Slope Instabilities on Perennially Frozen and Glacierised Rock Walls: Multi-Scale Observations, Analyses and Modelling

---

Dissertation
zur
Erlangung der naturwissenschaftlichen Doktorwürde
(Dr. sc. nat.)

vorgelegt der
Mathematisch-naturwissenschaftlichen Fakultät
der
Universität Zürich
von

Luzia Fischer

von
Winikon LU

Promotionskomitee
Prof. Dr. Wilfried Haeberli (Vorsitz)
Dr. Christian Huggel (Leitung der Dissertation)
Prof. Dr. Andreas Kääb
Dr. Ross S. Purves

Zürich, 2009

Summary

Slope failures from steep bedrock slopes have occurred in mountain areas throughout time. This is a consequence of the topography, geological characteristics, intense freeze-thaw activity and oversteepened slopes from glacier erosion. However, during the past decades, an increased number of periglacial rock avalanche events have been recorded in the European Alps and other high mountain ranges which are thought to be related to permafrost degradation and glacier shrinkage, indicating the potentially serious hazard related to slope instabilities originating from high-mountain faces.

The primary aim of this study is an interdisciplinary investigation of topographic, geological, cryospheric and climatic factors influencing high-mountain rock slope stability in view of the ongoing climatic change. The investigation of slope instabilities in high-mountain faces must account for the large variety of factors and processes and also consider the difficult conditions for data acquisition. The objectives of this study, where detachment zones of recent periglacial rock avalanches in the European Alps are investigated based on a multi-scale approach, can be divided in (a) the investigation and modelling of slope instabilities on periglacial high-mountain faces in order to better understand the different factors and processes leading to a slope failure, and (b) the application of different data acquisition and investigation techniques to test their suitability for steep faces in complex and difficult high-mountain terrain.

The implemented approaches consist of 1) a GIS-based statistical multi-factor analysis of detachment zones over the entire Central European Alps based on a rock avalanche inventory, 2) a GIS-based multi-factor analysis and detailed remote-sensing-based time-lapse topographic investigations of the Monte Rosa east face using LiDAR and digital photogrammetry, and 3) geomechanical analysis and numerical slope stability modelling of the Tschierva rock avalanche at the Piz Morteratsch.

This study has shown that in most cases a combination of several critical factors leads to a slope failure and no specific single primary factor was distinguished. The two factors slope angle and a pronounced discontinuity system are included in critical factor combinations at all failure magnitudes. The change in a factor and the time scale of change are considered to be more important than the individual factors. Rapid changes in a factor do not allow adequate stress redistribution within a flank and therefore, the critical shear strength may be exceeded. A large number of detachment zones were found to be located in areas with recent changes in glaciation and near the lower limits of local permafrost occurrence. Glaciers, mainly influencing the topography, and permafrost, mainly affecting the groundwater regime and geotechnical characteristics of discontinuities, are currently the predisposing factors having the fastest changes. However, slow processes such as progressive failure were also found to contribute to slope instabilities.

The present study demonstrates the benefits of a multi-scale approach and the combined application of conventional and novel techniques for the investigation of slope instabilities in high-mountain terrain. Furthermore, the findings provide a fundamental basis for prospective slope instability susceptibility analyses and subsequent hazard assessments.

Zusammenfassung

Felsstürze aus steilen Felswänden finden in Gebirgsregionen schon seit jeher statt. Dies ist bedingt durch die Topographie, aber auch durch geologische Charakteristiken, intensive Gefrier/Tau-Zyklen und übersteile Wände infolge Glazialerosion. Während der letzten Jahrzehnte wurde jedoch eine erhöhte Anzahl von Sturzereignissen registriert, sowohl in den europäischen Alpen wie auch in anderen Gebirgsregionen. Viele dieser Stürze werden mit Veränderungen im Permafrost und mit dem Gletscherrückzug in Verbindung gebracht, und sie zeigen die potentiellen Risiken im Zusammenhang mit solchen Instabilitäten in hochalpinen Steilwänden.

Das Hauptziel dieser Arbeit ist es, topographische, geologische, kryosphärische und klimatische Faktoren, welche die Hangstabilität beeinflussen, in einer interdisziplinären Untersuchung hinsichtlich der aktuellen Klimaveränderung zu untersuchen. Untersuchungen von Instabilitäten in hochalpinen Felswänden müssen einerseits die verschiedenen Faktoren und Prozesse miteinbeziehen, andererseits auch die erschwerten Bedingungen für die Datenerhebung berücksichtigen. Die Ziele dieser Arbeit, bei der Anrisszonen von periglazialen Felssturzereignissen in den europäischen Alpen auf verschiedenen Skalen untersucht wurden, lassen sich daher folgendermassen formulieren: (a) Die Untersuchungen und Modellierungen von Instabilitäten in periglazialen Felswänden sollen zur Verbesserung des Verständnisses der einzelnen kritischen Faktoren und der gesamten Prozesse beitragen, welche zu einem Sturzereignis führen. (b) Verschiedene Datenerhebungs- und Analysemethoden sollen verwendet werden, um ihre Anwendbarkeit in steilem, periglazialem Terrain zu testen.

Die verwendeten Ansätze bestehen aus 1) einer GIS-basierten Multi-Faktoren-Analyse, welche ein Felssturzinventar über die Zentralalpen auswertet, 2) einer GIS-basierten Multi-Faktoren-Analyse und hochauflösenden topographischen Analysen der Monte Rosa Ostwand basierend auf LiDAR-Daten und digitaler Photogrammetrie, und 3) geomechanischen Analysen und nummerischen Stabilitätsmodellierungen des Tschierva Felssturzes (Piz Morteratsch).

Die Resultate dieser Arbeit zeigen, dass meistens nicht ein einzelner Faktor, sondern eine Kombination von verschiedenen Faktoren für Hanginstabilitäten verantwortlich ist. Die Hangneigung und ausgeprägte Kluftsysteme kommen jedoch für jede Grössenordnung von Sturzereignissen in der Faktorkombination vor. Die Veränderung eines Faktors und der Zeitraum der Veränderung scheinen wichtiger zu sein als die einzelnen Faktoren. Eine schnelle Veränderung verhindert angemessene Spannungsumverteilung innerhalb einer Flanke und daher kann die kritische Scherfestigkeit eher überschritten werden. Viele Anrisszonen befinden sich in Gebieten mit kürzlichem Gletscherrückzug und in der Nähe der Untergrenze von lokalen Permafrostvorkommen. Gletscher, welche vor allem Einfluss auf die Topographie ausüben, und Permafrost, welcher hauptsächlich die Grundwasserverhältnisse und geotechnischen Eigenschaften von Diskontinuitäten beeinflusst, sind derzeit jene Faktoren, die sich am schnellsten ändern. Es gibt jedoch auch Prozesse, welche über lange Zeit zu Instabilitäten führen können, wie zum Beispiel die kontinuierliche Weiterentwicklung und das Öffnen von Klüften.

Die vorliegende Studie zeigt die Vorteile eines Multi-Skalen-Ansatzes und der kombinierten Anwendung von konventionellen und neuen Techniken zur Untersuchung von Hanginstabilitäten im Hochgebirge. Ausserdem bilden die Resultate eine wesentliche Grundlage für eine flächendeckende Abschätzung der Suszeptibilität und anschließende Gefahrenbeurteilungen.

Table of Contents

PART A: OVERVIEW

PART B: PAPERS

The thesis is based on four published and submitted papers (I, III-V) and one chapter containing work unpublished to date (II). The papers will be referred to in the text by Roman numerals. They are ordered according to thematic considerations, starting with a paper introducing the methodological focus, followed by papers incorporating the outcome of detailed local-scale studies and an integrative analysis of recent slope instabilities.

I **Fischer, L.,** and Huggel, C., (2008). Methodical design for stability assessments of permafrost affected high-mountain rock walls. *Proceedings of the 9th International Conference on Permafrost, Fairbanks, Alaska*, 439-444.

II **Fischer, L.,** Purves, R.S., Huggel, C., Noetzli, J., and Haeberli, W. (in prep.). On the influence of geological, topographic and cryospheric factors on slope instabilities: Statistical analyses of recent Alpine rock avalanches. *Natural Hazards and Earth System Science*.

III **Fischer, L**., Kääb, A., Huggel, C., and Noetzli, J. (2006): Geology, glacier retreat and permafrost degradation as controlling factors of slope instabilities in a high-mountain rock wall: the Monte Rosa east face. *Natural Hazards and Earth System Science*, 6, 761-772.

IV **Fischer, L.,** Eisenbeiss, H., Kääb, A., Huggel, C., and Haeberli, W. (subm.). Monitoring topographic changes in periglacial high-mountain faces using high-resolution DTMs, Monte Rosa east face, Italian Alps. *Permafrost and Periglacial Processes*.

V **Fischer, L.,** Amann, F., Moore, J.R., and Huggel, C. (subm.). The 1988 Tschierva rock avalanche (Piz Morteratsch, Switzerland): An integrated approach to periglacial rock slope stability assessment. *Engineering Geology*.

A complete list of publications with contributions by the PhD candidate is given on pages 75-77.

Table of Figures

List of Abbreviations

2-D, 3-D	2-dimensional, 3-dimensional
a.s.l.	above sea level
DInSAR	Differential Interferometric Synthetic Aperture Radar
DTM	Digital Terrain Model
GIS	Geographical Information Systems
GSI	Geological Strength Index
LGM	Last Glacial Maximum, about 21'000 y before present
LIA	Little Ice Age, period of major Holocene glacier re-advances, peaking around 1850
LiDAR	Light Detection And Ranging
RMS	Rock Mass Rating
SAR	Synthetic Aperture Radar
SAT-PP	SATellite Image Precision Processing (software by the Group of Photogrammetry and Remote Sensing, ETH Zurich)
UDEC	Universal Distinct Element Code (software by Itasca)

PART A: OVERVIEW

1 Introduction

1.1 Motivation

Global climate fluctuations over long time periods strongly affect mountain environments, especially those with alpine glaciers and permafrost occurrence (O'Connor and Costa, 1993). Due to their proximity to melting conditions, mountain glaciers and permafrost are particularly sensitive to climate changes (e.g., Haeberli and Beniston, 1998; Harris et al., 2001a; IPCC, 2007). As a consequence, climatic developments during the 20th century have caused pronounced effects in the glacial and periglacial belts of high mountain areas. The changes are made strikingly evident by the retreat of Alpine glaciers, with an overall area loss since 1850 of almost 50% in 2000 (Paul et al., 2004; Zemp et al., 2006). Less immediately visible but also very significant are changes in Alpine permafrost. During the past century, subsurface temperatures have warmed by about 0.5 to 0.8°C in the upper tens of meters (Harris and Haeberli, 2003; Harris et al., 2009). Since the Little Ice Age maximum (around 1850), the lower permafrost altitudinal limit is estimated to have risen vertically by about 1-2 m/year (Frauenfelder et al., 2001). Such fast changes in the Alpine cryosphere result in changed or enhanced periglacial processes such as increased sediment availability in recently deglaciated areas, formation and growth of ice-marginal and supraglacial lakes, floods and debris flows from the release of moraine- and glacier-dammed lakes, stable and unstable glacier length changes, rock and ice avalanches from steep valley walls, and debris flows (O'Connor and Costa, 1993; Evans and Clague, 1994; Kääb et al., 2006).

Slope failures from steep bedrock slopes have taken place in mountain areas throughout time. This is a consequence of the steep topography of these areas, their geological and structure-geological characteristics, intense freeze-thaw activity and oversteepened slopes from glacier erosion (e.g., Cruden and Hu, 1993; Ballantyne 2002; Evans et al., 2002; Hall et al., 2002). However, during the past century, an increased number of periglacial rockfall events have been recorded in the European Alps and other high mountain ranges which are thought to be related to permafrost degradation and glacier shrinkage, indicating the potentially serious hazard related to slope instabilities in alpine faces (e.g., Evans and Clague, 1994; Haeberli et al., 1997; Barla et al., 2000; Geertsema et al., 2006; Huggel, 2009; Papers II, III, IV). Rock avalanches often affect limited areas due to relatively short runout distances. However, as a trigger factor for other periglacial hazards such as floods and debris flows, slope failures from steep faces can be extremely hazardous and have the potential for far-reaching disasters, such as the extreme example of the Kolka/Karmadon rock avalanche (North Ossetia) that killed over 100 people in downstream areas (Kääb et al., 2003; Haeberli et al., 2004), or the ice avalanche linked with an earthquake-induced rock avalanche from Nevado de Huascarán (Peru) in 1970 that resulted in a mass movement killing thousands of people (Körner, 1983).

Climate change induces disturbance of glacial and periglacial belts and can shift hazard zones beyond historical knowledge. As a result, historical data alone are insufficient for hazard assessment. It is difficult to ascertain whether the frequency and magnitude of events have actually increased. However, situations with no historical precedent already occur and must be faced in the future.

So far, numerous investigations on slope failures have been performed on natural slopes in lowland areas as well as on artificial excavation slopes; periglacial rock avalanches, however, lack profound investigation. Most periglacial rock avalanche investigations have been conducted at a descriptive level and few detailed studies about slope failure processes are known (e.g., Barla and Barla, 2001; Noetzli et al., 2003; Eberhardt et al., 2004). Understanding the spatio-temporal variability of mass movement processes on high-alpine bedrock slopes requires an understanding of the processes relevant to local slope instability as well as knowledge about the spatial and temporal variability of the relevant boundary conditions. In addition, a better understanding of the impacts of climatic change on the high-mountain environment has become increasingly important, as human settlements and activities have extended progressively towards endangered zones in many alpine regions (Frauenfelder, 2005). Mountainous regions have experienced accelerated economic development during recent decades with growing tourism, associated transportation infrastructures and communication facilities, increasingly extending towards endangered zones in many regions (e.g. Turner and Jayaprkash, 1996).

Slope failures of different type, size and velocity may represent a significant threat to population, settlements and infrastructure worldwide. In order to optimize hazard recognition and early warning systems, knowledge about possible slope failure zones is necessary (e.g. Keefer and Larsen, 2007). Therefore, attention must also be paid to the processes leading to rock slope failures (e.g. Keusen 1997). Slope instability phenomena are related to a wide variety of factors involving the physical environment (Soeters and van Westen, 1996; Dikau and Glade, 2002). Thus, assessment of hazards from periglacial faces requires knowledge about these factors. For this reason it is necessary to apply multidisciplinary investigation techniques considering the different physical characteristics of these factors. Most engineering slope stability investigation approaches do not include cryospheric factors, and cryospheric studies tend to neglect the geological aspects. New investigation and modelling methods have to be evaluated and combined with established ones for hazard detection and management in steep periglacial faces. The ongoing changes in the glacial and periglacial zone pose the challenge of finding innovative observation and modelling approaches for related slope instabilities.

1.2 Objective and research questions

The primary objective of this study is to conduct an interdisciplinary investigation of the topographic, geological, cryospheric and climatic factors controlling high-mountain rock slope stability in view of ongoing climatic change based on a multi-scale approach. To further this aim, detachment zones of recent periglacial rock avalanches in the European Alps are investigated. The investigation of slope instabilities in high-mountain faces has to account for the influence of various factors and processes and must also consider the difficult conditions for data acquisition. The objectives of this study are, therefore: (a) the investigation and modelling of slope instabilities on glacierised and permafrost-affected high-mountain faces in order to better under-

stand the different factors and processes leading to a slope failure, and (b) to analyse different investigation techniques for documenting and studying steep faces in complex and difficult high-mountain terrain.

The main research question addressed is the following:

> What are the factors influencing slope instabilities in perennially frozen and glacierised steep rock walls and how can they be investigated?

This research question can be further divided into the following four sub-questions:

1. What are the primary factors that contribute to slope instabilities?

The basis for the understanding of slope failures is the knowledge of the different factors influencing slope stability. Few studies on high-mountain bedrock failures have included the influence of cryospheric changes induced by atmospheric warming.

2. What are appropriate techniques for data acquisition and measurement?

A major obstacle to data acquisition and closer examination of steep high-mountain rock walls is the complicated access. Therefore, appropriate techniques have to be evaluated and combined for data acquisition in situ and from remote sensing approaches.

3. What are feasible approaches for the assessment of slope instabilities?

The complexity of slope stability problems requires a number of different analysis techniques to consider the relevant physical processes and factors. The primary focus is to use and evaluate different methodological approaches.

4. What is the scale-dependence of the different factors and analysis methods?

Not all factors can be investigated on the same scale and with the same methodological approaches. The influence of this scale dependence on slope stability analysis should be evaluated.

1.3 Structure of the thesis

The thesis is divided into two parts (see Figure 1.1):

Part A provides a synopsis of the research conducted within the framework of this thesis and integrates it into a wider scientific context. It consists of six chapters. Following the present introduction, *Chapter 2* summarises the scientific background on which this study is based and creates the link between previous research and the present work. This review of the scientific background is divided into a process-oriented part, where the main characteristics of periglacial rock slope failures, observed rock avalanche events, controlling factors and their response to climate change are reviewed. The second part of the scientific background introduces the current state-of-the-art in data acquisition techniques, slope stability modelling methods and factor analyses. *Chapter 3* presents the approaches used in this study and describes the study sites. *Chapter 4* summarises the main research results derived from the publications on which this thesis is based. A general discussion of the main tasks and findings is given in *Chapter 5*. A summary of the main contributions and findings, concluding remarks and an outlook on the future research are formulated in *Chapters 6*.

Part B of this thesis contains full versions of the five papers which comprise the scientific work of this thesis (Figure 1.1).

Part A: Overview		Part B: Papers			
		Methodological		Technical/Case studies	Scale
1	Introduction	I	Methodical design for stability assessment of permafrost-affected high-mountain rock walls	II	On the influence of geological, topographic and cryospheric factors on slope instabilities: Statistical analyses of recent Alpine rock avalanches	10^2-10^4 km^2
2	Scientific background			III	Geology, glacier retreat and permafrost degradation as controlling factors of slope instabilities in a high-mountain rock wall: the Monte Rosa east face	10^0-10^1 km^2
3	Conceptual framework			IV	Monitoring topographic changes in steep periglacial high-mountain faces, Monte Rosa east face, Italian Alps	10^0-10^1 km^2
4	Main research Results			V	The 1988 Tschierva rock avalanche (Piz Morteratsch, Switzerland): An integrated approach to periglacial rock slope stability assessment	10^{-2}-10^0 km^2
5	General discussion					
6	Conclusions and perspectives					

Figure 1.1: Schematic structure of the thesis, showing the contents of the two main parts 'Overview' and 'Papers'. In the right column, the primary area/scale of investigation of the corresponding papers is specified.

2 Scientific Background

2.1 Rock slope instability in high-mountain areas

In this chapter, the scientific background of the research conducted in the thesis is outlined, focusing on the factors and processes influencing slope instability in high-mountain terrain affected by surface and subsurface ice. Firstly, the context of rock slope instability in high-mountain areas is outlined by introducing the characteristics of high-alpine faces, discussing the relevance of slope instabilities in such faces and recently observed Alpine rock avalanche events. Secondly, the environmental factors influencing slope stability and the response to climate change are described.

2.1.1 Characteristics of steep high-mountain rock walls

Steep high-alpine rock walls are characterised by their elevation, steep gradients, pronounced relative relief, periglacial environment, possible permafrost occurrence and glaciation on or adjacent to the face (e.g. Barsch and Caine, 1984). The periglacial zone is defined as a frost-dominated region peripheral to glaciers (Zepp, 2002; French, 2004). These areas are located in the vicinity of, and are influenced by, glacial environments that include glaciers and permafrost occurrence, and hence the lower limit of the periglacial zone varies regionally. In the European Alps, the lower limit of glaciation is currently about 1500 m a.s.l. and was roughly 200 m lower during the Little Ice Age. The lower limit of discontinuous permafrost occurrence in steep slopes depends mainly on slope aspect and varies roughly between 2500 m on northern aspects and 3000 m a.s.l. on southern aspects (e.g. Gruber et al., 2004a).

The surface coverage of steep high-alpine faces consists mostly of bedrock and ice with little to no talus material, given the steep slope angle (Figures 2.1a, 2.1b). Vegetation on steep periglacial faces is marginal, consisting mostly of only lichens and mosses. The ability to retain snow is inversely proportional to the slope gradient. Therefore, snow cover on steep slopes is usually shallow and intermittent, and its insulation effects are minimal (Gruber and Haeberli, 2007). Hence, the subsurface thermal regime is more directly coupled with the atmosphere than on less-inclined slopes. The subsurface thermal regime of the bedrock is often characterised by the occurrence of permafrost. Temperature and ice content may vary strongly depending on location, geological setting and water occurrence. Hanging glaciers and extensive ice coverage are a reliable sign of permafrost occurrence (Alean, 1985; Haeberli et al., 1997; Lüthi and Funk, 2001).

The ice cover in such faces can appear in the form of single hanging glaciers and firn fields (Figure 2.1c), connected hanging glaciers and firn fields (Figure 2.1b) or even consist of large-area ice and firn coverage building up ice faces (Figure 2.1a). The surface morphology can exhibit variances between rugged and highly weathered structures (Figure 2.1d), and smooth landforms from glacial overprints (Figure 2.1f).

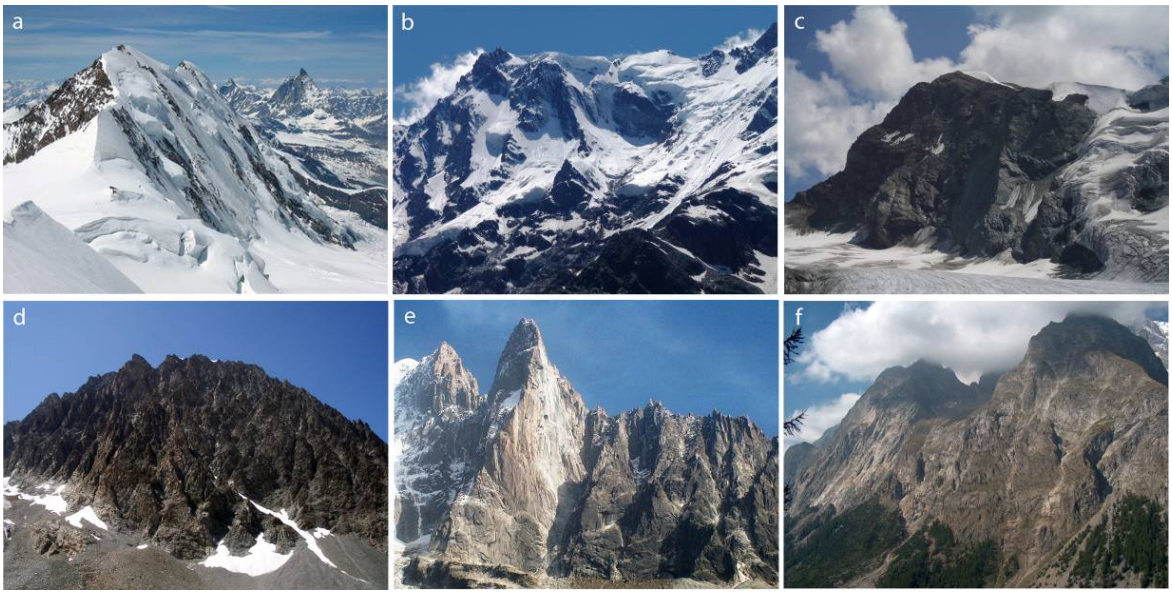

Figure 2.1: Photographs of different types of high-alpine faces. [a]-[c] show examples with varying degree of ice cover, from an ice face with several hanging glaciers to a sparsely ice-covered face. [d]-[e] show different morphological examples of non-glaciated high-alpine faces with varying surface characteristics. [a]: north face of Liskamm (Switzerland), [b]: east face of Monte Rosa (Italy), [c]: north face of Mont Brulé (Switzerland), [d]: east face of Mont Collon (Switzerland), [e]: west face of Les Drus (France), [f]: south-east face of M. Noir de Peuterey (Italy). Photographs [a] from www.stadler-markus.de, [b-f] taken by L. Fischer.

The slope gradient of steep bedrock faces ranges from about 35° to vertical, and even overhanging zones may occur. Zemp (2002) identified a threshold of 34° for the separation of debris-covered and bedrock slopes based on analyses of the rock signature in Swiss topographic maps. Gruber and Haeberli (2007) introduced a gradient of 37° as an approximate threshold of steep rock slopes. However, depending on local morphology, debris accumulation can also occur in concave topography steeper than this threshold, for example in couloirs. In the Swiss Alps, steep rock slopes with gradients over 35° and locations above 2000 m a.s.l. cover an area of about 3900 km^2 and hence 9.6 % of the area of Switzerland (Paper II).

2.1.2 Observed and investigated slope failure events

Numerous rock, ice and combined rock/ice avalanche events have taken place in high-mountain areas throughout history as they are an important geomorphic process on steep high-mountain rock walls (Sauchyn et al., 1998). This is a consequence of the steep topography of these areas and the high relief energy, but also geological and structure-geological characteristics, climatic factors such as intense freeze-thaw activity and erosion of steep slopes by glaciers (e.g., Cruden and Hu, 1993; Ballantyne 2002; Evans et al., 2002; Hall et al., 2002).

A mass movement is a downward and outward movement of slope-forming material under the influence of gravity and can range from slow deformation to very rapid detachment of material. In this work, only rapid mass movements from bedrock areas are considered and investigated. Failure mechanism in steep bedrock slopes can be fall, topple, slide and flow (Cruden and Varnes, 1996). However, the failure mechanisms are difficult to investigate and rarely known. Therefore, a classification will be made based on the volume of the failed rock mass alone. Rapid mass movements from bedrock failures are divided within this work into two classes based on the suggestion by Hungr et al. (2001): Rockfall typically involves relatively small volumes <10,000 m^3, whereas rock avalanches contain volumes of more than 10,000 m^3.

The motion of rock avalanches is massive, in that the bulk of the rock fragments moves as a semi-coherent flowing mass. Rockfall, in contrast, is more a talus-forming rolling, falling and bouncing of blocks. Slope failure events have been observed, reported and investigated throughout recorded history. Comprehensive information about rapid mass movements in the European Alps has been available sporadically since the beginning of the twentieth century, and documentation has increased during recent decades. This is probably related to enhanced and accelerated economic and touristic development in mountainous areas and increasing interest in recent climatic change and its impact on geosystems of high-mountain environments.

For prehistoric rock avalanches, mostly the deposit areas alone are identifiable, the location of the detachment zone is in many cases unknown or difficult to identify. Therefore, speculation about failure process and causes has its limits. In Matthews et al. (1997), available temporal and spatial information on large rapid mass movements during the Holocene in Europe, but also in other regions, are summarised and the nature of climatic controls on such mass movements considered. Detailed information on prehistoric and historic rock avalanche events in the European Alps can be found in Buck (1921), Heim (1932), Montandon (1933) and Abele (1974, 1994a, 1994b). Montandon (1933) developed an inventory of 160 historic mass movement events and Abele (1974) enlarged this inventory with a number of prehistoric and historic rock avalanches and landslides and presented comprehensive topographic and geological analyses of these events. Most of these large rock avalanches are considered to be influenced by an oversteepening of the slopes due to Pleistocene glaciation, although most of them did not fail immediately after the melting of the ice (Abele, 1994a).

During recent decades, a considerable number of contemporary rock and combined rock/ice avalanche events originating from alpine regions have been described and investigated, many of which are thought to be related to permafrost degradation and glacier shrinkage. Figure 2.2 shows the detachment zones of selected rock avalanche events. Rock and combined rock/ice avalanche events in the European Alps have been documented in Porter and Orombelli, (1980), Alean (1984), Eisbacher and Clague (1984), Noetzli et al. (2003), Deline (2001), Schoeneich et al. (2004), Ravanel and Deline (2008), and Paper II. Increased rock avalanche activity on the Monte Rosa east face (Italy) is documented in Haeberli et al. (2002), Kääb et al. (2004), Fischer (2004, 2006), Paper III, with major rock and ice avalanche events in 2005 and 2007 (Papers I, IV). Comprehensive data compilation and analyses of rockfall events in lowland to alpine areas of Switzerland have been performed by Gruner (2004), however most of these events were located below periglacial mountain belts.

Strikingly, a great number of rock avalanches with volumes of more than $1 \cdot 10^6$ m^3 have occurred in the European Alps during the last few decades. The Brenva rock avalanche in the Italian Aosta Valley (Januar, 1997) detached from recently deglaciated terrain and mobilised on its run out path a volume of about $2 \cdot 10^6$ m^3 of snow and ice from the Brenva glacier which developed into an airborne powder avalanche (Barla et al., 2000; Deline, 2001; Giani et al., 2001; Barla and Barla, 2001; Bottino et al., 2002; Figure 2.2A). At the same location, an earlier rock avalanche had occurred in 1920 (Deline, 2001). The detachment zone of the Val Pola landslide (Italy) in July, 1987 is situated at the altitude of the expected lower limit of mountain permafrost. This slope failure with a volume of about $40 \cdot 10^6$ m^3, containing blocks of ground ice from the uppermost part of the detachment zone, caused several casualties and significant damage (Dramis et al., 1995, Giani et al., 2001; Govi et al., 2002; Crosta et al., 2004). A recent very large event in the periglacial zone occurred from the Punta Thurwieser near Bormio (Italy) in September 2004 with a volume of about $2.5 \cdot 10^6$ m^3 (Cola, 2005; Sosio et al., 2008).

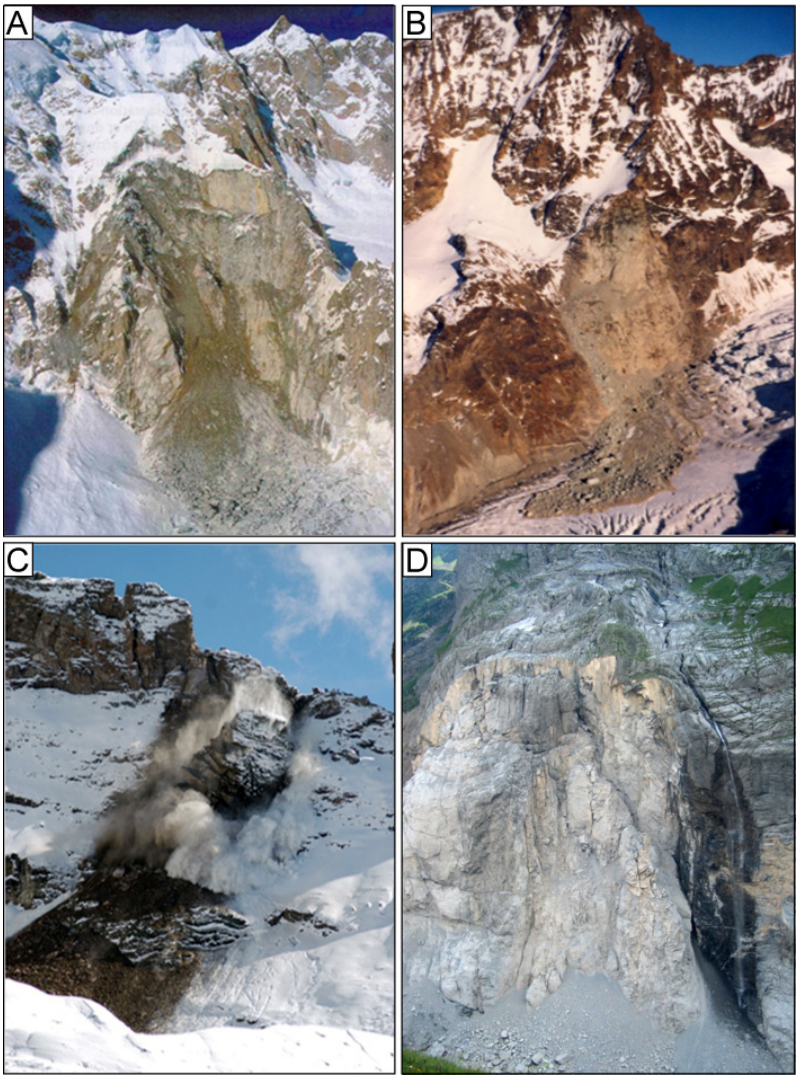

Figure 2.2: Selected examples of detachment zones of recent rock avalanche events in the European Alps. [A] Brenva, 1997 (G. Mortara), [B] Tschierva, 1988 (A. Amstutz), [C] Chärpf, 2007 (O. Adolph), [D] Eiger, 2006 (L. Fischer).

A much larger event occurred at Randa (Switzerland) in April, 1991, with a volume of about $30 \cdot 10^6$ m^3, destroying the main road and rail line and damming the Vispa river with subsequent flooding of a village (Sartori et al., 2003; Willenberg, 2004; Eberhardt et al., 2004). A collapse of a rock wall involving $2 \cdot 10^6$ m^3 occurred at the Eiger (Switzerland) in summer 2006, caused by recent glacier retreat (Oppikofer et al., 2008; Figure 2.2C). In October 2006, two rock avalanche events with volumes of around $1 \cdot 10^6$ m^3 occurred at Dents du Midi and Dents Blanches in the western Swiss Alps.

Outside of the European Alps, many events having a volume of more than one million cubic meters, some with catastrophic consequences, have been documented during recent decades, e.g., worldwide by Evans and Clague (1988, 1994), Hewitt et al. (2008) and Huggel (2009), for New Zealand by Cox and Allen (2009), McSaveney (1992, 2002), McSaveney et al. (1992), Chinn et al. (1992) and Augustinus, (1995a, 1995b), for North America by Evans and Clague (1988, 1994), Sauchyn et al. (1998), Evans et al. (2002), Geertsema et al. (2006), and Clague (2008). An enormous rock/ice slide occurred in September 2002 on the northern slope of the Kazbek massif, North Ossetia, Russian Caucasus (e.g., Haeberli et al., 2004; Kotlyakov et al., 2004; Huggel et al., 2005). The detachment zone was probably in a complex condition having

relatively cold/thick permafrost combined with warm, possibly unfrozen, parts with meltwater flow in very steeply inclined hanging glaciers with temperate firn introducing heterogeneous permeability (Haeberli et al., 2003). The impact of this massive rock/ice fall from the steep ice face on the Kolka glacier resulted in an almost complete erosion of a valley glacier (Kolka glacier) and led to a $>100 \cdot 10^6$ m^3 avalanche causing the death of over 100 people in downstream areas. This disaster is of worldwide importance since the erosion of a valley-type glacier due to impact from slope failure originating in an ice face has not been historically documented previously (Huggel et al., 2005). An event of such magnitude, in the relatively densely populated Alps, could have enormous consequences.

During the hot summer of 2003, an exceptional frequency of rockfalls was observed in the European Alps (Keller, 2003). Numerous smaller events occurred during the summer months, e.g., at the Monte Rosa east face, the Matterhorn, the Eiger north face, the Piz Bernina west face or at the Dent Blanche. These small-volume events are likely to be related to the fast thermal reaction of the subsurface of steep rock slopes by an extension of the active layer thickness and a corresponding destabilisation of ice-filled discontinuities (Gruber et al., 2004b).

2.1.3 Relevance of slope failures in high-mountain rock walls

The relevance of slope instabilities in mountain regions evolving in slope failures and rapid mass movements relates to two main fields: 1. formation of the alpine landscape, and 2. natural hazards.

The present-day landscape – including its topography, geological structures, and composition – is the result of millions of years of dynamic development and modification. The topographic features exposed on the surface are relatively young in age, but the geologic structures and composition from which the features were carved can be quite old (Rib and Liang, 1978). The high relief of the mountain areas results from endogenic forces of the plate tectonics and volcanism. Over a long time period, exogenous forces lead to the erosion of this high relief through physical factors (e.g., solar radiation, freezing processes), chemical factors (e.g. chemical weathering) and mechanical factors (e.g. glacial and fluvial erosion). Erosion can occur continuously area-wide as denudation, but also periodic large mass losses also contribute to erosion (Matsuoka et al., 1997, Sass, 2005). The collapse of cliff faces by rockfall and rock avalanches is a primary mode of bedrock erosion in alpine environments and exerts a first-order control on the morphometric development of these landscapes (Ballantyne, 2002; Moore et al., 2009). A number of field studies have been carried out on the distribution and quantity of rockfall as a contributor to erosion and rock wall recession (Rapp, 1960; Sass, 2005; Rabatel et al., 2008; Krautblatter et al., 2009).

Rock avalanches and rockfall present a major geological hazard in many parts of the world (e.g., Abele, 1974; Eisbacher and Clague, 1984; Evans et al., 2002; Haeberli et al., 2004). Hazard assessment is made difficult by a variety of complex initial failure processes and uncertain runout behaviour (Evans et al., 2002). It is often hindered by an incomplete understanding of the processes involved, and the episodic and catastrophic nature of related events limits the application of physically based models. Additionally, current climate change induces disturbance in glacier and permafrost equilibrium and can shift hazard zones beyond the historical-empirical knowledge.

Direct effects of slope failures from steep rock walls are generally restricted to limited areas, but can affect existing infrastructures and densely populated high-mountain regions. In combi-

nation with other periglacial hazard types, rock and ice avalanches have the potential for triggering far-reaching disasters (e.g. Kääb et al., 2005). Such process interactions can be, for example, combined rock and ice avalanches or a rock avalanche impacting a periglacial or supraglacial lake, triggering a lake outburst with possible far-reaching flooding and debris flow events. In fact, many of the largest known periglacial catastrophes featured hazard combinations and/or process chains (Plafker and Erickson, 1978; Körner, 1983; Röthlisberger, 1981; Richardson and Reynols, 2000; Huggel, 2004; Haeberli et al., 2002; Haeberli et al., 2003). Documented cases of rock avalanches in the European Alps and in other mountain regions indicate that their travel distances can be extended in glacial environments (Porter and Orombelli, 1981; Evans and Clague, 1988; Bottino et al., 2002). This is thought to be due to travel on low-friction snow/ice surfaces, fluidisation by snow and ice melting, generation of basal water pressure by frictional heating, and channelling or air launching by moraines (Evans and Clague, 1988). Furthermore, rock avalanches occurring in winter or impacting on a glacier have the potential to strongly increase their volume by the entrainment and incorporation of a significant amount of ice and snow, which may drastically enlarge runout distances (Evans and Clague, 1988; Barla et al., 2000; Bottino et al., 2002; Kääb et al, 2003).

For hazard assessment, the localisation of possible slope instabilities is fundamental. Therefore, sound knowledge about the nature and possible locations of slope instabilities and potential slope failures is essential for hazard assessment and mitigation. The general tendency in high-mountain areas with a scenario of accelerated future warming (e.g. IPCC, 2007) could be a widespread reduction in the stability of formerly glacierised and perennially frozen slopes and a marked shifting of hazard zones with considerable changes in the involved processes. However, the nature of slope instabilities and processes contributing to slope failure in periglacial high-mountain areas, including the factors permafrost and glaciers, are still insufficiently understood.

2.1.4 Environmental factors influencing slope stability

Slope stability is determined by the interplay of driving and resisting forces and is in equilibrium when all forces balance each other out. Slope instability occurs when gravitational and other types of shear stresses within a slope exceed the strength of the material that forms the slope (Terzaghi, 1950; Brunsden, 1985, 1993) and some form of mass movement, ranging from creep to avalanches, occurs.

What is required for slope instability formation is a critical combination of normal and shear stresses where the applied shear stress approaches, equals or exceeds the shear strength of the rock mass (Figure 2.3).

Shear stress: $\tau = \varrho h g \sin\beta$ (1)

Normal stress: $\sigma = \varrho h g \cos\beta$ (2)

where ϱ is rock density, h is the depth, g is gravity, and β is the slope angle

The shear strength of the rock mass may be defined as being composed of two components, cohesion and friction, as follows (Terzaghi, 1962; Wu and Sangrey, 1978):

$$s = c + \sigma'_n \tan\phi \quad (3)$$

where: s = shear strength, σ = normal stress
σ'_n = effective normal stress on the discontinuity ($\sigma'_n = \sigma - u$)
u = pore pressure, c = cohesion, ϕ = angle of friction

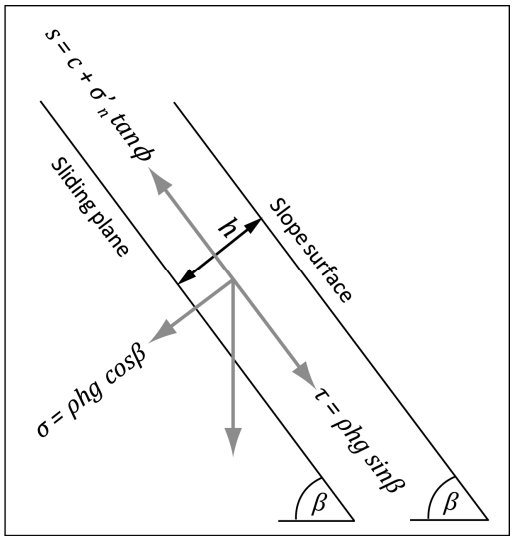

Figure 2.3: Normal and shear stress as well as an indicated shear strength in a simplified assumption of planar failure.

The stress field within a rock wall depends on a number of different factors and processes, which affect the state of stress inside and at the boundary of the slope (Figure 2.4). In this work a factor is defined as a physical component that occurs in and on a rock wall. Each factor has a given static state – a change in the state of a factor over time is induced by a specific process. Process is defined as a sequence of changes of a factor over a specific time, i.e. dynamic.

The characterisation and definition of the factors contributing to slope stability is complex and many different approaches have been introduced in engineering geology to date. Whalley (1974) summarised the basic criteria affecting the stability of a rock wall as follows: A) properties of the rock mass, B) geometric configuration of the rock mass, C) external factors affecting stability. In other studies, the predisposing factors are categorised into topographical, geomorphological, geological, geomechanical and hydrological factors (e.g., Cruden and Varnes, 1996; Eberhardt, 2006; van Westen, et al., 2008). Permafrost and glaciers are two additional environmental factors in high-mountain areas (Haeberli et al., 1997; Paper I) that have been rarely considered in engineering geology studies.

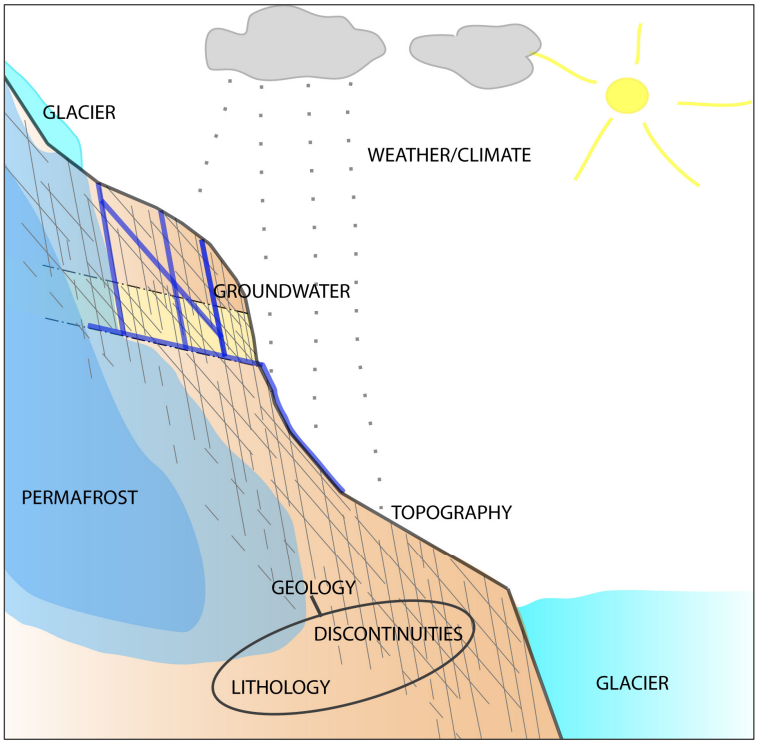

Figure 2.4: Schematic view of the environmental factors influencing the stability of periglacial faces.

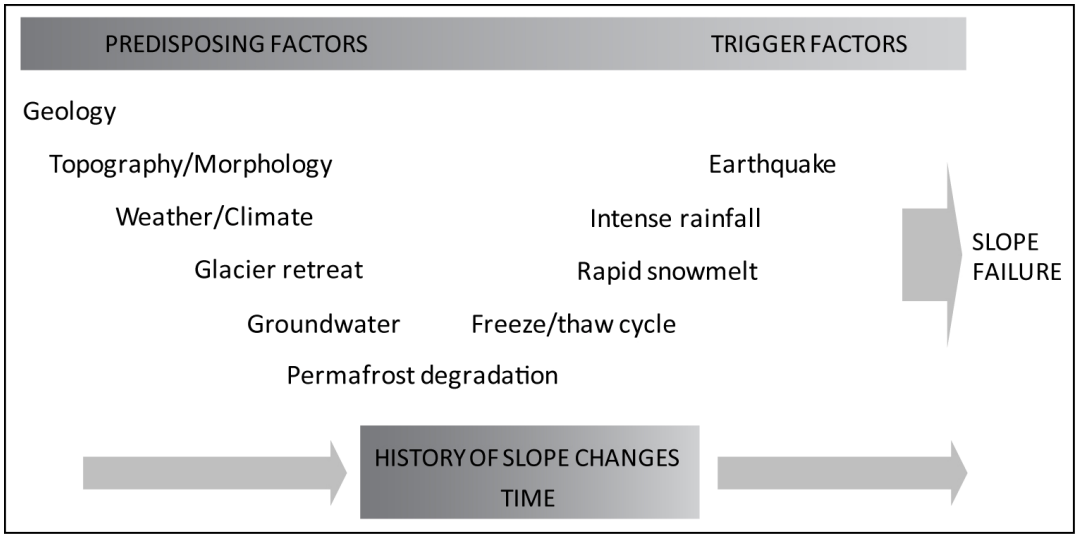

Figure 2.5: Cause-and-effect relationship between rock mass processes and slope instability problems (adapted from Eberhardt, 2006). This scheme reveals the fluent transition from predisposing to triggering factors.

According to Varnes (1978) a slope failure can have several causes and the eventual release of rock mass is driven by one or more triggering factors (Kienholz, 1997; Meissl, 1998; Figure 2.5). Triggering factors are by definition a stimulus causing a near-immediate response in the form of a slope failure by rapidly increasing stresses or reducing the strength.

Triggering factors include earthquakes (e.g. Keefer, 1984), intense rainfall and rapid snowmelt, volcanic eruptions and, rarely in high-mountain areas, disruptive human influence. However, slope failures may occur without an apparent trigger and result from the culmination of a process combination that gradually brings the slope to failure (Whalley, 1974; Wieczorek, 1996). A distinct separation of the predisposing and trigger factors is very difficult in many cases, as there are strong interactions and floating transitions from predisposing to triggering (Figure 2.5). The action period of these factors varies widely, and may range from a very short time in the case of strong earthquakes to a very long time, for example, in the case of progressive failure. Depending on the context, the same factor might act at one location as a disposition factor and at another location as a triggering factor, such as for example, frost weathering or water pressure. Therefore, the term 'environmental factor' will be used in the following for both predisposing and trigger factors.

In this work, **'environmental factors'** are divided into the following groups: topography, geology, glaciers, permafrost, groundwater, and weather (Figure 2.4). They are described in the next chapter and ordered according to their susceptibility to change. The factors topography and geology are the ones that are most constant over a long time period, glacier and permafrost can vary within a shorter timeframe and the groundwater, influenced by weather, is most prone to rapid changes. In nature these factors typically occur simultaneously, have complex interactions and these interactions may, in fact, provide an important clue to potential slope failure. These interactions, together with the history of slope changes, are fundamental to the development of slope instability.

2.1.4.1 Topography

Topography describes the ground surface geometry, implying the relief and the location of specific features. Topography results from a long-term interplay between endogenic and exogenic forces, mainly consisting of tectonic deformations and erosion. The topography and its evolution influence the occurrence and spatial distribution of slope instabilities due to the strong influence on stress and strain fields within a rock wall and therefore is a fundamental parameter for slope stability (Sowers and Royster, 1978; Evans et al., 2002). Relief characteristics and slope gradient are decisive for a rock mass to detach. Gerber and Scheidegger (1969) state: "The higher a rock wall, the larger is the overburden pressure, and the steeper a slope, the larger the stresses close to the slope surface". The curvature of a rock wall affects the stress field within itself: convex slopes experience more tensile stress whereas concave areas are more relieved (Meissl, 1998). Radiation and humidity may differ according to aspect, which in turn influences permafrost characteristics and, to a certain extent, the rock weathering intensity. Altitude primarily influences the temperature regime. Topography is closely connected to the geological setting and the geomorphological history of a rock wall (erosion, glacial overburden), which, in turn, also effectively influence the geomechanical setting.

2.1.4.2 Geological setting

The geological setting is determined by the lithology, the geological structures and the geotechnical properties of the intact rock mass, and the discontinuities. Except for the rare case of a completely unfractured rock unit, the majority of rock masses can be considered as assemblages of blocks delineated in three dimensions by a system of discontinuities (Norrish and Wyllie, 1996). The ***lithology*** designates mineralogical composition of the different rock types. The weathering susceptibility of mineralogical constituents might affect the development of microcracks and joints. Alteration of components may change shear strengths and pore spaces (Whalley, 1974). The strength parameters that are usually of greatest significance for slope stability analysis are the cohesion and friction angle of the rock mass (Willye and Norrish, 1996). However, both the resistance and compressive strength of the rock mass may be of importance, depending on the local geological and stress conditions. While the lithology of the rock mass plays a secondary role, the transition between different lithologies is important for slope stability, as lithology contrasts on rock walls may lead to differential erosion or different hydraulic regimes (Evans et al., 2002; Meissl, 1998; Papers III, V).

The stability of hard rock slopes is not only controlled by intact rock strength, but to a large extent by the ***geological structures*** (e.g., Sowers and Royster, 1978; Goodman, 1989; Giani, 1992). The geomechanical setting includes the discontinuities within intact rock mass, their occurrence, type, geometry, and properties. The controlling structural features are joints, bedding planes, fault zones, cleavage planes, schistositi, and folds. These structural features can be determined by the lithological setting, but are often formed as a reaction to changing stress fields due to tectonic activity, erosion or glacial debuttressing. The presence and geometry of discontinuities and their geotechnical characteristics (frequency, orientation, spacing, persistence, aperture, roughness, infilling) control the mechanical behaviour of a rock slope (Terzaghi, 1962; Bieniawski, 1989; Ballantyne, 2002). The most important structural parameter is the orientation of such discontinuities in space and relative to the rock face (Goodman, 1989; Sauchyn et al., 1998; Moore et al., 2009; Paper V). Discontinuities dipping out of slope must be carefully considered due to their high potential for instability (Piteau and Peckover, 1978). The shear strength as a

major parameter for stability is directly related to the geotechnical properties of discontinuities such as cohesion, friction angle, aperture, infilling, and weathering.

2.1.4.3 Glaciers

Glaciers influence the temperature and stress field as well as the hydrological setting of steep rock slopes. In the context of large mountain faces, two different glacier types can be identified that influence slope stability in different ways. Steep glacierisation including hanging glacier covers minor to large areas within a rock wall, while valley glaciers are situated below rock walls. Basal ice temperatures, which influence the thermal field in the underlying bedrock, may vary from temperate, close to the pressure-melting point, to cold temperatures largely below 0°C (Paterson, 1994; Suter, 2002). Ice temperatures depend on parameters such as air temperature, accumulation rate, solar radiation, clouds, surface albedo, wind, meltwater runoff, percolation and refreezing of meltwater, ice flow (Zagorodnov et al., 2006).

Hanging glaciers are often polythermal and then have two thermally different parts: (1) cold ice frozen to bedrock forms the vertical/impermeable ice cliffs where meltwater runs off immediately and ice lamellas break off as an important ablation process of these ice bodies, while percolation and refreezing of meltwater cause the existence of (2) much warmer or even temperate firn and ice below the less steep upper surfaces where snow accumulation predominates (Alean, 1985, Lüthi and Funk, 2001; Haeberli, 2005). The glaciers with zones of cold ice are thus connected to the permafrost environment (Etzelmüller and Hagen, 2005). Hanging glaciers on a face are therefore an indicator of permafrost. As hanging glaciers on steep faces are subject to shear stresses, their thickness is limited for the given steep slope gradients. They fail when the basal shear resistance or tensile strength is exceeded (Pralong, 2005). They usually do not exert as much influence on the stress field in the bedrock as valley glaciers. Alpine valley glaciers are mostly temperate glaciers with liquid water occurrence at the glacier bed. Therefore, bedrock below valley glaciers is considered not to be affected by permafrost. As long as the ice is present, a valley glacier supports adjacent bedrock faces (Abele, 1974). The erosion by, and retreat and down-wasting of, valley glaciers, in turn, may induce long-term change in the thermal and stress fields inside the rock wall (Wegmann et al. 1998, Eberhardt et al., 2004).

2.1.4.4 Permafrost

Permafrost or perennially frozen ground is defined as material of the lithosphere that remains at or below 0 °C throughout the year, for natural climatic reasons (cf. Brown and Péwé, 1973; van Everdingen, 1998). It is thus defined purely on the basis of temperature and time. Mountain permafrost has a complex spatial distribution that depends largely on altitude, radiation and snow distribution in space and time (Haeberli et al., 1983; Hoelzle et al., 2001; Harris et al., 2001a; Gruber et al., 2004a). The influence of permafrost on rock wall destabilisation is a very young field of research, but recent studies on the thermal conditions of rockfall starting zones confirm the importance of permafrost (Haeberli et al., 2003; Noetzli et al., 2003). Permafrost occurrence on a rock wall may influence the geotechnical characteristics of discontinuities. From a geotechnical viewpoint, the most important factors are the amount of ice content, its temperature, and unfrozen water content (Mellor, 1973; Davies et al., 2001). It is suggested that slow growth of segregation ice over long periods of time during permafrost formation may widen joints in their frozen state (Murton et al., 2001; Sass, 2005). Likely impacts of warming surface temperatures within the permafrost zone include active-layer thickening, basal melting causing permafrost thinning, and hydrogeological changes (Harris et al., 2001a). The shear

strength of ice-bonded discontinuities is strongly affected by the thermal regime in the subsurface and may be reduced by a rise in temperature with a stability minimum between -1.5 and 0°C (Davies et al., 2001; Harris et al., 2001a; Gruber and Haeberli 2007). The melting of ice-filled rock joints, in turn, also influences the hydrological regime, and may result in an increase in water pressure on the one hand, or higher permeability on the other.

2.1.4.5 Groundwater

The groundwater occurrence within a rock slope depends on surface topography, hydrogeological properties, and the infiltration of rainfall and melting snow. Groundwater flow affecting the hydraulic regime is one major factor that governs the stability of rock slopes (Terzaghi, 1962; Sowers and Royster, 1978; Erismann and Abele, 2001; Gugliemi, 2008). The hydraulic setting on a steep rock wall is closely connected to the topography, geological setting, geomechanical characteristics, glaciation, and permafrost occurrence. Piezometric measurements in rock slopes have shown that pressure distribution can be very complex, depending on rock joint systems (e.g. Watson et al., 2004). Water pressure is probably the most important factor affecting slope stability from an external source. According to Piteau and Peckover (1978), Terzaghi (1962), Serafim (1968), Müller (1964), and Giani (1992), existing groundwater within a flank and changes in hydraulic pressures can affect stability by 1. physically and chemically affecting the pore water and its pressure in joint infilling material, thus altering the strength parameters of the materials, 2. exerting hydrostatic pressure on joint surfaces, thus reducing the shearing resistance along potential failure surfaces by reducing the effective normal stresses acting on them, and 3. affecting intergranular shearing resistance, thus causing a decrease in compressive strength.

Krähenbühl (2004) showed, based on long-term measurements of meteorological and displacement data, that heavy precipitation in autumn may have a stronger influence on displacements than comparable events during summer and spring because fracture opening is largest in autumn and therefore maximal joint water pressure can be built up. Additionally, cyclic loading of fluid pressure in joints following precipitation or snowmelt events likely contributes to progressive failure of intact rock bridges. For groundwater, however, its flow pattern in rock masses is insufficiently known and quantitative analysis is highly uncertain (Hantz et al., 2003).

2.1.4.6 Climate and Weather

The climatic conditions determining the long-term precipitation and temperature regime of a region mainly influence glacier and permafrost occurrence and the erosion rate of the bedrock. The weather has more short-term influence on the slope stability and is an important dynamic factor influencing slope instabilities (Sowers and Royster, 1978). The two main weather components affecting slope stability are precipitation and air temperature. Wind can contribute to low-volume erosion and rockfall.

The groundwater regime of a slope is strongly linked with the weather, primarily with the precipitation. Heavy rainfall or fast snow-melting events can rapidly increase water pressure within a rock wall (e.g. Terzaghi, 1962). Bedrock weathering is influenced by different weather components. Changes in bedrock caused by weathering include wetting and drying processes, hydration, the removal of cementing agents, and freeze-thaw processes. The most important and effective form of weathering in high-mountain zones is frost weathering (Wegmann, 1998; Hall et al., 2002). Rocks may disintegrate under cycles of freezing and thawing or thermal expansion and contraction (Cruden and Varnes, 1996; Matsuoka and Murton, 2008). Frost weath-

ering depends on temperature variations, the available moisture, the lithology and structural geology. Discontinuities determine the size and form of the weathering product and moisture, and they also relieve convective heat transport is in these areas. Different models of frost weathering exist, but the key factor is always the freezing of water in the rock mass. Freezing water in a discontinuity can exert a very high pressure on the discontinuity walls (Hack, 2002). Frost weathering and rockfall activity is the subject of longstanding field observations and measurements (e.g., Matsuoka and Sakai 1999; Matsuoka 2001) and lab experiments (Murton et al., 2006). The two most important forms of frost weathering in high-mountain zones can be described using the volume expansion model (Matsuoka, 1991) and the segregation ice model (Hallet, 1983; Murton et al., 2006). Expansion of water due to freezing widens existing joints and may produce new ones, and acts mainly in superficial rock sections, while the segregation-ice process with the development of ice lenses is more effective at larger depths (Hallet et al., 1991). Many frost cycles lead to fatigue and an opening of the rock mass (Matsuoka, 1991). Investigations by Sass (2005) show that the occurrence of permafrost enhances frost weathering. Temperature cycles may cause movements in the bedrock. Fractures in brittle rock types may open at low temperatures due to contraction of the rock mass, whereas such deformations are stagnant or even reversed during warm seasons (Gruner, 2004).

2.1.4.7 Time and progressive failure

Time is another essential factor. Not only the current state of environmental factors influences the slope stability but also history of slope changes. Natural rock slopes undergo progressive failure over time (Piteau and Peckover, 1978). Murrell and Misra (1962) note that time-dependent strains occur when rock material is subjected to relatively high stresses for long periods. Most of the forces involved in such deformations are indeterminate functions of time, which are dependent on the effects of regional stresses, alteration processes in the mass, physical and chemical action of groundwater, and seasonal variations in temperature and rainfall. These lead to fatigue and the opening of cracks with irreversible deformations and progressive weakening of the mass (Piteau and Peckover, 1978; Paper V). In addition, slope deterioration can be affected by progressive failure processes that act to reduce rock mass strength. Progressive failure is predominately driven by the propagation of fractures through intact rock pieces connecting existing discontinuities (Einstein et al., 1983; Eberhardt et al., 2004; Prudencio and Van Sint Jan, 2007).

2.1.5 Response to climate change

Gradual or abrupt changes in one or more of the above-mentioned factors may change slope stability equilibrium and eventually lead to slope failure. Currently, permafrost and glaciers are the two environmental factors particularly prone to rapid changes in relation to ongoing climate change. Topography and geology react less strongly and more slowly to climatic changes. After Abele (1994a), climatic variations can affect slope stability in different ways: by changing the hydrological conditions, by glacier oscillation and by changing the thermal regime. Changes in distribution and ice temperatures of glaciers and permafrost occurrence can have large impacts on the local rock wall stress field, hydrologic and geomechanical properties (Evans and Clague, 1994; Wegmann et al., 1998; Davies et al., 2001; Gruber and Haeberli, 2007).

Glacial erosion and oversteepening, in combination with the relaxation of internal stresses after deglaciation (Evans and Clague, 1994; Augustinus, 1995a) and the associated propagation

of internal joint networks are considered to result in time-dependent rock-slope weakening (Sartori et al., 2003; Cossart et al., 2008). The removal of lateral support through glacial erosion and subsequent glacier retreat changes the in situ stress field and induces increased shear stresses in a face. The response of a rock slope to glacier downwasting may result in progressive slope deformations, rapid mass movements such as rockfall and rock avalanches, and deep-seated landslides (Evans and Clague, 1994; Augustinus, 1995a; Abele, 1994b; Ballantyne, 2002; Eberhardt et al., 2004). The three modes of response are all consequences of stress redistribution and release and may act in a combined way. The failure mode, scale and timing of periglacial rock-slope adjustment are strongly conditioned by rock mass strength, and in particular discontinuity sets (Ballantyne, 2002). Oversteepened slopes are generally thought to adjust rapidly to the changing stress conditions by a reduction of the slope gradient. Cruden and Hu (1993) proposed an exhaustion model of temporal distribution of rock slope failures which basically suggests that the number of failures exponentially decreases following deglaciation.

As a direct consequence of glacier retreat and ice surface lowering, previously ice-bonded rock walls become exposed, which in turn also induces changes in the temperature distribution inside the bedrock to great depths (Wegmann et al., 1998; Haeberli et al., 1999; Kääb, 2005; Paper III). Previously held at the pressure melting point (≈0°C) by temperate glacier ice, newly exposed rock walls become subject to local atmospheric conditions. Given the appropriate local temperature regime, retreat of temperate glaciers can enable the formation of permafrost (Wegmann et al., 1998; Kneisel, 2003). Thus, the penetration of a freezing front into previously thawed material has the potential to intensify rock destruction and affect hydraulic pressures and can, at least in part, be responsible for a decrease in rock wall stability (Hallet et al., 1991; Haeberli et al., 1997; Wegmann et al., 1998; Matsuoka et al., 1998; Kneisel, 2003). Additionally, freezing in the surface layers seals the rock wall. Such ice formation reduces the near-surface permeability of the rock walls involved and may cause increased hydraulic pressures inside non-frozen fissured rock sections (Tart, 1996; Wegmann et al., 1998; Paper V).

Permafrost degradation and a rise in the subsurface ice temperature have – especially in sections of relatively warm permafrost occurrence – a strong influence on the stability of steep rock walls (Wegmann et al., 1998; Davies et al., 2001; Noetzli et al., 2003). Ground temperatures in steep rock faces are more directly coupled to atmospheric influence than on flat or gently sloped terrain where snow, vegetation and soil cover effect a complex buffer. According to Gruber and Haeberli (2007), different physical processes may link warming permafrost and destabilisation of steep bedrock, such as the loss of ice bonding in fractures, reduction of shear strength and increased hydrostatic pressure. Extensive parts of currently perennially frozen rock walls will most probably warm up to depths of many decametres, thereby reaching temperatures of around 0°C, which are known to be especially critical for stability because of the simultaneous occurrence of ice and water in cracks and fissures (Harris et al., 2009). Permafrost degradation through advection by running water can rapidly lead to the development of deep thaw corridors along fracture zones in permafrost (Gruber and Haeberli, 2007) and potentially destabilise much greater volumes of rock than conduction can in the same time (Huggel, 2009). Cyclic variations and increase of water pressure in previously ice-filled fractures is also likely to contribute to a reduction in stability when permafrost thaws under conditions of warming. Davies et al. (2001) showed, on the basis of direct shear box tests, that a rise in temperature might lead to a reduction in the shear strength of ice-bonded discontinuities and eventually to a decrease in

slope stability. Warming permafrost is, therefore, thought to lead to increasing scale and frequency of slope failures, especially in combination with glacier retreat.

2.2 Measuring and modelling of steep rock walls

2.2.1 Requirement and challenges

Rock slope stability is complex and influenced by a number of different environmental factors, as described in the previous section. Data acquisition in high-mountain regions is particularly challenging due to difficult or impossible on-site access, complex topography and difficult acquisition geometry. Specific characteristics of high-mountain environments, such as glacier and permafrost occurrence, introduce further complexity (Paper I). Often, field data (e.g., geology, geological structure, rock mass properties, groundwater, etc.) is limited to surface observations and/or limited by inaccessibility, and can never be known completely, especially for the subsurface regime. For slope stability analysis it is important to consider all above-mentioned factors and processes, and therefore to use and combine different investigation techniques. In the following, relevant and suitable techniques for the acquisition of the different data sets in steep high-mountain faces and application examples are introduced, considering the relevant environmental factors described in 2.1. The main focus is the suitability for steep and complex periglacial terrain.

2.2.2 Basic data for factor analysis

For the generation of basic data, three different approaches can be distinguished: 1) remote sensing, 2) *in situ* measurements, and 3) modelling methods. Remote sensing is an increasingly important tool in high-mountain hazard assessment, particularly as new analytical techniques are being developed in line with emerging sensor technologies (e.g., Bishop et al., 2000; Kääb et al., 2005; Quincey et al., 2005; Paper IV). However, several surface and especially subsurface characteristics cannot be investigated using remote sensing techniques and hence *in situ* measurements have to be performed (Sowers and Royster, 1978). Some parameters such as permafrost distribution can be modelled based on topography and weather data. In the following, the different data acquisition methods are introduced based on the scheme in Figure 2.6. As the environmental factors vary in scale and extent, data acquisition at different scales has to be considered separately for each specific factor and purpose.

2.2.2.1 Remote sensing

Remote sensing techniques are well suited for data acquisition on ground surface features. They offer, with a range of sensors, flexibility in scale and timing (Quincey et al., 2005). Using this approach, terrain cover, geometry and dynamics of an area can be investigated without direct access. The applicability of remote sensing methods for determination of the topography, surface characteristics and their changes in time and space is predominantly governed by the spatial resolution, temporal resolution, timing of data acquisition, and available range of the electromagnetic spectrum (Kääb et al., 2005). The different data types appropriate for investigations in steep alpine faces include optical, microwave and LiDAR data.

ENVIRONMENTAL FACTOR	DATA ACQUISITION				SLOPE STABILITY ANALYSIS
	Remote sensing		*In situ* methodologies		
	Image classification	DTMs	Mapping/ manual measurement	Permanent installations	
1 Topography/ Morphology	10^0-10^2 m	10^0-10^2 m	10^0-10^1 m		GIS-based heuristic/statistical methods [1,2,4,5] 10^1-10^3 m
2 Geology	10^0-10^2 m		10^0-10^1 m		
3 Geomechanics	10^0-10^1 m	10^0-10^1 m	point	point	Kinematic methods [1,2,3] 10^0-10^1 m
4 Glacierisation	10^0-10^2 m		10^0-10^1 m		
5 Permafrost				point	Numerical stability modelling [1,2,3,4,5,6] 10^0-10^1 m
6 Groundwater	10^0-10^1 m		point	point	

Figure 2.6: Overview of methods for the data collection of environmental factors, indicating approximate resolution and possible slope stability analysis applications. The numbers in brackets indicate the necessary basis data for the corresponding slope stability analysis, and the approximate resolution is also specified. The methods that are applied within this work are marked in dark grey.

The data sets can be specified in spaceborne optical data (e.g., Corona, Ikonos, QuickBird, Landsat series, Aster), aerial images and terrestrial photographs including fix installed automatic cameras, spaceborne SAR and InSAR data (e.g., TerraSAR-X, Radarsat-2, ERS, Envisat, Shuttle Radar Topography Mission), airborne SAR and ground-based SAR, and aerial as well as terrestrial LiDAR. This data can be used for the creation of DTMs or for direct analysis of the optical data. The optimal spatial resolution of remote sensing data depends on the scale of the factors that have to be investigated. An overview of remote sensing methods and available sensors is given in Quincey et al. (2005), Metternicht et al. (2005) and Kääb (2008).

Image classification

The state of the environmental factors topography and geomorphology, geology, glacierisation and superficial water occurrence at a specific moment can be investigated based on image classification. Furthermore, the comparison of multi-temporal images is an effective technique to define spatial and temporal changes in surface characteristics. The most common application of remotely sensed image data for high-mountain hazard assessment is the interpretation and classification of the image content (Kääb et al., 2005; Kääb, 2008). In this way, both the spectral image information and the spatial context of such information are exploited. The technologically simplest form of image analysis is manual mapping of features of interest from the imagery

available. In particular under conditions of difficult topography and weak optical contrast, as is often the case with steep periglacial faces, manual image segmentation might be superior to semiautomatic and automatic techniques. However, for rapid, repeated, and/or large-area quantitative applications, automatic image classification offers valuable support (Lillesand and Kiefer, 2000; Kääb, 2005; Paul et al., 2004; Schowengerdt, 2007). Digital terrestrial and aerial photos have considerable potential for quantitative analyses of surface characteristics and their changes in a rock wall by georeferencing the photo based on a high-resolution DTM or photogrammetric techniques and image matching (Corripio, 2004; Roncella and Forlani, 2005). Furthermore, terrestrial photos often have the advantage of high temporal resolution, especially when data from an automatic camera is available. Satellite images are, for high-mountain faces, often lacking in spatial resolution or due to adverse acquisition geometry unsuitable for detailed analyses of detachment zones, but they provide valuable information in remote areas where no other high-resolution imagery material exists. Recently launched high resolution sensors with oblique stereo channels are still rarely used and could be quite useful in such cases.

Digital terrain models

Digital terrain models (DTMs), derived from optical stereo data, LiDAR or SAR data, are among the most important data sets for investigating high-mountain processes. The three-dimensional position of earth surface points and hence the topography can be described with a DTM (e.g. Weibel and Heller, 1991). Based on DTM analyses, information about the topography, geomorphology and structural geology can be extracted (e.g. Jaboyedoff et al., 2004a, 2004b). Furthermore, the comparison of repeat DTMs or DInSAR is an effective technique to exactly define terrain surfaces and their temporal changes in elevation (Kääb, 2002; Baldi et al., 2002; Kääb et al., 2005).

Derivation of DTMs from *stereoscopic satellite images* has considerable potential as satellite images are available over large areas and multi-temporal data is available (e.g., Kornus et al., 2006, Gruen et al., 2007). However, both DTM resolution and accuracy are typically in the range of decametres and may be even more reduced in steep mountain flanks (e.g., Bishop et al., 2003; Huggel, 2004; Kääb, 2008). This is often insufficient for detailed stability-related topographic analyses in high-mountain areas. Nevertheless, such DTMs can be useful for investigations in areas where no other data is available as well as for the landslide analyses in moderately inclined terrain (e.g. Nichol et al., 2006). *Digital photogrammetry* based on aerial or terrestrial images enables DTM and orthoimage generation. This is a particularly important method in view of the existing archives of analogue aerial images representing an invaluable source to investigate long-term topographic changes (Baltsavias, 1999; Kääb et al., 2005). Digital aerial photogrammetry has been applied in diverse studies in mountainous terrain, such as on volcanic faces (Baldi et al., 2002, 2008; Kerle, 2002), landslides (Dewitte et al., 2008) and steep rock walls (Buchroithner, 2002; Züblin et al., 2008). Terrestrial photogrammetry has only rarely been applied in studies in alpine slopes (e.g. Lerjen et al., 2003). However, photogrammetric processing of aerial images is very challenging for high-alpine rock walls due to large distortions of the images caused by the steepness and unfavorable data acquisition geometries, low image contrasts in glaciated areas and occlusion on vertical and overhanging slopes. It has, therefore, seldom been achieved in high resolution for such terrain.

Airborne and terrestrial laser scanning is a rapidly emerging and highly promising tool for acquiring very high-resolution DTMs for glacier and high-mountain areas (Baltsavias, 1999; Baltsavias

et al., 2001; Geist et al., 2003; Janeras et al., 2004). From repeated measurements it is also possible to derive terrain displacements (Kääb et al., 2005). Terrestrial laser scanning is increasingly applied for surveying small-sized rock walls for topographic and stability-related analyses in lowland as well as alpine terrain (Ruiz et al., 2004; Scaioni et al., 2004; Alba et al., 2005; Runqiu and Xiujun, 2008; Rabatel et al., 2008; Oppikofer et al., 2008). In high-alpine terrain, terrestrial laser scanning is mainly limited through difficult on-site access and the limited range of the scanner. Therefore, airborne laser scanning is a promising alternative. It has been used for different topographic analyses on rock slopes such as for example for coastal geomorphology (White and Wang, 2003; Lim et al., 2005; Rosser et al., 2005), earthquake-induced landslides (Chen et al., 2006) or landslide morphology (Glenn et al., 2006), but not on high-alpine steep slopes.

DInSAR is especially useful for area-wide detection of small superficial movements over long time periods and corresponding slope instabilities (e.g. Strozzi et al., 2004). In steep rock walls this technique has been rarely applied. Ground-based DInSAR technology is a capable tool for slope deformation studies (Luzi et al., 2007; Singhroy and Molch, 2004). However, this technique has so far been applied mainly for investigations of landslides in sedimentary material (e.g., Leva et al., 2003; Antonello et al., 2004) and rarely on steep bedrock faces. Nevertheless, the ground-based DInSAR performed for investigations of the Randa rock avalanche area provides valuable results about displacements and active release planes (Gischig et al., submitted). Another project for monitoring slope instabilities in the Monte Rosa east face belongs to the first ground-based DInSAR applications on steep rock walls (Luzi et al., 2007).

2.2.2.2 In situ methodologies

Mapping and on-site measurement

Information about the environmental factors topography, geomorphology, geology, geomechanics and superficial water occurrence can be extracted based on *in situ* mapping and manual measurements. Surface observations and mapping of surface characteristics provides the basis for slope stability analyses (Keaton and DeGraff, 1996). Basic tools and techniques for surface observation and geological mapping require access to the field site. Terrestrial surveying with theodolites, GPS (global positioning systems) and laser rangefinders can be used for the measurement of selected points. Salvini (2006) stated that in the last years automatic total station technology has shown very large improvements. It is nowadays suitable to be applied in geological surveying and monitoring. However, no area-wide topographic survey can be done with these methods (Kääb, 2005; Oppikofer et al., 2008).

On-site engineering-geologic investigations consist of the mapping of surface features of both the lithological and the geomechanical setting. Their purpose is to document surface conditions in order to provide a basis for projecting subsurface conditions. Preliminary rock mass characterisation can be performed in the field, for example based on the Rock Mass Rating systems RMS (Bieniawski, 1989) or the Geological Strength Index GSI (Hoek, 1994; Cai et al., 2004), which can be used for estimating the rock mass characteristics and strength from field observations. A preliminary assessment of the intact rock mass properties can be achieved for example using the Schmidt hammer method (Aydin and Basu, 2005). More precise measurements on rock mass strength can be performed in the laboratory. By on-site geological survey, structural discontinuities of the rock mass are mapped in detail and each feature is quantitatively characterised. The geological survey aims to measure a sufficient number of joints to allow sta-

tistical data analysis (cf. Section 2.2.3.2). The geomechanical and geotechnical properties of discontinuities can be assessed by measuring parameters such as orientation, frequency, spacing, aperture and surface characteristics based on the application of rock mass classification systems (Hack, 2002; Hoek and Brown, 1997; Wyllie and Mah, 2004). In the case of inaccessible ground conditions, these types of investigations can also be conducted in the surrounding area with similar lithological and geomechanical settings. Limited observations of the hydrological regime can also be done in-situ and from photographs, for instance observations of water inflow or outflow in a mountain face. Surface-water features can be mapped *in situ* or from imagery data. Springs and seeps near the crest of slope can supply recharge zones that provide groundwater to a potentially unstable slope. Springs and seeps near the base of a slope indicate a discharge zone that can be helpful in projecting piezometric surfaces in the slope (Keaton and DeGraff, 1996).

Permanent installations

Technical instrumentation and associated monitoring have made significant advances during recent decades. Such geophysical instrumentation can be used for the investigation of environmental factors that are not accessible to investigation based on optical and topographic techniques. Geophysical instrumentation for slope stability investigations in mountain regions can be divided into three main categories: geotechnical survey, thermal survey, and weather survey. In steep high-alpine environments, however, such permanent installations are difficult to install and maintain and hence have rarely been used until now. Technical instrumentation in steep high-mountain faces mainly concentrates on the near-surface zones as deep borehole installations are practically impossible in such terrain. Borehole installations, however, have been introduced in the vicinity of steep faces to observe subsurface patterns, deformation patterns, the hydrological regime or the thermal regime (e.g. Willenberg et al, 2002; Harris et al., 2001b).

Geotechnical survey includes slope displacement measurements and groundwater monitoring based on inclinometers, extensometers, and piezometers (e.g. Mikkelsen, 1996). Thermal survey includes point measurements of near-surface rock temperatures using temperature loggers installed a few cm to dm below the surface The resulting information can constrain permafrost distribution and the prevailing thermal regime (Gruber et al., 2003). More insights on infiltration, thawing, liquid water circulation and related deformation effects in rock slope on permafrost areas may come from more extensive near-surface installations (Hasler et al., 2008). Boreholes equipped with temperature loggers give an indication of temperature distribution at depth; equipped with inclinometers and piezometers they give geotechnical information. Geophysical techniques are powerful methods for indirect investigations of subsurface characteristics and are used to distinguish between frozen and unfrozen ground (Harris et al., 2001a). Georadar, electrical resistivity tomography and refraction seismics can be applied for the determination of subsurface structures and the distinction between frozen and thawing rock sections in alpine terrain (e.g., Hauck et al., 2004; Heincke, 2005; Krautblatter and Hauck, 2007; Hilbich et al., 2008). Geophysical investigations are mainly used as boundary conditions and reference values either for permafrost modelling or for analyses of the subsurface structures. However, such geophysical methods are difficult and complex in their application in steep rock walls and therefore rarely exploited (Krautblatter and Hauck, 2007).

2.2.2.3 Additional basic data

Additional basic data such as **weather data** and **seismic data** can be collected by different permanent measurement installations that should be located in the vicinity of the investigation

area for sufficient reliability. The climate data, as expressed in the various components of weather, can be measured with weather stations. In the European Alps, a dense network of weather stations exists, where precipitation, temperature, evaporation, wind, humidity, barometric pressure and other parameters are measured. The representativeness of such a weather station for a specific rock wall strongly depends on the distance and the topographic difference (Sowers and Royster, 1996). Information about seismic activity can be obtained from available seismic sensor networks, in the Swiss Alps, for instance, from stations of the Swiss Digital Seismic Network (SDSnet, www.seismo.etzh.ch).

Permafrost occurrence is only punctually measurable, but varies strongly in space. For spatial modelling of the permafrost distribution a number of models with varying levels of sophistication and at different spatio-temporal scales have been developed (e.g., Hoelzle et al., 2001, Gruber et al., 2003; Harris et al., 2009). Empirical models estimate, based on terrain parameters, the probability of permafrost occurrence or temperature (Haeberli, 1975). The three-dimensional temperature distribution and its evolution with climatic change is an important component for rock slope stability considerations, and can be assessed using physically based modelling by linking a surface energy balance model with a subsurface heat conduction scheme (Noetzli et al., 2007).

2.2.3 Slope stability analysis and modelling

Various methods with different levels of sophistication and detail can be used for the analysis and modelling of the stability of steep periglacial rock walls. The choice of an appropriate method depends primarily on the aim of the investigation, but is also strongly influenced by the size and conditions of the investigation zone and the availability of data.

Three types of approaches can be distinguished (e.g., Soeters and Westen, 1996; Guzzetti et al., 1999; Baillifard et al., 2003). These approaches are particularly popular in landslide research, but are also used for slope stability investigations in bedrock:

1. GIS-based heuristic/statistical methods comparing the distribution of observed rock avalanches (by means of an inventory) with the distribution of environmental factors thought to cause landslides either directly or indirectly (Carrara et al., 1995; Baillifard, 2003; Carrara and Pike, 2008).
2. Kinematic stability analyses using stereographic interpretations to assess possible failure mechanisms (e.g., Norrish and Wyllie, 1996; Jaboyedoff et al., 2004b).
3. Physically-based approaches that evaluate stability using physical laws (e.g. Stead et al., 2006).

2.2.3.1 GIS-based heuristic/statistical methods

Geographic Information Systems (GIS) can be used to store, display and analyse data, thereby enabling the selection of specific combinations of mass movement parameters to better understand spatial distribution of various slope failure types. GIS-based slope stability investigations include qualitative heuristic or quantitative statistical modelling techniques. For the most parts, different parameter maps are used and combined to define the spatial variability of geological, geomorphological, terrain and landslide inventory parameters (e.g., Carrara et al., 1995; Van Westen et al., 2003; Günther et al., 2004; Carrara and Pike, 2008). This approach is often used

for landslide susceptibility analyses in sedimentary material; applications for steep bedrock slopes are still rare.

In heuristic methods the expert opinion making the survey is drawn upon to classify the groups. This approach is based on a combination of different parameter maps with assigned qualitative weighting values (Soeters and van Westen, 1996). Statistical approaches involve the overlaying of parameter maps with statistical calculations, and quantitative predictions can be done for areas currently free of slope failures but where similar conditions exist (Soeters and van Westen, 1996). The importance of contributing factor combinations is calculated and weighting schemes can be introduced. The type and accuracy of the available data, however, is decisive for the use of a quantitative (statistic) method (Ruff and Rohn, 2008; Ruff and Czurda, 2008).

GIS-based factor and susceptibility analyses are widely used for landslide processes. However, for slope failures from bedrock, very few GIS-based factor studies exist. Giardino et al. (2004) performed qualitative classification of large slope instabilities in the Susa and Aosta Valleys (Italy). Marquínez et al. (2003) analysed the rockfall susceptibility over a 500 km^2 large area in the Cantabrian Range (North Spain). They found in a combined GIS-based analysis of talus scree, several topographic factors and lithology that the parameter topographic roughness was the most significant variable. Baillifard et al. (2003) used a GIS-based parameter rating approach for rockfall hazard mapping along a mountainous road in the Valais (Switzerland) over a length of 4 km. They performed an automatic assessment of susceptibility using the five criteria proximity to fault, scree slope, presence of a rock cliff, steep slope, and road for a limited area along an alpine road where a slope failure had already occurred.

Abdallah et al. (2004) used GIS-based analyses for establishing the relationships between mass movement occurrence and a comprehensive array of terrain parameters over a 2670 km2 large region of Lebanon. They demonstrate that remote sensing and GIS-based statistical correlations permit dual relations between the inherent parameters to mass movements to be defined, and the most significant ones relating to them to be detected. Their study includes all types of mass movement and not only rock slope failures. Eight parameters, i.e., lithology, proximity to fault zone, soil type, distance to drainage line, rainfall quantity, land cover/use, slope gradient and slope aspect were considered and the factor lithology was found to be the most influencing factor on mass movement occurrence.

Ruff and Rohn (2008) and Ruff and Czurda (2008) applied an index method for landslide hazard assessment in a 114 km^2 large area in the Eastern Alps on a working scale of 1:25,000 (Vorarlberg, Austria). Their work is based on 107 rock and soil slides. The factor layers geotechnical class, tectonic faults, bedding conditions, slope angle, slope aspect, vegetation and erosion were used in the assessment and each factor was weighted with an index ranging from 0 to 1 according to its importance and iteratively combined into a landslide susceptibility map. The geotechnical class and slope angle were found to have the strongest influence on slides. These studies reveal that the choice of factors has a strong influence on the results. Therefore, a preferably broad and complete range of factors should be considered to avoid unbalanced or even biased analyses. The investigated factors and level of detail is also related to the size of the investigation area and the investigation scale. The presented studies show that GIS-based analyses are applicable on different scales. However, the level of detail often decreases in studies over larger areas.

2.2.3.2 Kinematic stability analyses

Kinematic slope stability analysis can be used to evaluate the potential for failure and assess the failure mechanism (e.g., Goodman, 1989; Giani, 1992; Stead et al., 2001). The geometric relationship between the orientation of the discontinuity planes and the orientation of the topography determine the kinematic stability of a slope. The first step in assessing a kinematic failure potential is detailed evaluation of the rock mass structure. Interpretation of the geologic structural data requires the use of stereographic projections that allow the three-dimensional orientation data to be represented and analyzed in two dimensions. The most commonly used projections are the equal-area net and the polar net (e.g., Hoek and Brown, 1980; Hoek and Bray, 1981; Norrish and Wyllie, 1996; Figure 2.7.1). For such kinematic analyses the orientations of a large number of geological discontinuities have to be measured in situ.

New methods for the detection and measurement of geological discontinuities were developed based on high-resolution DTMs (Figure 2.7.2). The increasing availability and precision of DTMs aids in the assessment of landslide prone areas where is very limited availability of on-site data (e.g. Derron et al., 2005). From such DTMs with resolution in cm-dm range, topographic parameters, morpho-tectonic features and geological structures can be extracted. The main discontinuity sets can be distinguished and their geometrical pattern determined. Therefore, a preliminary assessment of potentially unstable areas may be performed with kinematic analyses using only a DTM (e.g., Jaboyedoff et al, 1999; Broccolato et al., 2006).

Further structural and stability analysis with a DTM is made possible by the recent development of geologically oriented GIS tools (e.g, Günther, 2003; Jaboyedoff et al., 2004c; Mote, 2005; Broccolato et al., 2006). Such tools have been applied, for example, for preliminary rockfall hazard assessment in Norway (Derron et al., 2005) and kinematic analyses of the Eiger rockslide in Switzerland (Oppikofer et al., 2008). Aksoy and Ercanoglu (2007) developed a different approach for kinematic analyses of discontinuity-controlled rock slope instabilities, where kinematic analyses of DTMs are combined with fuzzy set theory.

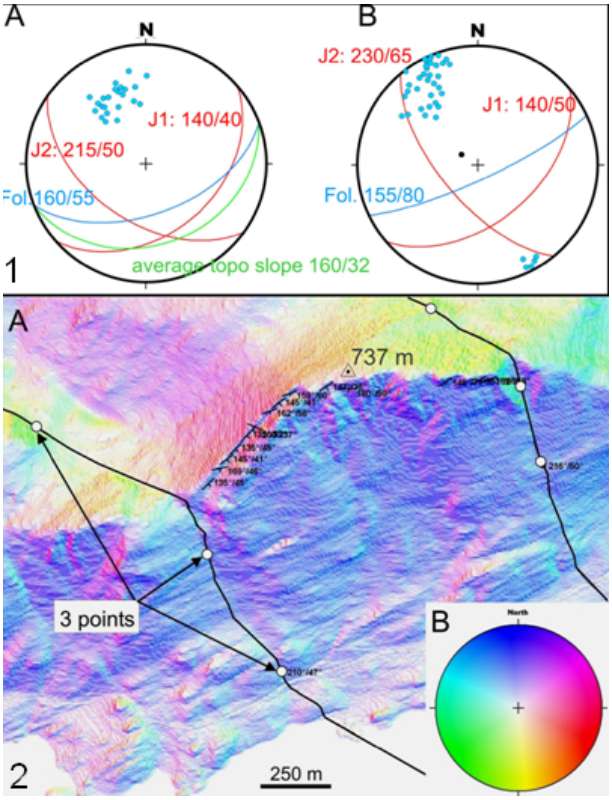

Figure 2.7: 2.7.1 shows a comparison of the measurements of poles and planes made on a DTM (A) and in the field (B) in the lower hemisphere stereographic projection. 2.7.2 shows a colour shaded DTM based on the COLTOP-3-D method by Jaboyedoff et al. (2007), where each position in the lower hemisphere stereographic projection has a corresponding colour value. (Source: Derron et al., 2005)

2.2.3.3 Numerical slope stability modelling

Numerical slope stability modelling methods provide a powerful tool for the assessment of failure mechanisms by giving approximate solutions with respect to physical processes, which would not be solvable using conventional techniques (e.g. kinematic analysis). Many rock slope stability problems involve complex geometry, lithology, *in situ* stresses, and hydraulic conditions, and are further complicated by coupling between these various parameters. For such complex slope stability analyses numerical methods are often required. Numerical methods used for rock slope stability analysis in 2-D and 3-D may be divided into three approaches: continuum, discontinuum and hybrid modelling. The different approaches are described in detail in Stead et al. (2001, 2006) and Eberhardt et al. (2004).

Detailed topographic, geomechanical and geotechnical characteristics of the rock mass are the basic input data necessary for numerical slope stability modelling. The quality of the input data made available for the analysis may vary such that the objective of the numerical analysis focuses on prediction of a slope failure when high quality *in situ* instrumentation data is present, or in cases where the data is limited, as providing a means to establish and understand the dominant mechanisms that may affect the behaviour of a slope (Eberhardt, 2006).

Bhasin et al. (2004) performed dynamic analysis and parametric studies for the rock slope stability problem at Oppstadhornet and Kveldsvik et al. (2009) for the Aknes rock slope (both western Norway) using the distinct element method UDEC. The purpose of analysis was to gain insight into the deformation mechanism of the rock slope and to estimate the volume of rock mass that could potentially slide when subject to dynamic forces such as earthquakes. This estimation was required in order to assess the runup heights of waves (tsunami) in a fjord that could potentially be caused by the rock slide. Similar analyses were performed in the area of the Tafjord slide (Norway, 1934), to assess whether subsequent slides were to be expected. For the Randa rock avalanche (Switzerland, Eberhardt et al., 2004; Willenberg, 2004), Brenva rock avalanche (Barla and Barla, 2001) and the Tschierva rock avalanche (Paper V), back-calculations of the slope failure were performed to evaluate failure mechanism and contributing factors. Coupled hydromechanical modelling was performed by Gugliemi et al. (2008), Bonzanigo et al. (2001) and Paper V to assess the influence of water pressure on slope instability.

Günther et al. (2006) developed a GIS-based specification tool for interactive setup and parameterisation of numerical models with GIS data to be processed with UDEC. They represent a first approach to interlinking a GIS (Geographical Information System) with a 2-D numerical simulation scheme (UDEC) for the modelling of rock slope instability phenomena on vertical 2-D cross sections through a GIS-based specification tool.

These selected studies have shown that numerical slope stability modelling is possible based on a range of elementary topographic, geological and geotechnical information. However, for sophisticated investigations and forecasting issues, extensive instrumentation of the slopes is required in order to obtain reference values of displacements, water pressure etc. Such permanent geophysical installations are very rare in high-alpine rock walls (c.f. chapter 2.2.2.2). Studies of alpine rock slope instabilities have shown that numerical models are a powerful tool for the assessment of failure mechanisms (e.g., Barla and Barla 2001; Eberhardt et al., 2004), but the necessary level of topographic and geotechnical detail limits their application for prediction issues.

3 Conceptual Framework

3.1 Methodological approach

The overview presented in the scientific background chapter reveals that the field of research on high-alpine bedrock slope instabilities is still limited, in terms of both the process-oriented and the technological part. Current process-oriented research is focused mainly on individual phenomena, such as geology, permafrost or glaciers and few multi-disciplinary approaches have been used. None of the GIS-based statistical methods or numerical slope stability modelling studies ever included the two key factors glacier and permafrost, but focused instead on topographic and geological factors. However, considering the fact that these two factors are currently prone to rapid changes, they must be included in a multi-disciplinary approach for analyses of slope stability in periglacial terrain. In the field of technology and methodology, highly promising advances were achieved during recent years, e.g. in LiDAR techniques, GIS-based methods or numerical slope stability analyses. A wide variety of conventional and novel data acquisition and modelling techniques have been used and tested in different projects, but only a few of these projects are actually situated in high-alpine terrain. Therefore, for most of the techniques introduced in the previous chapter, the applicability and potential at steep high-mountain faces is rarely known.

This work is based on a multi-scale approach and comprises different conventional as well as novel methodological approaches for data acquisition and the investigation of slope instabilities to test their applicability on high-mountain rock walls. The characteristics of the detachment zones of recent periglacial rockfall and rock avalanche events are considered as possible proxy information for the evaluation of essential predisposing factors and processes. The multi-scale approach consists of a regional-scale study covering the Swiss Alps and adjacent zones, considering a larger number of recent rock avalanche events and two local-scale studies concentrating each on specific rock walls with recent slope instabilities. Existing base data covering the entire investigation area include a digital elevation model with 25 m grid spacing (DHM25 Level 2; Swisstopo, 2004), a digital lithological map (based on the Swiss Geotechnical Map, 1:200,000), digital glacier inventories of the Swiss Alps for the years 1850, 1973 and 1998 (Paul, 2004), a recent permafrost map (FOEN, 2006), orthophotos and topographic maps. Additional data was acquired within this project, especially for the two local-scale study sites based on *in situ* field investigations, applying optical remote sensing techniques and by the use of digital photogrammetry and aerial LiDAR. The base data sets can be distinguished as point data and spatial data. *In situ* data acquisition methods mainly produce point data which provide a difficult basis for spatial exploration. For the acquisition of spatial data, a remote-sensing-based approach is more suitable.

As a brief summary, the different approaches concentrate on 1) a GIS-based statistical multi-factor analysis based on a rock avalanche inventory over the entire Swiss Alps, 2) a GIS-based multi-factor analysis and detailed remote-sensing-based topographic modelling of the Monte Rosa east face, and 3) geomechanical analysis and distinct element slope stability modelling of the Tschierva rock avalanche at the Piz Morteratsch.

3.2 Study sites

The different study sites are introduced here, as they represent the basis of the entire project and of the summary of research papers which follows.

3.2.1 Regional-scale approach

During recent decades, a considerable number of rock avalanche events originating from high-mountain regions have been described and investigated in scientific studies (cf. Chapter 2.1.2). The basis for the regional-scale approach is a rock avalanche inventory containing 57 rock avalanche events that occurred between 1900 and 2007 in the Swiss and adjacent Alps. The detachment zones of the considered events are located above 2000 m a.s.l and the volumes are estimated to be around or larger than 1000 m^3. The locations of the inventoried events are indicated by red dots in Figure 3.1.

3.2.2 Local-scale approaches

The east face of Monte Rosa, Italian Alps, is located at the Swiss-Italian border (Figure 3.2, A), and is among the highest and most impressive mountain faces in the European Alps (2200–4600 m a.s.l.). During recent decades, the ice cover of the Monte Rosa east face has experienced an accelerated and drastic loss in extent. New slope instabilities and detachment zones of rapid mass movements have developed in bedrock and ice. Increased rock and ice avalanche as well as debris flow activity have been observed. Besides frequent small-volume rock and ice avalanche events since around 1990, an ice avalanche with a volume of more than 1·106 m3 occurred in August 2005, and a rock avalanche of about 0.3·106 m3 detached in April 2007 from the upper part of the flank.

The 1988 Tschierva rock avalanche detached from the western flank of Piz Morteratsch in the eastern Swiss Alps (Figure 3.2, B). The Piz Morteratsch is located within the Bernina massive, Engadine, between Val Roseg and Val Morteratsch, and reaches an elevation of 3751 m a.s.l. The rock avalanche occurred on October 29, 1988, with a volume of 250,000 to 300,000 m^3.

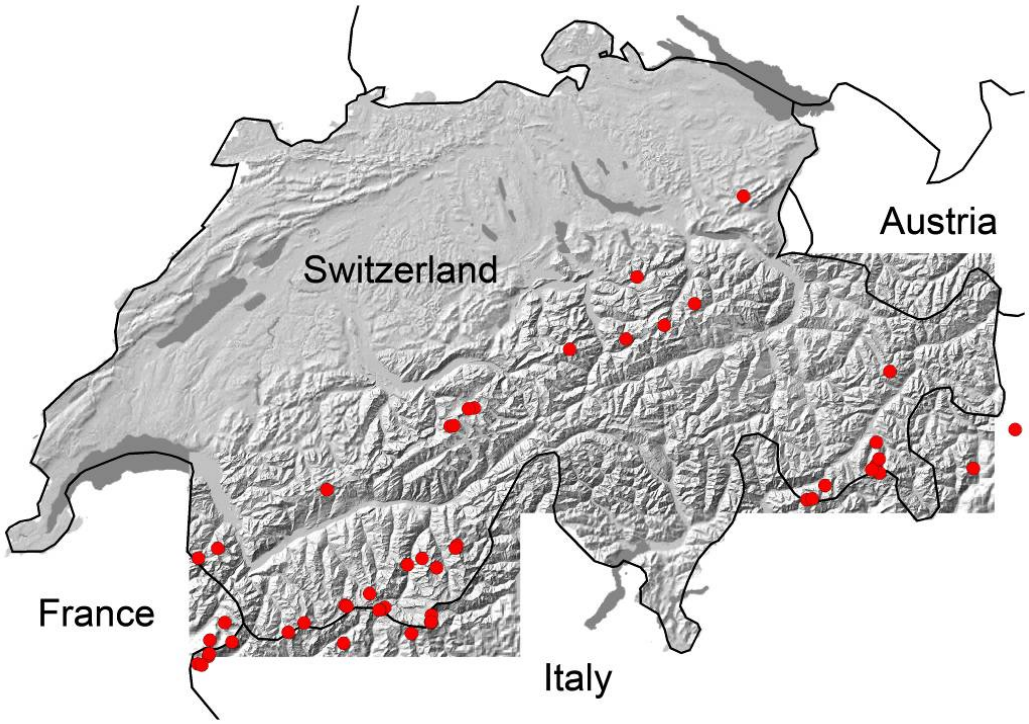

Figure 3.1: Overview of the spatial distribution of slope failure events.

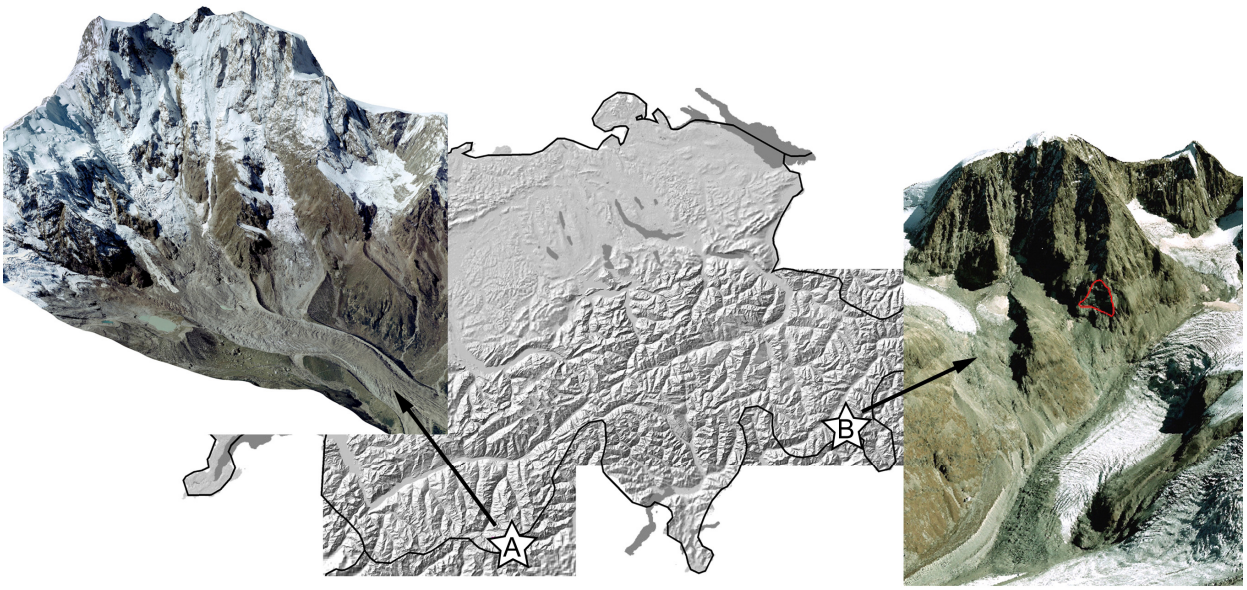

Figure 3.2: Location of the Monte Rosa east face (A) and the 1988 Tschierva rock avalanche, the detachment zone is marked in red (B).

4 Summary of Research Papers

I **Fischer, L.,** and Huggel, C., (2008). Methodical design for stability assessments of permafrost affected high-mountain rock walls. *Proceedings of the 9th International Conference on Permafrost, Fairbanks, Alaska*, 439-444.

This paper presents a methodological procedure for slope stability analyses, ranging from the basic data acquisition to eventual numerical slope stability modelling for high-mountain terrain. It discusses the complexity of slope stability problems, including the possible predisposing and triggering factors of slope failures in periglacial rock walls, and indicates the difficulties of data acquisition and investigations in complex high-mountain terrain. For an integrative assessment of slope stability, a better understanding of the state and changes in the predisposing factors is particularly important. Changes in the cryospheric environment can also affect other predisposing factors such as the topography, groundwater, geomechanical and geotechnical characteristics, and might reduce the stability of steep rock walls.

This article provides a review of investigation techniques and proposes a multi-disciplinary methodological design for comprehensive stability-directed investigations of predisposing factors in steep high-mountain rock walls which considers the particular difficulties of steep and partly inaccessible ground conditions, based on a combination of on-site and remote methods. Such combined approaches implementing different fields of research are particularly relevant in view of the effects of recent and future climate change on rock slope stability in such regions. The design presented in this paper does not claim to include all possible methods, rather it is based on investigation techniques and analyses that were applied and tested within past and ongoing projects in high-mountain terrain. Also, the rapidly advancing technology may require extension and adaptation of the design in the future.

The effective application and coupling of measurements, analyses and modelling methods is shown based on the two local-scale studies of this thesis:

- The case study of the Tschierva rock avalanche shows that appropriate method combination including classic geological field investigation techniques, terrestrial and aerial image analyses and permafrost modelling allows detailed numerical slope stability modelling to be performed and possible failure mechanisms to be evaluated.
- The much larger Monte Rosa east face with surface and subsurface ice subject to extremely fast changes, represents most challenging high-mountain conditions and required a more remote-based approach. Nevertheless, local field surveys could be integrated for a comprehensive spatial and temporal analysis of predisposing factors and the location of detachment zones in bedrock and ice.

II **Fischer, L.,** Purves, R.S., Huggel, C., Noetzli, J., and Haeberli, W. (in prep.). On the influence of geological, topographic and cryospheric factors on slope instabilities: Statistical analyses of recent Alpine rock avalanches. *Natural Hazards and Earth System Science.*

The present study seeks to evaluate and advance existing knowledge of regional distribution of recent slope failures on steep periglacial rock walls, especially their most important predisposing factors, by the application of statistical analyses. The focus hereby is on the applicability of the analyses over a regional scale, including the entire Swiss Alps.

Understanding the spatio-temporal variability of mass movement processes on high-alpine bedrock slopes requires an understanding of the processes relevant to local slope instability as well as knowledge about the spatial and temporal variability of the boundary conditions. Establishing statistical relationships between contemporary slope failures and the possible predisposing factors is an important task which aims to assess their influence and importance and to predict future events under the assumption that these would occur under geo-environmental conditions similar to the recent ones. Our approach relies on the use of a Geographical Information System (GIS) with different thematic layers and a Digital Terrain Model (DTM). Because of the relatively low number of rock avalanches in the study area, we concentrated on a more heuristic approach by a statistical comparison of the characteristics of the detachment zones with the settings over the entire area. In this heuristic approach, the factors lithology, elevation, slope gradient, glacierisation state and permafrost conditions were considered and an intercorrelation between environmental factors over the whole area and the same factors at the detachment zone was performed.

The compiled rock avalanche inventory is based on the work of Noetzli (2003) and enlarged with information from scientific publications, newspaper articles, field observations, and personal comments. Information on 57 periglacial rock avalanche events with volumes ranging from 1000 m^3 to more than $1 \cdot 10^6$ m^3 are available for the time period 1900 to 2007. The study area covers a 25,000 km^2 region in the Central European Alps, whereby only the areas above 2000 m a.s.l. were considered for the analyses in order to limit them mainly to the periglacial zones. The percentage of area decreases strongly from 45% between 2000 and 3000 m a.s.l. to only 5% above 3000 m a.s.l., whereas the proportion of detachment zones above 3000 m a.s.l. (60%) is higher than between 2000 and 3000 m a.s.l. (40%).

The main results can be summarised as follows:

- Slope gradient, elevation and recent glaciation changes were found to have the strongest influence on slope failures.
- The detachment zones are not evenly distributed over elevation but the proportion strongly increases at elevations above 2800 m a.s.l. and even more above 3400 m.
- As only 7% of the detachment zones show mean slope gradients below 40°, this value could be taken as a rough threshold for the critical slope gradient for rock avalanches in prospective susceptibility analyses.

- The lithology influences the volume rather than the frequency of a slope failure. Granite fails more in small-volume events, whereas gneiss and limestone lithologies are associated with both large- and small-volume events.
- Almost half of the rock avalanche events occurred in areas with recent deglaciation effects (i.e. since the end of LIA around 1850).
- Especially the slope failures of the volumetric classes from 10,000 m^3 to 100,000 m^3 are influenced by recent changes in glaciation.
- A large number of detachment zones are located close to the modelled lower boundary of permafrost. Especially for small-scale volumes, changes in the extent of the active layer and in water availability are influential. However, in order to draw further conclusions about the influence of permafrost, more detailed information on the thermal setting and ice content at each detachment zone would be required.

The results of this combined analysis of detachment zones and the entire area have shown that zones of increased susceptibility can be distinguished descriptively by identifying regions with critical factor combinations. However, investigations within this study have shown that more detailed topographic analyses require DTMs with higher resolution than 25 m. The factors structural geology and groundwater were not included in this multi-criterion approach as it is impossible to investigate them at the regional scale. However, local-scale analyses have shown (Paper V), that just these two factors might contribute largely to slope instabilities. Therefore, further research should be conducted to enable the investigation of these two factors at a regional scale.

III **Fischer, L.**, Kääb, A., Huggel, C., and Noetzli, J. (2006): Geology, glacier retreat and permafrost degradation as controlling factors of slope instabilities in a high-mountain rock wall: the Monte Rosa east face. *Natural Hazards and Earth System Science*, 6, 761-772.

This study investigates the present state of and recent changes in the Monte Rosa east face, taking into account the geological characteristics, the glacierisation and permafrost setting, and slope failures in both bedrock and ice. The integrated approach is based on a combination of remote sensing data and in situ field investigations, and complemented by modelled permafrost estimations. The main focus of this study is the assessment of the influence of the geological setting, glacier retreat and permafrost degradation on the current rock and ice avalanche activity.

The detachment zones of slope failures were mapped based on field investigations in 2003 and 2004 and supplementary analyses of aerial and terrestrial imagery. The investigation revealed strongly enhanced mass movement activity since about 1990 with successive formation of new detachment zones. Detailed geological mapping showed that the Monte Rosa east face is characterised by layers of two different lithologies, orthogneiss and paragneiss. Especially in the steep upper part of the face, the two lithologies alternate frequently, affecting many transition zones between the two lithologies.

The digital mapping of glacier outlines was based on topographic maps, orthophotos, terrestrial photographs and field observations, and allowed quantitative spatial analyses to be made of changes in glaciation since around 1900. An accelerated and drastic loss in glacierisation extent starting around 1990 was observed in the steep part of the face. Permafrost distribution was estimated by applying two empirical models. They showed that the upper half of the Monte Rosa east face was in a permafrost condition, and they localised the lower boundary of the permafrost occurrence at about 3100-3600 m a.s.l., depending on aspect, slope gradient, and snow/ice cover.

The results of the factor analyses were compiled in a GIS and the overlay of each investigated factor revealed spatial as well as temporal linkages between the individual factors, and allowed qualitative conclusions to be drawn concerning their influence on the formation of new slope instabilities. A comparison with observed detachment zones of rock avalanches showed that:

- a large number of them are situated in the transition zones between ortho- and paragneiss;
- most of the detachment zones on the Monte Rosa east face are located in areas where surface ice has disappeared recently;
- many detachment zones are located at the altitude of the lower boundary of the estimated permafrost distribution, where warm and degrading permafrost is presumed to exist.

This study indicates that the formation of detachment zones seems to be caused to a large extent by a combination of different predisposing factors and that the three investigated factors, geology, glacierisation and permafrost, represent a mere subset of a complex network of different factors, processes and feedback mechanisms in a steep rock wall. For further analyses and in particular for the prediction of hazardous zones, more factors and processes – such as topographic, geomechanical, hydrological, and climatic factors and changes – have to be investigated and their influence on rock wall stability assessed. Quantitative information on topographic changes in particular is required in order to draw detailed conclusions on the processes involved. This task is addressed in Paper IV.

IV **Fischer, L.,** Eisenbeiss, H., Kääb, A., Huggel, C., and Haeberli, W. (subm.). Monitoring topographic changes in periglacial high-mountain faces using high-resolution DTMs, Monte Rosa east face, Italian Alps. *Permafrost and Periglacial Processes*.

This paper describes a remote-sensing-based approach for detailed topographic investigations in steep periglacial high-mountain faces. The main objective of this study is to establish a methodology to investigate topographic changes in steep and complex terrain on a detailed scale over a long time period.

To this aim, time series of high-resolution digital terrain models (DTMs) from high-precision digital aerial photogrammetry and airborne LiDAR (Light detection and ranging) were developed. The applicability and quality of digital photogrammetry and LiDAR techniques for topographic monitoring tasks in steep and complex high-mountain terrain was of primary interest. Digital terrain models (DTMs) with 2 m resolution were developed from high-precision digital aerial photogrammetry for the years 1956, 1988 and 2001 and from airborne LiDAR for 2005 and 2007, and various aerial and terrestrial photographs were also considered. This approach enabled detailed investigations over past time periods to be made and a continuation of this allows prospective monitoring of hazardous situations in inaccessible areas to be carried out.

The main results and conclusions about the methodology can be summarised as follows:

- This study represents one of the most detailed and precise topographic data sets for a high-mountain face over a long time period.
- The use of sophisticated software such as SAT-PP enabled digital photogrammetry of aerial images to be applied, resulting in high-resolution DTMs even for such steep, glaciated terrain.
- Aerial LiDAR from airplane and helicopter has proven to be very beneficial for the acquisition of topographic data in steep periglacial terrain.
- Process understanding of periglacial slope instabilities cannot be gained from DTM analyses alone; additional observations in the field and the investigation of orthophotos and terrestrial images are essential.
- The transformation of individual DTMs to a common reference system is crucial in steep topography as minor offsets between DTMs introduce large errors into DTM comparisons.

The main results and conclusions about topographic changes and the involved processes can be summarised as follows:

- The individual detachment zones of slope failures can be located precisely, provided that the temporal resolution of the time lapse DTMs is high (i.e. for the time period 2001 to 2007).
- The rapid topography changes in the Monte Rosa east face have differed considerably in process, magnitude and timing and reveal strong stability coupling between permafrost-affected bedrock and adjacent hanging glaciers.

- The main slope failures are strongly spatially related. They started in 1990 on a small part of the face with combined rock and ice avalanche activity, proceeding progressively with a chain reaction of mass wasting processes until the whole Parete Innominata and Imseng Channel was ice-free in 2001.
- Considering the whole period over the past 50 years, a total volume loss of more than 20×10^6 m^3 of glacier ice and bedrock is revealed, whereby the major part of mass loss has occurred since 1990. This huge volume loss has no documented historical precedent of similar magnitude on a steep face in the European Alps.
- At some locations, a rapid ice accumulation and build-up of steep glaciers can be observed in eroded areas of an ice avalanche, whereas at other locations, no ice accumulation can be observed after mass loss. Such differences depend on the local topography and on the mass movement activity impacting these zones.
- The results provide valuable quantitative evidence of topographic changes to help scientists understand the nature and dynamics of change in inaccessible areas.

To conclude, the remote-sensing-based investigations provide a powerful database for the assessment of changes in glaciation, bedrock and slope instabilities as well as for detailed modelling tasks such as permafrost estimations and mass movement runout modelling. In particular the LiDAR data collection by helicopter and airplane proved to be an invaluable source of detailed and accurate topographic information in remote, steep and mountainous terrain. This novel method combination for steep periglacial terrain was tested at the example of the challenging Monte Rosa east face. Its main advantage is wide applicability to a range of geological and geomorphological problems in inaccessible terrain.

V **Fischer, L.,** Amann, F., Moore, J.R., and Huggel, C. (subm.). The 1988 Tschierva rock avalanche (Piz Morteratsch, Switzerland): An integrated approach to periglacial rock slope stability assessment. *Engineering Geology*.

This study focuses on the 1988 Tschierva rock avalanche (Engadine, Swiss Alps) as an example of a recent periglacial rock avalanche event. The objectives of this paper are to evaluate factors influencing the stability of the affected rock wall in an integrated manner, and to re-analyse the slope failure with kinematic and finite element modelling techniques, while focusing on the role of glacier retreat, geological setting and groundwater conditions. The study further contributes to a testing of possible approaches for slope stability assessment in high-mountain environments where access and site-specific data are typically limited (cf. Paper I).

Basis data was collected during *in situ* field work and deduced from multi-temporal aerial as well as terrestrial images, comprising detailed topographic profiles, a lithological map, rock mass characterisations and visual groundwater observations. In addition, information on the glaciation history based on a digital glacier inventory, modelled permafrost estimations and meteorological data from a nearby meteorological station were considered.

Kinematic analyses of discontinuity-controlled slope instabilities were based on a comparison of discontinuity orientation and friction angle with the geometry of the slope surface. The results of the kinematic analysis showed that the probability of planar sliding along existing discontinuities was significantly higher in the area of the slope failure than in the adjacent stable flank.

Numerical slope stability modelling was performed using the Universal Distinct Element Code UDEC (Itasca, 2004) to investigate the influence of different factors and underlying mechanisms contributing to this rock avalanche. Besides sensitivity analyses of the key geotechnical parameters, modelling experiments were performed with respect to (1) the retreat of LGM glaciers and (2) groundwater loading conditions. The glacial unloading of the LGM initiated progressive fracturing of discontinuities, which led to displacements within the rock wall along a stepped surface, corresponding well with the observed failure surface from the 1988 rock avalanche. Since the slope was stable for many thousands of years following retreat of LGM glaciers, we can assume that there were still intact rock bridges between discontinuities after deglaciation. The influence of glacier retreat can therefore be considered as preparatory degradation of rock mass strength but is not the primary reason for slope failure. The modelling of groundwater loading conditions indicated that water pressure not only induced reversible displacements by expansion, but also provoked irreversible vertical settlement in the area of the failed slope. Meteorological data documented significant precipitation events in the weeks preceding the rock avalanche that probably led to increased water pressure within the flank, especially during the pronounced freezing periods in the days before slope failure that could have led to a superficial freezing and consequently to a trapping of groundwater beneath surface ice.

The following main results can help to improve process understanding:

- Slow, progressive formation or extension of discontinuities following glacial debutressing at the end of the LGM likely played a key role in long-term degradation of rock mass strength.

- Similarly, cyclic loading of fluid pressure in joints following precipitation or snow-melt events likely contributed to progressive failure of intact rock bridges.
- The occurrence of permafrost within the failed flank may have influenced slope stability, as changes in the temperature and ice distribution related to ongoing atmospheric warming combined to reduce discontinuity shear strength while contributing to the formation of new groundwater flow paths.

Our approach of multi-factor analysis in combination with geomechanical modelling proved to be appropriate for failure analyses in such complex terrain, despite existing data limitations. However, the prevailing uncertainties in permafrost and groundwater conditions are a challenge for geomechanical modelling, and therefore more information from *in situ* installations such as, for instance, equipped boreholes, piezometers, temperature loggers and displacement measurements should be available for model calibration. This study has also pointed out that sufficient information on rock mass characteristics for reliable analyses can only be obtained by in situ investigations. This poses a particular challenge that can be overcome only in part by the use of advanced technology such as high-resolution remote sensing, and for example, by the extraction of structure-geological features from high-resolution DTMs.

5 General Discussion

In this chapter a discussion on the main tasks and findings of the thesis is given, linking together the research presented in Papers I-V. A more detailed discussion of methods and results can be found in the corresponding sections of the individual papers, appended in Part B of this work. The discussion is structured as follows: in 5.1, the inventoried rock avalanche events are discussed, as they provide the basis of the entire project; 5.2 summarises the benefits of the applied multi-scale approach; the identified influence of changes in predisposing factors on the slope stability are described in 5.3; and in 5.4 a short outlook on the possibilities of susceptibility analyses based on the results of this work is given.

5.1 Rock avalanche events as proxy data

The starting point of this work was the compilation of rockfall and rock avalanche events that occurred in the Central European Alps. In Switzerland, but also in many other countries, national databases on rockfalls and landslides exist for populated areas, but data about slope failures in high-mountain terrain are lacking. Therefore, information had to be compiled from diverse sources (Paper II).

The distribution and characteristics of the detachments zones were considered to serve as proxy data for the analysis of predisposing factors for slope instabilities. The compiled rock avalanche inventory includes only rapid mass movement processes from steep bedrock and contains around 80 rockfall and rock avalanche events from periglacial areas. Also other mass movement types such as debris flows, ice avalanches or slow-moving landslides occur within the periglacial zone. Their occurrence can also be influenced by recent changes in glacial and periglacial belts (e.g., Zimmermann et al., 1997; Papers III, IV). However, the influencing factors are probably slightly different, and combined statistical analyses of different slope failure processes as applied, for example, by Ruff and Rohn (2008) and Abdallah et al. (2005), have therefore to be treated with caution regarding conclusions about bedrock failures only.

In the inventory of this work, the volumes of the slope failures range from around 100 m^3 to more than 10^6 m^3. Taking this data set as proxy data, the difference in failure mechanism and contributing factors has to be kept in mind. Small-volume detachments are often influenced by superficial disaggregation of the bedrock due to enhanced weathering such as freeze/thawing effects, the occurrence of extreme weather events such as heavy rainfall and snowmelt, or extraordinary warm temperatures as observed in summer 2003. Small-volume detachments often occur immediately or soon after a factor being changed, as mostly the shear strength and tensile strength of single discontinuities alone have to be exceeded. Large-volume detachments evolve over much longer time periods, whereby climatic change and large-scale topographic changes play a significant role. For the detachment of a large volume, new persistent discontinuities have to be formed and the shear strength has to be exceeded over extensive areas.

The number of recorded periglacial slope failure increases after 1980 and especially from 2000-2007 (Paper II). Further back in time, less information is available, and only the large-volume events containing more than 10^5 m^3 or the ones that caused damage or casualties are known and reported. It is difficult to assess whether the number of slope instabilities has really increased during recent decades due to the influence of atmospheric changes and linked changes in periglacial terrain, or if this increased number of recorded periglacial slope failures stems only from increased recording activity during recent decades and more observations because of enhanced economic and touristic developments in mountainous areas. This uncertainty hinders the drawing of detailed conclusions about temporal characteristics of rock avalanche activity based on our inventory data.

However, we assume that the records of large-volume rock avalanche with volumes of more than 10^5 m^3 largely complete. From 1900 to 1980, zero to two events occurred with volumes larger than 10^5 m^3 per decade. The subsequent rise in number to six such events between 2000 and 2007 indicates a recent increase in large-volume events. The extraordinary high number of events during the summer of 2003 indicates a special situation. It remains unknown whether such a cumulation of small-volume events ever occurred in earlier times. However, summer heat waves like in 2003 in Europe are predicted to become more frequent in the future (e.g. Schär et al., 2004), and therefore such accumulations of slope failures might recur. Considering the small and temporally limited data set, no final conclusions can be reached on slope failure frequency, but the statistics indicate an increase in large-volume events, as also observed in northern British Columbia (Geertsema et al, 2006) and an extraordinary cumulation of small-volume events in an unusually hot summer.

5.2 Benefits of a multi-scale approach

This study is based on a multi-scale approach implementing a range of different base data sets and slope stability analysis methods. This chapter discusses the different approaches and the benefits of the combination of multiple investigation approaches at different scales.

Figure 5.1 shows the workflow scheme that builds the foundation for this work. The differences in the scale and level of details between the various approaches applied become obvious and the used linkages between the approaches are indicated. The dark grey arrows show the down-scaling approach, where information and results from simple statistical analyses over larger areas can be used for more detailed investigation steps. The light grey arrows show that the direction of up-scaling is also applicable and important. Within this study, workflow was performed in both directions. Based on initial regional-scale analyses of the rock avalanche inventory and available knowledge from existing projects, potential sites for the local-scale analyses were chosen. Results and insights from the detailed local-scale analyses about environmental factors and processes contributing to specific slope failures, in turn, provide the base for subsequent detailed statistical factor analyses of detachment zones at the regional-scale. They are valuable indicators of which factors should be considered and they enhance process understanding at all scales. Marked in orange are the steps recommended for further studies in the direction of susceptibility analysis, hazard assessment and finally the observation of hazardous situations (cf. Chapter 5.4)

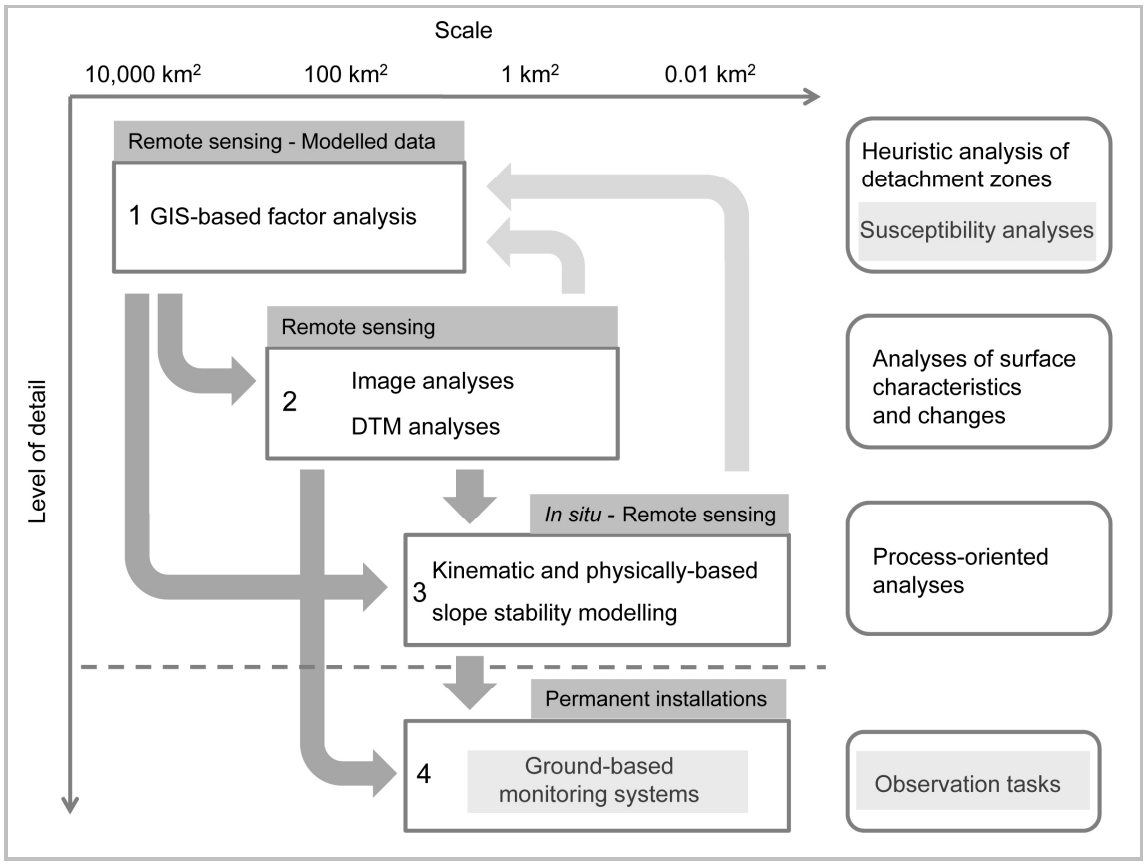

Figure 5.1. Workflow of a multi-scale approach for the detection and analysis slope instabilities in periglacial rock walls. This project includes investigations at the levels 1-3. Marked in light grey are the approaches and methods that are recommended as subsequent steps in the direction of hazard assessment.

5.2.1 Regional-scale GIS-based analysis

The regional-scale statistical factor analysis performed within this study is based on the compiled rock avalanche inventory over the entire Swiss Alps (Figure 5.1, level 1; Paper II). Such approaches were already performed by Abdallah et al. (2004) in Lebanon, and Ruff and Rohn (2008) in the Eastern European Alps, for example. However, the investigation area of around 12'000 km^2 in this project is 5 to 10 times larger than in the two projects mentioned, and only slope failures from bedrock are included and no soil slides. Furthermore, this study considers the cryospheric factors glacierisation and permafrost, which have rarely been integrated into regional-scale analyses before.

GIS-based factor analyses can be applied at different scales (Figure 5.1). The applicability strongly depends on the availability and quality of the basis data. One problem is the unsuitable resolution or inaccuracies of the basis data as already stated by Ruff and Rohn (2008). In our study this means, for example, the limited level of detail of the geological map, the constrictive resolution of the DHM25, uncertainties of coordinates and timing of rock avalanche events, or simply a total lack of information concerning what could lead to biased results. Another challenge is the implementation of point information. Point data sets that are spatially restricted can be implemented within a GIS, but the integration of such data in spatial analyses is delicate. Therefore, geotechnical and geomechanical data is difficult to use for a wide area, because these parameters cannot be extrapolated on a regional scale (e.g. Aleotti and Chowdhury, 1999), although they were found to be very important for slope stability (Paper V).

GIS technology provides a valuable tool, which is more efficient and faster than field observations for the extraction of the terrain parameters, e.g., from DTMs and optical data, and the investigation of the relations between mass movement occurrence and these parameters. A major advantage is that the spatial comparison of different factors can be performed over large areas and many different data sets can be included. Performed over smaller areas, such GIS-based spatial and statistical analyses provide also a valuable tool for more detailed assessments of individual rock walls, as performed for the Monte Rosa east face (Paper III).

5.2.2 Local-scale image and DTM analysis

The local-scale study of the Monte Rosa east face is based mainly on remote sensing data and complemented with observations from *in situ* field investigations. The different data sets are analysed using GIS-based multi-temporal spatial comparisons and with detailed topographic and volumetric change analysis. The implementation of multi-temporal orthophotos and DTMs, supplemented with terrestrial photographs, allow detailed time-lapse analyses of different factors in the face to be performed.

Topographic data provides the basis for all slope stability analyses. Currently available DTMs vary strongly in resolution. Area-wide DTMs derived from topographic maps are available with 25 m resolution. In Switzerland, LiDAR derived DTMs with resolutions of 1-5 m are available area-wide below 2000 m a.s.l. Above this altitude, such LiDAR data is still only available for few regions. This study made use of recent advances in technology and software for the acquisition and production of topographic data by airborne laser scanning and digital photogrammetry. Both technologies proved to be highly promising for the generation of detailed topographic data in steep and complex terrain. Time lapse high-resolution point clouds and DTMs enable a comparison of sequential data set in order to assess topographic and volumetric changes in detail and provide a powerful method for factor extraction and detailed localisation and dimensioning of detachment zones in re-analyses of slope failures. Wiss (2009) has shown, based on the example of the Monte Rosa east face, that automatic feature extraction from high-resolution DTMs is possible. A classification of six morphometric classes and the automatic extraction of features such as the steep fronts, crevasses and geological planes was performed on a LiDAR DTM with 1-10 m resolution. Similar analyses are also performed by Oppikofer et al. (2008) and Jaboyedoff et al. (2004c), for example, for the extraction of geological planes and failure mode analyses. Such feature extraction methods could provide useful data for susceptibility analyses in the future. These examples reveal the huge potential of high-resolution topographic data for detailed slope stability analyses. However, a high spatial resolution (i.e. 1-10 m resolution) is definitely required for such tasks. Analyses within this study have shown that such feature extraction is strongly limited from the DHM25 with 25 m resolution.

Process understanding of periglacial slope instabilities cannot only be gained from DTM analyses alone; additional observations in the field and the investigation of orthophotos and terrestrial images are essential. Imagery analyses (terrestrial, aerial and satellite images) are crucial for the classification of surface characteristics by the means of remote sensing. Such analyses can be performed at different scales (Figure 5.1), e.g. the factor glacierisation was detected from satellite images over the entire Swiss Alps (Paul, 2004) whereas current study extracted the same factor on a more detailed level from orthophotos for a single face (Paper III). Multi-temporal image analyses revealed to be crucial for the process understanding of topographic and glaciation changes in a periglacial face. Large slope failures show often (but not always) preceding

small volume rockfall and slope failures are often strongly spatially correlated with the sequence of the changes in topography and surface features. Such indications can only be revealed by repeat data sets at high temporal resolution.

5.2.3 Local-scale kinematic and physically based modelling

The combined kinematic and physically-based modelling approach used for the re-analysis of the Tschierva rock avalanche at the Piz Morteratsch presents the third investigation scale with the highest level of detail.

The kinematic analysis and the numerical slope stability modelling are based on detailed information over a relatively small area. Here, point data can be used, but the spatial extrapolation at the surface and even more the extrapolation into depth introduces large uncertainties. The resolution of in situ data is in the range of decimetres to decametres, the area coverage is about 10^2 to 10^3 m^2. Such detailed information is required for numerical slope stability analyses, for example finite element modelling approaches. The main requirement for this in situ approach is that access to the mountain face is possible. Barla and Barla (2001) approached the problem of inaccessibility with the help of an alpine guide attached to an helicopter by means of a 30 m long cable, the topographic coordinates of a number of points of the rock mass could be measured. At our site, access was partially possible, however restricted due to rockfall. This shows that the major problem for such detailed modelling tasks is already the acquisition of required input data. Nevertheless, our study has shown that field measurements are indispensable for the assessment of geomechanical and geotechnical characteristics.

2-D modelling tasks can be performed for restricted areas, such as one single rock wall, as they need detailed base data sets and are elaborative. They have been used for sensitivity analyses of individual factors rather than for the prediction of a slope failure. For more predictive tasks, much more information should be available from permanent monitoring systems such as data on subsurface structures from boreholes, piezometric measurements and displacement measurements (e.g. Stead et al., 2004). However, the distinct element modelling performed within this study contributes to improved process understanding.

Kinematic analyses provide a powerful tool to assess the potential of a slope failure based on the structure geological setting (Paper V), as also shown by Oppikofer et al. (2009). However, kinematic analyses based on manually measured discontinuity sets is restricted to small areas and often not applicable in steep periglacial terrain due to difficult access. These *in situ* field investigations could be replaced in parts by the extraction of geological structures from high-resolution DTMs acquired with LiDAR technologies (e.g., Derron et al., 2005; Jaboyedoff et al., 2007).

5.3 The effect of changes in predisposing factors

Predisposing factors may vary over time and the changing rate of the individual predisposing factors varies strongly. This study has shown that not only specific factors but primarily changes in one or more factors provoke slope instabilities. In the following, the temporal constraints of changes in predisposing factors as well as the influence on the stress field is discussed.

5.3.1 Topographic changes

Topography exerts a dominant control on the stress field in a flank and hence strongly influences the slope stability. Most topographic changes occur slowly over thousands of years. However, topographic changes can be strongly accelerated by glacier retreat, and slope failures also contribute to rapid topographic changes, possibly provoking further slope instabilities (Paper IV). Currently, the glacier retreat and downwasting is a main contribution to topographic changes. An oversteepening of a flank by fast erosion or mass loss as well as the removal of supporting ice contributes to increased shear stress in a flank. Failures induced by such topographic changes can occur on time scales of 10^0 to 10^4 years, depending on the glaciation history, topography, and geology (Cruden and Hu, 1993; Papers III, IV, V). The reaction of a flank to fast topographic changes is strongly dependent on the geological setting of the flank. Slow progressive failure of the bedrock induced by glacier retreat can lead to a delayed slope failure such as observed at the Tschierva rock avalanche (Paper V) or the Randa rock avalanche (Eberhardt et al., 2004), near-immediate (i.e. within few years) rock avalanche events were observed for example at the Monte Rosa east face (Papers II, III, IV). Given Cruden and Hu's (1993) proposed exhaustion model of temporal distribution of rock slope failures which suggests that the number of failures exponentially decreases following deglaciation, current rapid glacier downwasting probably promotes many rock slope failures at rather short time scales in the order of decades.

5.3.2 Geological changes

The geological setting varies marginally over long time periods. The lithology can be considered to be invariant over time periods of thousands of years. However, the geomechanical and geotechnical characteristics of rock mass may change over time by weathering processes and stress induced alteration (e.g. Augustinus, 1995a). The numerical slope stability modelling of the Tschierva rock avalanche showed that discontinuities can progressively develop over hundreds of years (Paper V). The geological setting contributes, depending on geotechnical characteristics of corresponding lithology, to low strength. Weathering processes, which are intense in periglacial areas due to enormous high temperature gradients, as well as progressive failure processes, contribute to reduced material strength. The two factors that might rapidly change the geotechnical and geomechanical properties of bedrock are changes in groundwater and ice-filled fractures.

5.3.3 Thermal and hydraulic changes

Laboratory experiments, theoretical considerations, observations and investigations of past periglacial rock slope failures indicate that permafrost degradation is an important transient stability factor for steep mountain rock walls, and zones in warm permafrost are especially sensitive (e.g., Davies et al., 2001; Gruber and Haeberli, 2007). A warming of an ice-filled fracture changes the geotechnical characteristic of this fracture. Laboratory experiments have shown that the shear strength of ice-bonded fractures decreases with warming temperature and is lowest at temperatures between -1.5 and 0°C (Davies et al., 2001). Thus, warming permafrost could introduce changes in geotechnical properties of ice-filled clefts and thereby reduce material strength. In addition, a warming and thawing of ice within bedrock increases the amount of liquid water content. Depending on the pattern of geological structures and the occurrence of still frozen, impermeable fractures, this liquid water cannot emerge. Higher water pressures within a

flank causes decreased shear strength as the effective normal stress is diminished by the water pressure. The regional-scale statistical analysis (Paper II) has shown a cumulation of detachment zones at the lower boundary of permafrost occurrence, where warm permafrost is assumed. The ongoing atmospheric warming will increase the area subject to warm permafrost temperatures. The progressive thermal changes into larger depths in the permafrost zones in particular can influence the size of the future slope failures and lead to increased rock avalanche volumes. However, 3-dimensional patterns of permafrost in the high-mountain rock walls and their changes are still being researched (e.g. Noetzli and Gruber, 2009), and the influence of advection by running water that can rapidly lead to the development of deep thaw corridors along fracture zones in permafrost is still poorly understood.

The exposure of the formerly glacier covered bedrock to atmospheric temperature can influence both the thermal and the hydraulic regime (e.g. Wegmann et al., 1998). Such changes were found to be of primary importance in areas where hanging glaciers and steep ice disappeared. The water pressure within a rock wall can vary quite rapidly, depending on water supply and permeability characteristics. Especially during a so-called 'lock-off situation', when the bedrock is frozen at the surface and therefore water outflow is blocked, very high water pressures might evolve and contribute to low shear strength. Such situations occur predominately in the autumn season and could have played a significant role in the Tschierva rock avalanche.

5.4 Implications for susceptibility analyses and hazard assessment

Hazard and risk assessment regarding mass movements from periglacial rock slopes is a complex topic and cannot be performed over large areas at a sufficient level of detail. Therefore, the hazard assessment of periglacial slope instabilities requires a systematic and integrative approach that implements different scales and level of details. In this study, the GIS-based approach was used for statistical factor analysis of the individual detachment zone. However, GIS-based approaches are also a valuable tool for area-wide factor analyses and can be used for a first-order assessment of slope instability susceptibility.

The calculation of risk requires information on the frequency and magnitude of slope failure events, which can be highly speculative at large study areas. Furthermore, such relationships are particularly difficult to estimate for periglacial rock avalanche events as the event documentation is non-uniform and incomplete. Van Westen et al. (2005) propose for medium to large investigation areas to concentrate on susceptibility zones rather than on risk assumptions, as detailed hazard assessments cannot be performed over large areas. Therefore, a first separation of more susceptible areas has to be performed using a tool that can be applied over a large area, while implementing spatially available data. Simple GIS-based spatial factor analyses can be used for such first-order susceptibility analyses and contribute to the detection of hot spots, where critical factor combinations occur. However, such first-order susceptibility assessments are far from being the equivalent of hazard assessment, as they can only help to identify areas where more detailed investigations should be performed.

Based on the findings of the GIS-based statistical analysis and the results from the complementary local-scale approaches within this study, relevant and susceptible factor combinations for slope instabilities in periglacial rock walls can be found. For the identification and investigation of hazardous rock walls, a multi-scale approach is recommended as shown in Figure 5.1.

For prospective hazard assessment tasks we recommend a downscaling approach from area-wide first-order assessments for systematically detecting hazard potentials (i.e. GIS-based factor analysis), to second-order assessments based on high-resolution remote sensing techniques (LiDAR, orthophotos), to detailed ground-based or airborne local investigations in high-risk areas (i.e., the domain of surveying, geophysical investigations, and permanent installations such as permanently installed cameras or displacement measurements). Furthermore, in order to obtain detailed knowledge about the influencing processes at a specific site, permanent in situ measurements of displacements, water pressure, subsurface temperatures, etc., could be performed. Such permanent installations are still very rare on high-alpine faces and present a large field of future research (e.g. Hasler et al., 2008). This study has shown that time-lapse image analyses provide a suitable tool for the analysis of changes in a rock wall. Large slope failures in particular are often preceded by rockfall activity or other indicators, such as the development and widening of tension cracks, bulging of the flank at the slope foot, or changed water occurrence. Such indications of slope instabilities can be detected based on multi-temporal optical data or even better by a permanently installed automatic camera.

Based on the findings of this study, such a first-order assessment of a spatial analysis of critical factor combinations should include the following combination: slope gradients greater than 40°, elevation close to the estimated lower permafrost boundary and recent deglaciation in the vicinity. For the areas defined on the basis of such a factor combination, a more detailed approach could be performed following the workflow scheme in Figure 5.1. Such first-order susceptibility analyses could also be coupled with GIS-based modelling tools of other high-mountain hazards such as ice avalanche, glacial lake outburst, and debris flow models, to address the possible process chain reactions that might lead to far-reaching disasters (e.g. Huggel et al., 2004).

6 Conclusions and Perspectives

The overall aim of this thesis was the investigation of the characteristics of periglacial slope instabilities in order to better understand the occurrence of slope failures from steep rock walls in general, and to assess the influence of different predisposing factors in particular.

6.1 Main contributions

The development and distribution of slope instabilities in periglacial faces are governed by a range of different factors that extend from local to regional scale, and which influence processes in the subsurface, at the surface, and in the atmosphere. In this study we developed a multi-scale approach to investigate these predisposing factors and their importance for slope stability.

The main contribution of this thesis is the implementation and combination of various approaches at different levels of detail within one project. This allowed a comparison of diverse methods and iterative factor analysis to be performed at different scales.

A number of GIS-based factor studies exist for the analysis of slope failure detachment zones and susceptibility analyses. This study is one of the first GIS-based statistical factor analyses of recent rock avalanches performed in high-mountain terrain that includes the cryospheric factors glacierisation and permafrost (Paper II).

Within this study, one of the most detailed and precise topographic data sets was developed for a high-mountain face over a long time period. This unique time-lapse data set is based on the combination of LiDAR and digital photogrammetry and demonstrates the novel technical possibilities as they have never been applied before in such difficult terrain (Paper IV). This high-resolution topographic analysis of the Monte Rosa east face is complemented with optical remote sensing data such as orthophotos and terrestrial photographs (Paper III) and presents one of the most detailed observation series of a high-mountain flank worldwide.

Only a few studies have used kinematic analysis and physically-based slope stability modelling for the re-analysis of rock slope failures on periglacial terrain (e.g. Barla and Barla, 2001). This study shows that an appropriate method combination including classic geological field investigation techniques, terrestrial and aerial image analyses and permafrost modelling allows detailed numerical slope stability modelling to be performed, possible failure mechanisms to be evaluated and process understanding to be improved, even with restricted base data (Paper V).

Based on the factor analyses at three levels of detail, we were able to evaluate and define the main environmental factors contributing to slope instabilities in periglacial rock walls.

6.2 Major results

The results are described in detail in Chapter 4 and in Publications I-V. The most important findings and conclusions of this thesis are summarised in this section and organised according to the research questions stated in the first chapter.

1. *What are the primary factors that contribute to slope instabilities?*

- The influencing factors depend on the volume of a slope instability. Large slope failures evolve over longer time periods and are therefore primarily affected by long-term changes, whereas small detachments often react to sporadic extreme events such as the extraordinary warm summer of 2003.

- No specific single primary factor was found based on our analyses, but a number of factor combinations that contribute significantly to slope stability emerged. However, the two factors slope angle and a pronounced discontinuity system are included in such factor combinations at all failure magnitudes.

- The change in a factor and the time scale of change are more important than the individual factors. Fast changes in a factor do not allow adequate stress redistribution within a flank and therefore, the critical shear strength may be exceeded. Glaciers, mainly changing the topography, and permafrost, mainly changing the groundwater regime and geotechnical characteristics of discontinuities, are currently the factors with the fastest changes.

- Slope gradient has a dominant influence on slope stability. The analyses have shown that gradients above 40° are prone to slope failures with a culmination of susceptibility between 45 and 60°.

- The lithological setting influences the magnitude rather than the frequency of slope failures. However, lithological transition zones and the presence of a fault zone enhance the probability of a slope failure.

- Groundwater is found to be a very important factor – both for causing of instabilities due to cyclic loading and possible freeze/thaw processes and for the eventual triggering. However, hydrologic data is very difficult to acquire and even more difficult to extrapolate spatially and at depth.

2. *What are the appropriate techniques for data acquisition and measurement?*

- This study makes clear that data acquisition in steep periglacial terrain is difficult and complex. A combination of remote sensing and in situ approaches was found to be most appropriate.

- Appropriate techniques for data acquisition and measurement depend strongly on the investigation scale. *In situ* approaches are based primarily on punctual measurements with a high level of detail, whereas remote-sensing-based approaches allow comprehensive data acquisition over larger areas.

- Remote sensing based approaches, including topographic as well as optical data, are very useful for dealing with the problem of difficult access and for providing spatial data. Strong improvements in high-resolution topographic data acquisition were achieved by the combination of digital photogrammetry and airborne LiDAR. In addition, time lapse DTMs provide a powerful basis for the assessment of topographic changes.

- Imagery analyses are important at all scales for the visual or automatic detection of surface characteristics. Repeat data sets are enormously important as they enable the analyses of temporal as well as spatial changes. Terrestrial photographs are useful for qualitative change analysis of surface characteristics, as they are, for the most part, available at higher frequency than any other base data.

- In situ field investigations are still very important for geotechnical and geomechanical investigations, as no detailed information about rock mass and discontinuity characteristics can be obtained from remote sensing data.

3. *What are feasible approaches for the assessment of slope instabilities?*

- The feasibility of an approach always depends on the available base data.

- All applied approaches are feasible. GIS-based factor analyses allow investigations to be conducted over large areas, but only factors with spatial information can be included. Numerical slope stability modelling, on the other hand, also includes point information and contributes to improved process understanding for a specific slope failure.

- Analyses of time-lapse high-resolution DTMs allow detailed topographic analyses to be made, and proved to be essential for slope stability analyses.

- Kinematic analyses are a powerful tool for the assessment of the failure potential, as the structural geology is one of the most important factors for slope instabilities.

- Numerical slope stability modelling is useful for re-analyses of a slope failure and sensitivity analyses of factors to improve process understanding. However, its use is often limited in high-mountain terrain because of a lack of information.

4. *What is the scale-dependence of the different factors and analysis methods?*

- The factors groundwater and structural geology could be investigated only on a local scale, and spatial extrapolation is difficult if not impossible.

- It is possible to investigate the factors geology, topography and glaciology on a large scale, however, their settings on a small scale, such as geological transition zones, are also important for slope stability analyses.

- The smaller the volume of a slope failure, the more limited the influencing area and factors, and hence, the higher the resolution of the base data sets should be.

- Numerical slope stability modelling is restricted to small areas, no area-wide investigations can be performed.
- GIS-based statistical analyses can be performed on a local and a regional scale, depending on the basis data. However, these analyses enable factor analyses to be made, at exclusion of process modelling.
- Kinematic stability analysis can partially bridge the gap between detailed small area process analyses and simple area-wide factor analysis.

In conclusion, this study has shown that advanced and combined technology applied at different scales can effectively contribute to improved assessments of slope instabilities, which is particularly important in view of ongoing glacial and periglacial changes. This is one of the first studies that includes the factors permafrost and glacier in GIS-based statistical analysis as well as finite element stability modelling. A better understanding of predisposing factors has been gained at different levels of detail and these findings provide a fundamental basis for prospective slope instability susceptibility analyses on a regional scale.

6.3 Perspectives – Further requirements and challenges

This thesis is a first step into a multi-disciplinary field with important and promising perspectives. The multi-disciplinary synergies gain benefits for the high-mountain cryosphere, the engineering geology and the remote sensing community, as well as a basis for informed and anticipative decisions on current and future high-mountain slope stability problems. Based on the results mentioned above, it can be concluded that future progress in periglacial rock slope stability research must focus on iterative multi-scale approaches including improved data acquisition and process-oriented modelling tasks, but also on the development of simple first-order assessment tools for area-wide susceptibility analyses.

Future research on slope instabilities in periglacial rock walls should focus on the following tasks:

- The recording of periglacial rockfall and rock avalanche events should be continued and standardised, to establish a more complete inventory and to enlarge the time series.
- GIS-based spatial factor analyses should be pursued in order to provide a simple first-order tool for the assessment of zones susceptible to slope instabilities. With such a tool, 'hot-spot' areas with increased susceptibility can be identified, where subsequent analyses can be performed at a more detailed level, as suggested in the workflow scheme in Figure 5.1.
- Our investigations have shown that it is very important to examine not only the current state of a flank but also to assess the changes in all contributing factors over time, both long-term and short-term changes. Therefore, comprehensive acquisition of time-lapse aerial images and LiDAR data assist enhanced analyses.
- It is important to conduct more extensive laboratory experiments (such as Davies et al., 2001) and field installations (such as Hasler et al., 2008) to improve process understand-

ing of permafrost in bedrock and the influence of changes in ice temperature and water content on the geotechnical behaviour of ice-filled fractures.

- A promising method bridging the gap between detailed local-scale approaches and regional-scale approaches is the automatic extraction of structure geological planes from high-resolution DTMs and subsequent kinematic analyses. Such analyses would allow better failure susceptibility analyses to be made over large areas and should be further improved.

- The collaboration and exchange between the different scientific fields, such as engineering geology, glaciology, remote sensing and GIS research, should be improved and expanded. Constructive communication and coorperation within the scientific disciplines involved is fundamental to deriving maximum benefit from the multi-disciplinary projects.

References

Abdallah, C., Chorowicz, J., Bou Kheir, R., and Khawlie, M. (2005). Detecting major terrain parameters relating to mass movements' occurrence using GIS, remote sensing and statistical correlations, case study Lebanon. *Remote Sensing of Environment*, 99: 448-461.

Abele, G. (1974). Bergstürze in den Alpen; ihre Verbreitung, Morphologie und Folgeerscheinungen. *Wissenschaftliche Alpenvereinshefte*, Heft 25: 230 p.

Abele, G. (1994a). Felsgleitungen im Hochgebirge und ihr Gefahrenpotential. *Geographische Rundschau*, 46(7+8): 414-420.

Abele, G. (1994b). Large rockslides: Their causes and movement on internal sliding planes. *Mountain research and development*, 14(4): 315-320.

Aksoy, H., and Ercanoglu, M. (2007). Fuzzified kinematic analysis of discontinuity-controlled rock slope instabilities. *Engineering Geology*, 89: 206-219.

Alba, M., Longoni, L. Papini, M. Roncoroni, F., and Scaioni, M. (2005). Feasibility and problems of TLS in modelling rock faces for hazard mapping. ISPRS WG III/3, III/4, V/3 Workshop "Laser scanning 2005", Eschede, the Netherlands, September 12-14, 2005.

Alean, J. (1984). Ice avalanches and a landslide on Grosser Aletschgletscher. *Zeitschrift für Gletscherkunde und Glazialgeologie*, 20: 9-25.

Alean, J. (1985). Ice avalanches: some empirical information about their formation and reach. *Journal of* Glaciology, 31(109): 324-333.

Aleotti, P., and Chowdhury, R. (1999). Landslide hazard assessment: summary review and new perspectives. *Bulletin of Engineering Geology and the Environment*, 58: 21–44.

Antonello, G., Casagli, N., Farina, P., Leva, D., Nico, G., Sieber, A. J., and Tarchi, D. (2004). Ground-based SAR interferometry for monitoring mass movements. *Landslides*, 1(1): 21-28.

Augustinus, P. (1995a). Rock mass strength and the stability of some glacial valley slopes. *Zeitschrift für Geomorphologie N.F.*, 39(1): 55-68.

Augustinus, P. C. (1995b). Glacial valley cross-profile development: the influence of in situ rock stress and rock mass strength, with examples from the Southern Alps, New Zealand. *Geomorphology*, 14(2): 87-97.

Aydin, A., and Basu, A. (2005). The Schmidt hammer in rock material characterization. *Engineering Geology*, 81: 1-14.

Baillifard, F., Jaboyedoff, M., and Sartori, M. (2003). Rockfall hazard mapping along a mountainous road in Switzerland using a GIS-base parmeter rating approach. *Natural Hazards and Earth System Science,* 3: 431-438.

Baldi, P., Bonvalot, S., Briole, P., Coltelli, M., Gwinner, K., Marsella, M., Puglisi, G., and Remy, D. (2002). Validation and comparison of different techniques for the derivation of digital elevation models and volcanic monitoring (Vulcano Island, Italy). *International Journal of Remote Sensing*, 23(22): 4783-4800.

Baldi, P., Coltelli, M., Fabris, M., Marsella, M., and Tommasi, P. (2008). High precision photogrammetry for monitoring the evolution of the NW flank of Stromboli volcano during and after the 2002-2003 eruption. *Bulletin of Volcanology*, 70: 703-715.

Ballantyne, C.K. (2002). Paraglacial geomorphology. *Quarternary Science Reviews*, 21: 1935-2017.

Baltsavias, E.P. (1999). A comparison between photogrammetry and laser scanning. *ISPRS J. Photogramm. Remote Sensing*, 54: 83-94.

Baltsavias, E.P., Favey, E., Bauder, A., Bösch, H., and Pateraki, M. (2001). Digital surface modelling by airborne laser scanning and digital photogrammetry for glacier monitoring. *The Photogrammetric Record*, 17(98): 243–273.

Barla, G., and Barla, M. (2001). Investigation and modelling of the Brenva Glacier rock avalanche on the Mount Blanc Range. ISRM Regional Symposium Eurock 2001, Balkema, Rotterdam, Espoo, Finlandia, 3-7 giugno, 2001, Espoo, Finlandia, Balkema.

Barla, G., Dutto, F., and Mortara, G. (2000). Brenva Glacier rock avalanche of 18 January 1997 on the Mont Blanc range, northwest Italy. *Landslide news*, 13: 2-5.

Barsch, D., and Caine, N. (1984). The nature of mountain geomorphology. *Mountain research and development*, 4(4): 287-298.

Bhasin, R., Kaynia, A., Blikra, L.H., Braathen, A., and Anda, E. (2004). Insights to the deformation mechanisms of a jointed rock slope subjected to dynamic loading. *International Journal of Rock Mechanics and Mining Sciences*, 41: 587-592.

Bieniawski, Z.T. (1989). Engineering rock mass classifications. Johns Wiley & Sons, New York.

Bishop, M.P., Kargel, J.S., Kieffer, H.H., MacKinnon, D.J., Raup, B.H., and Shroder, J.F., Jr. (2000). Remote-sensing science and technology for studying glacier processes in high Asia. *Annals of Glaciology*, 31: 164-170

Bishop, M. P., Shroder, J. F., and Colby, J. D. (2003). Remote sensing and geomorphometry for studying relief production in high mountains. *Geomorphology*, 55(1-4): 345-361.

Bonzanigo, L., Eberhardt, E., and Loew, S. (2001). Hydromechanical factors controlling the creeping Campo Vallemaggia landslide. Proceedings of the International Conference of Landslides - Causes, Impacts and Countermeasures, Davos.

Bottino, G., Chiarle, M., Joly, A., and Mortara, G. (2002). Modelling rock avalanches and their relation to permafrost degradation in glacial environments. *Permafrost and Periglacial Processes*, 13: 283–288.

Broccolato, M., Martelli D.C.G., and Tamburini, A. (2006). Il rilievo geomeccanico di pareti rocciose instabili difficilmente accessibili mediante impiego di laser scanner terrestre. Applicazione al caso di Ozein. *Geoingegneria Ambientale e Mineraria (GEAM)*, Anno XLIII(4): 39-46.

Brown, R.J.E., and Péwé, T.L., (1973). Distribution of permafrost in North America and its relationship to the environment, a review 1963 - 1973. Proceedings of the 2nd International Conference on Permafrost, F.J. Sanger and P.J. Hyde (Editors). National Academy of Sciences, Washington D.C., Yakutsk, USSR, 71-100.

Brunsden, D. (1985). Landslide types, mechanisms, recognition, identification. Proceedings of the Landslides in the South Wales Coalfield Symposium. The Poly. of Wales.

Brunsden, D. (1993). Mass movement; the research frontier and beyond: a geomorphological approach. *Geomorphology*, 7(1-3): 85-128.

Buchroithner M. (2002). Creating the virtual Eiger North Face. *ISPRS Journal of Photogrammetry and Remote Sensing,* 57(1-2): 114-125.

Buck, P.D. (1921). Stürzende, gleitende und fliessende Gesteinsbewegungen der Schweiz. Beigabe zum Jahresbericht der Stiftsschule Maria, Einsiedeln im Studienjahr 1920/21. Verlagsanstalt Benziger & Co., Einsiedeln, pp. 59.

Cai, M., Kaiser, P.K., Uno, H., Tasaka, Y., and Minami, M. (2004). Estimation of rock mass deformation modulus and strength of jointed hard rock masses using the GSI system. *International Journal of Rock Mechanics and Mining Sciences*, 41(1): 3-19.

Carrara, A., and Pike, R. J. (2008). GIS technology and models for assessing landslide hazard and risk. *Geomorphology*, 94: 257-260.

Carrara, A., Cardinali, M., Guzzetti, F., and Reichenbach, P. (1995). GIS technology in mapping landslide hazard. In: Carrara, A. and Guzzetti, F.: Geographical information systems in assessing natural hazards, Kluwer, 135–176.

Chen, R.-F., Chang, K.-J., Angeliera, J., Chan, Y.-C., Deffontaines, B., Lee, C.-T., and Lin, M.-L. (2006). Topographical changes revealed by high-resolution airborne LiDAR data: The 1999 Tsaoling landslide induced by the Chi–Chi earthquake. *Engineering Geology*, 88: 160-172.

Chinn, T.J., McSaveney, M.J., and McSaveney E.R. (1992). The Mount Cook rock avalanche of 14 December, 1991. *DSIR Geology and Geophysics*.

Clague, J.J. (2008). Effects of Recent Climate Change on High Mountains of Western North America. 9th International Confernce on Permafrost, Fairbanks, US, 2008, 269-273.

Cola, G. (2005). The large landslide of the south-east face of Thurwieser peak (Thurwieser-Spitze) 3658 m (Upper Valtellina, Italy). *Terra Glacialis,* 8: 38-45.

Corripio, J. (2004). Snow surface albedo estimation using terrestrial photography. *International Journal of Remote Sensing*, 25(24): 5705-5729.

Cossart, E., Braucher, R., Fort, M., Bourlès, D. L., and Carcaillet, J. (2008). Slope instability in relation to glacial debuttressing in alpine areas (Upper Durance catchment, southeastern France): Evidence from field data and 10Be cosmic ray exposure ages. *Geomorphology*, 95: 3-26.

Cox S.C., and Allen S.K. (2009). Vampire rock avalanches of January 2008 and 2003, Southern Alps, New Zealand. *Landslides*, 6(2): 161-166.

Crosta, G. B., Chen, H., and Lee, C. F. (2004). Replay of the 1987 Val Pola Landslide, Italian Alps. *Geomorphology*, 60: 127-146.

Cruden, D. M., and Hu, X. Q. (1993). Exhaustion and steady state models for predicting landslide hazards in the Canadian Rocky Mountains. *Geomorphology*, 8: 279-285.

Cruden, D. M., and Varnes, D. J. (1996). Landslide types and processes. In: Turner, A.K., Schuster, R.L. (Eds.), Landslides, Investigation and Mitigation. Transportation Research Board, Special Report 247, Washington D.C., USA, 36–75.

Davies, M. C. R., Hamza, O., and Harris, C. (2001). The effect of rise in mean annual temperature on the stability of rock slopes containing ice-filled discontinuities. *Permafrost and Periglacial Processes*, 12(1): 137–144.

Deline, P. (2001). Recent Brenva rock avalanches (Valley of Aosta): New chapter in an old story? *Suppl. Geogr. Fis. Dinam. Quat.*, V: 55-63.

Derron, M.-H., Jaboyedoff, M., and Blikra, L.H. (2005). Preliminary assessment of rockslide and rockfall hazards using a DEM (Oppstadhornet, Norway). *Natural Hazards and Earth System Science,* (5): 285-292.

Dewitte, O., Jasselette, J.-C., Cornet, Y., Van Den Eeckhaut, M., Collignon, A., Poesen, J., and Demoulin, A. (2008). Tracking landslide displacements by multi-temporal DTMs: A combined aerial stereophotogrammetric and LIDAR approach in western Belgium. *Engineering Geology*, 99(1-2): 11-22.

Dickau, R., and Glade, T. (2002). Gefahren und Risiken durch Massenbewegungen. *Geographische Rundschau*, 1: 38-45.

Dramis, F., Govi, M., Gugliemin, M., and Mortara, G. (1995). Mountain permafrost and slope instability in the Italian Alps: the Val Pola Landslide. *Permafrost and Periglacial Processes*, 6: 73-82.

Eberhardt, E. (2006). From cause to effect: using numerical modelling to understand rock slope instability mechanisms. Landslides from Massive Rock Slope Failure. S. G. Evans, G. Scarascia Mugnozza, A. Storm and R. L. Hermanns. Dodrecht, Nato Sciences Series, Springer. 49**:** 85-101.

Eberhardt, E., Stead, D., and Coggan, J.S. (2004). Numerical analysis of initiation and progressive failure in natural rock slopes - the 1991 Randa rockslide. *International Journal of Rock Mechanics and Mining Sciences*, 41: 69-87.

Einstein, H.H., Veneziano, D., Baecher, G.B.m and O'Reilly, K.J., (1983). The effect of discontinuity persistence on rock slope stability. *International Journal of Rock Mechanics and Mining Sciences, Geomech. Abst.*, 20(5): 227-236.

Eisbacher, G. H., and Clague, J. J. (1984). Destructive mass movements in high mountains: hazard and management. Geological Survey of Canada, Paper, 84-16.

Erismann T. H., and Abele, G. (2001). Dynamics of rockslides and rockfalls. Berlin, Springer.

Etzelmüller, B. and Hagen, J.O. (2005). Glacier - permafrost interaction in Arctic and alpine mountain environments with examples from southern Norway and Svalbard. Cryospheric Systems: Glaciers and Permafrost. c. M. Harris, J.B., Geological Society, London, Special Publications. 242**:** 11-27.

Evans, S.G., and Clague, J.J. (1988). Catastrophic rock avalanches in glacial environment. Proceedings of the 5th Symposium on Landslides, 10-15 July, Lausanne.

Evans, S.G., and Clague, J.J. (1994). Recent climatic change and catastrophic geomorphic processes in mountain environments. *Geomorphology*, 10: 107-128.

Evans, S.G., Scarascia Mugnozza, G., Strom, A.L., and Hermanns, R.L. (2002). Landslides from Massive Rock Slope Failure and Associated Phenomena. In: Landslides from Massive Rock Slope Failure. S.G. Evans, G. Scarascia Mugnozza, A.L. Strom, R.L. Hermanns, A. Ischuk and S. Vinnichenko, IV. Earth and Environmental Sciences. 49.

Fischer, L. (2004). Monte Rosa Ostwand - Jetziger Zustand der Wand und ihre Geschichte. Department of Earth Sciences, ETH Zurich. Diploma thesis.

Fischer, L. (2006). Monte Rosa Ostwand - Geologie, Vergletscherung, Permafrost und Sturzereignisse in einer hochalpinen Steilwand. *Bulletin für angewandte Geologie*, 11(1): 65-78.

Fischer, L., Kääb, A., Huggel, C. and Noetzli, J. (2006). Geology, glacier retreat and permafrost degradation as controlling factors of slope instabilities in a high-mountain rock wall: Monte Rosa east face. *Natural Hazards and Earth System Science*, 6: 761-772.

Fischer, L. and Huggel, C. (2008). Methodical Design for Stability Assessments of Permafrost Affected High-Mountain Rock Walls. 9th International Conference on Permafrost, Fairbanks, US, 2008.

FOEN (2006). Hinweiskarte Permafrost Schweiz, Federal Office for the Environment, Bern.

Frauenfelder, R. (2005). Regional-scale modelling of the occurrence and dynamics of rockglaciers and the distribution of paleopermafrost. PhD Thesis, University of Zurich, Zurich.

Frauenfelder, R., Haeberli, W., Hoelzle, M., Maisch, M. (2001). Using relict rockglaciers in GIS-based modelling to reconstruct younger dryas permafrost distribution patterns in the Err-Julier area, Swiss Alps. *Norwegian Journal of Geography,* 55 (4): 195-202.

French, H. M. (2004). Periglacial Geomorphology. In Geomorphology: Critical Concepts in Geography, D.J.A. Evans (ed.), London: Routledge, Vol 5.

Geertsema, M., Clague, J.J, Schwab, J.W., and Evans, S.G. (2006). An overview of recent large catastrophic landslides in northern British Columbia, Canada. *Engineering Geology*, 83: 120-143.

Geist, T., Lutz, E., and Stötter, J. (2003). Airborne laser scanning technology and its potential for applications in glaciology. *International Archives of Photogrammetry, Remote Sensing and Spatial Information Science*, Volume XXXIV, Part 3/W13, 101-106.

Gerber, E., and Scheidegger, A.E., (1969). Stress-induced weathering of rock masses. *Eclogae Geologicae Helvetiae*, 62: 401-416.

Giani, G. P. (1992). Rock Slope Stability Analysis. Rotterdam, Netherlands, A.A. Balkema/Rotterdam/Brookfield.

Giani, G. P., Silvano, S. and Zanon, G. (2001). Avalanche of 18 january 1997 on Brenva glacier, Mont Blanc Group, Western Italian Alps: an unusual process of formation. *Annals of Glaciology*, 32: 333-338.

Giardino, M., Giordan, D. and Ambrogio, S. (2004). G.I.S. technologies for data collection, management and visualization of large slope instabilities: two applications in the Western Italian Alps. *Natural Hazards and Earth System Science*(4): 197-211.

Gischig, V., Loew, S., Kos, A., Moore, J.R., Raetzo, H., and Lemy, F. (submitted). Identification of active release planes using ground-based differential InSAR at the Randa rock slope instability, Switzerland. *Natural Hazards and Earth System Science.*

Glenn, N.F., Streutker, D.R., Chadwick, D. J., Thackray, G.D., and Dorsch, S.J. (2006). Analysis of LiDAR-derived topographic information for characterizing and differentiating landslide morphology and activity. *Geomorphology*, 73: 131-148.

Goodman, R. E. (1989). Introduction to rock mechanics. John Wiley and Sons, New York.

Govi, M., Gulla, G., Nicoletti, P. G. (2002). Val Pola rock avalanche of July 28, 1987, in Valtellina (Central Italian Alps). *Geological Society of America, Reviews in Engineering Geology*, XV: 71-89.

Gruber, S. and Haeberli, W. (2007). Permafrost in steep bedrock slopes and its temperature-related destabilization following climate change. *Journal of Geophysical Research*, 112: F02S18.

Gruber, S., Peter, M., Hoelzle, M., Woodhatch, I., Haeberli, W. (2003). Surface temperatures in steep Alpine rock faces—a strategy for regional-scale measurement and modelling. Proceedings of the Eighth International Conference on Permafrost, 325–330.

Gruber, S., Hoelzle, M., and Haeberli, W. (2004a). Rock-wall temperatures in the Alps: Modelling their topographic distribution and regional differences. *Permafrost and Periglacial Processes*, 15(3): 299-307.

Gruber, S., Hoelzle, M., Haeberli, W. (2004b). Permafrost thaw and destabilization of Alpine rock walls in the hot summer of 2003. *Geophysical Research Letters*, 31((L13504)): doi:10.1029/2004GL0250051.

Gruen, A., Kocaman, S., and Wolff, K. (2007). High accuracy 3D processing of stereo satellite images in mountainous areas. Proceedings of the Dreilaendertagung 2007, Muttenz-Basel, Switzerland, 19-21 June.

Gruner, U. (2004). Klima und Sturzereignisse in Vergangenheit und Zukunft. *Bull. angew. Geol.*, Vol. 9/2: 23-37.

Guglielmi, Y., Cappa, F., Rutqvist, J., Tsang, C. F., and Thoraval, A. (2008). Mesoscale characterization of coupled hydromechanical behavior of a fractured-porous slope in response to free water-surface movement. *International Journal of Rock Mechanics and Mining Sciences*, 45(6): 862-878.

Günther, A. (2003). SLOPEMAP: programs for automated mapping of geometrical and kinematical properties of hard rock hill slopes. *Computers & Geosciences*, Volume 29(7): 865-875.

Günther, A., Carstensen, A., and Pohl, W. (2004). Automated sliding susceptibility mapping of rock slopes. *Natural Hazards and Earth System Sciences*, 4: 95-102.

Günther, A., Konietzky, H., and Wienhöfer, J. (2006). Incorporating GIS and numerical simulation for rock slope stability. *Geophysical Research Abstracts*, Vol. 8.

Guzzetti, F., Carrara, A., Cardinali, M., and Reichenbach, P. (1999). Landslide hazard evaluation: a review of current techniques and their application in a multi-scale study, Central Italy. *Geomorphology*, 31(1-4): 181-216.

Hack, R. (2002). An evaluation of slope stability classification. ISRM EUROCK 2002, Portugal, Madeira, Funchal, 25-28 November 2002.

Haeberli, W. (1975). Untersuchungen zur Verbreitung von Permafrost zwischen Flüelapass und Piz Grialetsch (Graubünden). Mitteilungen der Versuchsanstalt für Wasserbau, Hydrologie und Glaziologie der ETH Zürich, 17. ETH Zürich, Zürich, 221 pp.

Haeberli, W. (2005). Investigating glacier-permafrost relationships in high-mountain areas: historical background, selected examples and research needs. Geological Society London Special Publications 242(1): 29-37.

Haeberli, W., and Beniston, M. (1998). Climate change and its impacts on glaciers and permafrost in the Alps. *AMBIO*, 27(4): 258-265.

Haeberli, W., Hoelzle, M., Keller, F., Schmid, W., Vonder Mühll, D., and Wagner, S. (1983). Monitoring the long-term evolution of mountain permafrost in the Swiss Alps. Proceedings of the 6th International Conference on Permafrost, Beijing. Tapir Publisher: Trondheim; South China University of Technology, Vol 1: 214–219.

Haeberli, W., Wegmann, M., and Vonder Mühll, D. (1997). Slope stability problems related to glacier shrinkage and permafrost degradation in the Alps. *Eclogae Geologicae Helvetiae*, 90: 407–414.

Haeberli, W., Kääb, A., Hoelzle, M., Bösch, H., Funk, M., Vonder Mühll, D., and Keller, F. (1999). Eisschwund und Naturkatastrophen im Hochgebirge. Zürich, vdf Hochschulverlag an der ETH Zürich.

Haeberli, W., Kääb, A., Paul, F., Chiarle, M., Mortara, G., Mazza, A., Deline, P., and Richardson, S. (2002). A surge-type movement at Ghiacciaio del Belvedere and a developing slope instability in the east face of Monte Rosa, Macugnaga, Italian Alps. *Norwegian Journal of Geography*, 56: 104-111.

Haeberli, W., Huggel, C., Kääb, A., Polkvoj, A., Zotikov I., and Osokin., N. (2003). Permafrost conditions in the starting zone of the Kolka-Karmadon rock/ice slide of 20 December 2002 in North Ossetia (Russian Caucasus). Proceedings of the Eighth International Conference on Permafrost, Zurich, Switzerland, 1: 49–50.

Haeberli, W., Huggel, C., Kääb, A., Polkvoj, A., Zotikov I., and Osokin, N. (2004). The Kolka-Karmadon rock/ice slide of 20 September 2002: An extraordinary event of historical dimensions in North Ossetia, Russian Caucasus, *Journal of Glaciology*, 50(171): 533–546.

Hall, K., Thorn, C.E., Matsuoka, N., and Prick, A. (2002). Weathering in cold regions: some thoughts and perspectives. *Progress in Physical Geography*, 26(4): 577-603.

Hallet, B. (1983). The breakdown of rock due to freezing: A theoretical model. Proceedings of the VI. International Conference on Permafrost, Fairbanks Alaska 1, 433-438.

Hallet, B., Walder, J.S. and Stubbs, C.W. (1991). Weathering by segregation ice growth in Microcracks at sustained subzero temperatures: Verification from an experimental study using acoustic emissions. *Permafrost and Periglacial Processes*, 2: 283-300.

Hantz, D., Dussauge-Peisser, C., Jeannin, M. and Vengeon, J.M. (2003). Rock fall hazard assessment: from qualitative to quantitative failure probality. Fast Slope Movements, Naples.

Harris, C., and Haeberli, W. (2003). Warming permafrost in the mountains of Europe. *WMOBulletin* 52(3), 252–257.

Harris, C., Davies, M. C. R., and Etzelmüller, B. (2001a). The assessment of potential geotechnical hazards associated with mountain permafrost in a warming global climate. *Permafrost and Periglacial Processes*, 12(1): 145–156.

Harris, C., Haeberli, W., Vonder Mühll, D., and King, L. (2001b). Permafrost monitoring in the high mountains of Europe: the PACE project in its global context. *Permafrost and Periglacial Processes*, 12(1): 3–11.

Harris, C., Arenson, L.U., Christiansen, H.H., Etzelmüller, B., Frauenfelder, R., Gruber, S., Haeberli, W., Hauck, C., Hölzle, M., Humlum, O., Isaksen, K., Kääb, A., Kern-Lütschg, M.A., Lehning, M., Matsuoka, N., Murton, J.B., Nötzli, J., Phillips, M., Ross, N., Seppälä, M., Springman, S.M., Vonder Mühll, D., (2009). Permafrost and climate in Europe: Monitoring and modelling thermal, geomorphological and geotechnical responses. *Earth Science Reviews*, 92: 117-171.

Hasler, A., Talzi, I., Beutel, J., Tschudin, C., and Gruber, S. (2008). Wireless Sensor Networks in Permafrost Research: Concept, Requirements, Implementation, and Challenges. Proceedings of the 9th International Confe-

rence on Permafrost, Fairbanks, USA, 669-674.

Hauck, C., Isaksen, K., Vonder Mühll, D., and Sollid, J. L. (2004). Geophysical surveys designed to delineate the altitudinal limit of mountain permaforst: an example from Jotunheimen, Norway. *Permafrost and Periglacial Processes*, 15: 191-205.

Heim, A. (1932). Bergsturz und Menschenleben, Fretz & Wasmuth Zurich.

Heincke, B. (2005). Determination of 3-D fracture distribution on an unstable mountain slope using georadar and tomographic seismic refraction techniques. PhD Thesis, ETH Zurich, Zurich, 157 pp.

Hewitt, K., Clague, J.J., and Orwin, J.F. (2008). Legacies of catastrophic rock slope failures in mountain landscapes. *Earth-Science Reviews*, 87: 1-38.

Hilbich, C., Hauck, C., Hoelzle, M., Scherler, M., Schudel, L., Völksch, I., Mühll, D. V., and Mäusbacher, R. (2008). Monitoring mountain permafrost evolution using electrical resistivity tomography: A 7-year study of seasonal, annual, and long-term variations at Schilthorn, Swiss Alps. *Journal of Geophysical Research-Earth Surface*, 113(F1): F01S90.

Hoek, E. 1994. Strength of rock and rock masses, *ISRM News Journal*, 2(2), 4-16.

Hoek, E., and Brown, E.T. (1980). Empirical strength criterion for rock masses. *Journal of the geotechnical engineering division*, 106(9): 1013-1035.

Hoek, E., and Bray, J.W. (1981). Rock Slope Engineering, Institution for Mining and Metallurgy.

Hoek, E., and Brown, E.T. (1997). Practial Estimates of Rock Mass Strength. *International Journal of Rock Mechanics and Mining Sciences*, 34(8): 1156-1186.

Hoelzle, M., Mittaz, C., Etzelmüller, B., and Haeberli, W. (2001). Surface energy fluxes and distribution models of permafrost in European mountain areas: an overview of current developments. *Permafrost and Periglacial Processes*, 12: 53–68.

Huggel, C. (2004). Assessment of glacial hazards based on remote sensing and GIS modeling. PhD Thesis, University of Zurich, Zurich.

Huggel, C. (2009). Recent extreme slope failures in glacial environments: effects of thermal pertubation. *Quaternary Science Reviews*, 28: 1119-1130.

Huggel, C., Kääb, A., and Salzmann, N. (2004). GIS-based modeling of glacial hazards and their interactions using Landsat-TM and IKONOS imagery. *Norwegian Journal of Geography*, 58: 61-73.

Huggel, C., Zgraggen-Oswald, S., Haeberli, W., Kääb, A., Polkvoj, A., Galushkin, I. and Evans, S.G. (2005). The 2002 rock/ice avalanche at Kolka/Karmadon, Russian Caucasus: assessment of extraordinary avalanche formation and mobility, and application of QuickBird satellite imagery. *Natural Hazards and Earth System Sciences*, 5: 173-187.

Hungr, O., Evans, S.G., Bovis, M.J., Hutchinson, J.N. (2001). A review of the classification of landslides of the flow type. *Environmental and Engineering Geoscience* 7(3): 221.

IPCC (2007). Climate Change 2007: The Physical Science Basis. Contribution of Working Group 1 to the Fourth Assessment Report of the Intergovernmental Panel on Climate Change, Cambridge University Press, Cambridge, United Kingdom and New York, 996 pp.

Itasca (2004). Itasca Software Products – UDEC (Universal Distinct Element Code), Version 4.0. Itasca Consulting group Inc., Minneapolis.

Jaboyedoff M., Ballifard F., Marro C., Philippossian F., Rouiller J.D. (1999). Detection of rock instabilities: Matter-rock methodology". Proceedings of the Joint Japan-Swiss Scientific Seminar on Impact Load by Rock Falls and Design of Protection Structures, Kanazawa.

Jaboyedoff M., Baillifard F., Couture, R., Locat, J., Locat, P, and Rouiller, J.-D. (2004a). New insight of geomorphology and landslide prone area detection using DEM. Proceedings of the Symposium 1, Advances in Geomorphological Mapping, 9th International symposium on Landslides RIO 2004.

Jaboyedoff, M., Baillifard, F., Couture, R., Derron, M.-D., Locat, J., Locat, P. and Rouillier J.-D. (2004b). Modular and evolutive rock slope instabilities detection and hazard assessment methods: new tools to compute instability factors and examples of application. Proceedings of the 57eme Conference canadienne de geotechnique, Quebec, October 24-26, 2004.

Jaboyedoff, M., Baillifard, F., Philippossian, F. and Rouiller, J.-D. (2004c). Assessing fracture occurrence using "weighted fracturing densit": a step towards estimating rock instability hazard. *Natural Hazards and Earth System Science,* 4: 83-93.

Jaboyedoff M., Metzger R., Oppikofer T., Couture R., Derron M.-H., Locat J., and Turmel D. (2007). New insight techniques to analyze rock-slope relief using DEM and 3D-imaging cloud points: COLTOP-3D software. In: Eberhardt E., Stead D., Morrison T. (eds.) Rock mechanics: Meeting Society's challenges and demands. Proceedings of the 1st Canada - U.S. Rock Mechanics Symposium, Vancouver, Canada, May 27-31, 2007. Taylor & Francis, London, 61-68.

Janeras, M., Navarro, M., Arnó, G., Ruiz, A., Kornus, W., Talaya, J., Barberà, M., and López, F. (2004). LIDAR applications to rock fall hazard assessment in Vall de Núria. Proceedings of the 4th ICA Mountain Cartography Workshop, Vall de Núria, Catalonia, Spain.

Kääb, A. (2002). Monitoring high-mountain terrain deformation from air-and spaceborne optical data: examples using digital aerial imagery and ASTER data. *ISPRS Journal of Photogrammetry and remote sensing*, 57(1-2): 39-52.

Kääb, A. (2005). Remote sensing of mountain glaciers and permafrost creep. Research perspectives from earth observation technologies and geoinformatics. Schriftenreihe *Physische Geographie,* 48, University of Zurich, 266 pp.

Kääb, A. (2008). Remote sensing of permafrost-related problems and hazards. *Permafrost and Periglacial Processes*, 19(2): 107-136.

Kääb, A., Wessels, R., Haeberli, W., Huggel, C., Kargel, J., and Khalsa, S.J.S. (2003). Rapid ASTER imaging facilitates timely assessment of glacier hazards and disasters. *EOS Transactions, American Geophysical Union*, 84(13): 117-121.

Kääb, A., Huggel, C., Barbero, S., Chiarle, M., Cordola, M., Epifani, F., Haeberli, W., Mortara, G., Semino, P., Tamburini, A. and Viazzo, G. (2004). Glacier hazards at Belvedere glacier and the Monte Rosa east face, Italian Alps: Processes and mitigation. Proceedings of the International Symposium Interpraevent 2004 - Riva/Trient: 67-78.

Kääb, A., Huggel, C., Fischer, L., Guex, S., Paul, F., Roer, I., Salzmann, N., Schlaefli, S., Schmutz, K., Schneider, D., Strozzi, T., and Weidmann, W. (2005). Remote sensing of glacier- and permafrost-related hazards in high mountains: an overview. *Natural Hazards and Earth System Sciences*, 5: 527-554.

Kääb, A., Huggel, C., and Fischer, L. (2006). Remote sensing techologies for monitoring climate change impacts on glacier- and permafrost-related hazards. Proceedings of the 2006 ECI Conference on Geohazards, Lillehammer, Norway.

Keaton, J.R., and DeGraff, J.V. (1996). Surface observation and geologic mapping. In Turner, A.K., Schuster, R.L. (Eds.), Landslides: Investigation and Mitigation, Transportation Research Board National Research Council, Washington D.C., USA, National Academy Press, Special Report 247: 178-230.

Keefer, D.K. (1984). Rock avalanches caused by earthquakes: source characteristics. *Science,* 223: 1288-1290.

Keefer, D.K., and Larsen, M.C. (2007). Assessing landslide hazards. *Science*, 316: 1136-1138.

Keller, F. (2003). Kurzbericht über die Steinschlagereignisse im heissen Sommer 2003 im Bergell (Project report on rock fall 2003 to the Kanton Graubünden), Report, Inst. Für Tourismus und Landschaft Acad. Engiadina, Samedan, Switzerland.

Kerle, N. (2002). Volume estimation of the 1998 flank collapse at Casita volcano, Nicaragua: A comparison of photogrammetric and conventional methods. *Earth Surface Processes and Landforms*, 27: 759-772.

Keusen, H.-R., Bollinger, D., Lateltin, O., and Beer, C. (1998). Massenselbstbewegungen und ihre geologische Bedeutung. Geologische Naturgefahren in der Schweiz. S. S. F. f. Ingenieurgeologie**:** 11-28.

Kienholz, H. (1997). Naturgefahren und -risiken in Gebirgsräumen. Proceedings of the 51. Deutscher Geographentag, Bonn.

Kneisel, C. (2003). Permafrost in recently deglaciated glacier forefields – measurements and observations in the eastern Swiss Alps and northern Sweden. *Zeitschrift für Geomorphologie N.F.*, 47(3): 289–305.

Körner, H.J. (1983). Zur Mechanik der Bergsturzströme vom Huascaran, Peru. Hochgebirgsforschung (Innsbruck), 6, 71-110.

Kornus, W., Alamús, R., Ruiz, A., and Talaya, J. (2006), DEM generation from SPOT-5 3-fold along track stereoscopic imagery using autocalibration. *ISPRS Journal of Photogrammetry and Remote Sensing*, 60 (3): 147-159.

Kotlyakov, V.M., Rototaeva, O.V., Desinov, L.V., Zotikov I.A., and Osokin, N.I. (2004). Causes and effect of a catastrophic surge of Kolka glacier in the Central Caucasus. *Zeitschrift für Gletscherkunde und Glazialgeologie*, 38(2), 117–128.

Krähenbühl, R. (2004). Temperatur und Kluftwasser als Ursachen von Felssturz. *Bulletin für angewandte Geologie*, 9(1): 19-35.

Krautblatter, M., and Hauck, C. (2007). Electrical resistivity tomography monitoring of permafrost in solid rock

walls. *Journal of Geophysical Research*, 112, doi:10.1029/2006JF000546.

Krautblatter, M., Moser, M., Schrott, L., and Wolf, J. (2009). A study on sediment yield and geomorphic work comprising all rockfall magnitudes in an Alpine Catchment (Reintal, German Alps). *Geomorphology*.

Kveldsvik, V., Kaynia, A.M., Nadim, F., Bhasin, R., Nilsen, B., and Einstein, H.H. (2009). Dynamic distinct-element analysis of the 800 m high Aknes rockslope. *International Journal of Rock Mechanics and Mining Sciences,* 46: 686-698.

Lerjen M., Kääb, A., Hoelze, M., and Haeberli, W. (2003). Local distribution pattern of discontinuous mountain permafrost. A process study at Flüela Pass, Swiss Alps. Proceedings of the Eighth International Conference on Permafrost, Zurich, Switzerland, 2: 667-672.

Leva, D., Nico, G., Tarchi, D., Fortuny-Guasch, J., and Sieber, A.J. (2003). Temporal analysis of a landslide by means of a ground-based SAR interferometer. *IEEE Transactions on Geoscience and Remote Sensing*, 41(4): 745-752.

Lillesand, T. M. and Kieffer, R. W. (2000). Remote Sensing and image interpretation - fourth edition, Wiley, New York.

Lim, M., Petley, D.N., Rosser, N.J., Allison, R.J. and Long A.J. (2005). Combined digital photogrammetry and time-of-flight laser scanning for monitoring cliff evolution. *The Photogrammetric Record*, 20(110): 109-129.

Lüthi, M.P, and Funk, M. (2001). Modelling heat flow in a cold, high altitude glacier: interpretation of measurements from Colle Gnifetti, Swiss Alps. *Journal of Glaciology* 47(157): 314-324.

Luzi, G., Pieraccini, M., Mecatti, D., Noferini, L., Macaluso, G., Tamburini, A., and Atzeni, C. (2007), Monitoring of an Alpine Glacier by Means of Ground-Based SAR Interferometry. *Geoscience and Remote Sensing Letters, IEEE*, 4(3): 495-499.

Marquínez, J., Menéndez Duarte, R., Farias, P., and Jiménez Sánchez, M. (2003). Predictive GIS-based model of rockfall activity in mountain cliffs. *Natural Hazards*, 30: 341-360.

Matsuoka, N. (1991). A model of the rate of frost shattering: application of field data fom Japan, Svalbard and Antarctica. *Permafrost and Periglacial Processes*, 2: 271–281.

Matsuoka, N. (2001). Direct observation of frost wedging in alpine bedrock. *Earth Surface Processes and Landforms* 26: 601–614.

Matsuoka, N., and Sakai, H. (1999). Rockfall activity from an alpine cliff during thawing periods. *Geomorphology*, 28: 309–328.

Matsuoka, N., and Murton, J. (2008). Frost Weathering: Recent Advances and Future Directions. *Permafrost and Periglacial Processes*, 19: 195-210.

Matsuoka, N., Hirakawa, K., Watanabe, T., and Moriwaki, K., (1997). Monitoring of periglacial slope processes in the Swiss Alps: the first two years of frost shattering, heave and creep. *Permafrost Periglacial Processes*, 8, 155–177.

Matsuoka, N., Hirakawa, K., Watanabe, T., Haeberli, W., and Keller, F. (1998): The role of diurnal, annual and millennial freeze-thaw cycles in controlling alpine slope instability. Proceedings of the Seventh International Conference on Permafrost, Yellowknife, Canada, Collection Nordicana 57: 711-717.

Matthews, J.A., Brunsden, D., Frenzel, B., Gläser, B., and Weiss, M.M. (1997). Rapid mass movement as a source of climatic evidence for the Holocene. Publisher Paläoklimaforschung - Palaeoclimate Research, Vol. 19, 444 pp.

McSaveney, M.J. (1992). The Mount Fletcher rock avalanche of May 2, and again on September 16. *New Zealand Alpine Journal*, 45: 99-103.

McSaveney, M.J. (2002). Recent rockfalls and rock avalanches in Mount Cook National Park, New Zealand. *Geological Society of America, Reviews in Engineering Geology*, XV: 35-70.

McSaveney, M.J., Chinn, T.J., and Hancox, G.T. (1992). Mount Cook Rock Avalanche of 14 December 1991, New Zealand. *Landslide News*, 6: 32-34.

Meissl, G. (1998). Modellierung der Reichweite von Felsstürzen. Fallbeispeile zur GIS-gestützten Gefahrenbeurteilung aus dem Bayerischen und Tiroler Alpenraum. Innsbrucker Geografischen Studien 28, PhD Thesis, Universität Innsbruck, Innsbruck, Austria.

Mellor, M. (1973). Mechanical properties of rocks at low temperatures. In: Permafrost: North American contribution [to the] Second International Conference. Proceedings of the United States Planning Committee for the 2d International Conference on Permafrost, National Academy of Sciences (U.S.), 334-344.

Metternicht, G., Hurni, L., and Gogu, R. (2005). Remote sensing of landslides: An analysis of the potential contribution to geo-spatial systems for hazard assessment in mountainous environments. *Remote sensing of Environment*,

98: 284-303.

Mikkelsen, P.E. (1996). Field Instrumentation. In Turner, A.K., Schuster, R.L. (Eds.), Landslides: Investigation and Mitigation, Transportation Research Board National Research Council, Washington D.C., USA, National Academy Press, Special Report 247: 278-316.

Montandon, F. (1933). Chronologie des grand éboulements alpins, du début de l'ère chrétienne à nos jours. *Société de Géoography Genève, Matériaux pour l'étude des calamites*, 32, 271-340.

Moore, J. R., Sanders, J. W., Dietrich, W. E., and Glaser, S. D. (2009). Influence of rock mass strength on the erosion rate of alpine cliffs. *Earth Surface Processes and Landforms*, 34(10): 1339-1352.

Mote, T.I. (2005). 3D GIS-Based Kinematic Slope Stability Analysis. Joint Meeting Pacific Section, AAPG & Cordilleran Section GSA April 29–May 1, 2005, San José, California.

Müller, L. (1964). The stability of rock bank slopes and the effect of rock water on same. *International Journal of Rock Mechanics and Mining Sciences*, Vol. 1(4): 475-504.

Murrell, S.A., and Misra, A.K. (1962). Time-dependent strain on creep in rocks and similar non-metallic materials. Trans., Institution of Mining and Metallurgy, London, Vol. 71, 353-378.

Murton, J.B., Coutard, J.P., Lautridou, J.P., Ozouf, J.C., Robinson, D.A., and Williams, R.B.G. (2001). Physical modelling of bedrock brecciation by ice segregation in permafrost. *Permafrost and Periglacial Processes*, 12(3): 255-266.

Murton, J.B., Peterson, R., and Ozouf, J.-C. (2006). Bedrock Fracture by Ice Segregation in Cold Regions. *Science*, 314: 1127-1129.

Nichol, J.E., Shaker, A., and Wong, M.S. (2006). Application of high-resolution stereo satellite images to detailed landslide hazard assessment. *Geomorphology*, 76(1-2): 68-75.

Noetzli, J. (2003). Felsstürze aus Permafrost über Gletscher – Ansätze zur GIS-basierten Modellierung. MSc-Thesis, Department of Geography, University of Zurich, 122 pp.

Noetzli, J., Hoelzle, M., and Haeberli, W. (2003). Mountain permafrost and recent Alpine rock-fall events: a GIS-based approach to determine critical factors. 8th International Conference on Permafrost, Zurich, Balkema.

Noetzli, J., Gruber, S., Kohl, T., Salzmann, N., and Haeberli, W. (2007). Three-dimensional distribution and evolution of permafrost temperatures in idealized high-mountain topography. *Journal of Geophysical Research*, 112: F02S13, doi:10.1029/2006JF000545.

Noetzli, J., and Gruber, S. (2009). Transient thermal effects in Alpine Permafrost. *The Cryosphere*, 3: 85-99.

Norrish, N.I, and Wyllie, D.C. (1996). Rock slope stability analysis. In Turner, A.K., Schuster, R.L. (Eds.), Landslides: Investigation and Mitigation, Transportation Research Board National Research Council, Washington D.C., USA, National Academy Press, Special Report 247: 391-428.

O'Connor, J.E., and Costa, J.E. (1993). Geologic and hydrologic hazards in glacierized basins in North America resulting from 19th and 20th century global warming. *Natural Hazards*, 8(2): 121-140.

Oppikofer, T., Jaboyedoff, M., and Keusen, H.-R. (2008). Collapse at the eastern Eiger flank in the Swiss Alps. *Nature Geoscience*, 1: 531-535.

Paterson, W.S.B. (1994). The physics of glaciers, 480 pp, Pergamon, New York.

Paul, F., (2004). The new Swiss glacier inventory 2000 - Application of remote sensing and GIS. PhD Thesis, Department of Geography, University of Zurich, pp. 198.

Paul, F., Kääb, A., Maisch, M., Kellenberger, T., and Haeberli, W. (2004). Rapid disintegration of Alpine glaciers observed with satellite data. *Geophysical Research Letters*, 31: 33-44.

Piteau, D.R., and Peckover, F.L. (1978). Engineering of rock slopes. In: Landslides, Analysis and Control. Eds. R.L. Schuster and R.J. Krizek, Transportation Research Board, Special Report 176, 193-228.

Plafker, G. and Erickson, F.E. (1978). Nevados Huascaran avalanches, Peru. In: Vought, B. (Ed.), Rockslides and Avalanches, 1, Natural Phenomena, Amsterdam, Elsevier, 227-314.

Porter, S.C., and Orombelli, G. (1980). Catastrophic rockfall of September 12, 1717 on the Italian flank of the Mont Blanc massif. *Zeitschrift für Geomorphologie N.F.*, 24(2): 200-218.

Porter, S.C., and Orombelli, G. (1981). Alpine rockfall hazards - recognition and dating of rockfall deposits in the western Italian Alps lead to an understanding of the potential hazards of giant rockfalls in mountainous regions. *American Scientist*, Volume 69: 67-75.

Pralong, A. (2005). On the instability of hanging glaciers. Mitteilungen der Versuchsanstalt für Wasserbau, Hydrologie und Glaziologie der ETH Zürich, 189. ETH Zürich, Zürich, 156 pp.

Prudencio, M., and Van Sint Jan, M., (2007). Strength and failure modes of rock mass models with non-persistent joints. *International Journal of Rock Mechanics and Mining Sciences*, 44: 890-902

Quincey, D.J., Lucas, R.M., Richardson, S.D., Glasser, N.F., Hambrey, M.J., and Reynolds, J.M. (2005). Optical remote sensing techniques in high-mountain environments: application to glacial hazards. *Progress in physical geography*, 29(4): 475.

Rabatel, A., Deline, P., Jaillet, S., and Ravanel, L. (2008). Rock falls in high-alpine rock walls quantified by terrestrial lidar measurements: A case study in the Mont Blanc area. *Geophysical Research Letters*, 35(10): L10502.

Rapp, A. (1960). Recent development of mountain slopes in Kärkevagge and surroundings. *Northern Scandinavia. Geogr. Ann.* 42: 65-201.

Ravanel, L., and Deline, P. (2008). The West Face of Les Drus (Mont-Blanc massif): slope instability in a high-Alpine steep rock wall since the end of the Little Ice Age. *Géomorphologie: relief, processus, environnement*, 261-272.

Rib, H.T., and Liang, T. (1978). Recognition and identification. In: Landslides, Analysis and Control. Eds. R.L. Schuster and R.J. Krizek, Transportation Research Board, Special Report 176, 34-80.

Richardson, S.D., and Reynolds, J.M. (2000). An overview of glacial hazards in the Himalayas. *Quaternary International*, 65/66, 31-47.

Roncella, R., and Forlani, G. (2005). Extraction of planar patches from point clouds to retrieve dip and dip direciton of rock discontinuities. Proceedings of the ISPRS WG III/3, III/4, V/3 Workshop "Laser scanning 2005", Eschede, the Netherlands, September 12-14, 2005.

Rosser, N. J., Petley, D.N., Lim, M., Dunning, S.A., and Allison, R.J. (2005). Terrestrial laser scanning for monitoring the process of hard rock cliff erosion. *The Quarterly Journal of Engineering Geology and Hydrogeology*, 38(4): 363-375.

Röthlisberger, H. (1981). Eislawinen und Ausbrücke von Gletscherseen. Jahrbuch der Schweizerischen Naturforschenden Gesellschaft, wissenschaftlicher Teil 1978, 170-212.

Ruff, M., and Czurda, K. (2008). Landslide susceptibility analysis with a heuristic approach in the Eastern Alps (Vorarlberg, Austria). *Geomorphology*, 94: 314-324.

Ruff, M., and Rohn, J. (2008). Susceptibility analysis for slides and rockfall: an example from the Northern Calcareous Alps (Vorarlberg, Austria). *Environmental Geology*, 5: 441-452.

Ruiz, A., Kornus, W., Talaya, J., and Colomer, J.L. (2004). Terrain Modeling in an Extremely Steep Mountain: A Combination of Airborne and Terrestrial Lidar. *International Archives of Photogrammetry, Remote Sensing and Spatial Information Sciences*, Vol. XXXV, Part B3 pp. 4.

Runqiu, H., and Xiujun, D. (2008). Application of Three-Dimensional Laser Scanning and Surveying in Geological Investigation of High Rock Slope. *Journal of China University of Geosciences*, 19(2): 184-190.

Salvini, R. (2006). Monitoring of geological site by automatic total station, remote sensing and digital photogrammetry techniques. *Geophysical Research Abstracts*, Vol. 8.

Sartori, M., Baillifard, F., Jaboyedoff, M., and Rouiller, J.-D. (2003). Kinematics of the 1991 Randa rockslide (Valais, Switzerland). *Natural Hazards and Earth System Sciences*, 3: 423-433.

Sass, O. (2005). Spatial patterns of rockfall intensity in the northern Alps. *Zeitschrift für Geomorphologie N.F.*, Suppl.-Vol. 138: 51-65.

Sauchyn, D.J., Cruden, D.M., and Hu, X.Q. (1998). Structural control of the morphometry of openrock basins, Kananaskis region, Canadian Rocky Mountains. *Geomorphology*, 22: 313-324.

Scaioni, M., Giussani, A., Roncoroni, F., Sgrenzarolli, M., and Vassena, G. (2004). Monitoring of Geological Sites by Laser Scanning Techniques. Proceedings of the ISPRS WG VII/5, July 12-23, Istanbul, Turkey.

Schär, C., Vidale, P. L., Lüthi, D., Frei, C., Häberli, C., Liniger, M. A., and Appenzeller, C. (2004). The role of increasing temperature variability in European summer heatwaves. *Nature* 427: 332–336.

Schowengerdt, R.A. (2007). Remote sensing. Models and methods for image processing - third edition, Elsevier, Academic Press, 515 pp.

Schoeneich, P., Hantz, D., Vengeon, J.-M., Fraysinnes, M., Deline, P., Amelot, F., Savary, J., Rouiller, J.-D., and Paganone, M. (2004). A new Alpine Rockfall inventory. Proceedings of the Swiss Geoscience Meeting, Lausanne.

Serafim, J.L. (1968). Influence of interstitial water on the behavior of rock masses. In Rock Mechanics in Engineering Practice (Zienkiewicz, O.C., and Stagg, D., eds.), Wiley, New York, 55-97.

Singhroy, V., and Molch, K. (2004). Characterizing and monitoring rockslides from SAR techniques. *Advances in Space Research*, 33: 290-295.

Soeters, R., and Van Westen, C.J. (1996). Slope instability recognition, analysis, and zonation. *Landslides Investigation and Mitigation*: 129–177.

Sosio, R., Crosta, G.B., and Hungr, O. (2008). Complete dynamic modeling calibration for the Thurwieser rock avalanche (Italian Central Alps). *Engineering Geology*, 100: 11-26.

Sowers, G.F., and Royster, D.L. (1978). Field investigation. In Schuster and Krizek, (eds.), Landslides–analysis and control: Transportation Research Board. National Academy of Sciences, Special Report, 176: 81-111.

Stead, D., Eberhardt, E., Coggan, J., and Benko, B. (2001). Advanced numerical techniques in rock slope stability analysis - applications and limitations. In Kühne et al. (eds.), UEF International Conference on Landslides - Causes, Impacts and Countermeasures, Davos. Verlag Glückauf GmbH, Essen.

Stead, D., Eberhardt, E., and Coggan, J.S (2006). Developments in the characterization of complex rock slope deformation and failure using numerical modelling techniques. *Engineering Geology*, 83: 217-235.

Strozzi, T., Kääb, A., and Frauenfelder, R. (2004). Detecting and quantifying mountain permafrost creep from in-situ, airborne and spaceborne remote sensing methods. *International Journal of Remote Sensing* 25(15): 2919–2931.

Suter, S. (2002). Cold firn and ice in the Monte Rosa and Mont Blanc areas: spatial occurrence, surface energy balance and climatic evidence. PhD Thesis, Versuchsanstalt für Wasserbau, Hydrologie und Glaziologie der ETH Zürich. Zürich, ETH Zürich, 172: 188pp.

Swisstopo (2004). DHM25 - The digital height model of Switzerland. Product Information, http://www.swisstopo.admin.ch/internet/swisstopo/en/home/products/height/dhm25.html.

Tart, R.G., (1996). Permafrost. In Turner, A.K., Schuster, R.L. (Eds.), Landslides: Investigation and Mitigation, Transportation Research Board National Research Council, Washington D.C., USA, National Academy Press, Special Report 247: 620-645.

Terzaghi, K. (1950). Mechanism of landslides. *Application of geology to engineering practice: Berkey volume*: 83.

Terzaghi, K. (1962). Stability of steep slopes on hard unweathered rock. *Geotechnique* 12: 251-270.

Turner, A.K., and Jayaprakash, G.P. (1996). Introduction. In: Turner, A.K., Schuster, R.L. (Eds.), Landslides, Investigation and Mitigation. Transportation Research Board, Special Report 247, Washington D.C., USA, 3–11.

van Everdingen, R.O. (1998). Multi-language glossary of permafrost and related ground ice terms. International Permafrost Association.

van Westen, C.J., Rengers, N., and Soeters, R. (2003). Use of geomorphological information in indirect landslide susceptibility assessment. *Natural Hazards*, 30: 399-419.

Van Westen, C.J., van Asch, T.W.J., and Soeters, R. (2005): Landslide hazard and risk zonation—why is it still so difficult? *Bulletin of Engineering Geology and the Environment*, 65(2): 167–184.

van Westen, C.J., Castellanos, E., and Kuriakose, S. L. (2008). Spatial data for landslide susceptibility, hazard, and vulnerability assessment: An overview. *Engineering Geology*, 102: 112-131.

Varnes, D.J. (1978). Slope movement types and processes. In: Landslides, Analysis and Control. Eds. R.L. Schuster and R.J. Krizek, Transportation Research Board, Special Report 176, 11-33.

Watson, A.D., Moore, D.P., and Stewart, T.W. (2004). Temperature influence on rock slope movements at Checkerboard Creek. Proceedings of the International Symposium on Landslides. Balkema, Rio de Janeiro, 1293–1298.

Wegmann, M. (1998). Frostdynamik in hochalpinen Felswänden am Beispiel der Region Jungfraujoch-Aletsch. Versuchsanstalt für Wasserbau, Hydrologie und Glaziologie der ETH Zürich. Zürich, 161: 144.

Wegmann, M., Gudmundsson, G. H., and Haeberli, W. (1998). Permafrost changes in rock walls and the retreat of Alpine glaciers: a thermal modelling approach. *Permafrost and Periglacial Processes*, 9: 23-33.

Weibel, R., and Heller, M. (1991). Digital Terrain Modeling. In: Maguire, D.J., Goodchild, M.F. and Rhind, D.W. (eds.). Geographical Information Systems: Principles and Applications. London: Longman: 269-297.

Whalley, W. B. (1974). The mechanics of high-magnitude, low-frequency rock failure and its importance in a mountainous area. *Geographical Papers*, No. 27: 1-48.

White, S.A., and Wang, Y (2003). Utilizing DEMs derived from LIDAR data to analyze morphologic change in the North Carolina coastline. *Remote Sensing of Environment*, 85: 39-47

Wieczorek, G.F., (1996). Landslide triggering mechanims. In: Turner, A.K., Schuster, R.L. (Eds.), Landslides: Investigation and Mitigation, Transportation Research Board National Research Council, Washington D.C., USA, National Academy Press, Special Report 247: 76-90.

Willenberg, H. (2004). Geologic and kinematic model of a complex landslide in crystalline rock (Randa, Switzer-

land). Engineering Geology. Zurich, ETH Zurich. Doctoral Thesis.

Willenberg, H., Spillmann, T., Eberhardt, E., Evans, K., Loew, S., and Maurer, H. (2002). Multidisciplinary monitoring of progressive failure processes in brittle rock slopes - Concepts and system design. 1st European Conference on Landslides, Prague, Czech Republic.

Wiss, R. (2009). Extraction of features from an alpine rock face based on lidar data development of new methods using the Monte Rosa east face as an example. Diploma thesis, UNIGIS, University of Salzburg.

Wu, T.H., and Sangrey, D.A. (1978). Strength properties and their measurement. In: Schuster, R.L., Krizek, R.J. (Eds.), Landslides, Analysis and Control. Transportation Research Board, Special Report 176, Washington D.C., USA, 139–154.

Wyllie, D.C., and Norrish, N.I. (1996). Rock strength properties and their measurement. In Turner, A.K., Schuster, R.L. (Eds.), Landslides: Investigation and Mitigation, Transportation Research Board National Research Council, Washington D.C., USA, National Academy Press, Special Report 247: 372-390.

Wyllie, D.C., and Mah, C.W. (2004). Rock slope engineering: civil and mining. Spon Press/Taylor & Francis Group.

Zagorodnov, V., Nagornov, O., and Thompson, L. G. (2006). Influence of air temperature on a glacier's active-layer temperature. *Annals of Glaciology*, 43: 285.

Zemp, M. (2002). GIS-basierte Modellierung der glazialen Sedimentbilanz. Diploma thesis, Department of Geography, University of Zurich, 99 pp.

Zemp, M., Paul, F., Hoelzle, M., and Haeberli, W. (2006). Glacier fluctuations in the European Alps 1850–2000: an overview and spatiotemporal analysis of available data, in: The darkening peaks: Glacial retreat in scientific and social context, edited by: Orlove, B., Wiegandt, E., and Luckman, B., University of California Press.

Zepp, H. (2002). Geomorphologie: Eine Einführung, Schöningh.

Züblin, M., Fischer, L., and Eisenbeiss, H. (2008). Combining photogrammetry and laser scanning for DEM generation in steep high-mountain areas. The International Archives of the Photogrammetry, Remote Sensing and Spatial Information Sciences, Beijing, China.

Personal Bibliography

Peer reviewed articles

Fischer, L., Eisenbeiss, H., Kääb A., Huggel C. and Haeberli W. (submitted): Monitoring topographic changes in steep periglacial high-mountain faces, Monte Rosa east face, Italian Alps. *Permafrost and Periglacial Processes.*

Fischer, L., Amann, F., Moore, J.R. and Huggel C. (submitted): Geomechanical analyses of slope instabilities in glacierised environments. *Engineering Geology.*

Fischer, L., Purves, R.S., Huggel, C., Noetzli, J., and Haeberli, W. (in prep.). On the influence of geological, topographic and cryospheric factors on slope instabilities: Statistical analyses of recent Alpine rock avalanches. *Natural Hazards and Earth System Science.*

Fischer, L. and Huggel, C. (2008): Methodical design for stability assessments of permafrost affected high-mountain rock walls. Proceedings of the 9th International Conference on Permafrost, Fairbanks, Alaska, 439-444.

Fischer, L., Kääb, A., Huggel, C. and Noetzli, J. (2006): Geology, glacier retreat and permafrost degradation as controlling factors of slope instabilities in a high-mountain rock wall: the Monte Rosa east face. *Natural Hazards and Earth System Science*, 6, 761-772.

Fischer, L. (2006): Monte Rosa Ostwand – Geologie, Vergletscherung, Permafrost und Sturzereignisse in einer hochalpinen Steilwand. Bulletin für angewandte Geologie 11/1, 65-78.

Kääb, A., Huggel, C., Fischer, L., Guex, S., Paul, F., Roer, I., Salzmann, N., Schlaefli, S., Schmutz, K., Schneider, D., Strozzi, T., and Weidmann, Y. (2005): Remote sensing of glacier- and permafrost-related hazards in high mountains: an overview. *Natural Hazards and Earth System Science*, 5, 527-554.

Conference proceedings

Züblin, M., Fischer, L. and Eisenbeiss, H. (2008): Accuracy and reliability of DEM of Monte Rosa east face, a steep high-mountain flank in the European Alps. The International Archives of the Photogrammetry, Remote Sensing and Spatial Information Sciences. Vol. XXXVII. Part B6b, Beijing, China, pp. 37-43.

Huggel, C., Fischer, L. and Schneider, D. (2008): Gletscher- und Permafrost-Naturgefahren in der Perspektive sich ändernder Umweltbedingungen. Deutsche Gesellschaft für Geotechnik/Geowissenschaften, Fachsektion Ingenieurgeologie, Rundbrief 66, Sonderheft zur 18. Bodenseetagung der Deutschen, Oesterreichischen und Schweizerischen Fachgruppen der Ingenieurgeologie, 39-40.

Kääb, A., Huggel, C. and Fischer, L. (2006): Remote sensing technologies for monitoring climate change impacts on glacier- and permafrost-related hazards. 2006 ECI Conference on Geohazards. Paper 2, pp. 12.

Reports

GIUZ 2005. Analysis of amateur- and air-photos of the Monte Rosa east face and the Ghiacciaio del Belvedere (Kääb, A., Fischer, L., Huggel, C. and Haeberli, W.). Report Regione Piemonte. Glaciology and Geomorphodynamics Group, Department of Geography, University of Zurich, unpublished report, 59 pp.

GIUZ 2005. Data compilation and integration, Monte Rosa/Gh. del Belvedere, Macugnaga (Huggel, C., Kääb, A., Fischer, L. and Haeberli, W.). Report Regione Piemonte. Glaciology and Geomorpholdynamics Group, Department of Geography, University of Zurich, unpublished report, 57 pp.

Others

Mortara G., Tamburini, A., Ercole, G., Semino, P., Chiarle, M., Godone, F., Giuliano, M., Haeberli, W., Kääb, A., Huggel, C., Fischer, L., et al. (2009): Il Ghiacciaio del Belvedere e l'emergenza del Lago Effimero. A cura di G. Mortara e A. Tamburini, Regione Piemonte, 158 p.

Fischer, L. (2004): Monte Rosa Ostwand – Geologie, Vergletscherung, Permafrost und Sturzereignisse in einer hochalpinen Steilwand. Diploma thesis, Department of Earth Sciences, ETH Zurich.

Conference Presentations (first author presentations only):

L. Fischer, C. Huggel, A. Kääb, R.S. Purves, J. Noetzli, H. Eisenbeiss, F. Amann, J.R. Moore and W. Haeberli. *On the influence to topographic, geological and cryospheric factors on slope instabilities in steep periglacial rock walls.* Glacier Hazard Workshop, Vienna, Austria, 10.-13.11.2009

L. Fischer, C. Huggel, R.S. Purves and F. Amann. *On the influence of geological and cryospheric factors on slope instabilities in steep high-mountain flanks.* European Geosciences Union General Assembly 2009, Vienna, Austria. 19. – 24. 4.2009.

L. Fischer, H. Eisenbeiss, A. Kääb, C. Huggel and W. Haeberli. *Combined LiDAR and photogrammetry for stability-related change detection in glacierised and frozen rock walls - A case study in the Monte Rosa east face.* Swiss Geoscience Meeting, Lugano, Switzerland. 21.-22.11.2008.

L. Fischer, F. Amann and C. Huggel. *Multidisciplinary investigations and back-analysis of a periglacial rock fall event: Tschierva rock fall.* Swiss Geoscience Meeting, Lugano, Switzerland. 21.-22.11.2008.

L. Fischer. *Comparison of LIDAR and aerial photogrammetry for terrain analyses in steep high-mountain areas: Monte Rosa east face.* GriaAlp Meeting, Zurich, Switzerland. 13.-14.11.2008.

L. Fischer, and C. Huggel. *Methodical design for stability assessments of permafrost affected high-mountain rock walls*. IX International Conference on Permafrost, Fairbanks, Alaska. June 29 - July 3, 2008.

L. Fischer, H. Eisenbeiss, C. Huggel, M. Züblin, W. Haeberli and J. Vallet. *Helicopter-borne LIDAR and multi-platform aerial photogrammetry for stability related terrain analyses of steep high-mountain areas: Monte Rosa east face*. European Geosciences Union General Assembly 2008 Vienna, Austria. 13. – 18. 4.2008.

L. Fischer, C. Huggel, and A. Kääb. *Evolution of the Monte Rosa east face: studies and field survey*. Workshop: Advancements of remote sensing tools for glacier hazard monitoring: Demonstration on the Belvedere glacier. Macugnaga, Italy, August 31st – September 1st, 2007. (Invited talk)

L. Fischer, C. Huggel and F. Lemy. *Investigation and modelling of periglacial rock fall events in the European Alps*. European Geosciences Union General Assembly 2007, Vienna, Austria. 15. - 20. 4.2007.

L. Fischer, C. Huggel, and W. Haeberli. *High mountain slope instabilities related to climate change*. 5th International NCCR Climate Summer School, Grindelwald. 27.8. – 1.9.2006.

L. Fischer, C. Huggel, J. Nötzli and W. Haeberli. *Multidisciplinary analyses of the detachment zones of periglacial rock fall events in the European Alps*. European Geosciences Union General Assembly 2006, Vienna, Austria. 2. - 7. 4.2006.

L. Fischer, A. Kääb, C. Huggel and J. Nötzli. *Geology, glacier changes, permafrost and related slope instabilities in a high-mountain rock face: Monte Rosa east face, Italian Alps*. Swiss Geoscience Meeting, Zurich Switzerland. 18.-19.11.2005.

Acknowledgements

On the way through my PhD, I experienced a lively journey across impressive high-alpine landscapes with many steep rock walls, high peaks and deep valleys. There were many laborious and challenging ascents through the working labyrinth, but also as many outstanding summit experiences with wonderful panoramic views, when a problem was solved or a goal was reached. I would like to thank everybody who joined me on this journey, it would not have been possible without the help, guidance, support, and understanding of many people.

My sincerest thanks go to Wilfried Haeberli, for offering me the opportunity to pursue this adventurous journey within his research group. His continuous confidence, enthusiasm and motivation were essential for the completion of my work and I learned a great deal from his comprehensive knowledge and way of thinking.

I wish to express my deepest gratitude to Christian Huggel, who accompanied me as supervisor on my journey by giving me helpful inputs, leaving me considerable freedom to explore the scientific world, while still supporting all my ideas, and finding time for many interesting and fruitful discussions, sometimes even from abroad.

Special thanks go to Ross Purves for helping me with GIS questions, supporting me in the statistical part of this work with precise input and improving my English, but even more for advising me in the way of scientific thinking and debate.

I sincerely thank Andi Kääb for motivating me to take this PhD journey through such inaccessible high-mountain terrain by sparking my interest in the world of remote sensing. And special thank, also, for giving me the opportunity to work in Oslo, and a chance to get to know and appreciate Norway.

Frank Lemy from the Engineering Geology Group, ETH Zurich, brought me on the path of numerical slope stability modelling, and helped me negotiate the first steps with UDEC. He made a valuable contribution to the successful proposal, and for all these things has earned my enormous thanks.

With gratitude I acknowledge the instructive collaboration of Florian Amann from the Engineering Geology Group, ETH Zurich, and his enthusiastic help with UDEC and kinematic analyses. I also thank Jefferey Moore for his extensive contributions to the Tschierva paper and to fruitful discussions about slope stability, together with Florian, Andrew Kos and Mark Diedrichs.

I am greatly indebted to Henri Eisenbeiss from the Institute for Geodesy and Photogrammetry for the valuable collaboration and really helpful input, for giving me the opportunity to work at this institute using sophisticated digital photogrammetry programs. Many thanks also to Nusret Demir and Devrim Akca for the introduction to diverse software packages.

My gratitude is extended to Julien Vallet, his 'HELIMAP system' team, Remo Da Pra and Air Walser for the challenging LiDAR survey of the Monte Rosa east face, and for their flexibility.

Many special thanks go to my H68 officemates Lorenz Böckli, Andreas Linsbauer, and Demian Schneider and to all former office mates for the very pleasant (work) atmosphere in our little exclave! Furthermore, I would like to thank everyone from the 3G-Group for all the discussions and adventures, not only in-house and concerning science but also as friends for various outdoor activities. A huge thank you goes to Jeannette Noetzli for providing me with fundamental data from her work that established the basis of my project, the many scientific and non-scientific discussion about all the important things in the world, and all the adventures on snowy and rocky terrain. Special thanks go to Nadine Salzmann and Michi Zemp for so many really helpful and constructive discussions especially during the first steep ascent of my PhD which sometimes seemed to be overwhelming. Many thanks also to Frank Paul for providing me the glacier outline data. I am grateful to Lisbeth Nietlisbach and Helene Grüter for clearing away all the bureaucratic obstacles.

Many thanks go to Ivan Woodhatch and Susan Braun-Clarke, for their careful, skillful proofreading. Ivan helped me to get over the first huge obstacle of the SNF proposal even before I really started my PhD and Susan got me across the final barrier by proofreading the PhD and a major research article.

My most abundant thanks are extended to Regula Frauenfelder Kääb for providing me with all I needed to feel comfortable during my stay in Oslo and for her unfailingly sincere and helpful advices. Regula and Andi, many thanks for your generous hospitality, I am really happy to know you are in Norway, in view of my next adventure, in Trondheim.

I thank John Clague to contribute an external expertise of this work.

How greatly would I like to thank Hans Röthlisberger for the photographs of the Monte Rosa east face and for the fascinating discussion about this flank in earlier times. Sadly, I could not show him my final work as he passed away a few weeks ago.

I thank Arnold Amstutz for all the photographs and information he gave me about the Tschierva rock avalanche.

The collaboration with Andrea Tamburini, Marta Chiarle, Gianni Mortara, and Paolo Semino in Macugnaga was really interesting, enjoyable and instructive - grazie mille.

A special thank goes to Jeff Kargel, Rick Wessel, Maria Banks, Christian Huggel, Martin Hoelzle, and Isa Gärtner-Roer for making possible the outstanding fieldwork opportunity in Alaska and the chance to experience the huge dimension of Alaska's outback, glaciers and mountains.

Most special thanks go to Geotest, especially to Markus Liniger and Beat Kaufmann for giving me the opportunity to work in a geological office and to get to know the real world of gainful employment. I really appreciate the working atmosphere, a huge thank you to all of the Geotest Horw! My gratitude is extended to Hans-Rudolf Keusen for the chance to join him on several inspection rounds of fascinating natural hazard areas.

A thousand thanks to my very good friends Ruschle, Nici, Marc and Zedi for their friendship. Many thanks to Dani and Mauro, for having joined me a part of this journey. They all helped me to keep the balance between academic life and living a life.

My parents, Anneliese and Gerhard, I thank with all my heart for always supporting me in everything and for being my backbone in situations when mine was broken! Ganz härzleche Dank för euchi Unterstützig ond euches Interässe a minere Arbet!! Es esch sehr schön z'wösse, dass ech i allne Situatione uf euchi Hilf cha zelle! Special thanks, also, to my two sisters for all the moments we shared and the fun we have together. I thank Daniela and André for giving me the opportunity to share very special moments with their children Nicola, Luca and Maline, and thereby reminding me of the important things in life. Martina, thank you very much for your support, for being my 'ambulance driver' and the open doors in Arosa.

The present study was funded by a grant from the Swiss National Science Foundation (Project 200021-111967 / 2). The LiDAR survey was partially supported by University internal funds.

PART B: PAPERS

I

Methodical Design for Stability Assessments of Permafrost Affected High-Mountain Rock Walls

Luzia Fischer, Christian Huggel
Glaciology, Geomorphodynamics & Geochronology, Department of Geography, University of Zurich

Abstract

Slope stability of steep rock walls in glacierised and permafrost-affected high-mountain regions is influenced by a number of different factors and processes. For an integral assessment of slope stability, a better understanding of the predisposing factors is particularly important, especially in view of rapid climate-related changes. This study introduces a methodical design that includes suitable methods and techniques for investigations of different predisposing factors in high-mountain rock walls. Current state-of-the-art techniques are reviewed and their potential application for in-situ and remote studies assessed. A comprehensive array of analyses and modeling tools is presented, including data acquisition methods and subsequent stability analyses. Based on two case studies of recent slope instabilities in the European Alps the effective application and coupling of measurements, analyses and modeling methods is shown.

Keywords: climatic change; high-mountain rock walls; investigation techniques; predisposing factors; slope stability.

Introduction

Hazards related to rock fall, rock avalanches and combined rock/ice avalanches from steep glacierised and permafrost-affected rock walls pose a significant threat to people and infrastructure in high mountain regions. Due to ongoing climatic change, a widespread reduction in stability of formerly glacierised and perennially frozen slopes might occur and result in a shift of hazard zones (Haeberli et al.1997, Harris et al. 2001, Fischer et al. 2006). A major problem is the possible increase in magnitude and frequency of slope failures.

Slope stability of steep rock walls in glacierised and permafrost-affected high-mountain regions is influenced by a number of different factors such as topography, geological and geomechanical characteristics, hydrology as well as glaciation, permafrost distribution and thermal condition. Gradual or abrupt changes in one or more of these factors may reduce the slope stability and eventually lead to a rock fall event. Among these factors, permafrost and glaciers are particularly prone to rapid changes in relation to ongoing climate change. Although these two factors are, together with the hydrological regime, assigned a likely important role in current and future slope destabilization the effects are not clearly understood. A better understanding of the factors and mechanisms determining the slope stability of steep rock walls is thus a key factor and needs basic research.

The complexity of slope stability problems requires a number of different investigation and modeling techniques to consider the relevant physical processes and factors. However, high-mountain rock walls are an extremely challenging environment for currently existing technology and related investigations for a number of reasons. Often, the hazard source areas are situated in remote high-mountain regions and the on-site access to steep rock walls is mostly very difficult or prohibitively dangerous due to existing slope instabilities. Furthermore, the steepness complicates applications of airborne investigation techniques.

This article provides a review of current local-scale investigation techniques and introduces a multidisciplinary methodical design for comprehensive stability-directed investigations of predisposing factors in steep high-mountain rock walls which adequately considers the particular difficulties of steep and partly inaccessible ground conditions, based on a combination of on-site and remote methods. The design presented here does not claim to provide a complete approach, it rather bases itself on investigation techniques and analyses that were applied and tested within past and ongoing projects. Also, the rapidly advancing technology may require extension and adaptation of the design in the future.

Factors influencing slope stability

Predisposing and triggering factors can be distinguished with respect to slope stability of rock walls. In the following, a short definition of the two different types of factors is given. Proposed methodical design for slope stability assessment is mainly focused on the investigation of predisposing factors; analyses of triggering factors usually require permanent monitoring methods.

Predisposing factors are physically measurable processes and parameters that permanently affect stress and strain fields in a flank, also in the stable state. They can be broadly categorized in topographical, geomorphological, geological, hydrological and several other physically-based factors. In high-mountain areas, permafrost and glaciers are two additional important factors (Fig. 1).

Triggering factors can vary in time, space and magnitude and eventually provoke slope failure. They include, for example, earthquakes, rainfall and snow melt events that can result in increased water pressure and rather seldom in high-mountain areas, human interactions.

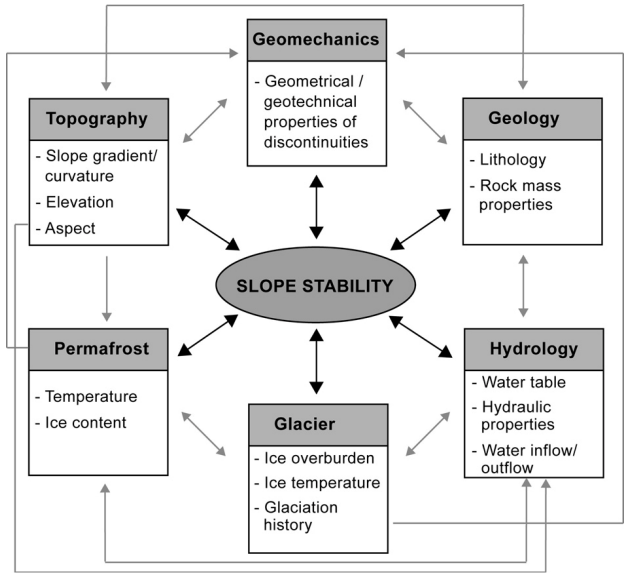

Figure 1: Predisposing factors influence the slope stability and have complex interactions among themselves which are represented by arrows.

Predisposing factors have complex interactions among themselves that influence slope stability (Fig. 1). Topography is a fundamental parameter for slope stability. Slope angle and morphology are important factors for the occurrence and spatial distribution of slope instabilities due to their strong influence on stress and strain fields within a flank. Topography is closely connected to the geological setting and the geomorphological history of a rock wall (erosion, glacial overburden), which, in turn, also effectively influence the geomechanical setting.

The geological setting is determined by the lithology and the geotechnical properties of the rock mass. The geological structures, i.e. discontinuities such as joints, bedding planes, schistosity and fault zones are fundamental for slope stability, especially their geometrical and geotechnical characteristics. The shear strength as a major parameter for stability is directly related to the geotechnical properties such as cohesion, friction angle, aperture, infilling and weathering.

Permafrost occurrence in a rock wall can strongly influence the geotechnical parameters of discontinuities, depending on ice content and temperature. The shear strength of ice-bonded discontinuities is strongly affected by the thermal regime in the sub-surface and may be reduced by a rise in temperature or finally the melting of ice-filled rock joints (Davies et al. 2001, Gruber & Haeberli 2007, Harris et al. 2001). This, in turn, also influences the hydrological regime, and may, for instance, result in an increase of the water pressure. The hydraulic setting in a steep rock wall is closely connected to the topography, geological setting, geomechanical characteristics, glaciation and permafrost occurrence. Changes in water table and water pressure, may significantly change the shear strength of the rock mass and therefore exert a strong influence on the slope stability.

Glacier ice may influence slopes differently. Hanging glaciers may have an impact on the thermal, hydraulic and hydrologic regime in adjacent areas (Haeberli et al. 1997). The erosion by and retreat and down-waste of valley glaciers, in turn, may induce long-term changes change in the stress field inside the rock wall (Wegmann et al. 1998, Eberhardt et al. 2004).

Among the factors outlined in Figure 1, glaciation and permafrost are presently those subject to the most direct and rapid changes due to climatic change. Changes in these parameters can significantly influence other factors such as hydrology, geomechanical and geotechnical properties in particular. The response of steep high-mountain rock walls to changes in these predisposing factors is, at the same time, strongly conditioned by the topography and the geological setting, in particular by the geometrical and geotechnical characteristics of discontinuities (Ballantyne 2002).

Investigation techniques and methodology

Data acquisition

In this section, current state-of-the-art techniques for the investigation of the predisposing factors are illustrated while in the following section subsequent analyses and processing methods are described (Fig. 2).

In-situ field investigations are useful to obtain detailed data. Traditional geological in-situ field studies are necessary to achieve data on geological and geomechanical characteristics of the rock mass. The lithological and geomorphological setting as well as geological structures can be mapped and a preliminary assessment of the intact rock mass properties can be achieved, for example using the Schmidt hammer method (Aydin & Basu 2005). The geomechanical and geotechnical properties of discontinuities can be assessed by measuring parameters such as orientation, frequency, spacing, aperture and surface characteristics based on the application of rock mass classification systems (Hack 2002, Hoek & Brown 1997, Wyllie & Mah 2004). In case of inaccessible ground conditions, these types of investigations can also be conducted in the surrounding area with similar lithological and geomechanical settings. Limited observations of the hydrological regime can also be done in-situ and from photographs, for instance observations of water inflow or outflow in a mountain flank.

Point measurements of near-surface rock temperatures using temperature loggers installed a few cm to dm below the surface can constrain permafrost distribution and the prevailing thermal regime (Gruber et al. 2003). Nearby boreholes equipped with temperature loggers give an indication of temperature distribution at depth.

Geophysical techniques are powerful methods for the investigation of subsurface characteristics, but in steep rock walls difficult and complex in their application and therefore rarely exploited until now. Georadar, electrical resistivity tomography and refraction seismic can be applied for the determination of subsurface structures and the distinction between frozen and thawing rock sections (Hauck et al. 2004, Heincke 2005, Krautblatter & Hauck 2007).

Remote sensing based techniques are crucial due to the inaccessibility of wide areas of high-mountain walls.

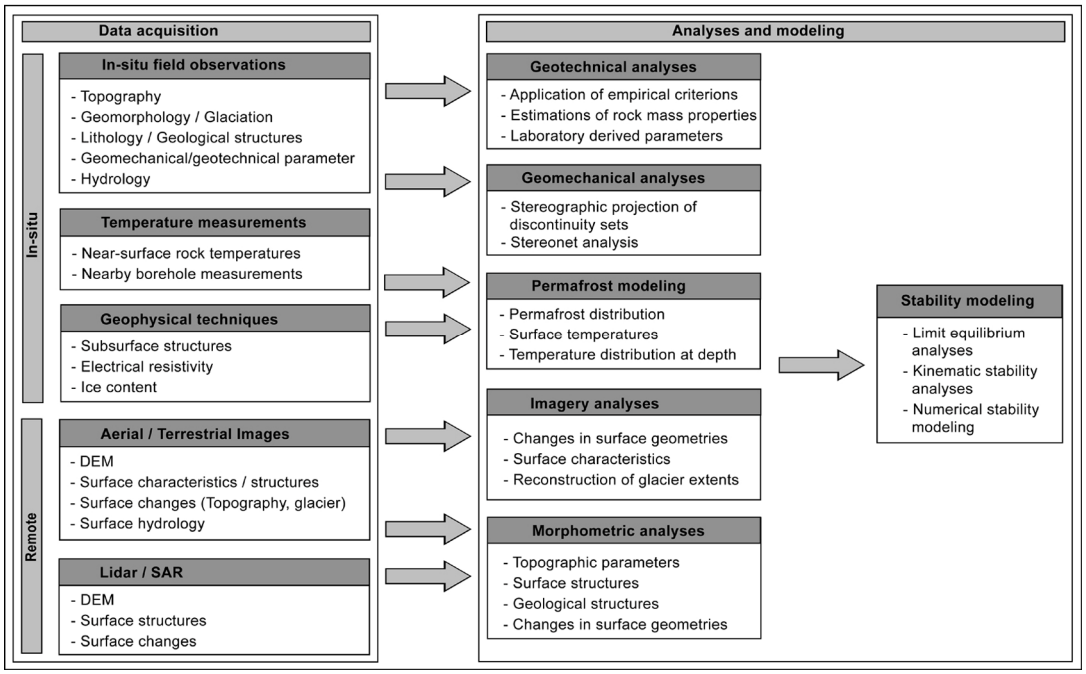

Figure 2: Methodical design for the assessment of slope stability in high-mountain areas containing different insitu and remote sensing based methods. The upper part shows techniques for the data collection, the lower part processing and analyses of acquired data.

Terrestrial and aerial imagery can be used for identifying geological structures and surface changes with respect to ice cover and topography. Aerial photography can also be used for the generation of digital elevation models (DEMs), the measurement of terrain displacements and for detailed interpretations (Baltsavias et al. 2001). In some specific studies, terrestrial photography was used for identifying changes with respect to ice cover and slope instabilities on steep ice faces (Fischer et al. 2006, Kääb et al. 2005). These studies have shown the considerable potential of such image analyses which should be further exploited. Automatic cameras are a commonly applied tool for monitoring acute slope instabilities.

Airborne and terrestrial laser scanning (LiDAR) is a rapidly emerging and highly promising tool for acquiring very high-resolution DEMs for high-mountain areas, and thus for detecting small-scale topographic structures (Baltsavias et al. 2001, Janeras et al. 2004). Laser scanning applications from helicopter allow perpendicular recording of LiDAR data and simultaneous acquisition of digital photographs with little geometric distortion (Skaloud et al. 2005). Repeated measurements are the basis to derive topographic changes. Ground-based synthetic aperture radar (SAR) technology is a capable tool for slope deformation studies (Atzeni et al. 2001, Singhroy and Molch 2004).

Analyses and modeling

Lithological and geomorphological data can be displayed on a map in a GIS for further applications or comparison with other parameters. The geomechanical and geotechnical data measured during field work typically have to be processed to get required parameters for the stability modeling, by using empirical criterions and rock mass classification systems (Hack 2002, Hoek & Brown 1997) or with adequate laboratory tests. Geomechanical data such as the orientation of discontinuities can be displayed in steregraphic projections and may be applied subsequently for kinematic analyses, limit equilibrium analyses and numerical modeling (Stead et al. 2006).

For the modeling of permafrost distribution a number of models with varying levels of sophistication and at different spatio-temporal scales have been developed (Hoelzle et al. 2001, Gruber et al. 2003). The three-dimensional temperature distribution and its evolution with climatic change is an important component for rock slope stability considerations, and has been assessed using numerical modeling by coupling a surface energy balance model with a subsurface heat conduction scheme (Noetzli et al. 2007). A modeling scheme that would directly include modeled permafrost distribution within slope stability models has yet to be developed but it can be considered for the model assumptions.

Geophysical investigations can mainly be used as boundary conditions and reference values either for permafrost modeling or for analyses of the subsurface structures.

The most common application of remotely sensed image data consists in the interpretation and classification of the image content. Terrestrial and aerial imagery can be used for the identification and mapping of different surface features in steep rock walls and also their temporal changes. Digital aerial as well as terrestrial photos have considerable potential for quantitative analyses of geomorphic structures and changes in a rock wall by georeferencing or matching images based on a high-resolution DEM or photogrammetric techniques (Roncella et al. 2005).

DEMs represent the core of any morphometric investigation of predisposing factors. They can be obtained from

stereo aerial and high-resolution terrestrial photos but also from LiDAR data (Kääb et al. 2005). From these DEMs, topographic parameters, large-scale morphotectonic features and geological structures can be extracted. A promising, yet not fully exploited method is the coupling of laser scanning data with photogrammetric analyses and terrestrial imagery analyses, to extract important topographic and structural-geological parameters from DEMs. Main discontinuity sets can be distinguished and their geometrical pattern determined. Therefore, a preliminary assessment of potentially unstable areas may be performed based on geomechanical parameters with limit equilibrium and kinematic analyses using the data from in-situ measurements or even only based on DEM analyses (Derron et al. 2005, Stead et al. 2001). Further structural and stability analysis with a DEM is made possible by the recent development of geologically oriented GIS tools (Günther 2003, Jaboyedoff et al. 2004).

For more complex slope stability assessments numerical methods are required. Numerical techniques used for rock slope analyses are generally divided into continuum and discontinuum approaches, or when combined, hybrid approaches (Barla & Barla 2001, Eberhardt et al. 2004, Stead et al. 2001, Stead et al. 2006). Numerical modeling is in fact a powerful tool for the assessment of failure mechanisms, but the level of topographic and geotechnical detail needed can limit the application.

Case studies

Tschierva rock avalanche event

The Tschierva rock avalanche occurred on October 19, 1988 from the western flank of Piz Morteratsch (3751 m asl, in the Engadin, Switzerland) on Tschierva glacier with an estimated volume of approximately $0.3x10^6$ m^3(Fig. 3).

For the reanalyses of the Tschierva rock avalanche, detailed numerical slope stability modeling was proposed. Therefore, in-situ field work and subsequent geotechnical and morphometric analyses have been done to obtain required accurate data (Fischer et al. 2007). The steps described here generally follow the scheme from Figure 2.

The in-situ field observations included:

- Preliminary analyses of rock mass properties (lithology, discontinuities, fault zones, water occurrence)
- Characterization of discontinuities (discontinuity sets, orientation, density, condition, aperture, filling)
- Surveying of detachment zone and adjacent area with manual rangefinder

Subsequent complementary analyses included:

- Geotechnical and geomechanical analyses by using field data, stereographic plots and empirical criterions
- Photogrammetric analyses of aerial images for the evaluation of topographic changes
- Analyses of aerial and terrestrial photos for detecting geological structures and water occurrence
- Modeling of the permafrost distribution
- Reconstruction of glacier extents based on satellite images and historical topographic maps

Figure 3: The western flank of the Piz Morteratsch with the Tschierva glacier in the foreground. In the middle of the photo visible is the detachment zone of the 1988 rock fall and the deposits on the glacier (photo by A. Amstutz, 1988).

Numerical slope stability modeling was then performed with the 2-D distinct-element method model UDEC (by Itasca) to examine the possible failure mechanisms. Modeling of the unloading of the pleistocene glacial overburden showed that subsequent redistribution of stress and strain fields in the flank had a strongly controlling influence on the geometry of the detachment zone. A sensitivity analysis of geotechnical parameters showed that the cohesion of the discontinuities was a fundamental parameter. The stability modeling for dry conditions also revealed that the failure mechanism was a combination of shear failure along preexisting discontinuities and development of brittle fractures propagation through the intact rock mass.

Coupled hydro-mechanical modeling demonstrated that slope stability was very sensitive to changes in water pressure. The existing fault zone crossing the rock slope induced an elevated water inflow due to the higher permeability and might therefore be, together with the long-lasting effects of ice unloading, a main factor for the slope instability.

Instabilities in the Monte Rosa east face

The Monte Rosa east face, Italian Alps, is one of the highest flanks in the Alps (2200–4600m asl). Steep hanging glaciers and permafrost cover large parts of the wall (Fig. 4). Since the end of the Little Ice Age (~1850), hanging glaciers and firn fields have retreated continuously. During recent decades, the glaciers of the Monte Rosa east face experienced an accelerated and drastic loss. Some glaciers have completely disappeared. New slope instabilities and detachment zones developed and resulted in enhanced rock fall and debris flow activity (Kääb et al. 2004, Fischer et al. 2006). In August 2005, an ice avalanche with a volume of more than $1x10^6$ m^3 occurred and in April 2007, a rock avalanche of about $0.3x10^6$ m^3 detached from the upper part of the flank.

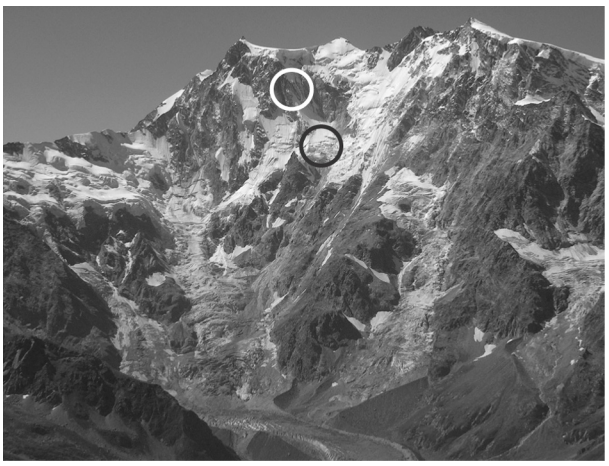

Figure 4: The Monte Rosa east face with the Belvedere glacier in the foreground (photo by L. Fischer, 2004). The detachment zone of the ice avalanche (2005) is marked with a black circle, the one of the rock avalanche (2007) in white.

Main focus of the investigations in the Monte Rosa east face was the assessment of the influence of glacier retreat and permafrost degradation on the current and possible future rock fall and ice avalanche activity (Fischer et al. 2006).

During field studies, the following data were compiled:

- Detailed geological and geomorphological mapping
- Current glacier extents
- Detailed map of the current detachment zones of mass movement activities

Due to difficult and dangerous in-situ access, this information was collected from distant ground-based and airborne observations.

Further analyses included:

- Modeling of the permafrost distribution
- Reconstruction of glacier extents since the early 20th century based on orthophotos and terrestrial photos

The results were compiled in a GIS and the overlay of each investigated factor revealed spatial as well as temporal linkages between investigated processes and their influence on the formation of new detachment zones.

The most important findings were that most detachment zones in the Monte Rosa east face are located in areas where surface ice has recently disappeared. In addition, many detachment zones are located at the altitude of the lower boundary of the estimated permafrost distribution, where presumably warm and degrading permafrost exists. A striking result is also that many detachment zones are situated in transition zones between orthogneiss and paragneiss. These findings demonstrate that the formation of detachment zones mostly seems to be caused by a combination of different factors.

Conclusion and perspectives

The investigation of slope stability in steep high-alpine rock wall is a major challenge, chiefly due to the difficulties in data acquisition and the complexity of the factors and processes influencing slope stability. In each case, the proceeding has to be adapted and different methodologies have to be applied concerning the possibilities of data acquisition and the required stability modeling method.

The case study of the Tschierva rock fall shows that the appropriate method combination including classic geological field investigation techniques, terrestrial and aerial image analyses and permafrost modeling allows to perform detailed numerical slope stability modeling and to evaluate possible failure mechanisms.

The much larger Monte Rosa east face with surface and subsurface ice subject to extremely fast changes, represents most challenging high-mountain conditions and required a more remote based approach. However, local field surveys could be integrated for a comprehensive spatial and temporal analysis of predisposing factors and their interaction.

In the future, measurement, analytical as well as modeling tools will be further advanced. For instance, ground-based SAR and helicopter-based LiDAR have only very recently been applied on large high-mountain walls and should be further developed. Advances are also expected with regard to a more comprehensive integration of high-technology data into slope stability assessment methods.

Acknowledgements

This project is funded by the Swiss National Science Foundation (project no. 200021-111967). We acknowledge constructive comments made by two reviewers and editor.

References

Aydin, A. & Basu, A. 2005. The Schmidt hammer in rock material characterization. *Engineering Geology* 81: 1-14.

Atzeni, C., Basso, M., Canuti, P., Casagli, N., Leva, D., Luzi, G., Moretti, S., PieraccinI, M., Sieber, A.J. & Tarchi, D. 2001. Ground-based radar interferometry for landslide monitoring and control. *Proceedings of the 'ISSMGE Field Workshop on Landslides and Natural/Cultural Heritage'. Trabzon (Turkey), 23-24 August 2001*: 195-209.

Ballantyne, C.K. 2002. Paraglacial Geomorphology. *Quarternary Science Reviews* 21: 1935-2017.

Baltsavias, E. P., Favey, E., Bauder, A., Boesch, H. & Pateraki, M. 2001. Digital surface modelling by airborne laser scanning and digital photogrammetry for glacier monitoring. *Photogrammetric Record* 17, 98, 243-273.

Barla, G. & Barla, M. 2001. Investigation and modelling of the Brenva Glacier rock avalanche on the Mount Blanc Range. *Proceedings of the ISRM Regional Symposium Eurock 2001, Espoo, Finlandia, 3-7 giugno, 2001*. 35-40.

Davies, M.C.R., Hamza, O. & Harris, C. 2001. The effect of rise in mean annual temperature on the stability of rock slopes containing ice-filled discontinuities. *Permafrost and Periglacial Processes* 12(1): 137-144.

Derron, M.-H., Jaboyedoff, M. & Blikra, L. H. 2005. Preliminary assessment of rockslide and rockfall hazards using a DEM (Oppstadhornet, Norway). *Natural Hazards and Earth System Sciences* 5: 285-292.

Eberhardt, E., Stead, D. & Coggan, J.S. 2004. Numerical analysis of initiation and progressive failure in natural rock slopes - the 1991 Randa rockslide. *Int. J. Rock Mech. Min. Sci.* 41: 69-87.

Fischer, L., Kääb, A., Huggel, C. & Noetzli, J. 2006. Geology, glacier retreat and permafrost degradation as controlling factors of slope instabilities in a high-mountain rock wall: the Monte Rosa east face. *Natural Hazards and Earth System Sciences* 6: 761-772.

Fischer, L., Huggel, C. & Lemy, F. 2007. Investigation and modelling of periglacial rock fall events in the European Alps. *EGU - Geophysical research abstracts*.

Gruber, S. & Haeberli, W. 2007. Permafrost in steep bedrock and its temperature-related destabilization following climate change. *Journal of Geophysical Research 112*: F02S18.

Gruber, S., Peter, M., Hoelzle, M., Woodhatch, I. & Haeberli, W. 2003. Surface temperatures in steep alpine rock faces – A strategy for regional-scale measurement and modeling. *Proceedings of the 8th International Confernce on Permafrost 2003, Zurich, Switzerland:* 325-330.

Günther, A. 2003. SLOPEMAP: programs for automated mapping of geometrical and kinematical properties of hard rock hill slopes. *Computer and Geosciences* 29: 865-875.

Hack, R. 2002. An evaluation of slope stability classification. *Proceedings of ISRM EUROCK 2002, Portugal, Madeira, Funchal, 25-28 Nov. 2002*: 3-32.

Haeberli, W., Wegmann, M. & Vonder Mühll, D. 1997. Slope stability problems related to glacier shrinkage and permafrost degradation in the Alps. *Eclogae geologicae Helvetiae* 90, 407-414.

Harris, C., Davies, M.C.R. & Etzelmüller, B. 2001. The assessment of potential geotechnical hazards associated with mountain permafrost in a warming global climate. *Permafrost and Periglacial Processes* 12(1): 145-156.

Hauck, C., Isaksen K., Vonder Mühll, D. & Sollid, J.L. 2004. Geophysical surveys designed to delineate the altitudinal limit of mountain permafrost: an example from Jotunheimen, Norway. *Permafrost and Periglacial Processes* 15:191-205.

Heincke, B. 2005. Determination of 3-D fracture distribution on an unstable mountain slope using georadar and tomographic seismic refraction techniques. *Doctoral thesis*, ETH Zurich.

Hoek, E. & Brown, E. 1997. Practical estimates of rock mass strength. *Int. J. Rock. Mech. Min. Sci. Abstr*. 27 (3): 1165-1186.

Hoelzle, M., Mittaz, C., Etzelmüller, B. & Haeberli, W. 2001. Surface energy fluxes and distribution models relating to permafrost in European mountain permafrost areas. *Permafrost and Periglacial Processes* 12: 53-68.

Jaboyedoff, M., Baillifard, F., Philippossian, F. & Rouiller, J.-D. 2004. Assessing fracture occurrence using "weighted fracturing densit": a step towards estimating rock instability hazard. *Natural Hazards and Earth System Science* 4: 83-93.

Janeras, M., Navarro, M., Arnó, G., Ruiz, A., Kornus,W., Talaya, J., Barberá, M. & López, F. 2004. LIDAR applications to rock fall hazard assessment in Vall de N´uria. *Proceedings of the 4th ICA Mountain Cartography Workshop, Vall de Núria, Catalonia, Spain*.

Kääb, A., Huggel, C., Barbero, S., Chiarle, M., Cordola, M., Epinfani, F., Haeberli, W., Mortara, G., Semino, P. Tamburini, A. & Viazzo, G. 2004. Glacier hazards at Belvedere glacier and the Monte Rosa east face, Italian Alps: Processes and mitigation. *Proceedings of the Interpraevent 2004 – Riva/Trient*.

Kääb, A., Huggel, C., Fischer, L., Guex, S., Paul, F., Roer, I., Salzmann, N., Schlaefli, S., Schmutz, K., Schneider, D., Strozzi, T. & Weidmann, I. 2005. Remote sensing of glacier- and permafrost-related hazards in high mountains: an overview. *Natural Hazards and Earth System Sciences* 5: 527-554.

Krautblatter, M. & Hauck, C. 2007. Electrical resistivity tomography monitoring of permafrost in solid rock walls. *Journal of geophysical research* 112: F02S20.

Noetzli, J., Gruber, S., Kohl, T., Salzmann, N. & Haeberli, W. 2007. Three-dimensional distribution and evolution of permafrost temperatures in idealizes high-mountain topography. *Journal of Geophysical Research* 112: F02S13.

Roncella, R. Forlani, G. & Remondino, F. 2005. Photogrammetry for geological applications: automatic retrieval of discontinuity in rock slopes. *Proceedings of SPIE-IS&T Electronc Imaging, SPIE* 5665: 17-27.

Skaloud, J., Vallet, J., Keller, K., Veyssiere, G. & Kölbl, O. 2005. HELIMAP: Rapid large scale mapping using handheld LiDAR/CCD/GPS/INS sensors on helicopters. *Proceedings of ION GNSS 2005 Congress, Long Beach, California*.

Singhroy, V. & Molch, K. 2004. Characterizing and monitoring rockslides from SAR techniques. *Advances in Space Research* 33: 290-295.

Stead, D., Eberhardt, E., Coggan, J. & Benko, B. 2001. Advanced numerical techniques in rock slope stability analyses-applications and limitations. Proceedings of the International Conference on Landslides-Causes, Impacts and Countermeasures, Davos 2001: 615-624.

Stead, D., Eberhardt, T. & Coggan, J.S. 2006. Developments in the characterization of complex rock slope deformations and failure using numerical modeling techniques. *Engineering Geology* 83: 217-235.

Wegmann, M., Gudmundsson, G.H. & Haeberli, W. 1998. Permafrost changes in rock walls and the retreat of Alpine glaciers: a thermal modelling approach. *Permafrost and Periglacial Processes* 9: 23-33.

Wyllie, D.C. & Mah, C.W. 2004. *Rock slope engineering, 4th ed.* New York: Spon Press, 431 pp.

II

On the influence of geological, topographic and cryospheric factors on slope instabilities: Statistical analyses of recent Alpine rock avalanches

Luzia Fischer*, Ross S. Purves**, Christian Huggel*, Jeannette Noetzli* and Wilfried Haeberli*

* Glaciology, Geomorphodynamics & Geochronology, Department of Geography, University of Zurich, Switzerland (luzia.fischer@geo.uzh.ch)

** Geographic Information Systems Unit, Department of Geography, University of Zurich, Switzerland

in preparation, NHESS

1 Introduction

Slope failures from steep rock walls have always taken place in mountain areas throughout history. This is a consequence of the steep topography of these areas and the high relief energy, but also of geological and structure-geological characteristics, climatic factors such as intense freeze-thaw activity and oversteepened slopes from glacier erosion (e.g. Cruden and Hu, 1993; Ballantyne 2002; Evans et al., 2002; Hall et al., 2002). However, during the past decades, an increased number of periglacial rock fall and rock avalanche events were observed in the European Alps and other high mountain ranges, and are thought to be related to some extent to changing conditions due to global warming, e.g., permafrost degradation or glacier shrinkage (e.g. Evans and Clague, 1994; Dramis et al., 1995; Barla et al., 2000; Fischer et al., 2006; Geertsema et al., 2006). Some events document the potential serious hazard related to slope instabilities in alpine flanks, such as the Brenva rock avalanche (Italy) in 1997, which detached from recently deglaciated terrain and increased the volume by erosion of snow and glacier ice on its runout path to about $2 \cdot 10^6$ m^3. This combined rock-ice avalanche killed two persons and damaged a hotel (Giani et al., 2001). An even more disastrous rock-ice avalanche occurred in 2002 on the northern slope of the Kazbek massive, Russian Caucasus. The impact of this massive rock/ice avalanche from the steep face on the Kolka glacier resulted in an almost complete erosion of the valley glacier and led to a $>100 \cdot 10^6$ m^3 avalanche causing the death of over 100 people in downstream areas (Haeberli et al., 2004). Rock avalanches often affect restricted areas due to limited runout distances. However, as a trigger factor for other periglacial hazards such as floods and debris flows, slope failures from steep faces can be highly hazardous and have the potential for far-reaching disasters. For hazard assessment, the location of possible slope instabilities is important. Furthermore, a better understanding of the impacts of climatic change on the high mountain environment and related slope instabilities has become increasingly important, not least because human settlements and activities have progressively extended towards endangered zones in many alpine regions.

Understanding the spatio-temporal variability of mass movement processes in high-alpine bedrock slopes requires the understanding of the processes relevant for local slope instability as well as knowledge about the spatial and temporal variability of the boundary conditions. Slope instability phenomena are related to a large variety of factors involving the physical environment (Cruden and Varnes, 1996). Thus, the assessment of slope instabilities in periglacial flanks requires knowledge about all these factors. The occurrence of these events is influenced by many quasi-static factors such as geology and terrain parameters (i.e., slope gradient, slope aspect, and elevation). Establishing statistical relationships between the present-day slope failures and the predisposing factors is one way to better understand the conditions under which such instabilities develop. This is important for the assessment of their impact and the anticipation of future events, assuming that future events would occur under similar geo-environmental conditions.

Different studies on the influence of geology, topography, permafrost (e.g. Noetzli et al., 2003) and some detailed analyses on individual slope failures have been performed (e.g. Barla and Barla, 2001; Eberhardt, 2004). GIS-based factor and susceptibility analyses are widely used for landslide processes. For slope failures from bedrock, some GIS-based factor studies exist (e.g. Ruff and Czurda, 2008; Baillifard et al., 2003). However, none of them included cryospheric factors. And for recent rock avalanches in the Central European Alps, neither comprehensive analyses of a large number of factors have ever been performed until now nor regional-scale analyses on periglacial slope failures.

To improve knowledge about landslide processes and their controlling factors in periglacial areas, we analyzed a large number of detachment zones of recent rock avalanche events in the Central European Alps. The major objectives of this study are (1) to reconstruct the topographic, lithological and cryospheric setting at the detachment zone and the history of slope change for observed rock avalanche events, and (2) to compare these factors with their spatial distribution and occurrence over the entire investigation area.

2 Background

The stability of mountain rock walls is given by different environmental factors including the topographic and geological setting, geomechanical properties, hydrogeology, glaciation, and permafrost occurrence. Changes in one or more of these factors may reduce slope stability and, often in combination with potential triggering factors such as earthquakes or heavy precipitation, lead to eventual slope failure (e.g. Cruden and Varnes, 1996; Fischer and Huggel, 2008). Currently, permafrost and glaciers are the factors most prone to changes due to their sensitivity to atmospheric warming. The changes are made strikingly evident by the retreat of Alpine glaciers, with an overall area loss since Little Ice Age (LIA) maximum around 1850 of almost 50% in 2000 (e.g. Zemp et al., 2006). Less immediately visible but also very significant are changes in Alpine permafrost. During the past century, subsurface temperatures have warmed by about 0.5 to 0.8°C in the upper tens of meters (e.g. Harris et al., 2009), and since the LIA maximum, the lower permafrost altitudinal limit is estimated to have risen vertically by about 1-2 m/year (Frauenfelder et al., 2001). Variations in glacier geometry or permafrost temperatures can have large impacts on the local rock wall stress field as well as the hydrologic and geomechanical properties and therefore influence rock wall stability (Evans and Clague, 1994; Haeberli et al., 1997; Wegmann et al., 1998; Davies et al., 2001). Different processes link warming permafrost and destabilisation of steep bedrock, such as the loss of ice bonding in fractures, reduction of shear strength, or increased hydrostatic pressure (e.g. Gruber and Haeberli, 2007). Oversteepened slopes due to glacial erosion and glacier retreat are generally thought to adjust rapidly to the changing stress conditions by a reduction of the slope gradient. Many historical landslides however are possibly conditioned by late Pleistocene deglaciation more than 10,000 years earlier (Cruden and Hu, 1993). In such cases, slope deterioration can be intensified by progressive failure processes over long time periods, which reduce rock mass strength. Progressive failure is predominately driven by the propagation of fractures through intact rock pieces between existing discontinuities (Einstein et al., 1983; Eberhardt et al., 2004; Prudencio and Van Sint Jan, 2007). The response of steep rock walls to changes as well as the failure mode, scale and timing is strongly determined by the topography and the geological setting, in particular the geometrical and geotechnical characteristics of discontinuities (Einstein et al., 1983; Ballantyne, 2002).

During the hot summer 2003, exceptional rock fall activity has been observed in the European Alps (Schiermeier, 2003; Keller, 2003; Gruber et al., 2004). These throughout small-volume events are likely related to the fast thermal reaction of the subsurface of steep rock slopes and an extension of

active layer thickness into ice-filled discontinuities (Gruber et al., 2004). Moreover, a large number of rockslides with volumes of more than $1 \cdot 10^6$ m^3 occurred in the European Alps during the past decades. Examples are the Brenva rock avalanches in the Italian Aosta Valley in January 1997 (total volume ca. $2 \cdot 10^6$ m^3; Barla et al., 2000; Giani et al., 2001; Bottino et al., 2002) and in November 1920 (Deline, 2001). The slope failure of the Val Pola landslide (Italy) in July, 1987 with a volume of about $40 \cdot 10^6$ m^3 caused several casualties and significant damage and detached at the altitude of the expected lower limit of mountain permafrost (Dramis et al., 1995, Giani et al., 2001; Govi et al., 2002; Crosta et al., 2004). A large event occurred in Val Zebrú near Bormio, from the Punta Thurwieser (Italy) in September, 2004 with a volume of about $2.5 \cdot 10^6$ m^3 (Cola, 2005; Sosio et al., 2008). An even larger event happened near Randa (Switzerland) in April, 1991, with a volume of about $30 \cdot 10^6$ m^3, destroying the main road and rail way line and damming the Vispa river with subsequent flooding of the village (Sartori et al., 2003; Willenberg, 2004; Eberhardt, et al., 2004). A collapse of a rock flank involving $2 \cdot 10^6$ m^3 occurred at the Eiger (Switzerland) in summer 2006, caused by recent glacier retreat (Oppikofer et al., 2008). And in October 2006, two rock avalanche events with volumes around $1 \cdot 10^6$ m^3 occurred at Dents du Midi and Dents Blanches in the western Swiss Alps. Such large-volume detachments evolve mostly over longer time periods than small ones and may be influenced by climatic and large-scale topographic rather than seasonal changes.

3 Regional setting

The study area covers a 25'000 km^2 region in the Central European Alps. The European Alps extend in a northward convex arc from Nice to Vienna and range from the Mediterranean sea level to a maximum altitude of 4'807 m a.s.l at Mont Blanc summit in the western part of the Alps. The Alpine range can be roughly divided into the Western Alps, the Central Alps and the Eastern Alps. The Central Alps compose quasi the connecting piece between the N-S oriented Western Alps in France and the E-W oriented Eastern Alps in Austria. In this study, mainly the area of the Central Alps is considered, including the entire Swiss Alps and the adjacent parts of the Italian and French Alps (see Fig. 1, inlet graphic).

The Alpine orogenesis started in the Cretaceous about 135 million years ago, proceeded during the Cenozoic and is still going on today with an uplift rate in the same magnitude as the erosion rate amounting to about 1 mm y^{-1} (Labhart, 1998). The Alpine range consists of different tectonic units, which are divided from north to south in the Helveticum, Penninicum, Austroalpine and Southern Alps (Labhart, 1998; Pfiffner, 2009). The Helveticum mainly consists of Mesozoic limestones, shales and marls that were originally deposited on the southern continental margin of the European continent. It forms the northern boundary of the Central Alps. The Penninicum has the highest metamorphic grade and is composed by large areas of gneiss from the crystalline basement and zones with ophiolite sequences and deep marine sediments, metamorphosed to phyllites, schists and amphibolites.

The Austroalpine contains parts of the African crystalline basement and sedimentary rocks. Main lithologies are schists, gneisses, dolomite and limestone that have only minor metamorphic overprint from the Alpine orogenesis. The Southern Alps are located south of the Insubric Line, the main suture zone in the European Alps and are composed of crystalline rock, volcanic rocks and Mesozoic sediments. In addition, the four massifs Aar Massif, Gotthard Massif, Aiguilles Rouges Massif and Mont Blanc Massif exist in the Central Alps, which mainly consist of gneiss and granite. Intrusions during the formation of the Alps are relatively sparse; the largest in the Central Alps is the Adamello granite.

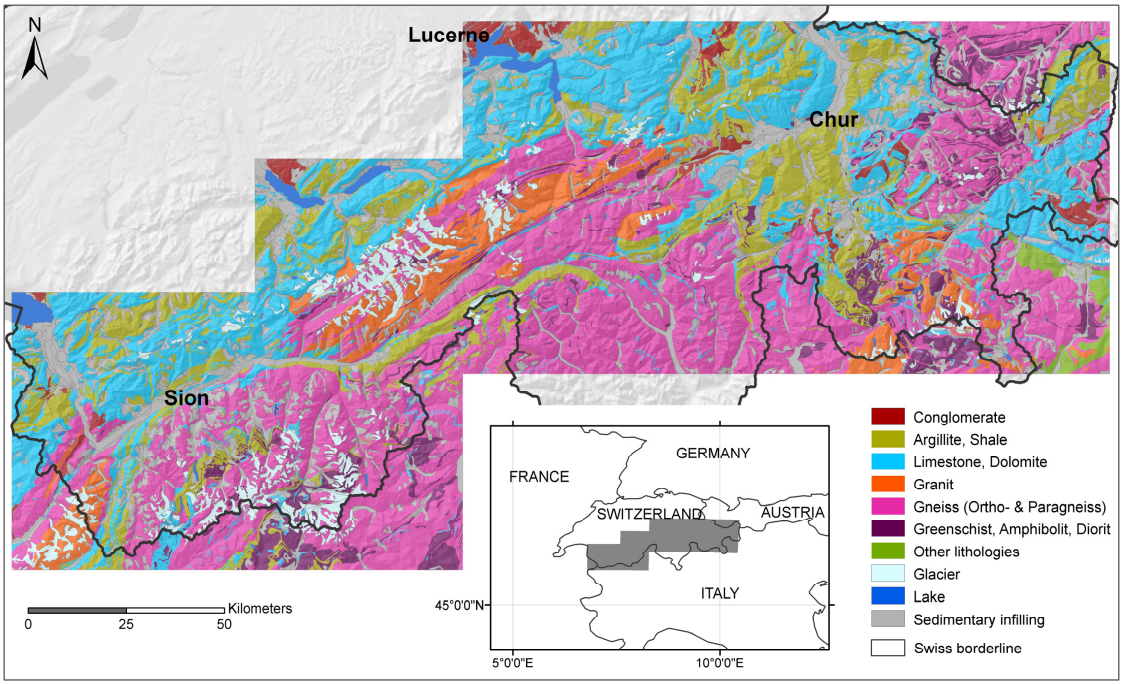

Fig. 1. Geological classification of the Central Alps derived from the Geotechnical Environmental Atlas of Switzerland V1/00 (© Swiss Geotechnical Commission; Geological basis data © Swiss Federal Office of Topography, Section Geological Survey).

Figure 1 shows a map with a simplified geological classification of the Central Alps deduced from the Geotechnical Environmental Atlas of Switzerland (© Swiss Geotechnical Commission; Geological basis data © Swiss Federal Office of Topography, Section Geological Survey). Note that this classification is based on lithology and not on tectonical units.

Late Pleistocene glacial cycles and periglacial weathering carved and shaped the European Alps. During the LGM (about 21,000 y BP), glaciers covered an area of about 150,000 km^2 in the European Alps (Keller and Krayss, 1998). With increasing air temperature after the LGM, glaciers started to retreat between 17,000 and 10,000 y BP (Keller, 1988). In 1999, the glaciers cover 2,270 km^2, which constitutes about half of the glacier-covered areas at the end of the Little Ice Age around 1850, when the glacier-covered area amounted to approx. 4,470 km^2 (Zemp et al., 2006). Figure 2 shows the distribution of glacier cover with respect to the elevation in the year 1999. The lower boundary of glaciation is at approximately 1600 m a.s.l. and glacier cover increases strongly with elevation. Above 3000 m a.s.l., 35–40% of the area is covered by glaciers.

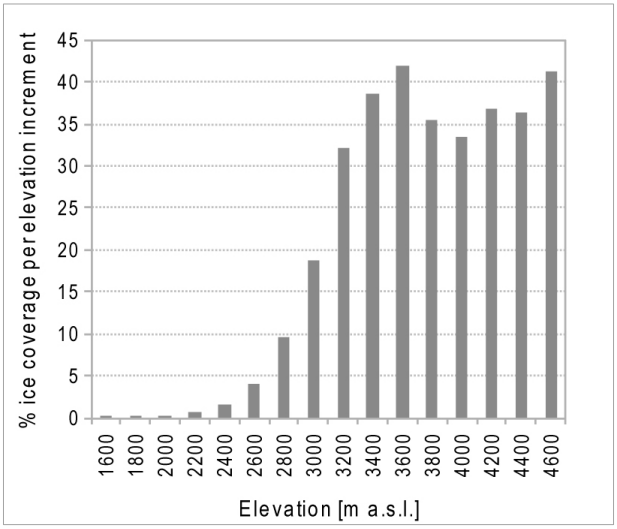

Fig. 2: Portion of glacier covered area with respect to elevation. The elevation is divided in 200 m increments, starting at 1600 m a.s.l.

Quaternary sediments are widespread in the periglacial zones, including alluvial cover, slope debris and moraine. These sediments can be found mainly in flat to moderately inclined slopes. Bedrock slopes show generally higher slope gradients from about 35° to vertical. Zemp (2002) identified a threshold of 34° for the separation of debris-covered and bedrock slopes based on analyses of the rock signature in topographic maps. Gruber and Haeberli (2007) introduced a gradient of 37° as an approximate threshold of steep rock slopes. In this study a threshold of 35° is chosen for the distinction between talus and bedrock. However, depending on local morphology debris accumulation can also occur in concave topography steeper than this threshold, for example in couloirs.

4 Data and Methodology

This study uses a GIS-based heuristic approach based on the intercorrelation of controlling environmental factors in the entire study area and at the detachment zones of recent rock avalanche events in the study area. A combination of different parameter maps were implemented by the use of GIS, as an important tool to provide the various functions for handling, processing, analyzing and reporting spatial data.

The primary basis of data used is a rock avalanche inventory, which contains 57 events that occurred between 1900 and 2007 in the Swiss Alps and adjacent areas in France and Italy. Figure 3 gives an overview of the spatial distribution of the events. The selection criteria for inclusion in the study are a detachment zone located above 2000 m a.s.l and an estimated volume around or larger than 1000 m^3. The study area is marked in colour in Figure 3. In addition, areas above 2000 m a.s.l. are marked in blue. Rapid mass movements from bedrock failures can be divided in classes, here by using the classification of Hungr et al. (2001): Rock fall typically involves relatively small volumes < 10’000 m3, whereas rock avalanches contain volumes of more than 10’000 m^3. To simplify matters, we use the term rock avalanche for the volumes between 1000-10’000 m^3, if both classes are included.

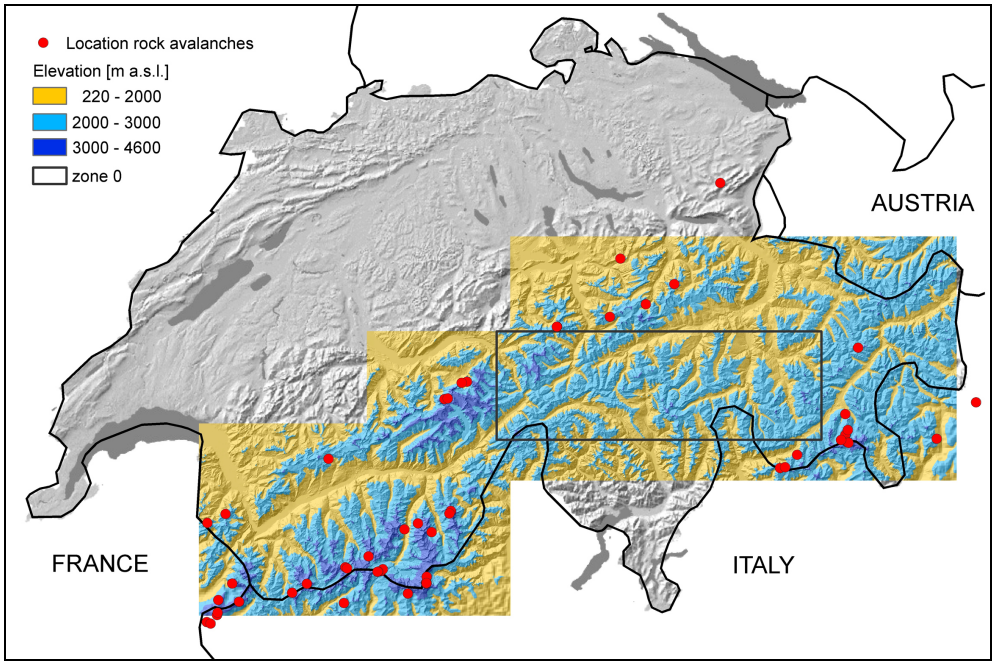

Fig 3. Investigation area and location of the rock avalanche events. For the DHM analyses, the coloured area was considered in this work including the alpine zone of Switzerland and adjacent areas. The black rectangle marks the specially investigated zone 0, where no rock avalanche events were recorded.

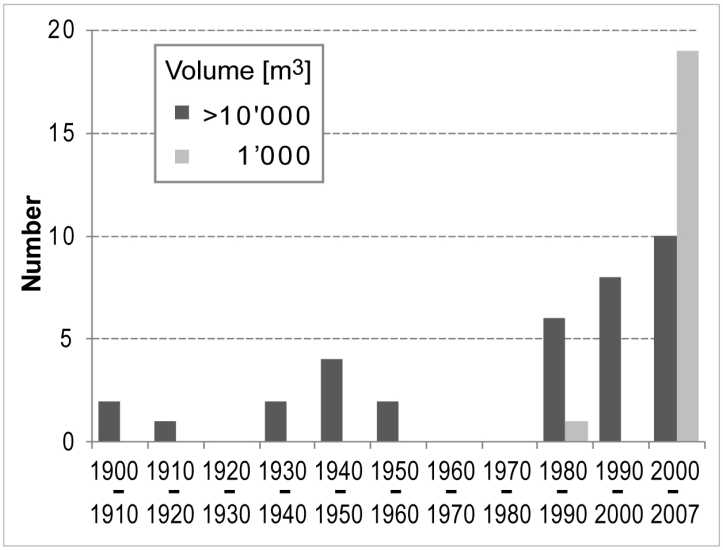

Fig. 4. Number of rock avalanche records per decade in the current and past century. The significant increase in number in the past three decades is difficult to interpret because of increased recording activities during this period.

The inventory is based on the one by Noetzli (2003), which has continuously been extended by information from scientific publications, newspaper articles, field observations, and personal comments. Since 1980 and especially between 2000–2007 more events were recorded than in the period before (Fig. 4). It is difficult to assess whether the number of slope instabilities has really increased during recent decades due to the influence of atmospheric changes and linked changes in periglacial terrain or if this increased number of recorded periglacial slope failures arises only from increased recording activity during recent decades and more observations because of enhanced economic and touristic developments in mountainous areas. However, the increased recording activity has to be considered in the analyses to prevent from a bias.

For the extraction of topographic attributes such as elevation, slope gradient or slope aspect, a digital elevation model with 25 m grid spacing (DHM25 Level 2, Swisstopo) was used. This dataset is based on the interpolation of contour lines from the Swiss National Map (1:25'000) and includes digitised lake perimeters, main break lines and spot heights (Swisstopo, 2004).

The geological setting of the study areas was deduced from the digital geotechnical map that is based on the Swiss Geotechnical Environmental Atlas (Swiss Geotechnical Commission). The classification was simplified to seven classes in order to allow investigations at a regional scale. The class *conglomerate* contains sandstone, marl, breccias; the class *shale/schist* contains Bündnerschiefer, argillite, shales, schists and similar lithologies; the class *limestone* contains limestone and dolomite; the class *granite* contains mainly granitic lithologies; the class *gneiss* contains both orthogneiss and paragneiss; the class *amphibolite* contains amphibolite, diorite, gabbro, peridotite, serpentinite, greenschist; and the class *others* contains radiolarian rock and quarzphyllite.

The glaciation history in the Swiss Alps since the maximum of the Little Ice Age (about 1850) was investigated to analyze the influence of glacier retreat on slope stability. The investigation was performed based on an existing digital glacier inventory of the Swiss Alps, which covers three periods. Maisch (1992) carried out a homogenous reconstruction of glacier extents around 1850 for glaciers of Grisons and the surrounding mountains based on the 'Siegfried map' series. For the year 1973 the data set was compiled from aerial photography (Müller et al., 1976), and for the year 1998 glacier outlines were reconstructed based on satellite images (Paul, 2004).

To estimate the lower boundary of the permafrost occurrence, a very basic approach was chosen. The primary factors determining the surface temperature of a rock wall are aspect (shortwave radiation) and altitude (sensible heat and longwave incoming radiation; cf. Noetzli et al., 2003).

The combination of these two topographic parameters was used and the elevation thresholds were adopted from the model PERMAKART (Haeberli, 1975; Keller, 1992). This model defines the lower limit of discontinuous permafrost occurrence in steep slopes to vary roughly between 2500 m in northern expositions and more than 3000 m a.s.l. in southern expositions (Haeberli, 1975; Gruber, 2004). Additionally, for the investigation of surface characteristics at the detachment zones of the rock avalanches, aerial images and terrestrial images were utilised and visually examined.

5 Results

5.1 Rock avalanches and topography

Elevation

This study focuses on periglacial rock slope failures and therefore analyses are concentrated on areas located above 2000 m a.s.l. (Fig. 3), which extend over 50% of the investigation area, areas below 2000 m a.s.l. are not included. The elevation interval between 2000 and 3000 m a.s.l. comprises an area of 13'500 km^2, which corresponds to 45% of the total area. The elevation interval between 3000 and 4600 m a.s.l. extends over 1'300 km^2, which corresponds to 5%. Fig. 4 shows the frequency distribution of the area in 200 m altitudinal intervals. In Figure 5, the bars in light grey concern the data set of the entire area above 2000 m a.s.l., while the ones in dark grey exclusively relate to the bedrock areas with slope gradients higher than 35° in the area the same altitudinal belt.

Comparing the elevation of bedrock areas with the elevation of the entire investigation area, a slight shift towards higher elevations is observed for bedrock areas. Looking at the distribution of the detachment zones of the events (marked in red in Fig. 5), the shift towards higher elevations becomes more pronounced. 40% of the rock avalanches (i.e. 22 events) started from the elevation interval between 2000 to 3000 m a.s.l. (i.e. 45% of the total area), whereas 60% of the rock avalanches (33 events) started above 3000 m a.s.l. (i.e., 5% of the total area).

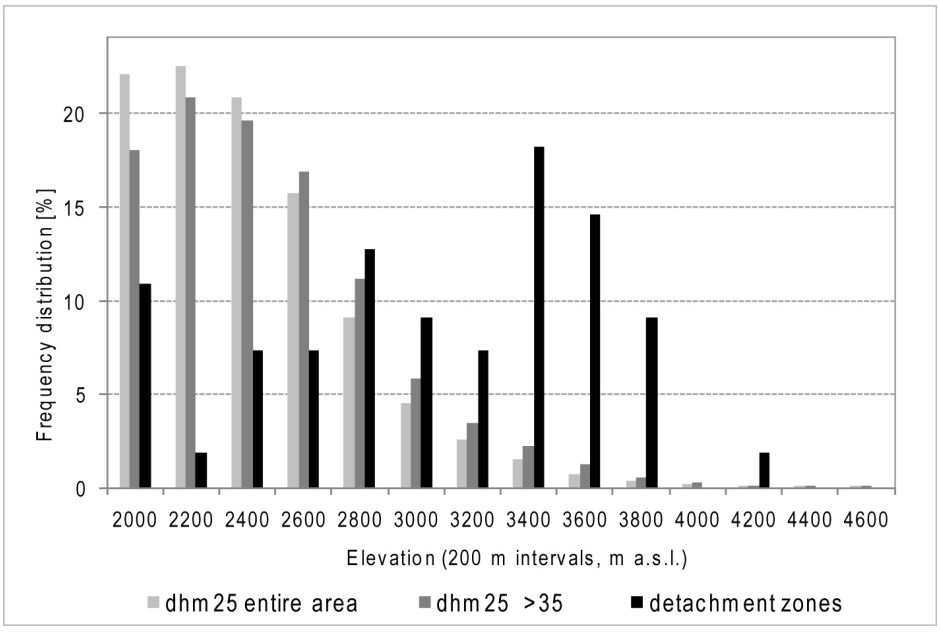

Fig 5. Area distribution with respect to elevation over the entire area (light grey), bedrock areas (dark grey) and rock avalanche detachment zones (black), calculated in 200 m elevation increments.

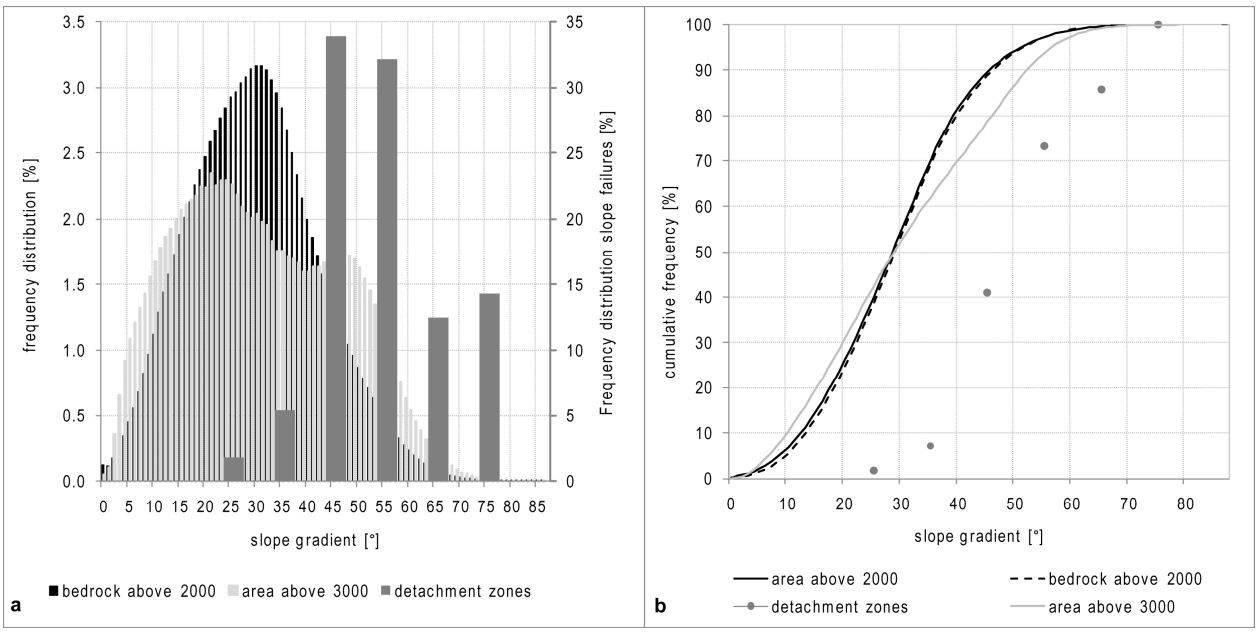

Fig. 6. Frequency distribution of slope gradients for the areas above 2000 m (black), the area above 3000 m a.s.l. (light grey), and the rock avalanche detachment zones (dark gray, in 10° intervals; 6a) and cumulative frequency of slope gradients for the same data sets (6b).

Slope gradient

As a fundamental driver of slope instability, the slope gradient is typically incorporated into bedrock failure analyses (e.g. Donati and Turrini, 2002; Ruff and Rohn, 2008). The slopes at higher elevations progressively become steeper. Between 1000 and 2800 m a.s.l., mean slope gradient calculated over the whole area is 27–30°, between 2800 and 3500 m a.s.l. 30–32° and above 3500 m a.s.l., mean slope gradient is around 35°. Similarly to the elevation ranges, the trend pattern of the slope gradient distribution was calculated for the area above 2000 m a.s.l. (light grey in Fig. 6), the bedrock areas above 2000 m a.s.l. (dark grey), areas above 3000 m a.s.l. (blue), and the detachment zones of the rock avalanches (red). The slope gradients of the bedrock areas are about 1° higher compared to the entire area above 2000 m a.s.l., which is clearly visible in the cumulative frequency distribution. The two samples above 2000 m show approximately normal distribution. The maximum of the slope gradient distribution of the entire area is at ca. 30° (Fig. 6a). The slope gradient frequency distribution only including areas above 3000 m, however, shows a different pattern: Two maxima exist at ca. 20° and 47° and a larger part of the area is located in flatter as well as steeper terrain than in the altitudinal belt 2000–3000 m. This is probably due to the occurrence of relatively more flat glaciers and steep bedrock areas. The rock avalanche detachment zones, in contrast, have very high slope gradients. Their frequency distribution is depicted in intervals of 10° in Figure 6. The highest frequency of detachment zones slope is between 40–60°. Higher values than 60° are common, but slope gradient values below 40° are rather rare. The cumulative frequency distribution of slope gradients at the detachment zones is about 20° higher than that over the entire area (Fig. 6b).

Slope aspect

Over the entire investigation area, the area proportion is roughly the same in all slope aspect directions. The detachment zones occur on slope of all aspects and no significant aspect-depending pattern could be observed. Therefore, the factor aspects will not be further discussed.

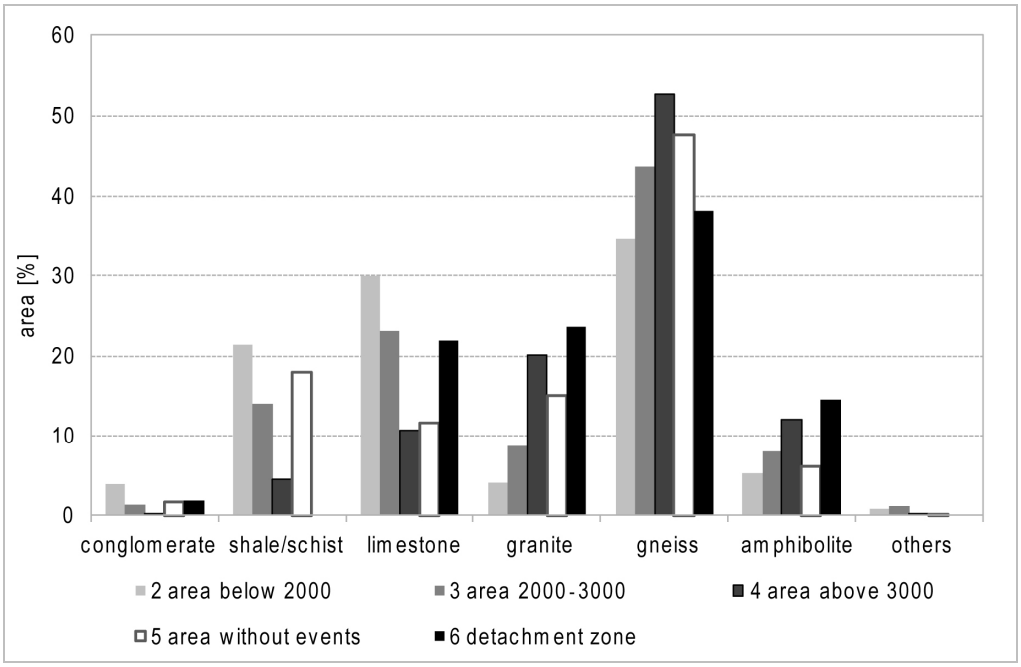

Fig. 7: Area proportion of the different lithological groups in different altitudinal belts (grey scales, statistics no. 2-4) and the lithological setting of the rock avalanche events (black, no. 6). Additionally, white bars depict the lithology distributions in the area without events recorded (no. 5).

5.2 Rock avalanches and lithology

Fig. 1 shows the spatial distribution of the lithological classes over the entire investigation area, Fig. 7 depicts the percental proportion of each class. The evaluations were performed for six data samples: Fig. 7 shows the lithology distributions for different altitudinal belts in grey scales (data sets 2-4), white bars (data set 5) depict the lithology distributions in a selected area without recorded events (c.f. Fig. 3) that will be discussed in Chapter 4.5, and the lithological setting at the detachment zones is displayed in black (data set 6).

With 40 %, *gneiss* covers the largerst proportion of the investigation area, followed by *limestone* (25%) and *shale* (17%). The proportion of all other lithology classes is less than 10%.The seven lithological classes are not equally distributed over altitude: *Conglomerates* and the class *others* do not exist above 3000 m a.s.l., and also the proportion of the groups *shale* and *limestone* decrease by 75% and 66% between the statistics 1 and 4. Contrastingly, the proportion of the lithologies *granite*, *gneiss* and *amphibolite* increases with elevation. *Gneiss* and *limestone* each cover an area of around 30% in the area below 2000 m a.s.l. Above 3000 m a.s.l. the proportion of *limestone* decreases to 10% whereas the one of *gneiss* strongly increases and is the predominant lithology with more than 50% area coverage. Most detachment zones are located in *gneiss* followed by *granite*, *limestone* and *amphibolite*. Figure 8 shows the proportion of the lithologies at the detachment zones normalised by the lithological proportions over the entire area in the two altitudinal belts 2000–3000 m a.s.l. and above 3000 m a.s.l. The value 1 denotes an equal lithological proportion of the detachment zones as over the entire area, values larger than 1 mean that proportionally more events occur in a lithology than this one is present over the entire area, and values below 1 indicate the opposite. In the area above 3000 m a.s.l., the proportion of the lithology at the detachment zones is comparable to the one over the entire area. In the altitudinal belt 2000–3000 m a.s.l., in contrast, large deviations from the lithology distribution of the entire area exist for all lithologies. In *limestone*, *granite* and *amphibolite* proportionally more events and in gneiss proportionally less events occured.

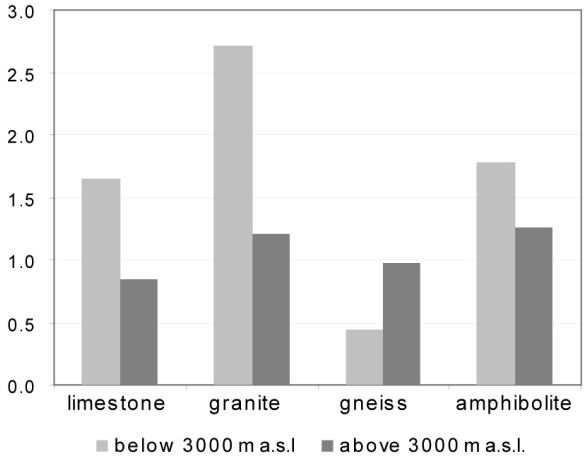

Fig. 8: Lithology of the detachment zones normalised by the lithology over the entire area for the two altitudinal belts 2000-3000 m a.s.l. and above 3000 m a.s.l

Fig. 9 shows the distribution of the cumulative frequency of slope gradients for each lithological group (different colours) for the entire area as well as for the bedrock area above 2000 m a.s.l. (black dashed). The lithological groups *conglomerate* and others have by far smaller slope gradients than the other lithologies and *limestone* and *granite* show higher slope gradients than the bedrock area. The differences in the pattern of cumulative slope gradients are strongly correlated with the elevation where the lithologies dominate. *Conglomerates* mainly occur in lower areas and build up flat topography whereas *granite* dominates in areas above 3000 m a.s.l. and forms steep slopes. However, *limestone* dominates more in areas below 3000 m a.s.l. but has comparable high slope gradients as *gneiss*. This indicates that slope gradients also depend on the geotechnical charactristics of a lithology and not only on the elevation as mentioned in 5.1.

The rock avalanche events were divided into four volumetric groups to analyse the connection of the lithological setting and the slope failure volume. For 54 events, a rough volume estimation was possible. The smallest volumetric class (1000m^3 – 10’000 m^3) contains 24 events, which corresponds to almost 50% of the data base.

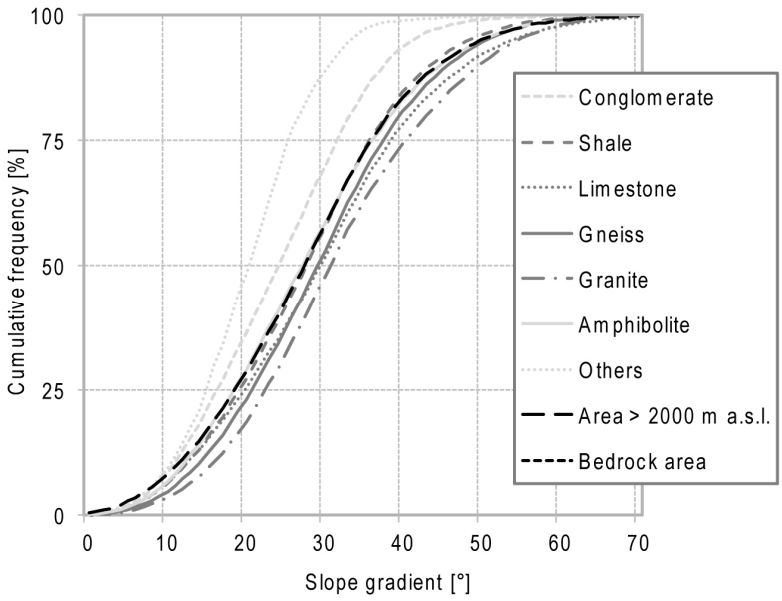

Fig. 9: Cumulative frequency of the slope gradient above 2000 m a.s.l.in the different lithological groups.

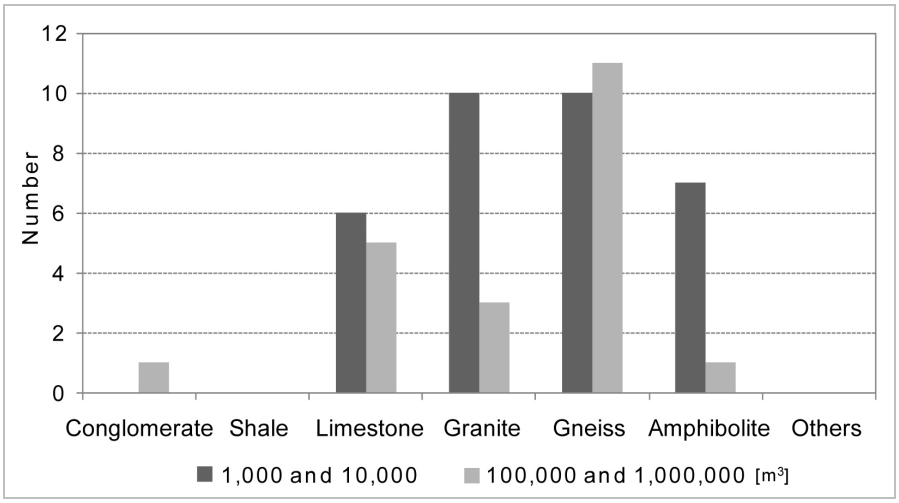

Fig. 10: Number of events of a particular volume class within the different lithologies.

Nine rock avalanche events had volumes larger than 10'000 m^3, the volume of 10 events exceeded 100'000 m^3 and 11 events were recorded with volumes > $1 \cdot 10^6$ m^3. Figure 10a shows the distribution of these volume classes among the lithologies, the two smaller and the two larger classes are combined. The lithology groups *conglomerate*, *others* and *schist* show zero or one record. This probably induces the fact that the portion of these lithologies are marginal, but also because they tend to other types of mass movements, e.g. slow moving deep-seated rotational landslides or continuous small-volume erosion.

The 1000 m^3 class is distributed over all other lithologies with a maximal count in *granite*. The classes g*ranite* and *amphibolites* show a pattern with a large number of small volume events and few events with very large volumes. The classes *limestone* and *gneiss*, on the contrary, show an equal number in both volume classes.

5.3 Rock avalanches and glaciation

About 35-40% of the surface above 3000 m a.s.l. is covered by glaciers and also at lower altitudes a considerable portion of the area is glacier covered (Fig. 2). Since the LIA, approximately half of the glacial cover disappeared (e.g. Zemp et al, 2006). The glacier retreat was proportionally largest between 1500 and 3000 m a.s.l. but is also documented above 4000 m a.s.l. Therefore, large areas of alpine rock walls are considered to be influenced by recent changes in glaciation.

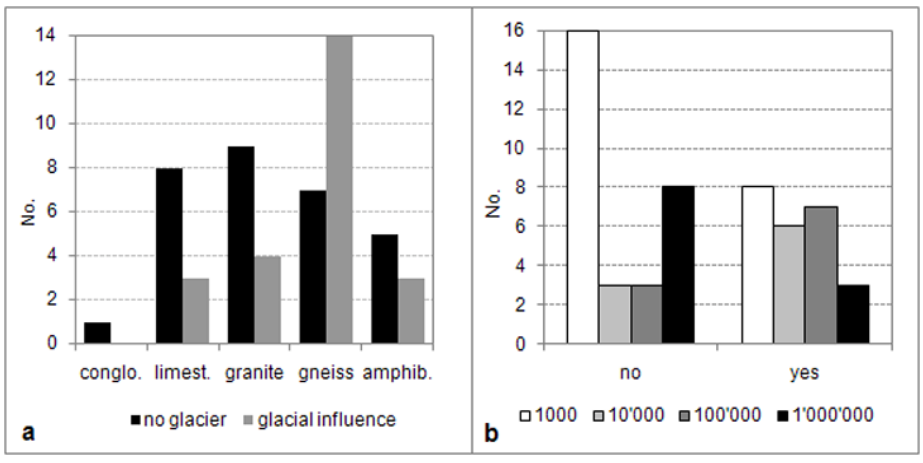

Fig. 11: a: Glaciation situation at failure time of each rock avalanche event, partitioned by the different lithologies. b: glaciation state distribution in the four volumetric classes (no = no recent glaciation, yes = adjacent glaciation).

In this study, the changes in glaciation since the LIA were assessed for each detachment zone. Based on the digital glacier inventory of the Swiss Alps, the glaciation state at and around the detachment zones was assessed for 1850, 1975 and 1998. The assessment of the glaciation at failure time was done based on visual comparisons of the location of the detachment zones with the glaciation map and additional information from the literature, maps, and photgraphs if available. 56% of the detachment zones were not glacier covered at failure time, but 44% of the detachment zones showed glaciation in direct vicinity.

Figure 11a displays the glaciation state for the slope failures, seperated in the different lithological classes. Figure 11b depicts the glaciation state of the detachment zones divided into the four volumetric classes. No glaciation (dark grey) means that there was no glacier in the flank or at the foot of the rockwall. Most of these locations were not affected by glaciation during the LIA, which means that the last glacial influence was likely during the LGM. The group with glacial influence (light grey) has either a valley glacier at the foot of the rockwall, which might directly impact the stress field in the flank, or glacier ice within the flanks. These locations were mostly ice covered during the LIA and we consider them to be influenced by recent glaciation and glacier retreat.

Fig. 11b reveals that in the smallest and largest volumetric classes, the count of glacial influenced detachment zones is only half of the one without recent glaciation. In the two intermediary classes, the pattern is inverted: The number of glacial influenced detachment zones is twice as much as without recent glaciation. Fig. 11a shows that in the lithologies *limestone* and *granite*, the number of events without glacier influence exceed the ones with glacier influence by far. In the *amphibolit* group, the distribution is similar. In the *gneiss* group, however, the number of events with glacier influence clearly exceeds the one without glacier. To check whether this is caused by the relatively higher portion of gneiss around the glaciers than granite and limestone, the frequency distribution of the lithologies in the vicinity of glaciers was calculated in a 100 m boundary zone around all glaciers. The frequency distribution of the lithologies at the glacier boundaries corresponds well with the regional frequency distribution over 3000 m a.s.l., where major glaciation is located.

Figure 12 shows the proportion of detachment zones with glacier presence normalised by the proportion of the glacier boundary lithologies. It becomes obvious that rock avalanche events in *gneiss* detach above proportion in glacier vicinity and *granite* below proportion in glacier vicinity.

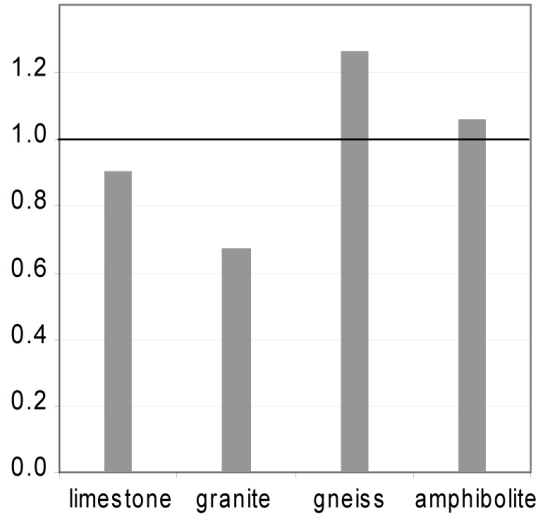

Fig. 12: Proportion of glacial influenced detachment zones normalised by the proportion of the glacier boundary lithologies.

Tab. 1. Seasonal distribution of the rock avalanche events, divided in the four volume classes.

Season	Volume [m^3]			
	>1‘000	>10‘000	>100‘000	>1‘000‘000
Dezember-March	1			3
April-Juni	2		3	2
Juli-Aug	16	1	4	2
Sept-Nov	1	3	2	4
unknown	4	5	1	

5.4 Rock avalanches and permafrost

Rock avalanche activity from steep bedrock walls varies in both, magnitude and seasonal timing. For the four volumetric classes of Fig. 11b, the seasonal distribution of the slope failures was analysed (Tab. 1), because processes involved in slope instabilities are presumably different for different volume classes and seasons. In the volume class between 1’000 and 10’000 m^3, a clear accumulation of events during the summer season is observed. A large number occurred during the extraordinary hot summer 2003. In the three larger volume classes no dominant pattern can be observed. Neither during summer months nor in the winter season an event accumulation can be observed and the distribution is quite equal over the whole year.

Rough estimations on possible permafrost occurrence at the detachment zones were based on the topographic location. Figure 13 displays the altitude of the detachment zones together with slope aspect. The two blue shades indicate the possible and probable permafrost occurrence based on the so-called ’rules of thumb’ by Haeberli (1975) implemented in the PERMAKART model (Keller, 1994). The two grey curves show the elevation of a modelled 0 °C-isotherm of near- surface temperatures in steep rock based on meteo data from the Corvatsch and Jungfraujoch stations as an indication of the lower permafrost boundary in steep rock (Gruber et al., 2004).

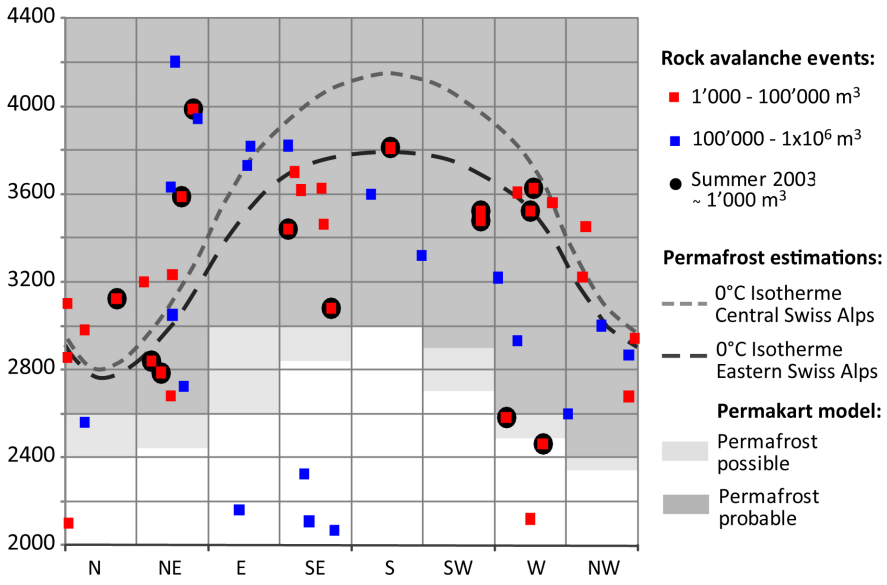

Fig. 13: The altitude of the detachment zones related to slope exposition as an information about the permafrost setting.The two blue shades indicate the possible and probable permafrost occurrence based on the PERMAKART, the two grey curves show the modelled 0 °C-isotherm based on meteo data from the Corvatsch and Jungfraujoch stations as an indication of the permafrost boundary (after Gruber et al., 2004).

The large difference in the permafrost boundary of 200–900 m altitude difference between the two methods mainly results from the basis of the two estimations. PERMAKART was calibrated for rock glacier areas in the Upper Engadine and tends to overestimate the permafrost occurrence in steep bedrock. The 0°C-isotherm is modelled for very steep rock and does not consider any snow cover. It therefore tends to underestimate the permafrost extent. The combination of the two, however, can be regarded as rough estimates of the lowest (PERMAKART) and uppermost (rock-0 °C-isotherm) altitude of the permafrost occurrence. For both methods it should be kept in mind that shading and local topography are not considered.

In Fig. 13, the rock avalanche events are divided again into two volumetric groups based on their volume. 6 events are located clearly outside permafrost, 12 are located above the rock-0 °C isotherm and therefore most likely in continuous permafrost. The other 34 detachment zones, hence the majority, are located below the 0 °C isotherm of Corvatsch but in areas where permafrost is possible or probable based on PERMAKART. The large volume events (green) generally detached at lower altitudes than the small volume events (red), except for 6 events with slope expositions NE and E. The distribution of the 46 detachment zones that are possibly located in permafrost shows a similar shape as the rock-0 °C isotherms. This might indicate similar thermal conditions and thermal influence on many of theses events. The above mentioned events of summer 2003 with volumes of around 1000 m^3 are additionally marked with a black framing. No obvious pattern in their distribution can be noticed. However, a slight concentration close to the modelled rock 0 °C isotherm of two-thirds of these events is observed.

5.5 Zone without rock avalanche records

In the central part of the Swiss Alps, a large area exists, where no rock avalanche was documented (Fig. 3). To investigate, whether there could be topographic, lithologic or other causes for the lack of rock avalanche events, a 4’800 km^2 large region (called zone 0) was investigated seperately and compared with the characteristics of the entire investigation area.Figure 7 shows that the frequency distribution of the lithology groups is comparable to the the entire area. Again, gneiss is the predominant lithology and the other main groups have percentage of around 10-15% each. However, a strongly increased proportion of schist exists, namely large areas of Bündnerschiefer.

Figure 14 depicts the elevation distribution in zone 0 normalised with the elevation distribution of the entire study area. Proportionally less area exist above 3000 in the zone 0 but slightly more between 2000 and 3000 m. Only 72 km^2 are located above 3000 m a.s.l. which corresponds to 1.5 % of the total area in zone 0, whereas over the entire area around 1200 km^2 are in this altitudinal belt, what corresponds to 5% of the entire area.

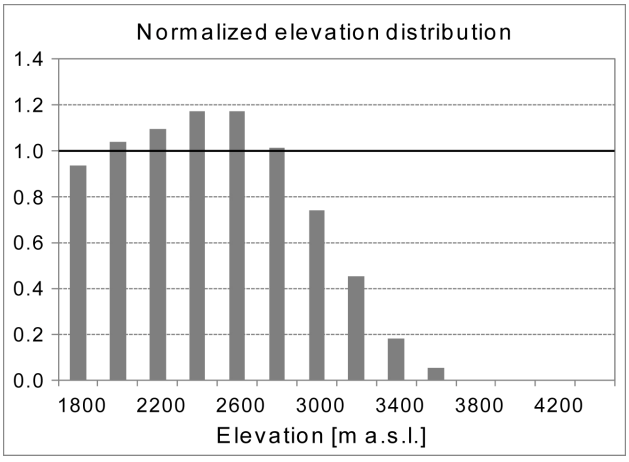

Fig. 14: Elevation distribution in zone 0 normalised with the elevation distribution over the entire area.

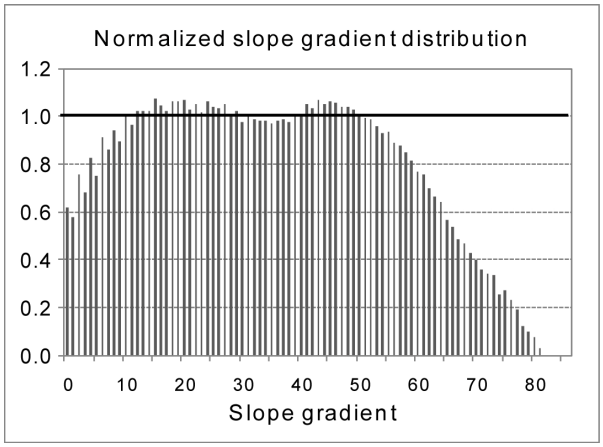

Fig. 15: Normalised slope frequency distribution of the zone 0.

A comparison of the slope gradients in the zone 0 with the ones over the whole investigation area was performed and the slope gradients of zone 0 were normalised with slope gradients over the whole area (Fig. 15). In the zone 0 proportionally less area with slope gradients larger than 50° occur. The proportion of areas in the zone 0 strongly decreases with increasing slope gradients.

6. Discussion

A rock avalanche inventory represents the spatial distribution of slope failure events and provides a fundament for the analysis of the empirical relation of instability and local predisposition factors. In this rock avalanche inventory study, slope failure susceptibility is explored with individual or combined predisposing factors such as elevation, slope gradient, geological setting, cryospheric factors and history of slope changes.

The number of events documented and the sampling technique are the first points that have to be considered when interpreting the results from statistical analyses. An increased frequency of rock avalanches was associated with climate change in other mountainous regions such as British Columbia (Geertsema et al., 2006). However, direct relationships between atmospheric warming, rock avalanche frequency and magnitude changes are difficult to establish, because historical records are especially for small-volume events almost certainly incomplete. We cannot draw conclusions about a possible increase in rock fall events based on the existing inventory because the recording activity strongly enhanced during the past decades because of both, increased activities in high mountain areas and higher public awareness of changing conditions in the Alps. This likely induces a bias in statements about the frequency of rock avalanche occurrences. Especially most small-volume events up to 10'000 m^3 were likely not documented before about the year 2000 if they did not have direct impact on people or infrastructure. Looking at large-volume events ($0.1 \cdot 10^6$ to $>1 \cdot 10^6$ m^3), however, a remarkable high number of 13 events during the past thirty years were documented. Only 8 events have been registered in the same volume class during the time period 1900–1980. Such large-volume events hardly remain unnoticed and we consider them to be known and documented for the whole time period since 1900 more or less completely. Based on these considerations, a recent increase in large-volume rock avalanche events is probable. A very interesting pattern of rock avalanche occurrence can be observed between 1900 and 1980. Between 1910 and 1930 and again between 1960 and 1980, very few records can be observed whereas between 1930 and 1960, comparably many events are recorded. The two periods without events correspond with two cold temperature periods, whereas the period with increasing records coincides with a warm temperature periods with strong glacier retreat. Although the number of events does not allow conclusions about this statistic, this pattern could indicate an increased rock avalanche activity during warm temperature periods with glacier retreat, as also assumed for the

recent increase of large slope failures since about 1980. Nevertheless, for both, large-volume as well as small-volume events, the inventory period has to be extended to allow for more reliable conclusions about frequency and magnitude trends.

Topography

Some remarkable results are found by comparing the topographic factors at the detachment zones with their occurrence in the entire investigation area. Detachment zones are not normally distributed with elevation, and the proportion of detachment zones is significantly increased at elevations above 2800 m a.s.l. and even more above 3400 m. The clearly smaller proportion of areas above 2800 m a.s.l. in the zone 0 could be one reason for the absence of rock avalanche in this zone, but does not entirely explain it The increased proportion of detachment zones above 3000 m a.s.l. could be a result of the higher glacier coverage in this altitudinal belt compared to areas below 3000 m a.s.l. and thus also relatively larger areas affected by recent glacier retreat. Although not considered in this study, these considerations also apply to permafrost occurrence, which inherently correlates with altitude. Below 2000 m a.s.l only little areas are within permafrost, above 3000 m a.s.l. permafrost is abundant and often continuous (BAFU MAP). The zone 0, on the contrary, shows very few glaciated areas.

The overall distribution of slope gradients at the detachment zones is shifted by about 15–20° towards steeper gradients compared to the area-wide slope gradients (Fig. 6b). The calculated slope gradients for the detachment zones are mean slope gradients and maximal values might be even higher. The slope gradients are calculated based on a DTM with 25 m grid resolution. This additionally leads to generally reduced slope gradients due to a smoothing of the topography. Slope gradients calculated from high-resolution DTMs with 1–2 m resolution, for example from LiDAR data, typically show slightly higher values in steep rock walls. Only 7% of the detachment zones show mean slope gradients below 40° and this value can be taken as a rough threshold for the critical slope gradient for rock avalanches in prospective susceptibility analyses.

Lithology

The classification of the lithologies required for a statistical analysis is a strong generalisation that might induce errors, because even similar lithologies can have very different geotechnical and geomechanical characteristics. A large part of the Central Alps constitutes of *gneiss*-type rock masses, containing both orthogneiss (from igneous rocks) and paragneiss (from sedimentary rocks); mineral constitution and metamorphic grade can vary strongly. Similarly, the mineral constitution can strongly vary in other lithological groups such as the *amphibolite* group. The classification has to be kept in mind when interpreting the results; for more detailed investigations of single detachment zones the lithological information has to be improved. The lithological groups are not equally distributed in the altitudinal belts. This is mainly a result of the location of the different tectonical units and their different geotechnical characteristics leading to differential erosion. The Helveticum and Penninicum containing main parts of the conglomerate, shale and limestone groups are located in the northern parts of the Alps with lower altitude, whereas the Austroalpine containing main parts of the gneiss, amphibolite and granite groups are located in the central to southern belts of the Alps showing higher elevations. Therefore, the proportion of conglomerate, shale, and limestone groups decreases at higher elevations, whereas the proportion of gneiss, granite and amphibolite increases (Fig. 7). The distribution of the lithologies of the detachment zones corresponds quite well with the area-wide lithology distribution. In high-alpine environments no lithology could be designated a significantly higher failure susceptibility than other lithologies. The normalisation of the detachment zones with the distribution of the lithologies over the entire area in Fig. 8, however, shows that granite has a proportionally high slope failure count in the

elevation belt between 2000 and 3000 m a.s.l., whereas in gneiss proportionally to the entire area less slope failures occur in this altitudinal belt. In the altitudinal belt above 3000 m a.s.l. the distribution of the detachment zones corresponds well with the portion of lithologies in the entire area.

The lithological setting seems to have a strong influence on the volume of the slope failures. The classes granite and amphibolite produce more smaller volumes, whereas gneiss and limestone produce small as well as large volumes. Such dependencies were already observed by Abele (1974).

Glaciation

Almost half of the rock avalanche events occurred in areas with recent changes in glaciation glacial influence, whereby recent means since the LIA. In the altitudinal belt 2000–3000 m a.s.l., for 6 of totally 21 detachment zones (29%) a glacier existed right below the failed area, above 3000 m a.s.l., 18 of totally 33 detachment zones (55%) had adjacent glacier cover. Several slope failures can be directly linked to recent glacier retreat, e.g., the Eiger rock slide (Oppikofer et al., 2008). Other events from the group without recent glacial influence are thought to be predisposed by the long-term effects of the retreat of the LGM glaciers, such as the Randa (Eberhardt et al., 2004) or Tschierva rock avalanche (Fischer et al., submitted).

Our investigations show that changes in glacier cover do not affect all volumetric classes in the same way. The smallest (<10'000 m^3) and largest volumetric groups (>$1 \cdot 10^6$ m^3) occur predominantly in areas without recent glacier influence. The latter are thought to be influenced by long-term effects of the retreat of the LGM glaciers, if there is a glacial influence at all. The smallest volumetric group shows many events in areas without glaciation. As most of these events are located in areas with probable permafrost occurrence (Fig. 14), they are probably more influenced by changes in the thermal regime. However, the intermediate volume classes seem to be often influenced or predisposed by glacier retreat. Cruden and Hu (1993) proposed an exhaustion model of temporal distribution of rock slope failures which basically suggests that the number of failures exponentially decreases with time following deglaciation. Accelerated and irreversible climate warming predicted for the coming century (IPCC, 2007), the continued down wasting of valley glaciers and unloading of adjacent rock walls, combined with a loss of steep ice and permafrost warming will negatively influence slope stability in the European Alps. The area of bedrock slopes influenced by glacier retreat will significantly increase and based on the assumptions of Cruden and Hu, the number of slope failures as a short-term reaction on the changes in topography, stress and thermal fields could first increase.

Permafrost

The permafrost boundaries are estimated with simple methods, and as no shadows and no detailed topography are considered, large uncertainties exist with both methods. A first assessment of the range of the lower altitudinal permafrost boundary is nevertheless possible. The comparison of the location of the detachment zones (altitude-aspect) with two basic permafrost altitudinal boundary estimates reveals a concentration of the detachment zones to areas between the estimated maximum and minimum permafrost boundaries. The detachment zones also show the same pattern in elevation as the permafrost boundaries with higher locations in southern and lower locations in northern direction. The zone between the estimated maximum and minimum permafrost boundaries can be interpreted as the marginal permafrost zone, probably most prone to changes. This is in agreement with ideas of Davies et al. (2001) and Haeberli et al., (1997) that warming ice in rock discontinuities becomes less stable a few degrees below the melting point, where mixtures of rock

water and ice exist. The marginal permafrost zones and the active layer zones are thought to be the areas where most recent changes have taken place concerning ice contents and hydrology.

The concentration of relatively small slope failures in the hot summer 2003 indicates changes in the near-surface parts of the permafrost, whereas the fact that several large-volume events occurred in winter time (e.g., the Brenva rock avalanche in January 1997) points to processes and changes that take place at greater depths and are related to long-term changes rather than to seasonal influences. Small-volume events correspond to changes and destabilisation of the near-surface layer (e.g., active layer thickening in the permafrost zone) and tend to react immediately to changes, large-volume events are more likely related to gradual warming at greater depths that are not influenced by seasonal variations of surface temperatures and develop over longer time periods. The ongoing atmospheric warming will increase the area subject to changes in permafrost temperatures. Especially the progressive thermal changes down to larger depths in the permafrost zones can influence the size of the future slope failures and lead to increased rock avalanche volumes. Important processes thereby may be convective heat transfer processes that can penetrate much faster and may be particularly favoured by rock discontinuity systems (Gruber and Haeberli, 2007). More detailed investigations on the thermal fields are required, such as e.g. the three-dimensional distribution and evolution of permafrost temperatures to enable a better process understanding (Noetzli et al., 2007).

7. Conclusions

Because of the relatively low number of rock avalanches in the study area, we concentrated on a more heuristic approach by comparing the characteristics of the detachment zones with the settings over the entire area. In this heuristic approach, the factors of lithological class, elevation, slope gradient, glacierisation state and permafrost conditions were included in the analyses. Slope gradient, elevation and recent glaciation changes were found to have the strongest deviations in their distribution in detachment zones and in the entire area and, hence, likely have a stronger influence on slope failures. Additionally, many slope failures occurred in areas of marginal permafrost, where warm permafrost is probable. Already minor changes in the subsurface temperatures could therefore strongly influence the slope stability in these areas. The lithology seems to influence the volume of a slope failure rather than the frequency.

The results of such factor analyses strongly depend on the quality of the basis data. One problem is the unsuitable resolution or inaccuracies of the basis data, for example the resolution of the geological map or uncertainties of coordinates and timing of rock avalanche events or simply a total lack of information what could lead to biased results. This study treats the detachment zones as point data as their location and exact extent are rarely known. However, mostly the topography of the surrounding area has also effects on the slope stability such as steepening, strong curvatures, etc. For further studies, the whole areas detachment zones should be considered for the investigation and also the surrounding area. However, investigations within this study have shown that more detailed topographic analyses require DTMs with higher resolution than 25 m.

The results of this analysis of detachment zones as well as the entire area have shown that areas of increased susceptibility could be distinguished descriptively identifying areas with critical factors. However, to enhance the significance of the statistical analyses a larger data base of rock avalanche events would be necessary. For susceptibility mapping over large areas, a multi-criterion approach based on the factors investigated within this study could be applied with an additional rating of the individual factors. Simple GIS-based spatial factor analyses can be used for such first-order susceptibility analyses and contribute to the detection of hot spots, where critical factor combinations occur.

References:

Abele, G.: Bergstürze in den Alpen; ihre Verbreitung, Morphologie und Folgeerscheinungen, Wissenschaftliche Alpenvereinshefte, 25, 230 pp., 1974.

Baillifard, F., Jaboyedoff, M., and Sartori, M.: Rockfall hazard mapping along a mountainous road in Switzerland using a GIS-base parmeter rating approach. Natural Hazards and Earth System Science, 3, 431-438, 2003

Ballantyne, C.K.: Paraglacial Geomorphology, Quarternary Science Reviews, 21, 1935-2017, 2002.

Barla, G., and Barla, M.: Investigation and modelling of the Brenva Glacier rock avalanche on the Mount Blanc Range, ISRM Regional Symposium Eurock 2001, Balkema, Rotterdam, Espoo, Finlandia, 2001.

Barla, G., Dutto, F., and Mortara, G.: Brenva Glacier rock avalanche of 18 January 1997 on the Mont Blanc range, northwest Italy, Landslide news 13, 2-5, 2000.

Bottino, G., Chiarle, M., Joly, A., and Mortara, G.: Modelling rock avalanches and their relation to permafrost degradation in glacial environments, Permafrost and Periglacial Processes, 13, 283–288, 2002.

Cola, G.: The large landslide of the south-east face of Thurwieser peak (Thurwieser-Spitze) 3658 m (Upper Valtellina, Italy), Terra glacialis, 8, 38– 45, 2005.

Crosta, G. B., Chen, H., and Lee, C. F.: Replay of the 1987 Val Pola Landslide, Italian Alps, Geomorphology, 60, 127-146, 2004.

Cruden, D.M., and Hu, X-Q.: Exhaustion and steady state models for predicting landslide hazards in the Canadian Rocky Mountains, Geomorphology, 8, 279-285, 1993.

Cruden D.M., and Varnes D.J.: Landslide types and processes. In: Landslides, Investigation and Mitigation, 36–75, 1996.

Davies, M. C. R., Hamza, O., and Harris, C.: The effect of rise in mean annual temperature on the stability of rock slopes containing ice-filled discontinuities. Permafrost and Periglacial Processes 12(1), 137–144, 2001.

Deline, P.: Recent Brenva rock avalanches (Valley of Aosta): New chapter in an old story?, Suppl. Geogr. Fis. Dinam. Quat. V, 55-63, 2001.

Donati, L., and Turrini, M.C.: An objective method to rank the importance of the factors predisposing to landslides with the GIS methodology: application to an area of the Apennines (Valnerina; Perugia, Italy), Engineering Geology, 63, 277-289, 2002.

Dramis, F., Govi, M., Gugliemin, M., and Mortara, G.: Mountain permafrost and slope instability in the Italian Alps: the Val Pola Landslide. Permafrost and Periglacial Processes, 6, 73-82, 1995.

Eberhardt, E., Stead, D., and Coggan, J.S.: Numerical analysis of initiation and progressive failure in natural rock slopes – the 1991 Randa rockslide, International Journal of Rock Mechanics and Mining Sciences, 41, 69-87, 2004.

Einstein, H.H., Veneziano, D., Baecher, G.B., and O'Reilly, K.J.: The effect of discontinuity persistence on rock slope stability, International Journal of Rock Mechanics and Mining Sciences Abst., 20(5), 227-236, 1983.

Evans, S. G. and Clague, J. J.: Recent climatic change and catastrophic geomorphic processes in mountain environments, Geomorphology 10, 107-128, 1994.

Evans, S. G., Scarascia Mugnozza, G., Strom, A. L., and Hermanns, R. L.: Landslides from Massive Rock Slope Failure and Associated Phenomena. In: Landslides from Massive Rock Slope Failure. S. G. Evans, G. Scarascia Mugnozza, A. L. Strom, R. L. Hermanns, A. Ischuk and S. Vinnichenko (eds.), IV. earth and Environmental Sciences, 49, 3-52, 2002.

Fischer, L. and Huggel, C.: Methodical design for stability assessments of permafrost affected high-mountain rock walls, in: Proceedings of the 9th International Conference on Permafrost, edited by: Kane, D.L., Hinkel, K.M., University of Alaska, Fairbanks, Alaska, Volume 1, 439-444, 2008.

Fischer, L., Kääb, A., Huggel, C. and Noetzli, J.: Geology, glacier retreat and permafrost degradation as controlling factors of slope instabilities in a high-mountain rock wall: Monte Rosa east face. Natural Hazards and Earth System Science, 6, 761-772, 2006.

Fischer, L., Amann, F., Moore, J.R., and Huggel, C.: The 1988 Tschierva rock avalanche (Piz Morteratsch, Switzerland): An integrated approach to periglacial rock slope stability assessment. Engineering Geology, submitted.

Frauenfelder, R., Haeberli, W., Hoelzle, M., Maisch, M..: Using relict rockglaciers in GIS-based modelling to reconstruct younger dryas permafrost distribution patterns in the Err-Julier area, Swiss Alps. Norwegian Journal of Geography, 55 (4), 195-202, 2001.

Geertsema, M., Clague, J.J, Schwab, J.W. and Evans, S.G.: An overview of recent large catastrophic landslides in northern British Columbia, Canada, Engineering Geology 83, 120-143, 2006.

Giani, G. P., Silvano, S. and Zanon, G.: Avalanche of 18 January 1997 on Brenva glacier, Mont Blanc Group, Western Italian Alps: an unusual process of formation, Annals of Glaciology, 32, 333-338, 2001.

Govi, M., Gulla, G. and Nicoletti, P. G.: Val Pola rock avalanche of July 28, 1987, in Valtellina (Central Italian Alps), Geological Society of America, Reviews in Engineering Geology XV, 71-89, 2002.

Gruber, S., Haeberli, W.: Permafrost in steep bedrock and its temperature-related destabilization following climate change. Journal of Geophysical Research, 112, F02S18, 2007.

Gruber, S., Hoelzle, M., and Haeberli, W.: Permafrost thaw and destabilization of Alpine rock walls in the hot summer of 2003, Geophysical Research Letter, 31, L13504, doi:10.1029/2004GL0250051, 2004.

Haeberli W.: Untersuchungen zur Verbreitung von Permafrost zwischen Flüelapass und Piz Grialetsch (Graubünden), Mitteilungen der Versuchsanstalt für Wasserbau, Hydrologie und Glaziologie, 17, ETH Zürich, 1975.

Haeberli, W., Wegmann, M., and Vonder Mühll, D.: Slope stability problems related to glacier shrinkage and permafrost degradation in the Alps, Eclogae Geologicae Helvetiae, 90, 407–414, 1997.

Haeberli, W., Huggel, C., Kääb, A., Polkvoj, A., Zotikov I., and Osokin, N.: The Kolka-Karmadon rock/ice slide of 20 September 2002: An extraordinary event of historical dimensions in North Ossetia, Russian Caucasus, Journal of Glaciology, 50(171), 533–546, 2004.

Hall, K., Thorn, C. E., Matsuoka, N., and Prick, A.: Weathering in cold regions: some thoughts and perspectives. Progress in Physical Geography, 26(4), 577-603, 2002.

Harris, C., Arenson, L.U., Christiansen, H.H., Etzelmüller, B., Frauenfelder, R., Gruber, S., Haeberli, W., Hauck, C., Hölzle, M., Humlum, O., Isaksen, K., Kääb, A., Kern-Lütschg, M.A., Lehning, M., Matsuoka, N., Murton, J.B., Nötzli, J., Phillips, M., Ross, N., Seppälä, M., Springman, S.M., Vonder Mühll, D.: Permafrost and climate in Europe: Monitoring and modelling thermal, geomorphological and geotechnical responses. Earth Science Reviews, 92, 117-171, 2009.

Hungr, O., Evans, S.G., Bovis, M.J., Hutchinson, J.N.: A review of the classification of landslides of the flow type. Environmental and Engineering Geoscience 7(3), 221 , 2001.

IPCC: Climate Change 2007: The Physical Science Basis. Contribution of Working Group 1 to the Fourth Assessment Report of the Intergovernmental Panel on Climate Change (eds. S. Solomon, D. Qin, M. Manning, Z. Chen, M.C. Marquis, K. Averyt, M. Tignor and H.L. Miller). Intergovernmental Panel on Climate Change, Cambridge and New York, 2007.

Keller, F.: Kurzbericht über die Steinschlagereignisse im heissen Sommer 2003 im Bergell (Project report on rock fall 2003 to the Kanton Graubünden), Inst. Für Tourismus und Landschaft Acad. Engiadina, Samedan, Switzerland, 2003.

Keller, O.: Ältere spätwürmzeitliche Gletschervorstösse und Zerfall des Eisstromnetzes in den nördlichen Rhein-Alpen (Weissbad-Stadium/Bühl-Stadium). Schriftenreihe Physische Geographie, 27, Band A & B: 241 pp. & 291 pp, 1988.

Keller, O. & Krayss, E.: Datenlage und Modell einer Rhein-Linth- Vorlandvergletscherung zwischen Eem-Interglazial und Hochwürm, In: Ikinger, A. (ed.): Festschrift Wolfgang Schirmer, GeoArchaeoRhein, 2, 121–138, 1998.

Labhart, T.P.: Geologie der Schweiz. Ott Verlag, 211 pp., 1998.

Maisch, M.: Die Gletscher Graubündens. Rekonstruktion und Auswertung der Gletscher und deren Veränderungen seit dem Hochstand von 1850 im Gebiet der östlichen Schweizer Alpen (Bündnerland und angrenzende Regionen), Geographisches Institut der Universität Zürich, Physische Geographie, 33, Part A: 324 pp., Part B: 128 pp., 1992.

Müller, F., Caflish, T., and Müller, G.: Firn und Eis der Schweizer Alpen, Gletscherinventar. Geographisches Institut, vdf-Verlag, ETH Zürich, 57, 174 pp., 1976.

Noetzli, J.: Felsstürze aus Permafrost über Gletscher – Ansätze zur GIS-basierten Modellierung, MSc-Thesis, University of Zurich, 122 pp., 2003.

Noetzli, J., Hoelzle, M., and Haeberli, W.: Mountain permafrost and recent Alpine rock-fall events: a GIS-based approach to determine critical factors, in: Proceedings of the 8th International Conference on Permafrost, Zurich, Switzerland, 2, 827-832, 2003.

Noetzli, J., Gruber, S., Kohl, T., Salzmann, N., and Haeberli, W. Three-dimensional distribution and evolution of permafrost temperatures in idealized high-mountain topography. Journal of Geophysical Research, 112, F02S13, doi:10.1029/ 2006JF000545, 2007.

Oppikofer, T., Jaboyedoff, M., and Keusen, H.-R.: Collapse at the eastern Eiger flank in the Swiss Alps, Nature Geoscience, 1, 531-535, 2008.

Paul, F.: The new Swiss glacier inventory 2000 - Application of remote sensing and GIS, PhD Thesis, University of Zurich, 198 pp., 2004.

Pfiffner, A.: Geologie der Alpen, UTB, Stuttgart, 2009.

Prudencio, M., Van Sint Jan, M.: Strength and failure modes of rock mass models with non-persistent joints, International Journal of Rock Mechanics and Mining Sciences, 44, 890-902, 2007.

Ruff, M., and Czurda, K.: Landslide susceptibility analysis with a heuristic approach in the Eastern Alps (Vorarlberg, Austria). Geomorphology, 94, 314-324, 2008.

Ruff, M., and Rohn, J.: Susceptibility analysis for slides and rockfall: an example from the Northern Calcareous Alps (Vorarlberg, Austria), Environmental Geology, 55(2), 441-452, 2008.

Sartori, M., Baillifard, F., Jaboyedoff, M., and Rouiller, J.-D.: Kinematics of the 1991 Randa rockslide (Valais, Switzerland), Natural Hazards and Earth System Sciences, 3, 423-433, 2003.

Schiermeier, Q.: Alpine thaw breaks ice over permafrost's role, Nature, 424, 712, 2003.

Sosio, R., Crosta, G. B., and Hungr, O.: Complete dynamic modeling calibration for the Thurwieser rock avalanche (Italian Central Alps), Engineering Geology, 100(1-2), 11-26, 2008.

Swisstopo (2004). DHM25 - The digital height model of Switzerland. Product Information, http://www.swisstopo.admin.ch/internet/swisstopo/en/home/products/height/dhm25.html.

Wegmann, M., Gudmundsson, G. H., and Haeberli, W.: Permafrost changes in rock walls and the retreat of Alpine glaciers: a thermal modelling approach, Permafrost and Periglacial Processes, 9, 23-33, 1998.

Willenberg, H.: Geologic and kinematic model of a complex landslide in crystalline rock (Randa, Switzerland), Engineering Geology. Zurich, ETH Zurich. Doctoral Thesis, 2004.

Zemp, M.: GIS-basierte Modellierung der glazialen Sedimentbilanz, Diplomarbeit, Geographisches Institut, Universität Zürich, 99 pp., 2002.

Zemp, M., Paul, F., Hoelzle, M., and Haeberli, W.: Glacier fluctuations in the European Alps 1850–2000: an overview and spatiotemporal analysis of available data, in: The darkening peaks: Glacial retreat in scientific and social context, edited by: Orlove, B., Wiegandt, E., and B. Luckman, University of California Press, 152–167, 2006.

Nat. Hazards Earth Syst. Sci., 6, 761–772, 2006
www.nat-hazards-earth-syst-sci.net/6/761/2006/

Natural Hazards and Earth System Sciences

Geology, glacier retreat and permafrost degradation as controlling factors of slope instabilities in a high-mountain rock wall: the Monte Rosa east face

L. Fischer, A. Kääb, C. Huggel, and J. Noetzli

Glaciology and Geomorphodynamics Group, Department of Geography, University of Zurich, Winterthurerstrasse 190, 8057 Zürich, Switzerland

Received: 21 February 2006 – Revised: 3 July 2006 – Accepted: 18 August 2006 – Published: 11 September 2006

Abstract. The Monte Rosa east face, Italian Alps, is one of the highest flanks in the Alps (2200–4500 m a.s.l.). Steep hanging glaciers and permafrost cover large parts of the wall. Since the end of the Little Ice Age (about 1850), the hanging glaciers and firn fields have retreated continuously. During recent decades, the ice cover of the Monte Rosa east face experienced an accelerated and drastic loss in extent. Some glaciers have completely disappeared. New slope instabilities and detachment zones of gravitational mass movements developed and enhanced rock fall and debris flow activity was observed. This study is based on multidisciplinary investigations and shows that most of the detachment zones of rock fall and debris flows are located in areas, where the surface ice disappeared only recently. Furthermore, most of these detachment zones are located in permafrost zones, for the most part close to the modelled and estimated lower boundary of the regional permafrost distribution. In the view of ongoing or even enhanced atmospheric warming and associated changes it is therefore very likely that the slope instabilities in the Monte Rosa east face will continue to represent a critical hazard source.

1 Introduction

Perennially frozen and glacierised mountain regions react very sensitively to changes in atmospheric temperature (Haeberli and Beniston, 1998; Harris et al., 2001). As a consequence, climatic developments during the 20th century have caused pronounced effects in the glacial and periglacial belts of high mountain areas. The changes are made strikingly evident by, for example, the retreat of Alpine glaciers (Paul et al., 2004; Zemp et al., 2006). Less immediately visible but also very significant are changes in Alpine permafrost. During the past century, it has warmed by about 0.5 to 0.8°C in the upper tens of meters (Harris and Haeberli, 2003; Harris et al., 2003). Since the Little Ice Age maximum (about 1850), the lower permafrost limit is estimated to have risen vertically by about 1 m/year (Frauenfelder, 2005).

Steep high-mountain rock walls, which are often characterised by hanging glaciers and firn fields covering extensive parts of the flank as well as widespread permafrost occurrence, are also strongly influenced by these changes. The slope stability of such flanks is influenced by a number of factors. The temperature and stress fields in rock and ice as well as the hydrological regime, however, have a significant influence (Davies et al., 2001). Changes in surface and subsurface ice might change these factors strongly and, especially in combination with unfavourable geological factors – discontinuities and lithology – slope instabilities can develop and cause enhanced mass movement activities such as rock fall, debris flows and ice avalanches (Haeberli et al., 1997; Ballantyne, 2002). However, interactions and processes are extremely complex and some major aspects of such slope instabilities are still understudied or even unknown. Especially the interactions between glacier and permafrost in steep flanks and their interaction with other factors are poorly understood.

The shrinkage of hanging glaciers in steep rock walls may uncover large areas of bedrock and leads to changed temperature and stress fields in the rock to great depths (Wegmann et al., 1998; Haeberli et al., 1999; Kääb, 2005). Additionally, the formerly ice covered rock is unprotected from mechanical and thermal erosion. The penetration of the freezing front into previously thawed or unfrozen material has the potential to intensify rock destruction through ice formation in cracks and fissures (Hallet et al., 1991; Haeberli et al., 1997; Matsuoka et al., 1998; Kneisel, 2003). Such ice formation, in turn, reduces the near-surface permeability of the rock walls involved and may cause increased hydraulic pressures inside the non-frozen fissured rock sections.

Correspondence to: L. Fischer
(luzfisch@geo.unizh.ch)

Published by Copernicus GmbH on behalf of the European Geosciences Union.

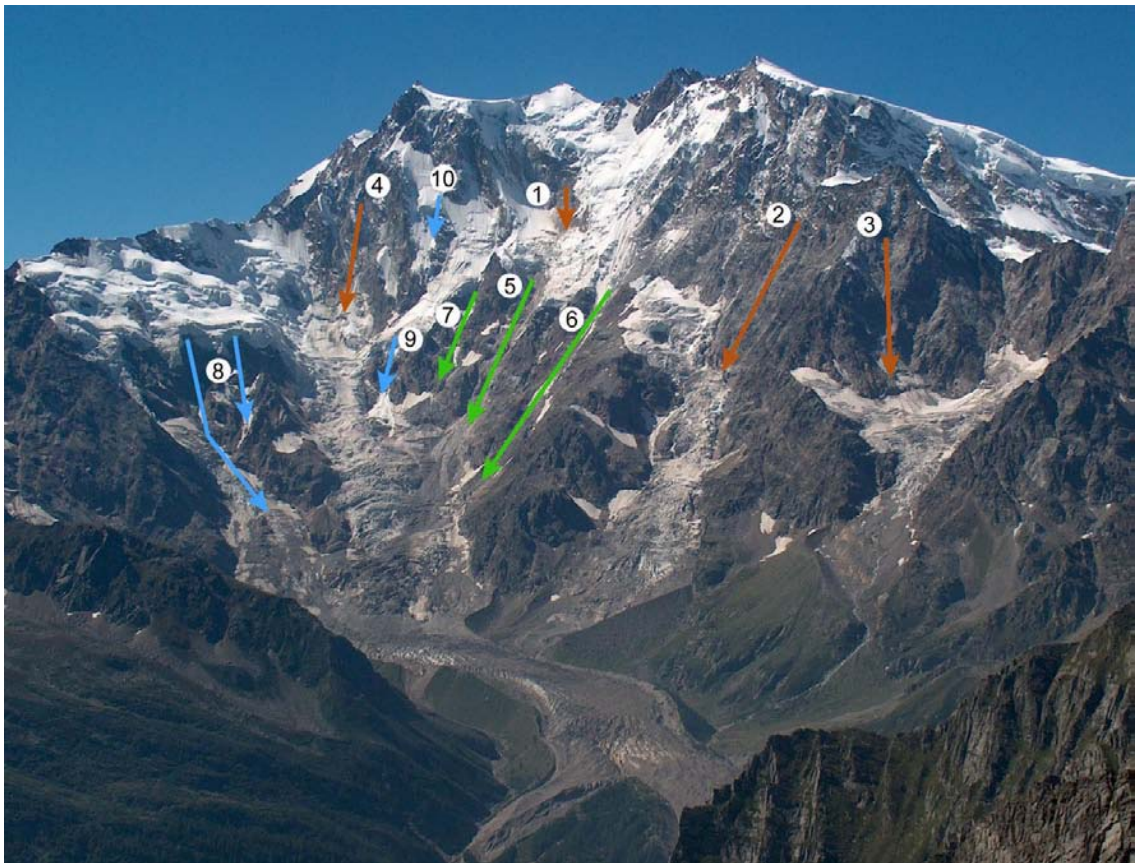

Fig. 1. Monte Rosa east face and Belvedere glacier, seen from Monte Moro. The arrows indicate the main active mass movement zones in the rock wall; rock fall areas are signed in brown, debris flow channels in green and ice avalanche areas in blue. The numbers replace the site names described in Sect. 2.

Permafrost degradation and a rise of the sub-surface ice temperature have – especially in sections of relatively warm permafrost occurrence – a strong influence on the stability of steep rock walls (Wegmann et al., 1998; Davies et al., 2001; Noetzli et al., 2003). Extensive parts of currently perennially frozen rock walls will most probably warm up to depths of many decametres, thereby reaching temperatures of around 0°C, which are known to be especially critical for stability because of the simultaneous occurrence of ice and water in cracks and fissures. Davies et al. (2001) showed on the basis of direct shear box tests, that a rise in temperature might lead to a reduction in the shear strength of ice-bonded discontinuities and reduce the factor of safety of a rock wall. Warming permafrost is, therefore, likely to lead to increasing scale and frequency of slope failures.

The Monte Rosa east face is an actual example for such changes and developments in a high alpine flank. During the last two decades, the ice cover has strongly changed and the mass movement activity has apparently increased. Scope of this study was in a first step to analyse and illustrate the actual geological and glaciological conditions in the Monte Rosa east face and their developments in the last century. Therefore, three different factors – geology, glaciation and permafrost – were investigated in a multidisciplinary approach using airborne photogrammetry, oblique photos, topographic maps, visual observations, field mapping and modelling. Second purpose was to analyse the linkages and spatial relationships between those three factors, on one hand, and the observed increasing slope instabilities in the Monte Rosa east face, on the other hand. To assess and evaluate the influence of the different examined factors, they are visually analysed and compared. Investigation techniques are well established ones, but the most important contribution of this study is the combined analysis of the above mentioned factors. Many papers, in fact, deal with rock wall stability, but not specifically for high altitude, glacierized rock walls, as this study does.

2 Study site and observed mass movement activity

2.1 Monte Rosa east face

The Monte Rosa east face (Fig. 1) is one of the highest steep flanks in the Alps (2200–4500 m a.s.l.), situated in the upper Valle Anzasca above the village Macugnaga, northern Italy (Fig. 2). With the Dufourspitze, Nordend, Zumsteinspitze and Signalkuppe, multiple peaks of over 4500 m a.s.l. are located at the top of the rock wall. Large parts of the Monte Rosa east face are covered by steep hanging glaciers and firn fields. Since the end of the last maximum glacier extent (Little Ice Age, about 1850), the hanging glaciers and firn fields have retreated slightly (Mazza, 2000). During recent decades, however, the ice cover of the Monte Rosa east face experienced an accelerated and drastic loss in extent and thickness (Haeberli et al., 2002; Kääb et al., 2004; Fischer, 2004). Also the permafrost distribution, even though not directly visible, is believed to have experienced changes in extent and ground-temperatures, as in large parts of the European Alps (Harris et al., 2003).

2.2 Belvedere glacier

The Belvedere glacier is located at the foot of the Monte Rosa east face. It is a humid-temperate, heavily debris-covered glacier fed by hanging glaciers, ice and snow avalanches as well as rock falls from the Monte Rosa east face (Mazza, 2000). Between summer 2000 and summer 2001, the Belvedere glacier started a surge-type movement with ice velocities increasing by one order of magnitude and showed in parts a strongly uplifted glacier surface by 10 to 25 m (Kääb et al., 2004). At the foot of the Monte Rosa east face, however, a large depression developed on the Belvedere glacier and the glacier surface was lowered by 15 to 35 m. Possibly as a consequence of enhanced englacial water pressure or other processes related to the surge-type movement, the supraglacial lake Effimero formed in this depression on the glacier in September 2001 and in the following two summers with a maximum volume of 3×10^6 m^3 (Haeberli et al., 2002; Kääb et al., 2004; Tamburini and Mortara, 2005). The continuously grown topographic depression at the location of the former lake represents a retention basin for small-to-medium rock and ice avalanche events. However, in the case of a water-filled supraglacial lake, a medium mass movement event from the Monte Rosa east face reaching the lake could trigger disastrous chain reactions such as flood or debris flow.

2.3 Mass movement activity

Mass movement processes have taken place all times because of the height and steepness of the Monte Rosa east face. Over the recent two decades, however, the mass movement activity in the Monte Rosa east face has drastically increased and new detachment zones of rock falls, debris flows and ice avalanches have developed. The analysis of the mass movement activity is based on observations during fieldwork in summer 2003 and summer 2004, reports of local people as well as analyses of photos since 1885 and air photos since 1956. It reveals that before about 1985 debris fans hardly existed on the glacier in the lower part of the Monte Rosa east face. Since 1990, pronounced debris fans can be observed.

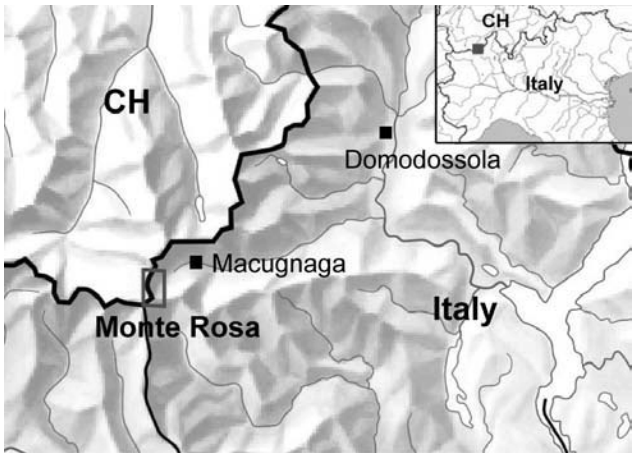

Fig. 2. Sketch map of the investigated area.

The main mass movement processes in the face are rock falls, debris flows and ice avalanches (Fig. 1), as observed during fieldwork. The detachment zones of rock fall are situated in the very steep rock walls above 3500 m a.s.l. and are distributed over the whole Monte Rosa east face. The most active zone of rock falls is from the Parete Innominata (Fig. 1, no. 1) to the hanging glacier below and in the upper part of Channel Imseng (no. 5). In the zones below Jägerjoch (no. 2) and Jägerhorn (no. 3) and on the Signalkuppe east face (no. 4) occasional rock fall can be observed. The debris deposits are mostly accumulated in the channels and on the hanging glaciers in the face, no observed rock fall events have reached the foot of the rock wall.

During spring, summer and autumn, rock fall events, which are strongly varying in size and reach, occur repeatedly. During fieldwork in the extraordinary hot summer 2003, rock fall events from different detachment zones could be observed almost every day. Even during the winter the gravitational mass movements – though reduced – take place. This indicates in some places a strongly reduced stability in the bedrock and shows that rock fall activity is not only affected by thawing and melting water during summertime, but rather by changed glacier, permafrost and bedrock conditions.

The debris flows mostly occur in the channels Imseng and Marinelli (Fig. 1, no. 5 and 6), occasionally also in the channel Zapparoli (no. 7). This mass movement process forms from debris deposits in the channel, which are accumulated because of the rock fall activities and physical weathering of the bedrock. The debris flows are a mixture of rock

Fig. 3. Transition zone and deposit area of the ice/rock avalanche in August 2005. The reach of the solid part of the avalanche (rock and ice) is marked in red; the reach of the powder avalanche is marked in yellow. No. 1 indicates the location of the hut Zamboni, no. 2 points to the location of the Lake Effimero, which is not visible on this aerial photograph from 1999.

and water, some are additionally mixed with considerable amounts of ice. They occur particularly during summertime when a lot of melting water is available in the Monte Rosa east face. During summer of 2003 – the extraordinary hot summer – almost daily activity was observed.

In steep high-mountain areas, relatively small and frequent ice avalanches often correspond to the natural ablation of steep hanging glaciers (Alean, 1985; Margreth and Funk, 1999), as seen on the Monte Rosa east face (Fig. 1, Ghiacciaio del Signal, no. 8; Ghiacciaio del Monte Rosa, no. 9). However, some large-scale events have occurred recently, especially in the area of channel Imseng (Fig. 1, no. 5). Between 1999 and 2001, about 350 m in length of this hanging glacier disappeared, most likely as a result of several ice avalanche events. A major ice avalanche, whose breakoff volume was estimated to be of the order of 1.1×10^6 m^3 (A. Tamburini, personal communication), occurred in August 2005 in the same area. The avalanche volume increased furthermore along its path by eroding underlying debris and ice. The main part of the material was deposited on the glacier Belvedere, particularly in the – fortunately almost empty – depression of the former lake Effimero (Fig. 3, red marking). The powder-part of the avalanche including ice and debris fragments, however, overtopped the lateral moraine of the Belvedere glacier and covered the plain around the hut Zamboni (Fig. 3, yellow marking). Fortunately, this ice avalanche occurred at night when nobody stayed at the frequently visited plain around the Rifugio. During the day, with a lot of tourists upwards to the plain and moraine, a number of injured persons or even casualties could have been possible.

3 Methods

Three different predisposing factors were studied in a multidisciplinary approach in order to assess their influence on the slope stability of the Monte Rosa east face: (i) geology, (ii) permafrost distribution and (iii) changes in glaciation. In a first step, the three factors were analysed separately to assess the recent changes and contemporary conditions. The results of this step are discussed in Sect. 4. In a second step, the results from the first analyses were compiled for a comparison with the current detachment zones of the ongoing mass movements. These analyses have been done visually by comparing the three analysed factors with the positions of the actual detachment zones. The detachment zones are indicated in each figure of the three investigated factors and therefore a direct comparison can be done. The findings of this second step are discussed in Sect. 5.

3.1 Detachment zones

The detachment zones were detected and analysed based on the combination of daily visual observations during fieldwork, photogrammetry and oblique photos. The fieldwork has taken place in summer 2003 and summer 2004, therefore the investigated detachment zones are the actual ones of these years. Detachment zones, transfer channels and frequency of the gravitational mass movement processes were observed and recorded during fieldwork (cf. Sect. 2 and Fig. 1). Due to the uncertainties from remote mapping and the multiple events at rather the same zone, detachment zones are only marked with a dot or circle. For the comparison with the geology, the detachment zones are classified in two groups, those from ice avalanche and those from rock falls/debris flows. The detachment zones of rock falls and debris flows are combined due to the fact that most debris flows are closely connected to the rock fall zones because of the available debris.

3.2 Geology

Geology is a fundamental parameter for slope stability. Therefore, the geological setting of the Monte Rosa east face was investigated during field work and a geological map was

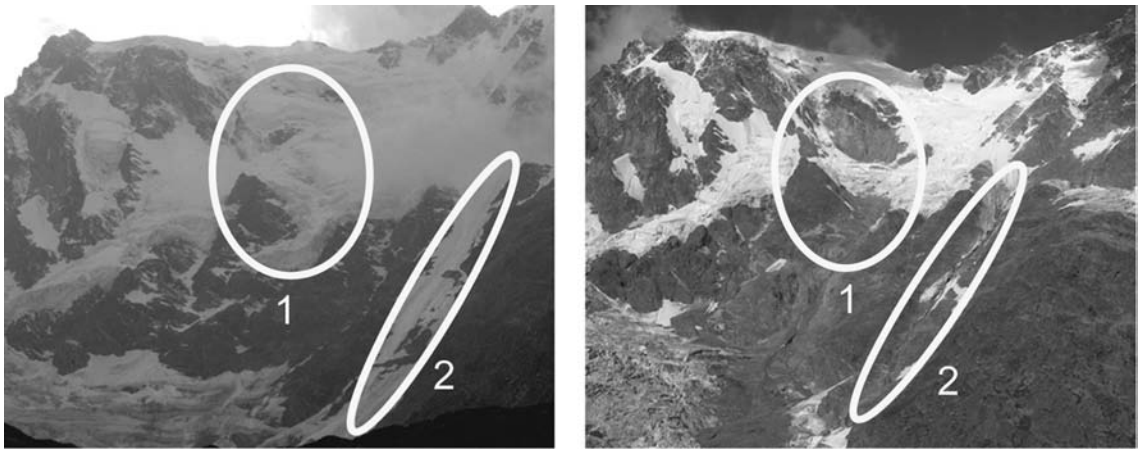

Fig. 4. Glacier extents on the Monte Rosa east face in September 1983 (left, W. Haeberli) and August 2003 (right, L. Fischer). Marking 1 indicates the Parete Innominata and the upper part of the Imseng channel, 2 indicates the Marinelli channel, zones with the most striking changes in glacier extent and also the highest mass movement activity.

compiled. Due to inaccessibility of most parts of the Monte Rosa east face it was mostly mapped remotely from the opposite slope. As a basis for the mapping the topographic maps Zermatt (Swisstopo, sheet no. 1348) and Monte Moro (Swisstopo, sheet no. 1349) were used. Furthermore, the Geological Atlas of Switzerland (Schweizerische Geologische Kommission), scale 1:25 000, and the study of Bearth (1952) were used for the classification of the lithology. For further investigations the geological field map was digitised in the GIS (Geographic Information System).

3.3 Permafrost distribution

To assess the permafrost distribution in the Monte Rosa east face and its possible linkage to the slope stability problems, two different models were applied aiming at estimating the lower boundary of the permafrost occurrence. This area is characterized by warm permafrost with temperatures marginally below 0°C and liquid water content thus presumably present and therefore is the most sensitive zone to permafrost degradation.

In a first approach the model PERMAKART (Keller, 1992) was applied. PERMAKART is based on the so-called "rules of thumb" to predict permafrost occurrences as developed earlier for the eastern Swiss Alps by Haeberli (1975). Based on an input DEM, PERMAKART primarily considers radiation effects as related to aspect, air temperature as related to altitude and snow cover as related to slope foot areas (long lasting snow cover caused by avalanche deposits). As these empirical rules are deduced and calibrated for the Upper Engadine in the Eastern Swiss Alps, they are first fitted to the Monte Rosa region using the 0°C-isotherm altitude and temperature gradient from the meteo station of Plateau Rosa/Testa Grigia at 3488 m a.s.l. (Mercalli et al., 2003). Based on a MAAT of −5.8°C of the Plateau Rosa station and lapse rate of 0.57°C/100 m (Mercalli et al., 2003), a 0°C isotherm altitude of 2470 m a.s.l. results. The calculations were based on a 25 m gridded DEM (DHM25 Level 2, Swisstopo) with a vertical accuracy of 4–6 m. However, due to the extreme topography in the Monte Rosa east face and its marginal position on the Swiss boundary larger errors of vertical elevations exist.

A second model is deduced from rock temperature calculations by Gruber et al. (2004) and called ROCKFROST in this paper. On the basis of meteo data, energy fluxes were modelled and eventually the spatial distribution of mean annual rock surface temperatures was calculated for climate conditions in the central (Corvatsch, Engadine) and northern Alps (Jungfraujoch, Bernese Alps) for a time period of 1982–2002. On a long-term basis the mean elevation of the 0°C-isotherm of the ground surface temperature corresponds to the lower limit of permafrost distribution in steep rock. By approximating the relation between the elevation of the 0°C-isotherm and aspect with a polynomial function for different slope values, the permafrost occurrence in steep rock can be assessed within a GIS. For these calculations the same DEM was used as in the first approach. Grid cells with a minimum slope of 45° were considered as steep rock.

3.4 Glacier extent

In order to reconstruct changes in glacier extents on the Monte Rosa east face, oblique photos (e.g. Figs. 4 and 5), historic maps and orthorectified air-photos were analysed. The glacier extents for different years were reconstructed by two approaches using different data sets. Both approaches were conducted by digitising glacier contours for different years since the early 20th century.

In a first approach, glacier extents were reconstructed on the basis of field observations in summer 2003, various old

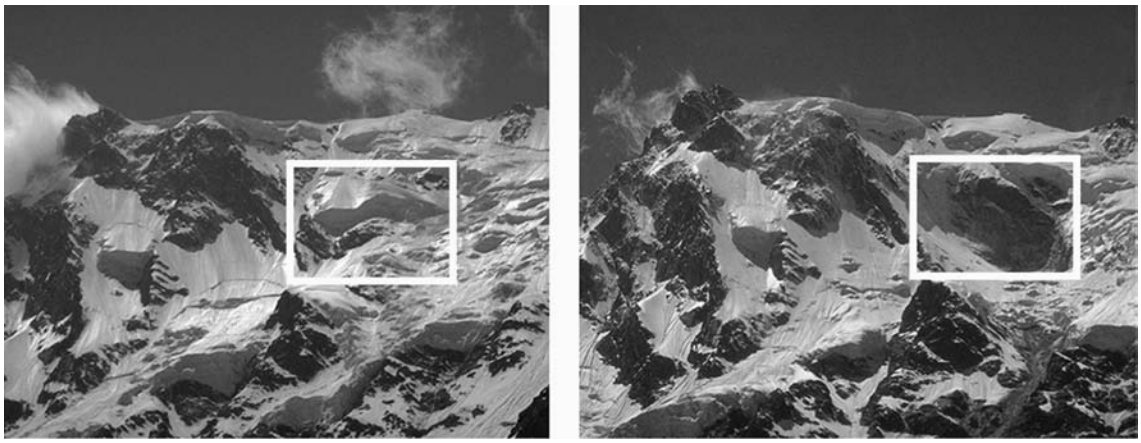

Fig. 5. Comparison of the glacier extent in the upper part of the Monte Rosa east face between June 1986 (left, H. Röthlisberger) and July 2002 (right, W. Haeberli). The white square indicates Parete Innominata, where a whole hanging glacier disappeared uncovering this steep rock wall.

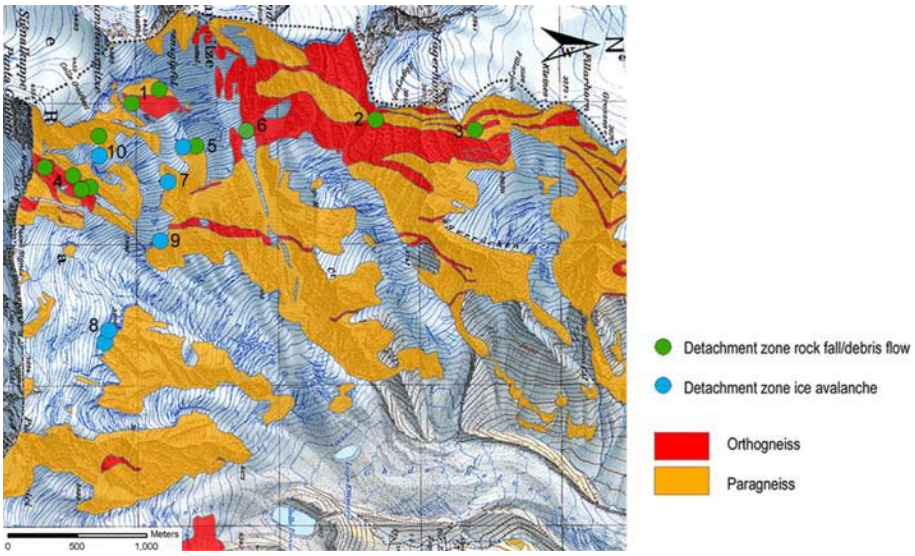

Fig. 6. Detachment zones of rock fall/debris flow events and ice avalanches in the Monte Rosa east face. The locations are marked by green and blue dots. Furthermore, the geology of the Monte Rosa is shown, orthogneiss in red and paragneiss in orange colour. Numbering is corresponding to Fig. 1. Topographic map is reproduced by permission of Swisstopo (BA067953).

oblique photos since 1885 and a historical topographic map. The procedure is mainly based on the visual comparison of different photos. The Italian topographic map dated from 1924 was georeferenced thus allowing glacier outlines to be digitised. The delineation of glacier extent in 1982 and 1999 was exclusively based on oblique photos. These photos were examined visually and the outlines were estimated manually in the GIS based on the digital topographic maps "Zermatt" and "Monte Moro". The glacier extent of 2003 was mapped during the field work and from oblique photos. An overlay of the different years shows the resulting glacier extents and corresponding retreat through time.

In a second approach, air-photos (taken by the Swisstopo) of the years 1956, 1977, 1988, 1999 and 2001 were orthorectified with the program PCI OrthoEngine on the basis of the DHM25 Level 2 from Swisstopo and map-derived ground control points. The identification of ground control points in the air-photos for the orthorectification turned out to be difficult due to the steepness of the Monte Rosa east face and consequent strong distortions of the air-photos. Due to some larger errors in vertical elevations in the DEM some horizontal inaccuracies occur in the orthophotos. However, this can be accounted for while delineating the outlines of the glaciers manually in the GIS.

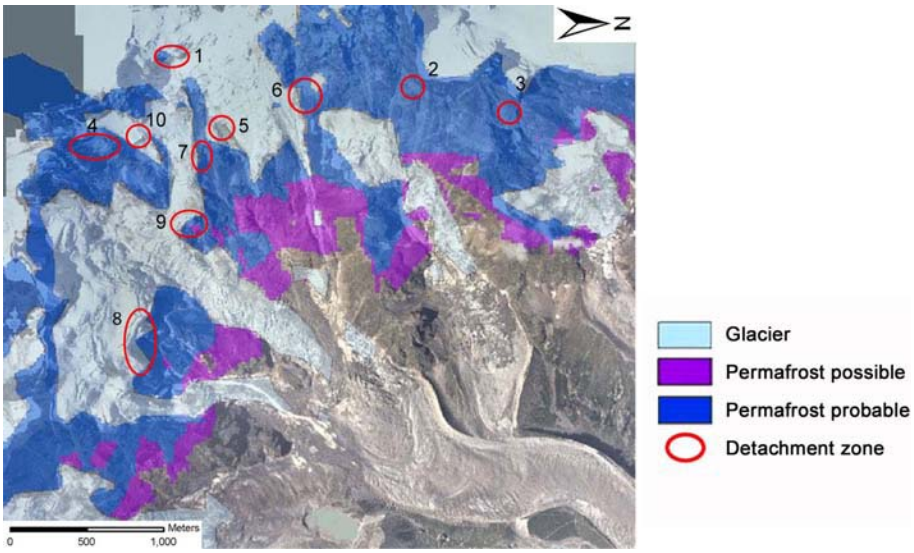

Fig. 7. Permafrost distribution based on the PERMAKART model with indicated active detachment zones, numbering is corresponding to Fig. 1. DHM25 © swisstopo (BA067953).

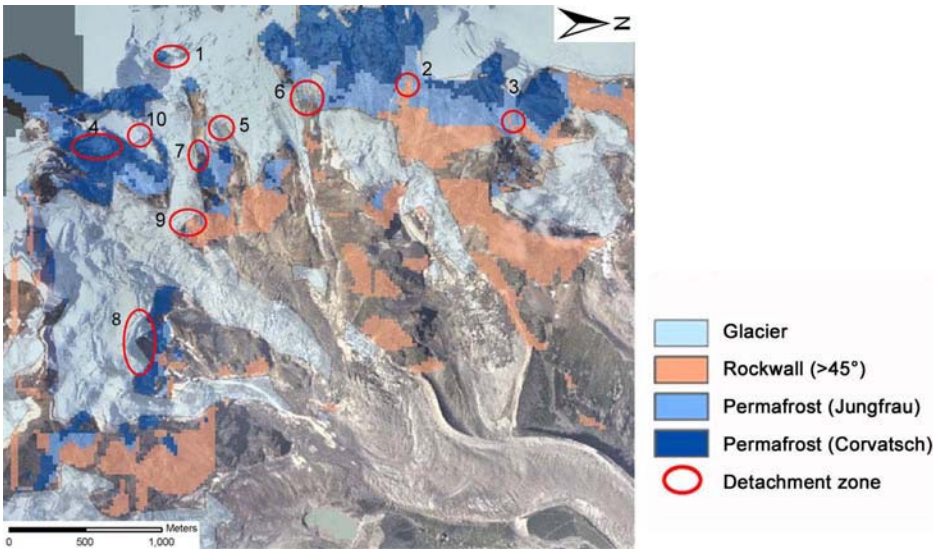

Fig. 8. Permafrost distribution based on the ROCKFROST model with indicated active detachment zones. DHM25 © swisstopo (BA067953).

4 Results

4.1 Geology

The geology of the Monte Rosa east face is characterized by layers of two different lithologies: orthogneiss and paragneiss (Bearth, 1952; Fischer, 2004). The two lithologies stem from the cristallyne of the penninic Monte Rosa nap. Ortho- and paragneiss can be well distinguished in the field based on the containing minerals, structures and their colour.

The composition of orthogneiss varies considerably throughout the Monte Rosa east face but the predominant constituent minerals are always quartz, kalifeldspar, plagioclase, muscovite and biotite. The structure of the orthogneiss varies from bulky to parallel texture. Paragneiss contains either biotite or muscovite as a main part, often combined as well and garnet, quartz and feldspar as a minor part. The paragneiss shows a pronounced parallel texture (schistosity) with varying formation from schist to gneiss. The geological setting of the Monte Rosa is strongly alternating between the two lithologies (Fig. 6). In most parts of the rock wall, the lithological stratification is clearly visible. Hence, many transition zones between the two lithologies occur.

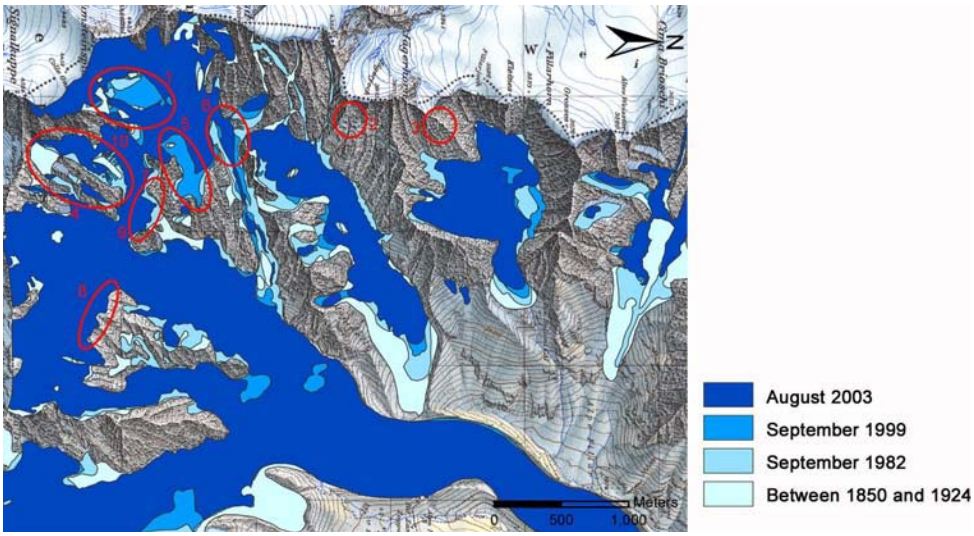

Fig. 9. Reconstruction of glacier extent derived from oblique photos and a historic map from 1924. The active detachment zones are indicated in red. Topographic map is reproduced by permission of Swisstopo (BA067953).

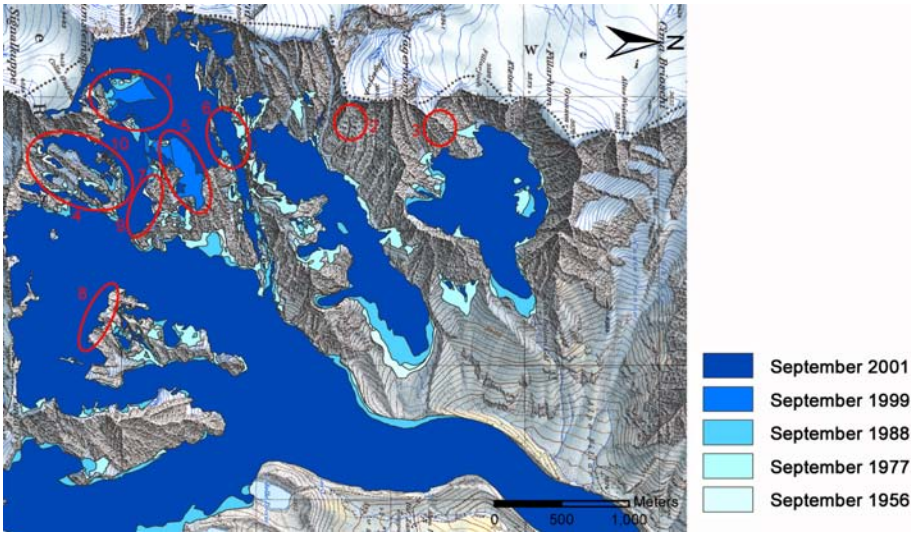

Fig. 10. Reconstruction of the glacier extent derived from orthorectified airphotos. The active detachment zones are indicated in red. Topographic map is reproduced by permission of Swisstopo (BA067953).

4.2 Permafrost distribution

Applying PERMAKART, the lower boundary of the possible permafrost occurrence (where locally permafrost may occur) is modelled at an altitude of 2700–2800 m a.s.l. (Fig. 7). The lower limit of probable permafrost (where continuous permafrost is supposed) is located between 2900 and 3200 m a.s.l., depending on the exposition and inclination of the rock wall. Since the model is based on rules of thumbs deduced in rather gentle as well as debris- and snow-covered slopes the PERMAKART model tends to overestimate the permafrost distribution in steep rock and, hence, can be consulted for an indication of the maximum permafrost occurence in the Monte Rosa east face.

Based on the ROCKFROST calculations, the lower boundary of the permafrost distribution is estimated to be between 3000–3300 (Jungfrau) and 3200–3500 m a.s.l. (Corvatsch) depending on the exposition and inclination of the rock wall (Fig. 8). The two classes Jungfrau and Corvatsch correspond to inner and slightly colder northern Alpine climate conditions, respectively. For the lower limit of permafrost occurrence, the model results for northern Alpine conditions are regarded to be the more likely for near-vertical snow-free areas of such steep rock walls like the Monte Rosa east face.

However, the ROCKFROST model might slightly underestimate the permafrost distribution, since shadowing effects and potential local small snow deposits lower ground temperatures but are not taken into account. According to the calculations by Gruber et al. (2004) the uncertainties of this approach are in the range of ± 2°C, which corresponds to roughly ± 200 m vertically.

Together, the models indicate the sensitive areas around the lower boundary of the permafrost occurrence that can be localised between about 3100–3600 m a.s.l. This large range is mainly due to the different aspects found on the flank.

4.3 Glacier extent

The reconstruction of the glacier retreat based on the first approach is shown in Fig. 9. This map shows the continuous retreat of hanging glaciers and firn fields since the end of the Little Ice Age. Unlike the strong retreat of many valley-type glaciers since about 1850, the changes of the steep glaciers in the Monte Rosa east face were not very distinctive from this time until the 1980s. However, during the last few decades an accelerated loss in extent of the ice cover becomes evident. Some glaciers (or parts of glaciers) disappeared within only a few years and they seem to decay through mass wasting. The analysis based on field observations, various old oblique photos and a historic map represents a qualitative analysis and the result provides a good overview of the changes in glaciation since the last glacier maximum (Little Ice Age). Another advantage of this approach is the existence of maps and oblique photos since the end of the 19th century.

The results of the second approach are shown in Fig. 10 and reveal a slight but progressive deglaciation in the Monte Rosa east face since 1956 and in some parts of the face a drastic loss of the ice-covered area in the last 10–15 years. The analysis of the orthophotos also reveals an occasional increase in the extent of certain firn fields and some hanging glaciers. This approach demonstrates that airborne remote sensing and analyses of orthophotos offer efficient methods for glacier mapping even on steep flanks. The mapping based on orthophotos is more detailed than that with oblique photos. However, due to the higher degree of details the general picture of change decreases in places. Another disadvantage is the lack of air-photos before 1956.

Together, the two methods give an overview over the glacier retreat and reveal the areas with the most pronounced changes in glaciation. In Canalone Marinelli the ice-covered area has decreased drastically since about 1995. The most striking changes took place in the hot summer of 2003 when the entire channel became almost ice-free. In Canalone Imseng a large part of the glacier tongue disappeared between 1999 and 2001 leaving a zone of instable rock. In the same zone, the ice avalanche in August 2005 with a break-off volume of more than 1×10^6 m^3 occurred. The ice cover of the Parete Innominata, currently the most active rock fall zone, has retreated stronly since 1990 and the present active detachment zone has become ice-free since around 2000.

5 Discussion

In this section, the analyses of relationships between the development of slope instabilities, on one hand, and geology, glacier retreat and permafrost degradation, on the other hand, are presented and discussed. Figure 6 shows the geological setting in the Monte Rosa east face and the positions of the actual detachment zones. It reveals that all detachment zones of rock falls and debris flows (green dots) are situated in the upper part of the rock wall, between 3400 to 4100 m a.s.l. In addition, a concentration of detachment zones at transition zones between orthogneiss and paragneiss becomes apparent (Fig. 6, detachment zones no. 1–5 and 7, see also Table 1). This indicates that the transition zones between orthogneiss and paragneiss could favour or cause instabilities because of the different geotechnical properties of the two lithologies. The detachment zones of ice avalanches are also situated in the upper part of the flank, but most of them cannot directly be related to the geological setting. In some zones, though, where ice avalanches are influenced by rock fall and debris flows, lithological transition zones may have an indirect impact on the glaciers.

The comparison of changes in glacier extent with current detachment zones shows that many rock fall and most debris flow events originate in recently deglaciated parts of the Monte Rosa east face (Figs. 9 and 10, Table 1). Today, Parete Innominata (1), channel Imseng (5) and channel Marinelli (6) represent the most active zones of both, glacial changes and mass movement activity. An important observation is the spatial shifting of the active detachment zones with decreasing glacier extent. Around 1990, the channel Zapparoli (7) was the only active detachment zone. At that time, the hanging glacier above the channel Zapparoli decreased drastically in extent and induced enhanced mass movement activity. Today, this zone is not very active anymore. This observation points out that changes in glacier extent might affect slope stability significantly due to drastic changes in surface and also subsurface conditions in the deglaciated areas. The major ice avalanches observed during recent decades occurred particularly in zones with significant glacial changes, the Parete Innominata (1) and channel Imseng (5). The Ghiacciaio del Signal (8), however, is hardly affected by changes in glacier extent. These ice avalanches occur as natural ablation due to the cliff position of this glacier. This shows that the reactions of hanging glaciers on a rise in atmospheric temperature are varying considerably.

Furthermore, modelling analyses suggest a probable linkage between permafrost degradation and the formation of detachment zones (Figs. 7 and 8). These figures reveal that many detachment zones of the present rock fall and debris flow events (2–7) and also some starting zones of ice

Table 1. Compilation of the active detachment zones of the summer 2003. This compilation reveals the influence of the three investigated factors geology, glacier retreat and permafrost on slope stability. For each active detachment zone the possible influencing factors are marked with ×.

Detachment zone		Geology (close to a transition zone)	Glacier (areas with glacier retreat)	Permafrost (most probably warm permafrost)
Parete Innominata, upper part (1)	Rock fall	×	×	
Parete Innominata, lower part (1)	Rock fall	×	×	
Jägerjoch (2)	Rock fall	×		×
Jägerhorn (3)	Rock fall	×		×
Signalkuppe east face, upper part (4)	Rock fall		×	
Signalkuppe east face, lower part (4)	Rock fall	×	×	×
Channel Imseng (5)	Rock fall	×	×	×
Channel Marinelli (6)	Debris flows		×	×
Channel Imseng (5)	Debris flows	×	×	×
Channel Zapparoli (7)	Debris flows	×	×	×
Ghiacciaio del Signal (8)	Ice avalanche			
Ghiacciaio del Monte Rosa (9)	Ice avalanche			×
Channel Zapparoli (7)	Ice avalanche	×	×	×
Channel Imseng, upper part (5)	Ice avalanche	×	×	
Channel Imseng, lower part (5)	Ice avalanche		×	×
Signalkuppe hanging glacier (10)	Ice avalanche		×	

avalanches (5, 7, and 9) are situated in areas of most probably warm permafrost at the lower boundary of permafrost occurrence (Table 1). This fact confirms the assumption, that instabilities may be formed in part due to increased temperatures in warm permafrost occurrence, which in turn may lead to decreased shear strength in the rock wall and enhanced water pressure. However, some of the detachment zones of rock fall are situated at higher altitudes where occurrence of cold permafrost is predicted. This suggests that not all rock fall events are directly connected to changes in ground-thermal conditions. A rise in permafrost temperatures may also laterally influence the thermal regime of hanging glaciers and have a destabilizing effect on cold hanging glaciers. Rising temperatures can thereby induce higher ice temperatures and more percolating melt water at the glacier bed and thus increase the stresses at the front of steep glaciers.

The performed analyses based on the combination of different methods such as airborne photogrammetry (Kääb et al., 2005), oblique ground-based photo comparisons, local field surveys and modelling in the GIS represent a useful approach for visually detecting the spatial and temporal relationship between different factors and processes in steep rock walls. Each investigated factor and process can be illustrated as a separate GIS-layer and an overlay of two or more layers reveals spatial as well as temporal linkages between investigated processes and their influence on the formation of new detachment zones. The visual processing and presentation of different processes and factors in the Monte Rosa east face with GIS-techniques provides a basis for direct comparisons.

6 Conclusion and perspectives

In the following the most important results of this study are summarised (see also Table 1):

- During recent decades, the ice cover of the Monte Rosa east face experienced an accelerated and drastic loss in extent.
- Enhanced mass movement activity was observed since about 1990 and new detachment zones were developed.
- Most of the detachment zones on the Monte Rosa east face are located in areas where surface ice has recently disappeared.
- Many detachment zones are located at the altitude of the lower boundary of the estimated permafrost distribution, where presumably warm and degrading permafrost exists.
- Many detachment zones are situated in transition zones between orthogneiss and paragneiss.
- The formation of detachment zones mostly seems to be caused by a combination of different factors.

The presence of lithological transitions zones seems to be a crucial factor for the development of instabilities in rock. However, also glacier retreat and permafrost degradation as a consequence of atmospheric warming have significant consequences on slope stability. The magnitude of observed rock

fall events during recent decades was rather small but they occurred frequently. These events could have happened as a consequence of permafrost thawing at the lower boundary of the permafrost distribution as well as the thawing of the near-surface permafrost layers in other parts of the rock wall. Changes in permafrost temperature into greater depths caused by long-term temperature changes could also cause large-size rock fall events.

In many unstable areas, a combination of the three main mass movement processes – rock falls, debris flows and ice avalanches – can be observed. Detachment zones of debris flows are mostly connected to the zones of rock fall due to the available debris. Ice avalanches occur on one hand due to the natural ablation of hanging glaciers, on the other hand however, some of them seem to be strongly related to instabilities in bedrock. In some parts of the Monte Rosa east face, e.g. channel Imseng, ice avalanche activity is influenced by rock falls and debris flows. Thus, an indirect influence of geology and permafrost on ice avalanche activity can be assumed. The compilation in Table 1 reveals that almost all observed detachment zones of rock fall, debris flows and ice avalanches in the Monte Rosa east face seem to be influenced by at least one of the investigated factors, but mostly by two or all of them. This indicates the importance of the combination and interaction of different processes and factors affecting the stability of steep slopes and the formation of detachment zones.

However, the three investigated factors represent still just a subset out of a complex net of different factors, processes and feedback mechanisms in a steep rock wall. For further analyses and mainly for the prediction of hazardous zones, more factors and processes – such as geological, geomechanical, geomorphologic, topographic, glaciological and climatic factors – have to be investigated and their influence on rock wall stability has to be assessed. A particularly important aspect is the geomechanical setting. Discontinuities such as layering, schistosity and rock joints are crucial predisposing factors for slope stability in steep rock walls, especially for the size and potential failure mode of rock falls (e.g. Abramson et al., 2001). Hence, further investigations should be directed to geomechanical aspects and the dependence on changes in surface and subsurface ice.

Due to the ongoing or even enhanced changes in surface and subsurface ice related to the atmospheric warming, large magnitude events in rock and ice cannot be ruled out in the Monte Rosa east face, as indicated with the large ice avalanche in August 2005. Chain-reactions of mass movement processes have also to be taken into account for further investigations. In case of a major supraglacial lake on the Belvedere glacier at the foot of the rock wall, as in summer 2002 and 2003, large mass movement events from the Monte Rosa east face could trigger disastrous chain reactions such as floods or debris flows, which could endanger populated areas.

Edited by: G. Wieczorek
Reviewed by: M. Chiarle and another referee

References

Abramson, L. W., Lee, T. S., Sharma, S., and Boyce, G. M.: Slope stability and stabilization methods, John Wiley & Sons, New York, 2001.

Alean, J.-C.: Ice avalanches: some empirical information on their formation and reach, J. Glaciol., 31, 324–333, 1985.

Ballantyne, C. K.: Paraglacial geomorphology, Quart. Sci. Revi., 21, 1935–2017, 2002.

Bearth, P.: Geologie und Petropraphie des Monte Rosa, Beiträge zur Geologischen Karte der Schweiz, Bern, 1952.

Davies, M. C. R., Hamza, O., and Harris, C.: The effect of rise in mean annual temperature on the stability of rock slopes containing ice-filled discontinuities, Permafrost and Periglacial Processes, 12, 137–144, 2001.

Fischer L.: Monte Rosa Ostwand – Geologie, Vergletscherung, Permafrost und Sturzereignisse in einer hochalpinen Steilwand, M.Sc.-Theses, Department of Geography, University of Zurich, 2004.

Frauenfelder, R.: Regional-scale modelling of the occurrence and dynamics of rockglaciers and the distribution of paleopermafrost, Schriftenreihe Physische Geographie, Glaziologie und Geomorphodynamik, University of Zurich, 2005.

Gruber, S., Hoelzle, M., and Haeberli, W.: Rock-wall temperature in the Alps: modeling their topographic distribution and regional differences, Permafrost and Periglacial Processes, 15, 299–307, 2004.

Haeberli, W.: Untersuchungen zur Verbreitung von Permafrost zwischen Flüelapass und Piz Grialetsch (Graubünden). Zürich: Mitteilung Nr. 17 der Versuchsanstalt für Wasserbau, Hydrologie und Glaziologie der ETH Zürich, 1975.

Haeberli, W. and Beniston, M.: Climate change and its impacts on glaciers and permafrost in the Alps, Ambio, 27/4, 258–265, 1998.

Haeberli, W., Wegmann, M., and Vonder Muehll, D.: Slope stability problems related to glacier shrinkage and permafrost degradation in the Alps, Eclogae geologicae Helvetiae, 90, 407–414, 1997.

Haeberli, W., Kääb, A., Hoelzle, M., Bösch, H., Funk, M., Vonder Mühll, D., and Keller, F.: Eisschwund und Naturkatastrophen im Hochgebirge. Schlussbericht NFP31, vdf Hochschulverlag ETH Zürich, 1999.

Haeberli, W., Kääb, A., Paul, F., Chiarle, M., Mortara, G., Mazza, A., Deline, P., and Richardson, S.: A surge-type movement at Ghiacciaio del Belvedere and a developing slope instability in the east face of Monte Rosa, Macugnaga, Italian Alps, Norwegian Journal of Geography, 56, 104–111, 2002.

Hallet, B., Walder, J. S., and Stubbs, C. W.: Weathering by segregation ice growth in microcracks at sustained subzero temperatures: Verification from experimental study using acoustic emissions, Permafrost and Periglacial Processes, 2/4, 283–300, 1991.

Harris, C. and Haeberli, W.: Warming permafrost in the mountains of Europe, World Meteorological Organization Bulletin, 52(3), 252–257, 2003.

Harris, C., Davies, M., and Etzelmüller, B.: The assessment of potential geotechnical hazards associated with mountain permafrost

in a warming global climate, Permafrost and Periglacial Processes, 12, 145–156, 2001.

Harris, C., Vonder Mühll, C., Isaksen, K., Haeberli, W., Sollid, J. L., King, L., Holmlund, P., Dramis, F., Guglielmin, M., and Palacios, D.: Warming permafrost in European mountains, Global and Planetary Change, 39, 215–225, 2003.

Kääb, A.: Remote sensing of mountain glaciers and permafrost creep, Schriftenreihe Physische Geographie, University of Zurich, 48, 264 pp, 2005.

Kääb, A., Huggel, C., Barbero, S., Chiarle, M., Cordola, M., Epifani, F., Haeberli, W., Mortara, G., Semino, P., Tamburini, A., and Viazzo, G.: Glacier hazards at Belvedere glacier and the Monte Rosa east face, Italian Alps: Processes and mitigation. International Symposium, Interpraevent 2004 – Riva/Trient, 2004.

Kääb, A., Huggel, C., Fischer, L., Guex, S., Paul, F., Roer, I., Salzmann, N., Schlaefli, S., Schmutz, K., Schneider, D., Strozzi, T., and Weidmann, Y.: Remote sensing of glacier- and permafrost-related hazards in high mountains: an overview, Nat. Hazards Earth Syst. Sci., 5, 527–554, 2005, http://www.nat-hazards-earth-syst-sci.net/5/527/2005/.

Keller, F.: Automated mapping of mountain permafrost using the program PERMAMAP within the geographical information system ARC/INFO, Permafrost and Periglacial Processes, 3(2), 133–138, 1992.

Kneisel, C.: Permafrost in recently deglaciated glacier forefields – measurements and observations in the eastern Swiss Alps and northern Sweden, Zeitschrift für Geomorphologie, 47, 3, 189–305, 2003.

Margreth, S. and Funk, M.: Hazard mapping for ice and combined snow/ice avalanches - two case studies from the Swiss and Italian Alps, Cold Regions Science and Technology, 30, 159–173, 1999.

Matsuoka, N., Hirakawa, K., Watanabe, T., Haeberli, W., and Keller, F.: The role of diurnal, annual and millennial freeze-thaw cycles in controlling alpine slope instability, Proceedings of the Seventh International Conference on Permafrost, Yellowknife, Canada, Collection Nordicana, 57, 711–717, 1998.

Mazza, A.: Some results of recent investigations on Ghiacciaio del Belvedere (Anzasca Valley, Western Alps) taking into account the glacier mechanics, Geogr. Fis. Dinam. Quat., 23, 59–71, 2000.

Mercalli, L., Cat Berro, D., Montuschi, S., Castallano, C., Ratti, M., Di Napoli, G., Mortara, G., and Guidani, N.: Atlante climatico della Valle d'Aosta, Societa Meteorolgica Subalpina, Torino, 2003.

Noetzli, J., Hoelzle, M., and Haeberli, W.: Mountain permafrost and recent Alpine rock-fall events: a GIS-based approach to determine critical factors, in: 8th International Conference on Permafrost, Proceedings, edited by: Phillips, M., Springman, S., and Arenson, L., 2, Zurich, Swets & Zeitlinger, Lisse, 827–832, 2003.

Paul, F., Kääb, A., Maisch, M., Kellenberger, T. W., and Haeberli, W.: Rapid disintegration of Alpine glaciers observed with satellite data, Geophys. Res. Lett., 31, L21402, doi:10.1029/2004GL020816, 2004.

Swisstopo, DHM25: Das digitale Hoehenmodell der Schweiz, Level 2, Bundesamt fuer Landestopographie, Wabern, Switzerland, 2002.

Tamburini, A. and Mortara, G.: The case of the "Effimero" Lake at Monte Rosa (Italian Western Alps): studies, field surveys, monitoring, in: Progress in Surface and Subsurface Water Studies at Plot and Small Basin Scale, Proceedings of the 10th ERB Conferece, Turin, 13–17 October 2004, Unesco, IHP-VI Technical Documents in Hydroloy, 77, 179–184, 2005.

Wegmann, M., Gudmundsson, G. H., and Haeberli, W.: Permafrost changes in rock walls and the retreat of Alpine glaciers: a thermal modelling approach, Permafrost and Periglacial Processes, 9, 23–33, 1998.

Zemp, M., Paul, F., Hoelzle, M., and Haeberli, W.: Glacier fluctuations in the European Alps 1850–2000: an overview and spatio-temporal analysis of available data, in: The darkening peaks: Glacial retreat in scientific and social context, edited by: Orlove, B., Wiegandt, E., and Luckman, B., University of California Press, in press, 2006.

IV

Monitoring topographic changes in periglacial high-mountain faces using high-resolution DTMs, Monte Rosa east face, Italian Alps

Fischer Luzia *, Eisenbeiss Henri**, Kääb Andreas***, Huggel Christian* & Haeberli Wilfried*

* Glaciology, Geomorphodynamics & Geochronology, Department of Geography, University of Zurich, Switzerland (luzia.fischer@geo.uzh.ch)

** Institute of Geodesy and Photogrammetry, ETH Zurich, Switzerland

*** Department of Geosciences, University of Oslo, Norway

submitted to Permafrost and Periglacial Processes

Abstract

Permafrost characteristics, periglacial/glacial process dynamics and the stability of steep rock walls in cold mountain regions are strongly affected by atmospheric warming. Appropriate documentation of the changes involved requires high-precision long-term monitoring. This paper describes a remote-sensing-based approach using digital terrain models (DTMs) from high-precision digital aerial photogrammetry and airborne LiDAR. The resulting time series of high-resolution DTMs with a 2 m resolution represents a unique new way of documenting and quantitatively assessing topographic changes and slope instabilities in steep periglacial terrain, enabling detailed investigations over past time periods and allowing for prospective monitoring of hazardous situations in inaccessible areas.

This study was conducted at one of the highest periglacial rock walls in the European Alps, the partially glacierized east face of Monte Rosa. Since about 1990, strongly increased rock and ice avalanche activity in this permafrost-affected rock wall has been causing massive topographic changes. The DTM comparisons performed provide an exceptional quantitative assessment of these topographic changes over the past 50 years, precisely locate the detachment zones of slope failures and reveal a total volume loss of more than 20×10^6 m^3 of glacier ice and bedrock and indicate a strong stability coupling between permafrost-affected bedrock and adjacent hanging glaciers.

1. Introduction

Atmospheric warming during the 20th century has caused pronounced effects in the periglacial and glacial belts of high-mountain areas (Haeberli and Beniston, 1998; IPCC, 2007). The coexistence of permafrost and hanging glaciers in high-mountain areas thereby gives rise to complex thermal and hydrological processes (Wegmann *et al*., 1998; Haeberli *et al*., 1999; Haeberli, 2005; Fischer *et al*., 2006; *Huggel*, in press). Changes in the distribution and temperature of surface and subsurface ice can have large impacts on the thermal and stress fields in both rock and ice, on geotechnical properties, as well as on the groundwater regimes of steep high-mountain faces and therefore strongly influence slope stability (Evans and Clague, 1993; Haeberli *et al*., 1997; Wegmann *et al*., 1998; Harris *et al*., 2001; Davies *et al*., 2001; Eberhardt *et al.*, 2004). With continued atmospheric warming, extended parts of rock walls that are still perennially frozen will most probably warm up to depths of tens if not hundreds of meters, thereby reaching temperatures slightly below 0°C, which are known to be especially critical for slope stability because of the simultaneous occurrence of ice and water in cracks and fissures (Davies *et al*., 2001; Gruber and Haeberli, 2007). A special complication with high-mountain slopes is the existence of cold to polythermal hanging glaciers, which introduce deep-seated geothermal anomalies and extremely complex hydrological/hydraulic

regimes. Deglaciation, in turn, may enable the penetration of a freezing front into previously non-frozen bedrock, and near-surface frost-related processes have the potential to intensify the weathering of newly exposed bedrock (Wegmann *et al*., 1998; Kneisel, 2003).

Reduced slope stability conditions may result in natural threats and disasters such as rock avalanches, ice avalanches, or combined events (e.g. Evans and Clague, 1994; Ballantyne, 2002; Bottino *et al*., 2002; Fischer *et al.,* 2006; Gruber and Haeberli, 2007). During recent decades, a number of extraordinary and catastrophic rock and ice avalanche events with volumes between 10^6 and 10^7 m^3 occurred in periglacial environments, and were thought to be related to changes in permafrost and glacierization conditions. These slope failures include the combined rock/ice avalanche at the Kolka Glacier, Caucasus, Russia, causing the death of over 100 people in downstream areas (Haeberli, 2004; Huggel *et al.,* 2005), the Brenva rock avalanche, killing two persons (Barla et al., 2000), the Thurwieser rock avalanche (Cola, 2005) and the Monte Rosa ice avalanche (Fischer *et al*., 2006), the latter three in the European Alps, all in partially glacierized areas with permafrost occurrence.

A major obstacle to close examination and better understanding of periglacial high-mountain rock walls is their difficult accessibility and the lack of detailed topographic data. Steepness, ice cover, difficult terrain and also safety problems hinder direct access. Therefore, remote-sensing-based investigations are fundamental to the assessment of changes in glaciation and bedrock, as well as slope instabilities (Kääb *et al*., 2005, Quincey *et al.*, 2005, Fischer and Huggel, 2008, Kääb, 2008). DTMs from remotely sensed data represent the basis of most topographic, geomorphic and morphometric analyses and DTM time series are very effective when used to accurately define temporal changes of terrain surfaces elevation (Kääb, 2002; Baldi *et al.*, 2002; Kääb *et al*., 2005). The generation of detailed DTMs for steep high-mountain flanks is complicated by the steepness and unfavorable data acquisition geometries, poor image contrasts in glaciated parts and occlusion by vertical to overhanging slopes. For tasks requiring ground resolution and accuracy in a meter scale, aerial photographs and LiDAR data are the most appropriate data for DTM generation (Baltsavias *et al*., 2001; Buchroithner, 2002). Digital photogrammetry based on digitized hard-copy aerial images or digital imagery is a particularly important method in view of the existing archives of analogue aerial images, which represent a valuable source of data on long-term topographic changes (Baltsavias, 1999; Kääb *et al*., 2005). Terrestrial and airborne laser scanning, in turn, is a rapidly emerging and highly promising tool for acquiring high-resolution topographic information (Baltsavias, 1999; Rabatel *et al*., 2008; Oppikofer *et al*., 2008). Some projects have already taken advantage of the coupling of digital photogrammetry and LiDAR for multi-temporal topographic analyses of rock walls (Bitelli *et al*., 2004; Dewitte *et al*., 2008), as well as for the detection of changes in valley glaciers (Baltsavias *et al*., 2001). The combination of the two techniques for time series of topographic data for steep permafrost-affected and glacierized high-mountain rock walls has not been applied so far.

The main objective of this study was to establish a methodology to investigate topographic changes in steep periglacial rock walls on a detailed scale. For this purpose, time series of high-resolution digital terrain models (DTMs) from high-precision digital aerial photogrammetry and airborne LiDAR (Light detection and ranging) were developed. The main focus was on the applicability and quality of digital photogrammetry and LiDAR techniques for topographic monitoring tasks in steep and complex high-mountain terrain was of central interest. The case study area was the Monte Rosa east face, Italian Alps. This is one of the largest high-mountain faces of the European Alps. Based on time series of DTMs over the past 50 years, temporal and spatial changes in surface topography were evaluated to assess terrain changes quantitatively and to improve process understanding of the slope instabilities and glaciation dynamics in a large periglacial rock wall.

2. Study site

The east face of Monte Rosa, Italian Alps, is located at the Swiss-Italian border (45°56'N, 7°53'E, Figure 1), and is among the highest and most impressive faces in the European Alps (2200–4600 m asl). During recent decades, this area was subject to striking changes in permafrost-affected bedrock and steep glaciers, resulting in a number of hazardous slope failures that are all very susceptible to chain reactions, especially with the newly formed supraglacial lake, as described in Haeberli *et al*. (2002), Kääb *et al*. (2004), Tamburini and Mortara (2005) and Fischer *et al*. (2006). The Monte Rosa east face is very steep in the upper half with average slopes between 55-70° on exposed bedrock and 40-50° in glaciated areas, while in the lower part of the rock wall the average slope is between 25 and 40°. Surface temperature measurements and modeling have shown that large parts of the rock wall are affected by permafrost (Zgraggen, 2005; Fischer *et al*., 2006). The upper part of the face is assumed to be under continuous permafrost conditions, and the horizontal grey bar in Figure 1 indicates the approximate lower boundary of permafrost occurrence, where presumably discontinuous permafrost dominates. The permafrost distribution is assumed to have experienced changes in extent and ground temperature during the 20th century, as in large parts of the European Alps (Harris *et al*., 2003, 2009; Gruber and Haeberli, 2007).

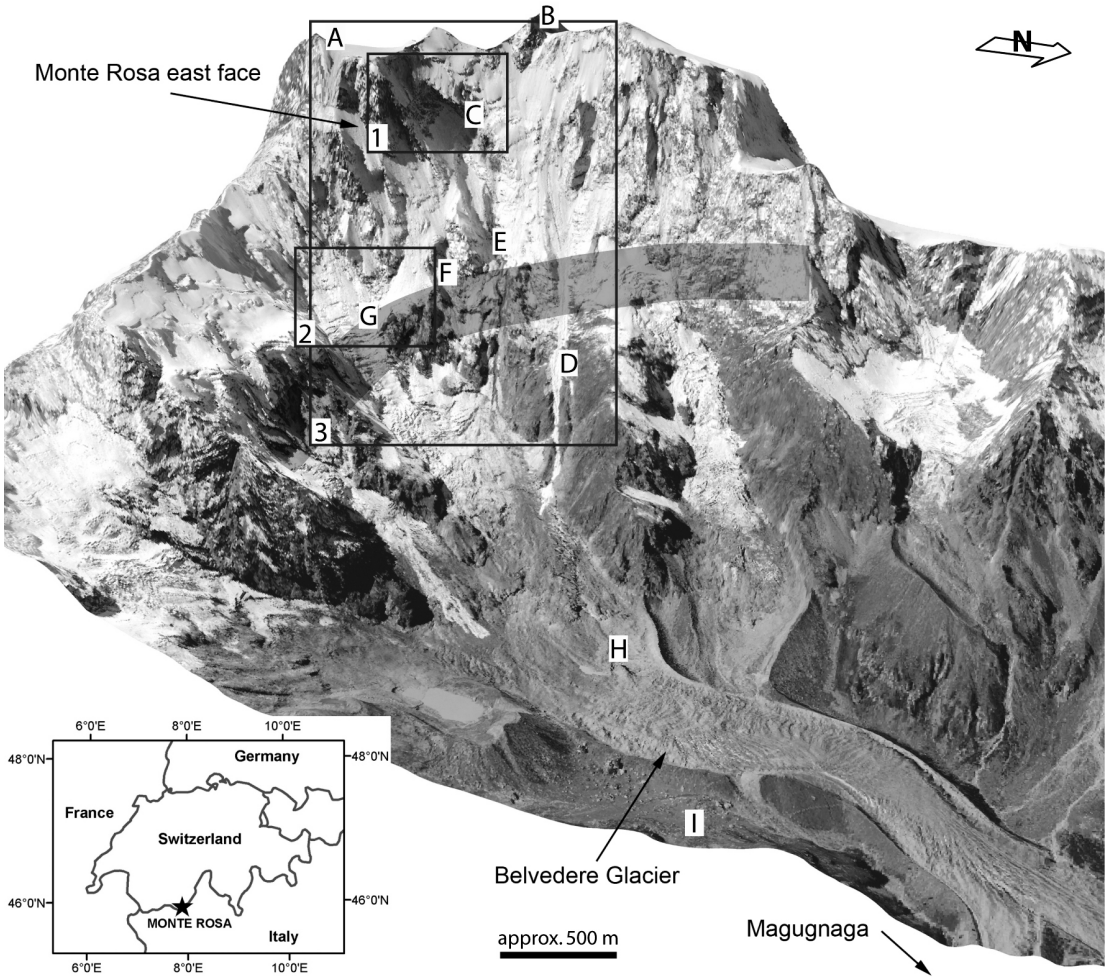

Figure 1. Oblique view on the Monte Rosa east face and the Belvedere glacier from the northeast. The synthesized view is computed from an orthophoto of 2005 and a photogrammetric DTM from 2001. The approximate lower limit of the permafrost occurrence based on corresponding modeling studies by Fischer et al. (2006) is shown in gray. A: Signalkuppe, B: Dufourspitze, C: Parete Innominata, D: Marinelli Channel, E: Imseng Channel, F: Zapparoli Channel, G: Monte Rosa Glacier, H: Lake Lago Effimero, I: Alpine hut Zamboni. The extent of Figure 4 is marked by the rectangles 1 and 2, and that of Figure 5 by rectangle 3.

Steep hanging glaciers and firn/ice fields cover large parts of the wall. During recent decades, the ice cover has experienced an accelerated and drastic loss in extent and thickness with rates that had not been observed before (Haeberli *et al*., 2002; Kääb *et al*., 2004; Fischer *et al*., 2006). Some glaciers completely disappeared within a few years, especially in the area of the Parete Innominata (Figure 1, C), Marinelli Channel (D) and Imseng Channel (E).

Since about 1990, striking new slope instabilities developed in permafrost-affected bedrock and hanging glaciers (Kääb *et al*., 2004; Fischer *et al*., 2006). Frequent small-scale as well as several large-scale rock and ice avalanches have been observed. A first major rock avalanche was reported in summer 1990 and several large rock and ice avalanche events followed. Most recently, an ice avalanche with a volume of more than 1×10^6 m^3 occurred in August 2005, and in April 2007, a rock avalanche of about 0.2×10^6 m^3 detached from the upper-most part of the face, where continuous permafrost occurrence is expected. The debris from both events was deposited on the Belvedere glacier in the depression of former lake Lago Effimero (H). The pressure wave from the 2005 ice avalanche, containing small ice and rock particles, affected much larger areas on the valley floor, however, and extended as far as the Alpine hut Zamboni (I). The volume of this ice avalanche is among the greatest documented in the European Alps over the past 100 years (Tufnell, 1984; Alean, 1985; http://www.glacierhazards.ch; http://glaciology.ethz.ch/inventar). In view of the ongoing or even enhanced atmospheric warming and the associated changes in a periglacial face, it is very likely that such slope failures from bedrock and hanging glaciers will continue to represent a critical hazard source for this densely populated and touristic region.

Additionally, the Belvedere Glacier located at the base of the Monte Rosa east face showed exceptional changes. In summer 2001, the Belvedere glacier started a surge-type movement with strongly increased surface velocities. The supraglacial lake Lago Effimero (H) developed in a glacier depression at the foot of the Monte Rosa in September 2001 and the two following summers with a maximum volume of 3×10^6 m^3 (Haeberli *et al*., 2002; Kääb *et al*., 2004; Tamburini and Mortara, 2005). This development posed a significant hazard source, especially with the potential for rock and ice avalanches from the Monte Rosa east face into a full lake that could trigger a catastrophic lake outburst with a far-reaching range of destruction. Luckily, no rock or ice avalanche event reached the lake during its existence and the drainage of the lake occurred, in the end, without a hazardous flood event.

3. Data sets

For the generation of multi-temporal DTMs of the Monte Rosa east face a combination of different optical remote sensing techniques was used for the data acquisition, using airplane- and helicopter-borne sensors (Table 1). In the following, the data sets are described.

3.1 LiDAR data

Two airborne LiDAR data sets are available for the Monte Rosa east face. In September 2005, LiDAR data were acquired by the Swissphoto Group over a 650 km^2 high-mountain area in the southern Valais from an airplane. Technical equipment consisted of an ALTM3100 System from Optech that was combined with a Trimble GPS receiver and the inertial measuring system Applanix POS-AV to obtain position and orientation during data acquisition. Acquisition geometry was invariably vertical. For the present study a sector of about 6.5 km^2 was considered, containing approximately 18.5×10^6 points (Table 1) with a point spacing of less than 2 m and vertical point accuracy better than 0.3 m (Luethy and Stengele, 2005).

Table 1. Date and main parameters of available optical data.

Date	Type of data	Camera/ sensor type	Quantity of data used	Focal length	Flight height	Ground resolution	Point density	Area of produced DTM
Sept 1956	Aerial images	Wild RC 5	3 images	115.26 mm	5020 m asl	6-23 cm	-	4 km^2
Sept 1988	Aerial images	Wild RC 10	4 images	153.37 mm	6100 m asl	11-24 cm	-	25 km^2
Sept 2001	Aerial images	Wild RC 10	3 images	153.28 mm	6700 m asl	16-28 cm	-	20 km^2
Oct 2005	LiDAR (airplane-based)	Optech ALTM3100	18.5×10^6 Pts	-	not available	-	2-3 Pt/m^3	6 km^2
Sept 2007	LiDAR (helicopter-based)	Riegl LMS-Q240i-60	4.8×10^6 Pts	-	various heights	-	1-3 Pt/m^3	3 km^2
Sept 2007	Small-scale aerial images (oblique)	Hasselblad H1	300 images	55 mm	-	4-8 cm	-	3 km^2

In September 2007, both LiDAR data and high-resolution oblique photographs were acquired from a helicopter for this study. The Helimap system of the company UW+R SA (Vallet, 2007; Vallet and Skaloud, 2004) includes a Riegl LMS-Q240i-60 laser scanner, a digital camera and coupled GPS/INS antenna, to obtain position and orientation during data acquisition. It can be installed on standard helicopters and is operated manually and so can be tilted to allow acquisition geometry almost perpendicular to the rock wall. This is a major advantage in steep terrain and prevents geometric degradation (Skaloud *et al*., 2005). Data acquisition was done along fourteen horizontal flight lines that were arranged parallel to each other at different heights to cover the whole face. The point cloud of this LiDAR data consists of 4.8×10^6 points and covers a total area of 3 km^2 with a point density of 1-3 pt/m^2 and vertical point accuracy better than 0.2 m (Table 1; Skaloud *et al*., 2005). With laser scanner wavelengths of 1064nm (Optech) and 905nm (Riegl), scanning on snow and glacier surfaces is possible, as the reflectivity of such surfaces is high at these wavelengths. However, both data sets show some gaps in the point cloud. These occur mainly due to occlusion during data acquisition in very steep to overhanging zones, as well as in complex topography with strong changes in horizontal and vertical curvature. The airplane-based data set shows fewer gaps in the point cloud because of the larger acquisition distance and less short-distance occlusions.

3.2 Analogue aerial images

Analogue aerial images from the Monte Rosa east face exist as from around 1950 and have been taken repeatedly in time intervals of 5 to 10 years by both the Swiss Federal Office of Topography (swisstopo) and the Italian Instituto Geografico Militare (IGM). For this study, the best suitable sets of stereoscopic aerial images from 1956, 1988 and 2001 were selected (swisstopo, Table 1). The selection criteria aimed at a well-distributed chronological sequence, good image quality with little snow coverage and preferably little distortion. The image scales within the individual images vary strongly due to the large height differences in the area, and range from 1:6,000 to 1:23,000 (1956), from 1:11,000 – 1:24,000 (1988) and 1:16,000 – 1:28,000 (2001). Image scale is calculated with the ratio focal length divided by the flight altitude above terrain. The black and white photographs were scanned at 10-µm resolution using a Vexcel photogrammetric scanner, resulting in ground

resolutions from 6 cm to 28 cm. The quality of the aerial images varies significantly between 1956 and 2001 (Züblin *et al*., 2008). The images from 1956 show coarse-grain image quality, while later images have better image quality. Large distortions exist due to the vertical acquisition geometry and the steepness of the Monte Rosa east face, especially in the steepest upper part of the face. Contrast is reduced on snow and ice surfaces and in areas of shadow.

Additionally, terrestrial amateur photos taken over several decades are available. They were taken by various persons with different uncalibrated cameras. Poorly known information about image position and cameras make photogrammetric processing for quantitative analyses difficult. Therefore, these images were used mainly for visual interpretations of surface characteristics in combination with generated DTMs.

4. Methods

4.1 LiDAR data processing

The raw data processing of the LiDAR data sets was done by Swissphoto for the 2005 data and by Helimap System SA for the 2007 data. This processing included the fitting of flight lines, and automated as well as manual filtering of ground points, outliers and artifacts. More information about the data processing is given in Luethy and Stengele (2005), Skaloud et al. (2005) and Vallet (2007).

The conversion of the processed LiDAR point clouds of 2005 and 2007 into a grid raster was done using the SCOP++ (inpho) software that is especially designed for processing a large number of points. The automatic LiDAR classification tool uses efficient robust interpolation techniques with flexible adaptation to terrain type and terrain coverage. The final DTM grids were generated at a 2 m resolution to allow direct comparison with the photogrammetric DTMs. However, even higher resolutions would be feasible with the given point density and distribution of the point cloud.

4.2 Analogue aerial image processing

4.2.1 Image triangulation

In a first step, the scanned analogue aerial images had to be oriented to recover the exterior parameters of the camera. This was done with Leica Photogrammetry Suite (LPS; Wang et al., 2004). For each investigated year an image block was set up, containing three aerial images for 2001 and 1988 and containing four aerial images for 1956. Camera calibration protocols on the interior orientation were available for all aerial images from swisstopo.

Table 2. The σ_0 of the exterior orientation of the three image blocks calculated in LPS and root mean square error (RMSE) of the control points. XYZ: Ground coordinates und xy: stereo intersection accuracy of the GCPs in image coordinates.

DTM	σ_0 (Pixel)	Control point RMSE (X in m, x in pixel)
2001	0.48	X: 1.3, Y: 0.6, Z: 1.5 x: 0.21, y: 0.57
1988	0.60	X: 1.9, Y: 1.3, Z: 2.5 x: 0.15, y: 0.66
1956	0.99	X: 1.6, Y: 1.5, Z: 1.7 x: 0.62, y: 0.34

Tie points were measured manually to obtain the relative orientation of the image block. Because of the extremely steep terrain and associated strong distortions in the aerial images, automatic tie point extraction could barely be applied. The absolute orientation of the image blocks requires manually measured ground control points (GCP). Because of the lack of survey points on the Monte Rosa east face, the coordinates of the GCPs were extracted from a topographic map (swisstopo, sheet no. 1348, edition 2003, 1:25,000) and the DHM25, a digital elevation model with 25 m grid spacing (DHM25 Level 2, swisstopo). Existing buildings such as alpine huts and pronounced unmovable surface features were taken as GCPs. LPS uses a one-step bundle adjustment for tie points and GCPs. The bundle adjustment yielded at a global accuracy of σ_0 = 0.48, 0.6 and 0.99 pixel for the different image blocks (Table 2). This corresponds to about 10-20 cm in object space, considering an averaged image scale. The variation of the σ_0 value from 0.48 to 0.99 pixel for 2001 to 1956 respectively, can be explained by the better image quality for the more recent aerial images. The global accuracy of the exterior orientation is very high for all image blocks, with values of 10-20 cm in object space.

The root mean square error (RMSE) value of the control points describes the accuracy of the GCPs and ranges from 0.6 to 2.5 m in planimetry and height (Table 2, XYZ values). This deviation was caused mainly by the imprecise GCP coordinates and the inaccuracy of manual point measurements. However, the stereo intersection accuracy of the GCPs in image coordinates resulted in half of a pixel (Table 2, xy values), which showed the high quality of the orientation considering the height and steepness of the rock wall.

4.2.2 DTM generation

DTM generation from the oriented aerial images was subsequently done in SAT-PP (Satellite image Precision Processing, ETH Zurich). The main component of this software package is an enhanced multiple image matching algorithm for the extraction of image correspondences and the generation of 3D data. The approach uses a coarse-to-fine hierarchical solution with an effective combination of several image matching algorithms and automatic quality control (Zhang, 2005; Wolff and Gruen, 2007). The exterior orientation parameters recovered in LPS were imported into SAT-PP. Once the pre-processing of the original images (noise reduction, edge enhancement, production of image pyramids) was completed, it was possible to begin the extraction and matching of feature points, grid points and edges. This image matching produced a large number of points for the subsequent DTM generation and attained pixel level accuracy. Least squares matching methods were used to achieve more precise matches for all the matched features and for the identification of some false matches. Detailed mathematical descriptions of the SAT-PP software package are given in Gruen *et al*. (2005), Zhang (2005), Zhang and Gruen (2006).

In preparation for the automatic point extraction and matching process of the aerial images in SAT-PP, seed points had to be measured manually in each stereo pair of the image blocks. Here, a factor of ten-times more points than is usually necessary had to be measured manually in flat and ice-free areas because of the complex and steep topography as well as the widespread ice coverage. Some large vertical errors occurred due to incorrect automatic matching, mainly in steep and shadowy areas, and at damaged or polluted points or areas on the diapositives of the aerial images. Improvements in these areas were obtained via enhanced manual measurements of seed points as well as vertical lines. Point density resulting from the matching process with several points/m^2 on average was as high as, or even higher than, the LiDAR point clouds. Taking into account the ground resolution of the aerial images (0.06-0.28 m, Table 1), the final DTM grids were generated at a ground resolution of 2 m.

4.2.3 Co-registration of DTMs

A direct comparison of multi-temporal DTMs requires the definition of a common reference system to avoid errors due to shifts in the individual DTMs. Due to inaccuracies of the GCPs used in planimetry and height of 0.6 to 2.5 m and a minimal number of GCPs within the face, the photogrammetrically derived DTMs showed offsets between each other of several meters. To reduce such differences, all DTMs had to be transformed into a common reference system. Therefore, the LiDAR DTM acquired in 2007 has been taken as reference surface for all other processed DTMs.

Automatic co-registration of the DTMs on the reference DTM was conducted with LS3D (Least Squares 3D Matching; Akca and Gruen, 2007). The LS3D method estimates the transformation parameters of one DTM to a reference one, using the Generalized Gauss-Markoff model, minimizing the sum of squares of the Euclidean distances between the surfaces (Gruen and Akca, 2005). This method is a one-step solution for the matching and georeferencing of multiple 3D surfaces that are globally matched and simultaneously georeferenced. In a first step, called registration, each DTM was transformed onto the 2007 LiDAR-DTM. Only unchanged surfaces were transformed on the corresponding surfaces of the reference DTM, errors and also areas with topographic changes were excluded. These unchanged surfaces were manually selected in known stable bedrock (five zones with a size of at least 1000 m^2), equally distributed over the whole face. The transformation of individual DTMs to the reference DTM allowed, in addition, assessment of their relative accuracy. In a second step, the difference between the entire areas of the transformed DTMs was calculated. For this DTM comparison, errors as well topographic changes were included in the calculations (in the following termed ‘comparison’). These comparisons quantitatively revealed topographic changes that occurred within the investigated periods.

5. Results

5.1 Digital terrain models

5.1.1 LiDAR DTMs

The DTMs of 2005 and 2007 show a very high level of detail. Figure 2 depicts two representative shaded reliefs of LiDAR and photogrammetrically derived DTMs for 2005 and 1988, respectively, and for comparison an orthophoto of the corresponding year. The 2005 LiDAR DTM (Figure 2, right) shows a very precise reproduction of the topography. Topographic features such as crevasses in ice and bedrock structures can be identified clearly. The DTM is smooth on ice- and snow-covered surfaces, a fact that corresponds with visual observations based on the orthophotos. The particularly sound representation of planar segments is clearly a major advantage of the LiDAR technique. Edges and linear features, though, are less distinctly reproduced, as the laser beam does not always hit these features directly.

5.1.2 DTMs from analogue aerial images

The multi-image matching approach in SAT-PP enabled the generation of high-resolution DTMs, even in such steep and complex terrain. The photogrammetric DTMs also showed a high level of detail (Figure 2). Due to the feature and line extraction during the image matching process in SAT-PP, linear features in particular were well defined in the DTMs (Figure 2). Topographic structures are visible with a high resolution and linear features such as crevasses and edges are well defined. However, some drawbacks exist in planar areas, where undulated interference features are visible on bright glacier and snow surfaces. The problem in these zones is the low radiometric contrast that hinders effective feature, point and edge extraction for the matching process.

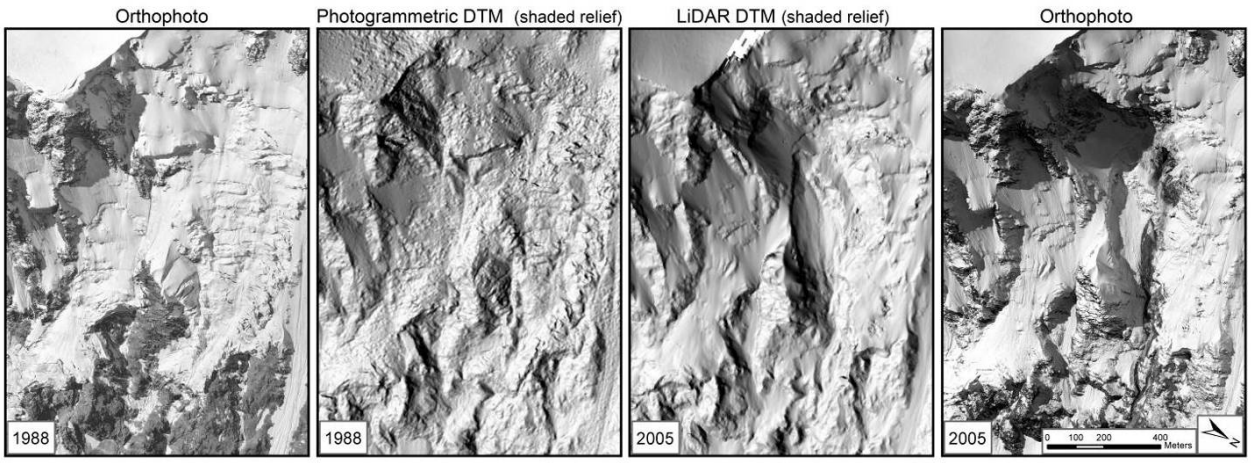

Figure 2. Comparison of the shaded relief models of the1988 DTM from vertical aerial images (middle left) and the LiDAR DTM from 2005 (Swissphoto, middle right; © BSF Swissphoto). The surface characteristics (glacier or bedrock) can be seen on the corresponding orthophoto (left, resp. right). Both DTMs show a very high level of detail, where different surface characteristics can be well distinguished. Conspicuous on the 1988 DTM is the undulated surface on bright glacier surfaces that originate from insufficient radiometric contrast for effective image matching.

The comparison of the LiDAR DTMs with the photogrammetric DTMs from vertical aerial images shows that the processing of aerial images with SAT-PP results in DTMs with comparable quality and point density as LiDAR data.

5.1.3 Relative DTM accuracy

The transformation of each DTM into the reference coordinate system of the 2007 LiDAR DTM allowed relative accuracy estimation through the registration process. For the registration, the σ_0 of analyzed DTMs from the reference DTM lay between 1 m and 2 m (Table 3). This shows the very high relative DTM accuracy after the transformation using areas with no topographic changes within the investigated period.

The σ0 of the DTM registrations using only unchanged areas can be compared with the σ0 of the DTM comparisons including all topographic changes over the entire face. The σ_0 of the comparisons between the 1988 DTM, the 1956 DTM and the 2007 LiDAR DTM was at 16.3 and 19.4 m, clearly larger than the σ_0 of corresponding registration. This indicates the large topographic changes in the Monte Rosa east face in these time periods. The σ_0 of the comparison of the 2001 and 2005 DTMs with 4.3 and 2.4 m were more consistent with the corresponding registration, a finding that can be explained by lower cumulative topographic changes within these two short periods.

Table 3. The σ_0 of the registration and comparison of all DTMs with the 2007 LiDAR DTM.

DTM	σ_0 of registration (m)	σ_0 of comparison (m)
2005	1.6	2.4
2001	1.5	4.3
1988	1.3	16.3
1956	1.9	19.4

5.1.4 Comparison of e- and z- distance

Differences between the surfaces of two DTMs were measured using different quantities. In the following, two of them are introduced and their usability for steep topography is assessed.The z-distance is the vertical elevation difference between two DTMs (Figure 3). It is the result of a difference calculation of the z-values between two DTMs and is usually the standard application in the commercial GIS (Geographic Information System). The e-distance (Euclidean distance) is the shortest distance between discrete points on two data sets (cf. Figure 3). Here, the e-distance was calculated in LS3D, where for each defined discrete point on one DTM the closest located discrete point on the other DTM is found and the Euclidean distance calculated, after LS3D minimized the square sum of e-distances by iteratively fitting one DTM on the other.

Figure 4 shows z- and e-distances in areas with significant differences between both quantities marked by dashed ellipses. In addition, the slope angles of the corresponding zones are calculated from the 2005 LiDAR DTM. The areas with significant differences are located very steep zones, or even more pronounced in strongly varying terrain with transition from relatively flat to steep terrain and vice versa, as can also be seen in Figure 3. In uniform and relatively flat terrain, the two distance quantities correspond well.

In geomorphometric studies, the z-distance is most commonly applied. However, as can be observed in Figures 3 and 4, z-distance measurements are less suitable for quantifying differences in steep areas with slope angles higher than ~50°. The actual topographic changes can be overestimated. A severe problem of z-distances is that even very minor horizontal shifts or errors between DTMs induce large errors in the DTM difference calculations when the z-distance is used.

The e-distance measurement is suitable for such strongly varying and steep topography because the influence of slope angle on surface difference measurements is minimized and accordingly shifts between DTMs have a much smaller influence. Furthermore, changes in strongly varying topography can be evaluated more reliably. Within this study, both methods have been applied but in the multi-temporal DTM comparison, only the results based on the e-distance are shown due to its better suitability for the steep topography of the Monte Rosa east face.

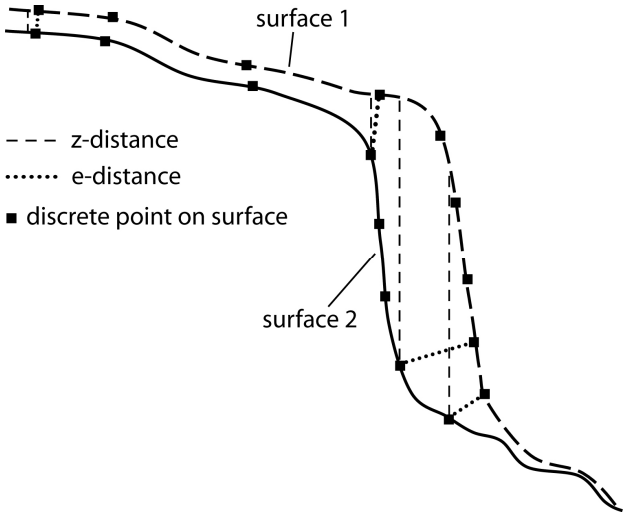

Figure 3. Comparison of z- and e-distance measurements in complex and steep topography. The discrete points are the original measurement points from LiDAR or aerial-photogrammetric matching of stereo-parallaxes. The e-distance is the line between an individual measurement point and its closest neighbour in the other data set.

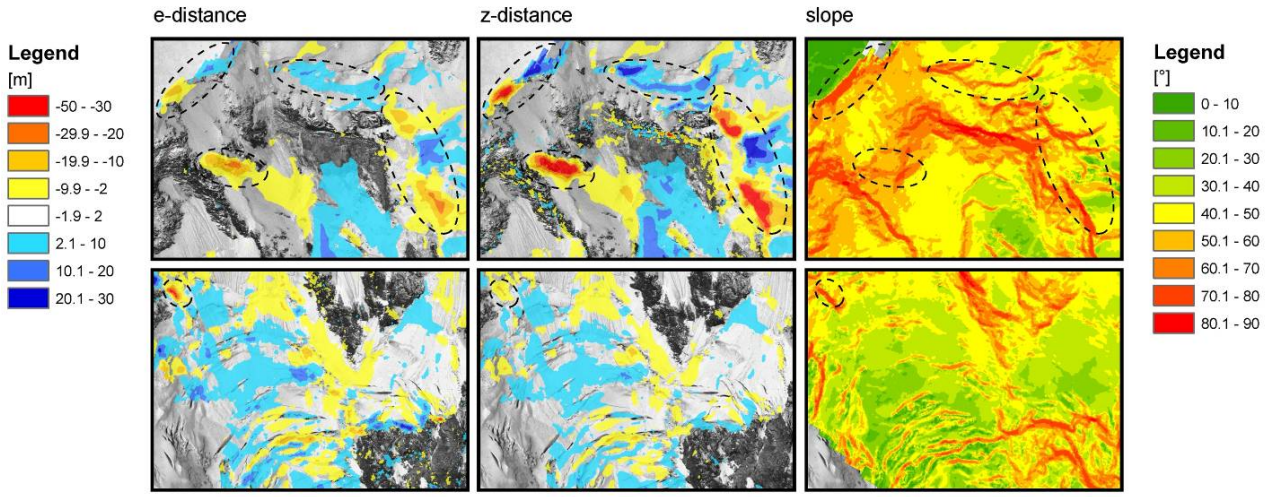

Figure 4. Comparison of DTM subtractions with z- and e-distance measurement. Topographic changes are obtained by the subtraction of the 2005 and 2007 LiDAR DTMs, slope angles are calculated from the 2005 LiDAR DTM. The upper row shows the DTM comparison in a very steep part of the Monte Rosa east face, where large differences can be seen between e- and z-distance (marked with black ellipses). In flatter terrain (lower row), the two measurement methods show similar results.

5.2 Topographic changes from DTM time series

The photogrammetrically derived DTMs from 1956, 1988 and 2001 and the LiDAR DTM from 2005 and 2007 were considered for the calculations of topographic changes. Figure 5 shows the differences between consecutive DTMs for a selected area of the rock wall (cf. Figure 1), given as e-distance. The cumulative topographic changes larger than +-5 m are displayed. By looking at the individual time intervals, the chronology of topographic changes and their locations becomes obvious.

Between 1956 and 1988, very few topographic changes were detected in the bedrock area (Figure 5a). In snow, firn and ice areas, accumulation as well as ablation was observable in equal measure. The e-distance changes with an average of about 10 m and a maximum of 30 m in restricted areas within 30 years correspond to normal processes of volume gain and loss of glaciers as well as moderate rockfall activity on such a steep rock wall. This result and additional interpretation of amateur photographs from 1895, 1911, 1983 and 1986 showed consistent patterns of glaciation, and only minor changes in glacier geometries and thickness can be recognized (Figure 6). The large surface differences in the area s1 are deceptive. They are caused by local errors in the 1956 DTM.

Figure 5b shows totally different patterns. In the time period between 1988 and 2001, major changes were evident that appear to be related to mass movement processes. Mass loss of up to 120 m in e-distance can be observed in the central area of the face (e1-e4; red/orange color). The total volume of this mass loss exceeded 20×10^6 m^3. This detached mass included both glacier ice and also underlying bedrock. A comparison of terrestrial photographs from 1986 and 2002 (Figure 6, upper row) confirmed the striking changes in the area of the Parete Innominata, where a whole hanging glacier and large parts of bedrock disappeared within a few years and a steep rock wall became newly exposed (e1, e2). The temporal resolution of the DTM time series did not allow conclusions to be drawn about the chronology of the topographic changes. Additional interpretations of terrestrial and aerial photographs and in situ observations by locals revealed that the slope failures started after 1988 at the location of e1, and subsequently, the hanging glacier and underlying bedrock, marked as e2 in Figure 5, disappeared in a combination of one major and several small-scale rock and ice avalanche events. Interaction between rock avalanche events and glacier retreat has intensified and accelerated mass loss further upwards in the face.

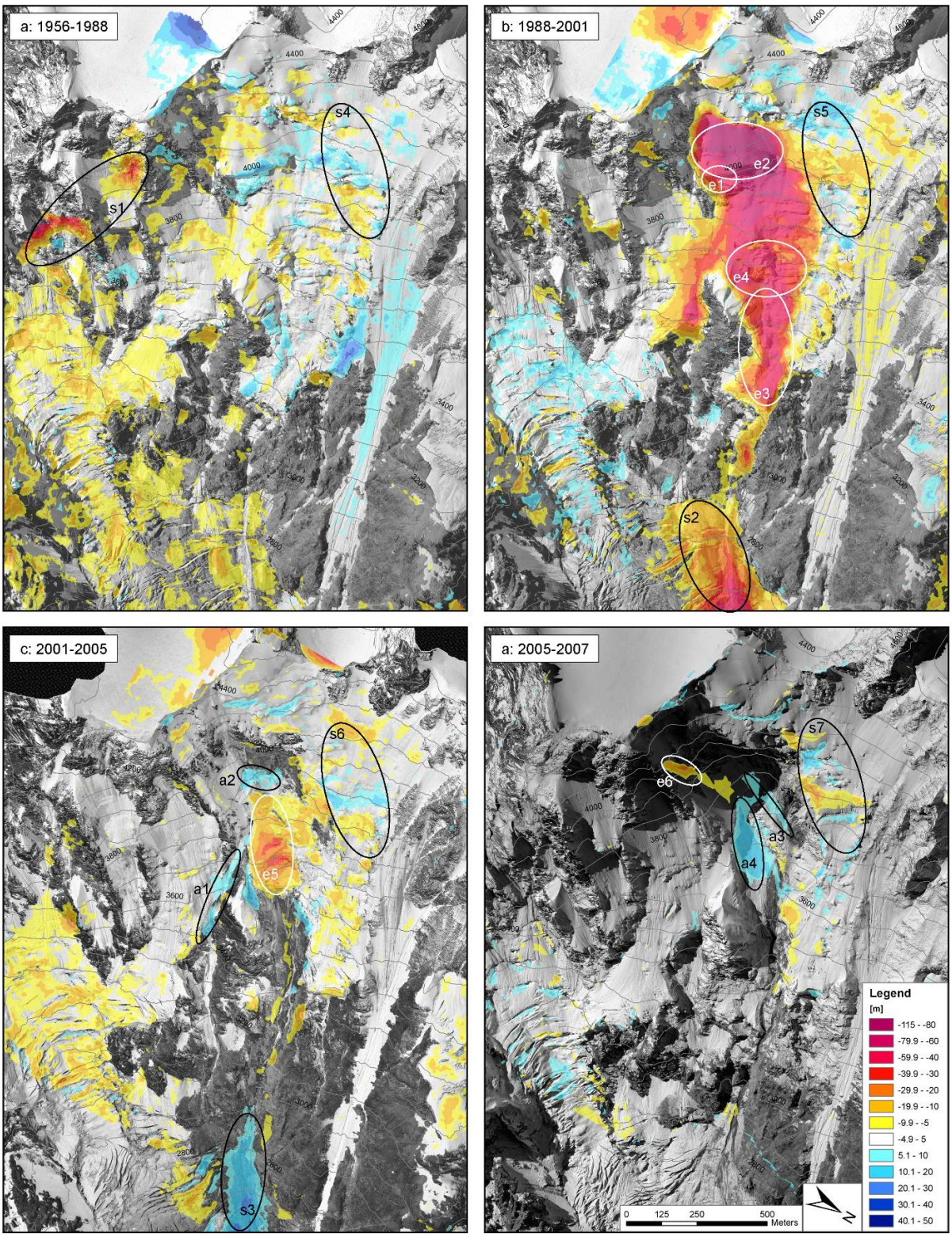

Figure 5. Evolution of the central part of the Monte Rosa east face in the form of e-difference maps with colour coding from red (volume loss) to blue (volume gain) observed between a: 1956 and 1988, b: 1988 and 2001, c: 2001 and 2005 and d: 2005 and 2007. The elevation differences are plotted on the orthophotos of a: 1988, b: 1988, c: 2001 and d: 2005; the equidistance of contours is 100 m. Significant mass failure events are marked with e1 to e6, zones with striking volume gain are marked with a1 to a4 and special features are marked with s1 to s7; explanations are given in the text.

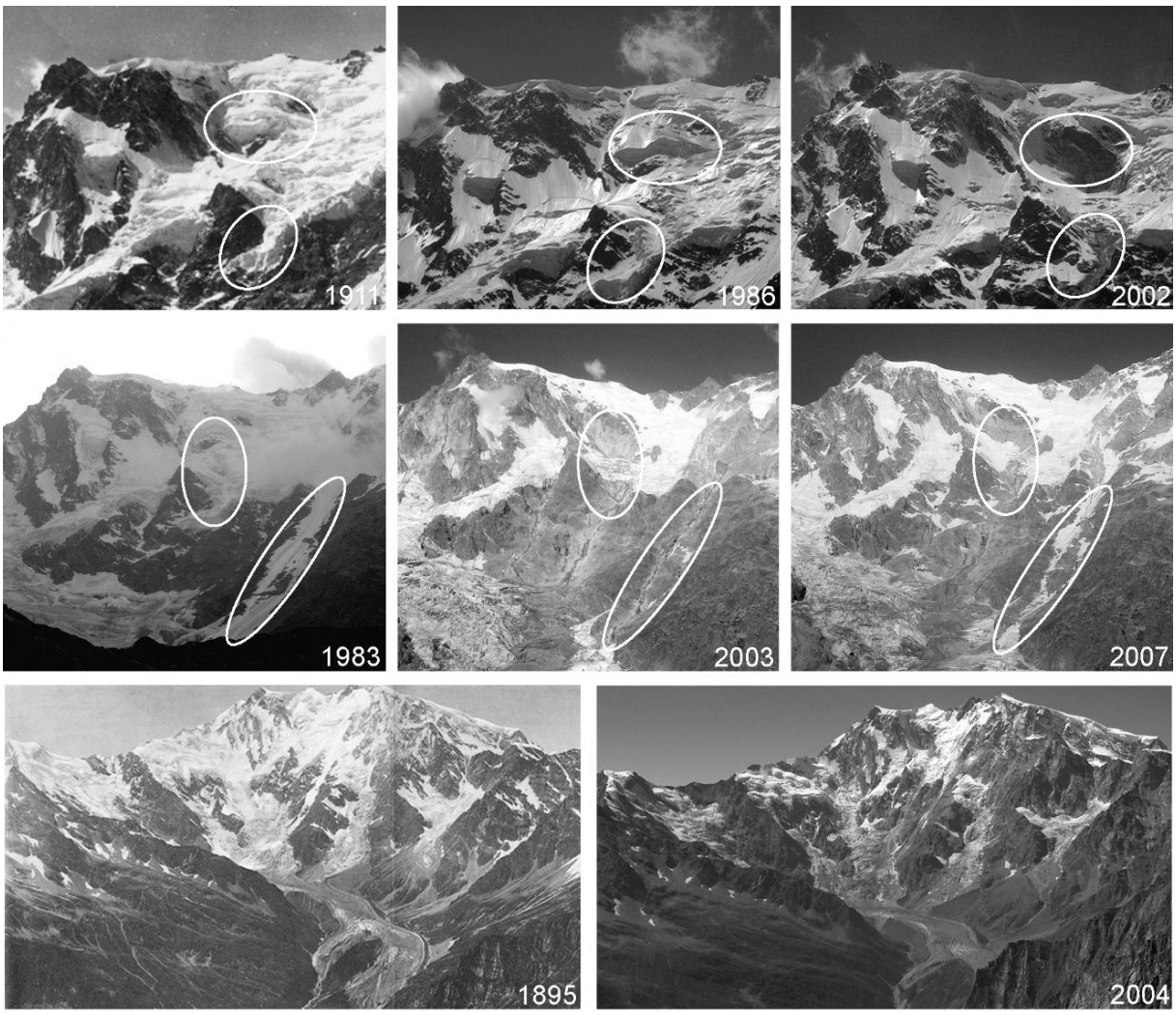

Figure 6. Time series of selected terrestrial photographs of the Monte Rosa east face from 1911 to 2007 from different perspectives. The top row shows a detail view of the upper part of the Monte Rosa east face at different times, the middle row presents the main part of the face, and the bottom row gives an overview of the entire area. The zones with the most significant changes in glaciation and topography are marked in white; for detailed descriptions see text. The photographs are from: top row: Sella (1911), H. Röthlisberger (1986), W. Haeberli (2002); middle row: W. Haeberli (1983), Fischer (2003 and 2007); bottom row: Sella (1895), Fischer (2004).

In the Imseng Channel (e3, e4 in Figure 5b), the lowermost part of the glacier detached with a mass loss of up to 60 m thickness between 1999 and 2001. Terrestrial photographs and observations of locals point to a combination of repeated small-scale and one major ice avalanche events. The mass failures started in the lowest part of the glacier (e3) and proceeded progressively upwards. This intensive mass movement activity caused the glacier beneath (s2) to be eroded up to 40 m along the runout channel. By contrast, in other parts of the face, moderate but large-area ice accumulation was observed on glaciers. The lower part of the Monte Rosa glacier in particular showed an increase in ice thickness of 5 to 15 m.

In the time period from 2001 to 2005, distinct topographic changes are again observable (Figure 5c). The mass loss in the Imseng Channel (e5) corresponds to one single ice avalanche event with a volume of more than 1×10^6 m^3 that occurred in August 2005. This ice avalanche occurred directly above the area, where major parts of the glacier have detached since 1999 (e3, e4). Below the Parete Innominata, a small area of mass gain can be observed (a2). This is the accumulation of rockfall debris from the newly ice-free rock wall 'Parete Innominata' above. Accumulation of debris and ice can be observed in the area s3, where erosion took place in the period 1988-2001. This

indicates that the intensity and magnitude of the mass movement activity diminished. Local glacier ice volume gain can be observed at site a1. Ice accumulated in the area where the main runout channel of the mass movements from e1 and e2 was situated before 1999. As this runout channel was inactive due to a shift of rock fall detachment zones, ice accumulated here. Within a period of five years, an ice ridge of up to 20 m thickness built up.

In the time period from 2005 to 2007 (Figure 5d) several distinct topographic changes can be observed. Considerable ice volume gain is evident in the Imseng Channel (a4). In the area of the former detachment zone of the 2005 ice avalanche, ice accumulated to a thickness of up to 20 m within only two years. The detachment zone of the April 2007 rock avalanche (e6; 0.2×10^6 m^3) is clearly visible. The difference between the LiDAR DTMs from 2005 and 2007 suggests a thickness of the detached rock mass of 15-30 m. The mass loss in the area between e6 and a4 was due to erosion of ice by the rock avalanche event. Below the rock wall Parete Innominata mass accumulation is visible at a3. This rock wall shows evidence of small-scale rockfall activity since the disappearance of the hanging glacier (e1, e2).

An interesting displacement pattern of steep glacier ice can be observed in the areas s4-s7. The steep glacier below the Dufourspitze shows a complementary pattern of decrease as well as increase of ice thickness. The glacier displacement seems to have accordion-like behavior, with alternating areas of extension and thinning, and areas of compression. Such patterns resulted from varying positions of steep and crevassed ice fronts and flatter areas and do not directly imply changes in general ice thickness.

6. Discussion

6.1 Methods

This study shows that LiDAR data collection by helicopter and airplane proved to be an invaluable source of detailed and accurate topographic information in remote, steep and mountainous terrain. High-precision DTM data facilitate detection of topographic changes at meter-scale and reveal subtle geomorphic features to an accuracy of 1-3 m. Helicopter-based LiDAR data acquisition is especially advantageous for relatively small areas (less than about 5-10 km^2) with high altitude differences, airplane-based data acquisition is more suitable for larger areas with lower altitude differences. However, in such high-mountain environments, several logistic and technical challenges have to be considered for both methods: complicated acquisition geometry, difficult weather conditions such as for example strongly varying wind fields and local clouding, limitations of GPS satellite reception and the optimal skills required of the helicopter pilot.

The comparison of the two LiDAR point clouds reveals that though the acquisition geometry of the helicopter-based method perpendicular to the wall seems intuitively better suited, the airplane-based method has a denser area-wide point distribution with fewer gaps. The point density of the airplane-based data set is significantly higher, especially in steep and complex areas. This is due to the ten times higher acquisition rate of the laser scanner used on the airplane. The high acquisition rate enables faster flight speed and larger distances to the face, reducing the problem of occlusions. Optical imagery taken simultaneously with the LiDAR acquisition provides additional information that is invaluable for understanding the observed geometry changes.

For investigations of time periods before the advent of LiDAR technology, aerial images are the best available quantitative data source. Aerial images have high spatial resolution and the great advantage of more than fifty years of images. However, photogrammetric processing of aerial images is seriously challenging for such high-mountain rock walls due to the steepness and low levels

of contrast in glaciated areas. With the application of a sophisticated photogrammetric processing approach, for the first time the generation of a highly accurate multi-temporal series of high-resolution DTMs could be completed for such a large high-mountain face. The point density of the image matching process is similarly to that of the LiDAR data and allows the generation of high-resolution DTMs with grid size in the order of 2 m. Nevertheless, time-consuming processing and local errors in the DTMs have to be taken into account.

The transformation of individual DTMs to a common reference system using LS3D is a suitable method for reducing offsets between DTMs that were introduced by slightly different GPS positions, for example. The investigations have shown that small offsets result in large DTM differences, especially in steep areas. In future, a solution to eliminate the offset errors with the photogrammetric method would be the triangulation of aerial images in multi-temporal image blocks, as used for instance for matching terrain displacements (Kääb, 2002). Thus, the aerial images of all years could be triangulated in one step with the identical ground control points and multi-temporal tie points (Kääb, 2002). In addition, a valuable approach for reducing errors and misinterpretations in DTM comparisons is the application of the Euclidean Distance (e-distance). However, DTM subtraction also implies that individual DTM errors can be incorporated in the comparison and lead to overestimations of topographic changes. Therefore, an examination of the calculated terrain changes has to be conducted based on the aerial images and terrestrial photographs. A major advantage of amateur terrestrial photographs is first, their availability and secondly, their temporal resolution compared to aerial images. The different angles of view can also be advantageous.

Considering all these advantages and disadvantages, three-dimensional reconstruction of the ground surface (DTM), derived from airborne photogrammetric surveys and LiDAR data, has proven to be a powerful tool to investigate inaccessible areas such as steep periglacial high-mountain faces at high spatial resolution. The combination of LiDAR and photogrammetric methods is particularly suitable for extending the temporal resolution and time period covered, and thus the time span of precise surface topography. Moreover, in future studies the integration of a LiDAR system into an autonomous flying UAV would allow a precise data acquisition following a predefined flight path. This technique will establish itself, especially in small-scale areas, where the access for manned aircraft is impossible or the risk of endangering human life too high.

6.2 Glacial and periglacial processes

The analysis of multi-temporal DTMs provides detailed information on topographic changes in the Monte Rosa east face and, especially in combination with visual inspection of terrestrial photographs (cf. Figure 6), enables conclusions to be drawn about processes affecting slope stability in such an area. The quantitative analysis of DTMs reveales complex patterns of terrain changes (cf. Figures 5 and 6). These diverse geomorphic patterns point to the simultaneous occurrence of different processes in a high-mountain face. The following topographic changes could be distinguished and quantitatively assessed:

- accumulation and ablation of ice over large areas of a glacier;
- rapid mass loss due to frequent small-scale or single large-scale rock and/or ice avalanche events;
- erosion of debris and/or glacier ice in the runout channel by rock and/or ice avalanche events;
- accumulation of debris material from gravitational mass movement processes;

- rapid ice accumulation and build-up of steep glaciers in eroded areas after mass movement processes;
- accordion-like displacement pattern of steep glaciers with varying positions of ice fronts.

The most striking observations were the exceptionally large loss of ice and bedrock. The DTM comparisons from 1988 to 2007 show how the glacierization of such a steep face, in contrast to valley glaciers, can change massively within a few years, remarkable in terms of both volume loss and gain. Rapid changes in surface geometry and the size of hanging glaciers are known to be comparably independent from climatic conditions, also for other high-mountain faces (Pralong and Funk, 2006; Post and Lachapelle, 1971). However, since about 1990 numerous large rock and ice avalanche events with a total volume of more than $20 \cdot 10^6$ m^3 have occurred with no documented historical precedence of similar magnitude in the European Alps. We suspect that such developments indicate the massive problems relating to permafrost, steep glaciation and rock-wall stability, which are expected to occur also in other steep high-mountain faces under similar conditions as those at the Monte Rosa east face.

The comparison of the slope failure zones (Fig. 5) with the modeled permafrost distribution (Figure 1) shows that all detachment zones are located in permafrost areas. The glacierization in these areas is assumed to consist of mainly of cold ice, however, hanging glaciers often have polythermal patterns with sections of much warmer or even temperate firn and ice (Alean, 1985; Haeberli, 2005). Such polythermal pattern may locally influence temperatures in the bedrock down to great depths. The small-scale rockfall events occurred in the area of the Imseng Channel, the Parete Innominata and elsewhere in the face can be related either to changes within the near-surface active layer of the permafrost or to enhanced frost weathering after the deglaciation. The large-volume rock avalanches such as 2007 event, however, cannot be only due to changes in the thermal field. For this rock avalanche, the striking and rapid topographic changes in the surrounding area with an enormous mass loss of over 15×10^6 m^3 ice and bedrock in this area may have had significant effects on the stability by influencing the topographic and geomechanical conditions of the remaining bedrock and thereby inducing changed stress fields in the bedrock. At the same time, the response of steep bedrock areas to glacier retreat is strongly conditioned by the geological setting, in particular by the geometrical and geotechnical characteristics of discontinuities, as in the 2007 case with an unfavorable, surface-parallel setting of the rock discontinuities.

The DTM comparisons and additional imagery analyses have revealed that the sequence of the topographic changes and slope failures is strongly spatially correlated. The slope failures started in 1990 on a small part of the Parete Innominata with combined rock and ice avalanche activity, proceeding with a chain reaction of mass wasting processes until the whole Parete Innominata and Imseng Channel was ice-free in 2001. Slope instabilities in the permafrost-affected bedrock can diminish the stability of hanging glaciers, and unloading effects due to glacier retreat may induce changed stress fields in the bedrock. Due to rock or ice avalanches, the terrain may become oversteepened and the internal stress field is changed. Subsequently, terrain adjustments implying mass movement activity occur to recover equilibrium. The analyses show a strong stability coupling between permafrost affected bedrock and adjacent hanging glaciers.

Looking at the glacierization, increased area-wide ice loss could be observed since 1956, probably to be explained by the trend towards increased air temperatures of about 0.5 to 1.5°C in this area. However, between 1988 and 2001, the lower part of the Monte Rosa glacier showed mass accumulation even though in other areas of the face, large ice loss occurred by ice avalanche events. Hence, simultaneous volume gain and volume loss can be observed in the glaciated areas at the

same time. These observations suggest complex glaciation/deglaciation processes in such high-mountain faces.

Another noticeable phenomenon is the surprisingly fast accumulation of ice at distinct zones, where it was eroded by preceding mass movement events, e.g. in the Zapparoli Channel and the Imseng Channel. The accumulation rate is in these areas with up to 10 m per year higher than the assumed local precipitation rate. Strikingly, the areas with fast accumulation are located in flatter, depression-like terrain. These high accumulation rates are most likely influenced by snow redistribution due to complex wind fields, and snow and ice avalanches from steeper parts. Considering the photographs from 2003 and 2007 (Figure 6), it can be seen that the Marinelli Channel was totally ice-free in 2003 and shows again some ice cover in 2007. The ice and firn thickness in the Marinelli Channel is about 5 to 15 m. Such thin ice covers react extremely fast to temperature and precipitation changes, and can recover rapidly after having completely vanished.

7. Conclusion and perspectives

The results of the multi-temporal DTM comparison in this study represent a unique new way of documenting and quantitatively assessing topographic changes in bedrock and ice in a large periglacial area. The combination of LiDAR data and photogrammetrically processed aerial images allows detailed investigations over long time periods. Large numbers of terrestrial photographs and orthophotos provide insights that help to interpret processes influencing slope stability. Processes that influence glacier and rock slope stability, however, cannot be determined from DTM analyses alone; additional observations in the field and the investigation of orthophotos and terrestrial images are essential.

Permafrost and glaciers in cold mountain regions will continue to be affected by climate change. In other steep periglacial mountain faces comparatively strong changes may develop, or have already developed. Consequently, further hazardous situations are likely to emerge. Therefore, remote sensing methods for the investigation and monitoring of high-mountain faces should be further developed and applied. The combination and integration of different technologies help to improve our understanding of the involved processes and corresponding hazard assessments. The acquisition of LiDAR at regular intervals would be important for establishing a detailed data base that documents topographic changes. For continuous monitoring and hazard assessment fixed installation of automatic cameras taking photographs with higher temporal resolution provide additional information at high temporal resolution.

Acknowledgements

The authors thank H. Röthlisberger, G. Mortara, M. Chiarle, P. Semino and A. Tamburini for providing imagery data and valuable information about the Monte Rosa east face. We acknowledge the support and funding from the Swiss National Science Foundation (project no. 200021-111967).

References

Akca D, Gruen A. 2007. Generalized least squares multiple 3D surface matching. In *International Archives of the Photogrammetry, Remote Sensing and Spatial Information Sciences*, Vol. XXXVI, Part 3 / W52, 1-7.

Baldi P, Bonvalot S, Briole P, Coltelli M, Gwinner K, Marsella M, Puglisi G, Remy D. 2002. Validation and comparison of different techniques for the derivation of digital elevation models and volcanic monitoring (Vulcano Island, Italy). *International Journal of Remote Sensing* **23**: 4783– 4800.

Ballantyne CK. 2002. Paraglacial geomorphology. *Quaternary Science Reviews* **21**: 1935-2017.

Baltsavias EP. 1999. A comparison between photogrammetry and laser scanning. *ISPRS Journal of Photogrammetry and Remote Sensing* **54**: 83-94.

Baltsavias EP, Favey E, Bauder A, Bösch H, Pateraki M. 2001. Digital surface modelling by airborne laser scanning and digital photogrammetry for glacier monitoring. *The Photogrammetric Record* **17**(98): 243–273.

Barla G, Dutto F, Mortara G. 2000. Brenva Glacier rock avalanche of 18 January 1997 on the Mont Blanc range, northwest Italy. *Landslide news* **13**: 2-5.

Bitelli G, Dubbini M, Zanutta A. 2004. Terrestrial laser scanning and digital photogrammetry techniques to monitor landslide bodies. In *Proceedings of ISPRS WG V/2*, Istanbul, Turkey. 246-251.

Bottino G, Chiarle M, Joly A, Mortara G. 2002. Modelling rock avalanches and their relation to permafrost degradation in glacial environments. *Permafrost Periglacial Processes* **13**: 283-388.

Buchroithner M. 2002. Creating the virtual Eiger North Face. *ISPRS Journal of Photogrammetry and Remote Sensing* **57**(1-2): 114-125.

Cola G. 2005. The large landslide of the south-east face of Thurwieser peak (Thurwieser-Spitze) 3658 m (Upper Valtellina, Italy). *Terra Glacialis* **8**: 38– 45.

Davies MCR, Hamza O, Harris C. 2001. The effect of rise in mean annual temperature on the stability of rock slopes containing ice-filled discontinuities. *Permafrost Periglacial Processes* **12**(1): 137-144.

Dewitte O, Jasselette J-C, Cornet Y, Van Den Eeckhaut M, Collignon A, Poesen J, Demoulin A. 2008. Tracking landslide displacements by multi-temporal DTMs: A combined aerial stereophotogrammetric and LIDAR approach in western Belgium. *Engineering Geology* **99**(1-2): 11-22.

Eberhardt E, Stead D., Coggan JS. 2004. Numerical analysis of initiation and progressive failure in natural rock slopes - the 1991 Randa rockslide. *International Journal of Rock Mechanics and Mining Sciences* **41**: 69-87.

Eisenbeiss H, 2008. The autonomous mini helicopter: A powerful platform for mobile mapping. *The International Archives of the Photogrammetry, Remote Sensing and Spatial Information Sciences*. Vol. XXXVII. Part B1, 977-983.

Evans SG, and Clague JJ. 1994. Recent climatic change and catastrophic geomorphic processes in mountain environments. *Geomorphology* **10**: 107-128.

Fischer L, Huggel C. 2008. Methodical design for stability assessments of permafrost affected high-mountain rock walls. In *Proceedings of the 9th International Conference on Permafrost 2008,* Kane DL, Hinkel KM (eds). Institute of Northern Engineering, University of Alaska: Fairbanks, Alaska. Volume 1: 439-444.

Fischer L, Kääb A, Huggel C, Noetzli J. 2006. Geology, glacier retreat and permafrost degradation as controlling factors of slope instabilities in a high-mountain rock wall: Monte Rosa east face. *Natural Hazards and Earth System Science* **6**: 761-772.

Gruber S, Haeberli W. 2007. Permafrost in steep bedrock slopes and its temperature-related destabilization following climate change. *Journal of Geophysical Research* **112**: F02S18. DOI:10.1029/2006JF000547

Gruen A, Akca D. 2005. Least squares 3D surface and curve matching. *ISPRS Journal of Photogrammetry and Remote Sensing* **31**(3B): 151-174.

Gruen A, Zhang L, Eisenbeiss H. 2005. 3D precision processing of high-resolution satellite imagery. In *Proceedings of the ASPRS 2005 Annual Conference.* Baltimore, Maryland, USA.

Haeberli W. 2005. Investigating glacier-permafrost relationships in high-mountain areas: historical background, selected examples and research needs. In *Cryospheric Systems: Glaciers and Permafrost* Harris C, Murton JB. (eds). The Geological Society of London, Special Publication, **242**: 29-37.

Haeberli W, Beniston M. 1998. Climate change and its impacts on glaciers and permafrost in the Alps. *Ambio* **27**(4): 258-265.

Haeberli, W, Wegmann, M,Vonder Muehll D. 1997. Slope stability problems related to glacier shrinkage and permafrost degradation in the Alps, *Eclogae Geologicae Helvetiae*, 90, 407-414.

Haeberli W, Kääb A, Hoelzle M, Bösch H, Funk M, Vonder Mühll D, Keller D. 1999. *Eisschwund und Naturkatastrophen im Hochgebirge*. Schlussbericht NFP31, v/d/f Hochschulverlag ETH Zürich.

Haeberli W, Kääb A, Paul F, Chiarle M, Mortara G, Mazza A, Deline P, Richardson S. 2002. A surge-type movement at Ghiacciaio del Belvedere and a developing slope instability in the east face of Monte Rosa, Macugnaga, Italian Alps, *Norwegian Journal of Geography* **56**: 104-111.

Haeberli W, Huggel C, Kääb A, Zgraggen-Oswald S, Polkvoj A, Galushkin I, Zotikov I, Osokin N. 2004. The Kolka-Karmadon rock/ice slide of 20 September 2002: an extraordinary event of historical dimensions in North Ossetia, Russian Caucasus. *Journal of Glaciology* **50**(171): 533-546.

Harris C, Davies MCR, Etzelmüller B. 2001. The assessment of potential geotechnical hazards associated with mountain permafrost in a warming global climate. *Permafrost and Periglacial Processes* **12**(1): 145–156.

Harris C, Arenson LU, Christiansen HH, Etzelmüller B, Frauenfelder R, Gruber S, Haeberli W, Hauck C, Hoelzle M, Humlum O, Isaksen K, Kääb A, Kern-Lütschg MA, Lehning M, Matsuoka N, Murton JB, Noetzli J, Phillips M, Ross N, Seppälä M, Springman SM, Vonder Mühll D. 2009. Permafrost and climate in Europe: Monitoring and modelling thermal, geomorphological and geotechnical responses. *Earth Science Reviews* **92**(3-4): 117-171.

Huggel C. 2009. Recent extreme slope failures in glacial environments: effects of thermal pertubation. *Quaternary Science Reviews* **28**: 1119-1130.

Huggel C, Zgraggen-Oswald S, Haeberli W, Kääb A, Polkvoj A, Galushkin I, Evans SG. 2005. The 2002 rock/ice avalanche at Kolka/Karmadon, Russian Caucasus: assessment of extraordinary avalanche formation and mobility, and application of QuickBird satellite imagery. *Natural Hazards and Earth System Sciences* **5**: 173-187.

IPCC 2007. *Climate Change 2007: The Physical Science Basis*. Contribution of Working Group 1 to the Fourth Assessment Report of the Intergovernmental Panel on Climate Change. Solomon S, Qin D, Manning M, Chen Z, Marquis MC, Averyt K, Tignor M, Miller HL. (eds). Intergovernmental Panel on Climate Change, Cambridge and New York.

Kääb A. 2002. Monitoring high-mountain terrain deformation from repeated air- and spaceborne optical data: examples using digital aerial imagery and ASTER data, *ISPRS Journal of Photogrammetry and Remote Sensing* **57**(1-2): 39-52.

Kääb A. 2008. Remote sensing of permafrost-related problems and hazards. *Permafrost Periglacial Processes* **19**: 107-136.

Kääb A, Huggel C, Barbero S, Chiarle M, Cordola M, Epifani F, Haeberli W, Mortara G, Semino P, Tamburini A, Viazzo G. 2004. Glacier hazards at Belvedere glacier and the Monte Rosa east face, Italian Alps: Processes and mitigation. In *Proceedings of the Interpraevent 2004*. Riva/Trient. Volume I: 67-78

Kääb A, Huggel C, Fischer L, Guex S, Paul F, Roer I, Salzmann N, Schlaefli S, Schmutz K, Schneider D, Strozzi T, Weidmann W. 2005. Remote sensing of glacier- and permafrost-related hazards in high mountains: an overview. *Natural Hazards and Earth System Sciences* **5**: 527-554.

Lim M, Petley DN, Rosser NJ, Allison RJ Long AJ. 2005. Combined digital photogrammetry and time-of-flight laser scanning for monitoring cliff evolution. *The Photogrammetric Record* **20**(110): 109-129.

Luethy J, Stengele R. 2005. Mapping of Switzerland - challenges and experiences, In *Proceedings of ISPRS WG III/3, III/4, V/3 Workshop "Laser scanning 2005",* Enschede, Netherlands, September 12-14, 2005, 42-47.

Oppikofer T, Jaboyedoff M, Keusen H-R. 2008. Collapse at the eastern Eiger flank in the Swiss Alps. *Nature Geoscience* **1**: 531-535.

Post A, Lachapelle ER. 1971. *Glacier ice*. University of Toronto Press; 110 pp.

Pralong A, Funk M. 2006. On the instability of avalanching glaciers. *Journal of Glaciology* **52**(176): 31-48.

Quincey DJ, Lucas RM, Richardson SD, Glasser NF, Hambrey MJ, Reynolds JM. 2005. Optical remote sensing techniques in high-mountain environments: application to glacial hazards. *Progress in Physical Geography*, **29**(4): 475-505.

Rabatel A, Deline P, Jaillet S, Ravanel L. 2008. Rock falls in high-alpine rock walls quantified by terrestrial lidar measurements: A case study in the Mont Blanc area. *Geophysical Research Letters* **35**(10): L10502, doi:10.1029/2008GL033424.

Rosser NJ, Petley DN, Lim M, Dunning SA, Allison RJ. 2005. Terrestrial laser scanning for monitoring the process of hard rock cliff erosion. *The Quarterly Journal of Engineering Geology and Hydrogeology* **38**(4): 363-375.

Ruiz A, Kornus W, Talaya J, Colomer JL. 2004. Terrain modeling in an extremely steep mountain: A combination of airborne and terrestrial lidar. In *International Archives of Photogrammetry, Remote Sensing and Spatial Information Sciences*, Vol. XXXV, Part B3 pp. 4.

Skaloud J, Vallet J, Keller K, Vessière G, Kölbl O. 2005. Helimap: Rapid large scale mapping using handheld LiDAR/CCD/GPS/INS Sensors on Helicopters. In *Proceedings of the ION GNSS Congress*, Long Beach, Sept. 2005.

Tamburini A, Mortara G. 2005. The case of the "Effimero" Lake at Monte Rosa (Italian Western Alps): studies, field surveys, monitoring. In *Proceedings of the 10th ERB Conference, Turin, 13–17 October 2004, Unesco, IHP-VI Technical Documents in Hydrology,* **77**: 179–184.

Tufnell L. 1984. *Glacier hazards*. Longman: London and New York; 97 pp.

Vallet J. 2007. GPS-IMU and LiDAR integration to aerial photogrammetry: Development and practical experiences with Helimap System®. *Vorträge Dreiländertagung 27. Wissenschaftlich-Technische Jahrestagung der DGPF*. 19-21 June 2007, Muttenz.

Vallet J, Skaloud J. 2004. Development and experiences with a fully-digital handheld mapping system operated from a helicopter. *The International Archives of the Photogrammetry, Remote Sensing and Spatial Information Sciences*, Vol. XXXV, Part B, Commission 5.

Wang Y, Yang X, Stojic M, Skelton B. 2004. Toward higher automation and flexibility in commercial digital photogrammetric system. *The International Archives of the Photogrammetry, Remote Sensing and Spatial Information Sciences*, 838-841.

Wegmann M, Gudmundsson GH, Haeberli W. 1998. Permafrost changes in rock walls and the retreat of Alpine glaciers: a thermal modelling approach. *Permafrost Periglacial Processes* **9**: 23-33.

Wolff K, Gruen A. 2007. DSM generation from early ALOS/PRISM data using SAT-PP, *ISPRS Hannover Workshop "High-Resolution Earth Imaging for Geospatial Information",* Hannover, Germany, 29 May-1 June.

Zgraggen A. 2005. Measuring and modeling rock surface temperatures in the Monte Rosa east face. Diploma thesis. ETH Zurich.

Zhang L. 2005. Automatic Digital Surface Model (DSM) generation from Linear Array Images. Ph.D. thesis, Report No. 88, Institute of Geodesy and Photogrammetry, ETH Zurich, Switzerland.

Zhang L, Gruen A. 2006. Multi-image matching for DSM generation from IKONOS imagery, *ISPRS Journal of Photogrammetry and Remote Sensing* **60**(3): 195-211.

Züblin M, Fischer L, Eisenbeiss H. 2008. Combining photogrammetry and laser scanning for DEM generation in steep high-mountain areas. *The International Archives of the Photogrammetry, Remote Sensing and Spatial Information Sciences* Vol. XXXVI, Part B6b: 37-43.

V

The 1988 Tschierva rock avalanche (Piz Morteratsch, Switzerland): An integrated approach to periglacial rock slope stability assessment

Luzia Fischer[a]*, Florian Amann[b], Jeffrey R. Moore[b] and Christian Huggel[a]

[a] Glaciology, Geomorphodynamics & Geochronology, Department of Geography, University of Zurich, Switzerland

[b] Engineering Geology, Department of Earth Sciences, ETH Zurich, Switzerland

submitted to Engineering Geology

Abstract

The 1988 Tschierva rock avalanche in the eastern Swiss Alps involved several complex mechanisms relating to geological, geomechanical, glaciological, and hydrologic processes for which no clear trigger can be assigned. This paper investigates the periglacial slope failure based on a multi-disciplinary approach combining qualitative analysis of contributing factors with quantitative geomechanical modeling. The problem of data acquisition in complex high-mountain terrain is addressed, and an approach for slope stability analysis is presented that comprehensively copes with the existing data limitations.

Results from multi-factor analyses of morphology, geology, glaciation history, permafrost, hydrology, and climate allowed first conclusions to be drawn about the influence of these factors on slope stability. For more detailed process investigations, however, geomechanical modeling was performed. Results from kinematic analyses demonstrated the strong influence of discontinuity and slope geometry on the degree of kinematic freedom and stability of local rock slopes. Discontinuum modeling was then applied to investigate the both influence of glacier retreat and variable groundwater conditions. The results suggest progressive rock mass strength degradation through failure of intact rock bridges connecting non-persistent discontinuities following release of lateral support by deglaciation. The influence of an unfavorable groundwater setting was addressed using a conceptual hydro-mechanical approach, and demonstrated that repeat cycles of water pressure can result in irreversible slope displacements. Changes in permafrost are suggested to have influenced groundwater flow paths and the shear strength of ice-filled discontinuities. The combined results of this study reveal the strong influence of discontinuity orientation with respect to the rock slope, and the long-term effect of progressive development of persistent discontinuities induced by glacier retreat and groundwater loading cycles, in leading to the eventual rock avalanche.

Keywords: rock slope stability, periglacial, kinematics, numerical modeling, progressive failure

1. Introduction

Rock avalanches in the European Alps and other high mountain ranges document the potential hazard related to slope instabilities in alpine flanks (e.g. Evans and Clague, 1988, 1994; Dramis et al., 1995; Barla et al., 2000; Haeberli et al., 2004; Cola, 2005; Geertsema et al., 2006). Several recent alpine rock avalanches have been investigated in detail (e.g. Barla and Barla, 2001; Bottino et al., 2002; Noetzli et al., 2003; Fischer et al., 2006; Oppikofer et al., 2008; Huggel, 2009), but generally only single environmental factors have been considered in these investigations. The failure causes and process interactions controlling most alpine slope instabilities remain poorly understood.

The stability of mountain rock walls is influenced by a number of internal and external factors including the topographic and geological setting, geomechanical properties, hydrogeology, glaciation, and permafrost occurrence. Changes in one or more of these factors, often in combination with potential external forcings such as earthquakes or heavy precipitation, may reduce slope stability and lead to eventual failure (Wegmann et al., 1998; Ballantyne, 2002; Fischer and Huggel, 2008). Permafrost and glaciers are particularly sensitive to climate change (e.g. Harris et al., 2003, 2009; Zemp et al., 2006), and variations in their extent or geometry can have a large influence on rock wall stability. The response of steep mountain flanks to changes in these factors is strongly conditioned by the topography and geological setting, in particular by the geometrical and geotechnical characteristics of discontinuities (Einstein et al., 1983; Ballantyne, 2002). The stability of hard rock slopes is controlled not only by intact rock strength, but to a large degree by discontinuity properties and geometry (Hoek and Bray, 1981; Goodman, 1989; Giani, 1992).

Changes in the distribution and temperature regimes of alpine glaciers and permafrost can have a large impact on the local rock wall stress field and hydrologic and geomechanical properties (Evans and Clague, 1993; Haeberli et al., 1997; Wegmann et al., 1998; Harris et al., 2001; Davies et al., 2001). Different physical processes may link warming permafrost and destabilization of steep bedrock, such as the loss of ice bonding in fractures, reduction of shear strength, and increased hydrostatic pressure (Gruber and Haeberli, 2007). A large number of recent rock avalanches are thought to be related to ongoing changes in permafrost occurrence (Bottino et al., 2002; Noetzli et al., 2003), for example the 2.5 x 10^6 m^3 rock avalanche from Punta Thurwieser, Italy, in 2004 (Cola, 2005), the 2-3 x 10^6 m^3 Brenva rock avalanche, Mont Blanc region, Italy, in 1997 (Barla et al., 2000), and the ~1 x 10^6 m^3 rock avalanches from Dents du Midi and Dents Blanches, Switzerland, in 2006. Glacial erosion and oversteepening, in combination with subsequent debuttressing accompanying glacier retreat, may result in slope instabilities such as progressive slope failures, rock avalanches, and deep-seated landslides (Evans and Clague, 1994; Augustinus, 1995; Ballantyne, 2002; Eberhardt et al., 2004). The failure mode, scale, and timing of periglacial rock slope adjustment are strongly conditioned by rock mass strength, and in particular by discontinuities (Ballantyne, 2002; Moore et al., 2009). Oversteepened slopes are generally thought to adjust rapidly to changing stress conditions by a reduction of the slope angle; however, many historical landslides may have been conditioned by late Pleistocene deglaciation more than 10,000 years earlier (Cruden and Hu, 1993). In such cases, slope deterioration can be additionally affected by progressive failure processes that act to reduce rock mass strength. Progressive failure is predominately driven by the propagation of fractures through intact rock pieces connecting existing discontinuities (Einstein et al., 1983; Eberhardt et al., 2004; Prudencio and Van Sint Jan, 2007).

The complexity of slope stability problems in glaciated and permafrost terrain requires a combination of different investigation and modeling techniques in order to resolve the relevant physical processes. High-mountain rock walls are an extremely challenging environment for data acquisition due to the complex topography and difficult access. The first step in assessing rock slope stability is detailed evaluation of the lithology and rock mass structure. Kinematic analyses based on rock wall and joint geometry can give an initial indication of failure potential (e.g. Goodman, 1989; Giani, 1992; Stead et al., 2001; Sartori et al., 2003). Many rock slope stability problems, however, involve complex geometry, lithology, in situ stresses, and hydraulic conditions, and are further complicated by coupling between these various parameters. For such complex slope stability analyses numerical modeling methods are often required; different approaches are described by Stead et al. (2001, 2006) and Eberhardt et al. (2004). Studies of alpine rock slope instabilities have shown that numerical models are a powerful tool for assessment of failure

mechanisms (e.g. Barla and Barla 2001; Eberhardt et al. 2004), but the necessary level of topographic and geotechnical detail can limit their application.

In this study, we focus on the 1988 Tschierva rock avalanche (Engadin, Swiss Alps) as an example of a recent periglacial rock avalanche event. The objectives of this paper are to analyze a broad range of factors influencing slope stability in an integrated manner, to evaluate slope stability with kinematic and numerical techniques focusing on the role of glacier retreat, permafrost and groundwater conditions, and finally to discuss the role of geological, geomechanical, and glaciological factors in leading to the rock avalanche. The study further contributes to developing a framework for slope stability assessment in high-mountain environments where access and site-specific data are typically limited. This is particularly relevant in view of the effects of recent and future climate change on rock slope stability in these regions.

2. Study site and 1988 rock avalanche

The 1988 Tschierva rock avalanche detached from the western flank of Piz Morteratsch in the eastern Swiss Alps (Fig. 1 and 2). The Piz Morteratsch is located within the Bernina massive, Engadin, between Val Roseg and Val Morteratsch, and reaches an elevation of 3751 m a.s.l. The Tschierva glacier is situated at the south-western foot of the Piz Morteratsch. Minor debris cover on this valley glacier, except for the deposit of the investigated rock avalanche, indicates that no larger mass movements occurred in this area during the last century.

The rock avalanche occurred on October 29, 1988, shortly before midnight. A volume of 250'000 - 300'000 m^3 of rock, estimated from the deposition area and thickness of deposits (Schweizer, 1990) as well as by the extent of the detachment zone (current study), detached at about 3180 m a.s.l. from the front of a steep west-facing ridge. The rock mass fell down onto the Tschierva glacier, incorporating material from below the detachment zone, finally coming to rest on the glacier at an elevation of about 2700 m a.s.l. The runout distance was approximately 1000 m and the drop height 480 m, corresponding to an average slope angle of 26°.

The detachment zone extends over an area of about 7000 - 8000 m^2. The shape is a triangular form about 150 m wide at the base and with the apex touching the ridge (Fig.1). The upper boundary of the detachment zone is located at an elevation of about 3180 m a.s.l., the lower boundary at 3050 m a.s.l. The surface is stepped in the form of three prominent large-scale benches (Fig. 3). The deposit is clearly delineated atop the otherwise relatively clean glacial ice and contains large boulders up to 200 m^3. The average thickness of the deposit was estimated to be 1 to 3 m immediately after the rock avalanche (Schweizer, 1990), but the thickness subsequently decreased due to dispersion of the debris by the flowing glacier.

Increased but small-volume rockfall activity was observed in the area during the months prior to the rock avalanche (personal communication A. Amstutz). During field work in summer and fall 2006, occasional minor rock fall activity was also observed. As earthquakes are known to trigger slope failure and the Engadin region shows occasional earthquake activity, the Swiss Macroseismic Earthquake Catalogue was consulted. Analysis of this seismic database showed that there was no seismic event within the timeframe of the slope failure. Thus, an earthquake can be excluded as a possible trigger of the Tschierva rock avalanche.

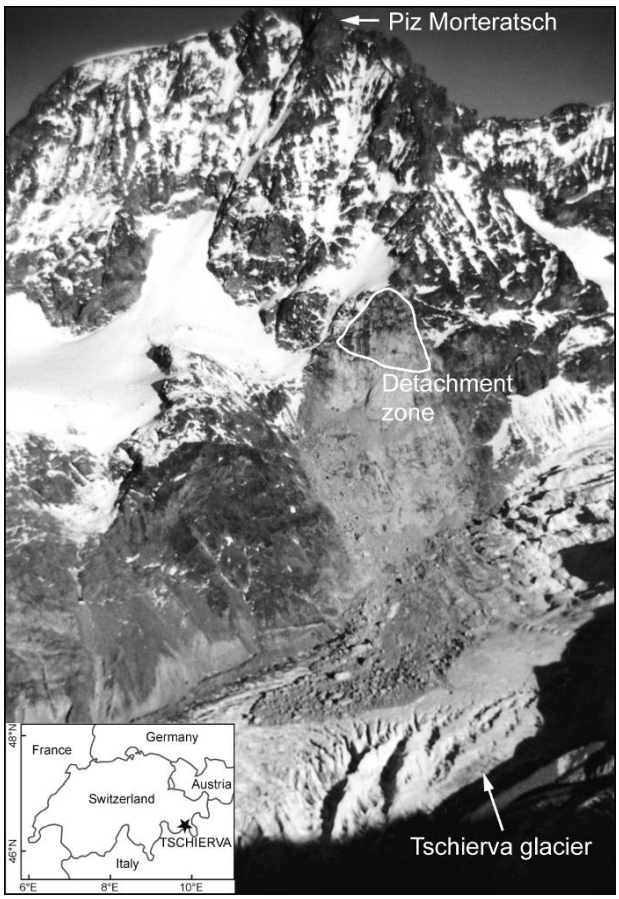

Fig. 1. Western flank of the Piz Morteratsch with the Tschierva glacier in the foreground. The detachment zone of the 1988 rock avalanche (outlined) and the deposits resting on the glacier are visible in the middle of the photograph (A. Amstutz, 1988).

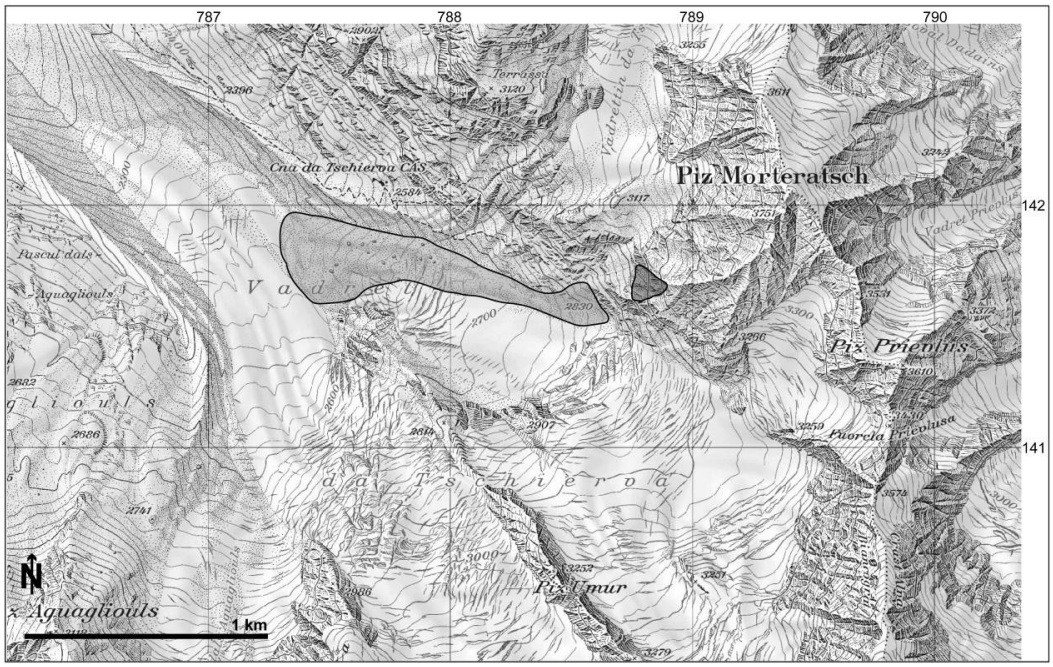

Fig. 2. Topographic map of the Piz Morteratsch and Tschierva Glacier. The detachment zone and deposit on the glacier (date of the map: 2003) are marked in gray. Topographic map is reproduced by permission from Swisstopo (BA091428).

3 Site investigation

3.1 Topography and morphology

The area around the Piz Morteratsch lies within an altitude range of 2500 to 4000 m a.s.l. The regional landforms show a strong influence of both Late Pleistocene and current glaciers. Only the highest peaks in the area remained ice free during the Last Glacial Maximum (LGM), while the lower flanks were sculpted and partially oversteepened by valley glaciers into strong U-shaped forms. Rock wall slope angles vary between 40° and 75°, while debris-covered, recently deglaciated slopes are inclined between 20° and 40°.

A topographic survey was conducted at the site to determine geometrical features and to obtain representative surface profiles. Due to difficult and dangerous access, the post-failure slope geometry was measured from a fixed position below the detachment zone with a laser rangefinder and inclinometer. The pre-failure surface was extracted from orthophotos dating from 1985 (Fig. 3). Details of the topography of the investigated flank including the detachment zone are illustrated in Fig. 3. In the upper-most area, the profile is divided into two parts: section [1] shows the ridge topography above the detachment zone, while section [2] displays the topography of the cirque located to the north above the detachment zone (cf. Fig. 1).

The 1988 Tschierva rock avalanche detached at the lowest part of the steep western ridge of the Piz Morteratsch, where the frontal section of the ridge widens to a steep, triangular flank. The ridge shows a shoulder-like morphology, steepening below the rounded edge then ending at the bottom of the flank in low angle debris-covered terrain. The upper part of the failed slope was gently inclined and rounded prior to the rock avalanche, while the lower portion was steeply inclined similar to the current slope. A small cirque is located slightly above the northern side of the ridge, directly adjacent to the frontal flank. This cirque holds snow nearly throughout the entire year.

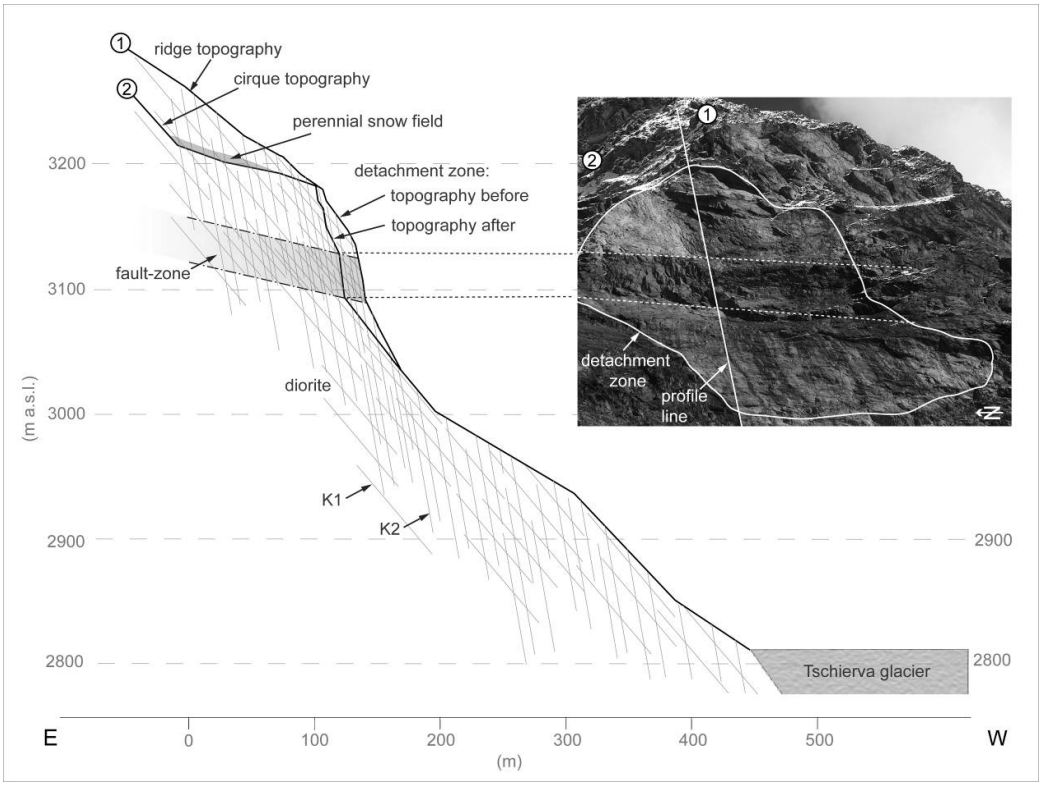

Fig. 3. Topographic profile and geological model of the investigated area, including the detachment zone of the Tschierva rock avalanche. Sections 1 and 2 show the two different neighboring topographies above the detachment zones, K1 and K2 are the predominant discontinuity sets. The profile line indicated in the photograph is used later in numerical slope stability modeling.

3.2 Geology and rock mass characterization

Geological mapping and rock mass characterization were conducted during field investigations and supplemented with additional geological data from Spillmann and Trommsdorff (2005). Rock mass characterization was performed in compliance with empirical rating schemes, such as the Geological Strength Index (GSI; Hoek and Brown, 1980, 1997) and the Rock Mass Rating system (RMR; Bieniawski, 1989). In this study, the uniaxial compressive strength (UCS) was estimated from reported literature values and the application of the Hoek-Brown failure criterion (Hoek and Brown, 1997) on field data (GSI). The rock mass characteristics are listed in Table 1.

The study area is located within the Lower Austroalpine nappe, in the crystalline rocks of the Bernina nappe system. The area of the Tschierva rock avalanche includes two primary lithologies: diorite is predominant throughout, while kataclastic-mylonitic altered rocks occur in the fault zone crossing the flank (Fig. 3). The fault zone has a thickness of 20 to 40 m and extends laterally over several kilometers. Similar fault zones can be observed elsewhere in the surrounding area. The local fault zone crosses the ridge horizontally through the detachment zone and dips out of the slope at approximately 15° to 20° (Fig. 3). The fault zone is a tectonically-modified rock mass consisting of greenschist to amphibolitic rock. This amphibolitic rock is foliated, and slicken-sides can be found on the surfaces of many discontinuities. The structure of the diorite is generally massive to blocky, and the minerals are marginally aligned.

Discontinuities (i.e. faults and joints) were analyzed in the field with regard to their geometrical and mechanical properties in order to provide a basis for subsequent kinematic and numerical modeling. Orientation measurements were performed manually at different sites close to and within the detachment zone. Four joint sets were mapped and characterized, based on statistical clustering of orientation measurements.

The predominant joint set, K1 (mean dip direction and dip angle: 250 / 56; Fig. 3), dips moderately to the west unfavorably out of slope (orientation of failed slope: 260-270 / 55-70), and can be found throughout the entire ridge. The second joint set, K2, dips steeply to the west (285 / 84; cf. Fig. 3). These two joint sets combine to create the primary surfaces of the detachment zone, where K1 forms large flat surfaces and K2 creates a series of steep scarps. There were two additional joint sets noted, K3 (300 / 66) and K4 (180 / 28), though they are less frequent and not persistent throughout the ridge. Joint frequency increases strongly within the fault zone compared to the dioritic rock mass, and additional indicators of shear displacements (slickensides) can be found on discontinuity surfaces in this area (Table 1). Joints in the faulted domain are often open or have mineral infillings.

Table 1. Rock mass properties of the two primary lithologies

		Diorite	Amphibolitic fault zone
UCS		150-200 MPa	130-180 MPa
GSI		55-65	45-55
Joint spacing		0.4 – 1.2 m	0.2 – 0.8 m
Joint condition	Persistence	3-10 m	3-10 m
	Aperture	0.1-1 mm	1-5 mm
	Roughness	slightly	smooth to slickensided
	Infilling	none to hard infilling < 5 mm	hard infilling > 5 mm
	Weathering	slightly to moderately weathered	moderately to highly weathered
Groundwater	Joint/Flow	dry/no	wet/occasional
	Description	dry	flowing

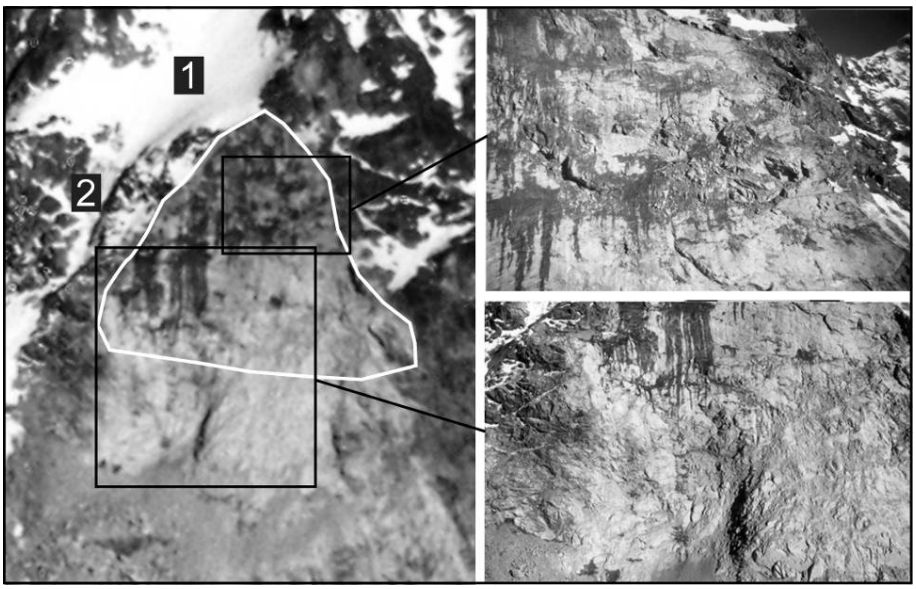

Fig. 4. Water discharge in the upper part of the detachment zone following the 1988 rock avalanche (A. Amstutz, 1988). The detachment zone is marked in white, [1] indicates the main infiltration zone and [2] the occasional surface water drainage.

3.3 Hydrological setting

Groundwater information was compiled from visual observations in 1988 and 2006, and through analysis of aerial and terrestrial photographs from different years. Strong water discharge was observed directly after the rock avalanche in the upper portion of the detachment zone in the area of the fault (cf. Fig. 4; personal communication A. Amstutz). Water outflow was also observed in this area during field work in the summer of 2006. At the end of September 2006, however, no water outflow could be observed, but prominent water staining could be seen in the area of the fault-zone and adjacent surfaces (photograph in Fig. 3). The strong water outflow observed after the slope failure in October 1988 is notable considering the low air temperatures around 0° C during the days before the rock avalanche that impeded enhanced melting (cf. Fig. 6 and section 3.7).

The primary water infiltration zone is assumed to be the cirque directly above and behind the crest of the detachment area (Fig. 1 and 3). Long-lasting snow patches persist nearly all year and may provide ample water supply (Fig. 1 and 4). Occasional surface water drainage from this cirque can be observed during summer along a small channel adjacent to the failed flank (Fig. 3 and 4). The hydrological transport properties of the bedrock are highly anisotropic, with flow largely controlled by discontinuities. Higher fluid conductivity due to more frequent and persistent discontinuities is expected within the fault zone. The sparsely jointed dioritic rock mass below the fault zone acts as a nearly impermeable barrier for water percolating from above. Therefore, discontinuities dipping out of slope at the lower boundary of the fault zone act as seepage paths. Significant water pressures may develop within the fault zone following periods of prolonged rainfall or intense snow melt. Such water pressure can act as a key triggering factor for slope instabilities.

3.4 Glaciation history

The history of glaciation in the Piz Morteratsch area was investigated in order to analyze the effects of glacier retreat on slope stability and deduce the relevant timescales. Our investigation was based on an existing digital glacier inventory of the Swiss Alps for the years 1850, 1973, and 1999. These

reconstructions of glacier extents were compiled from historical maps, aerial photographs, and satellite images (Müller et al., 1976; Maisch, 1992; Maisch et al., 2000; Paul, 2004). Fig. 5 shows the three past glacier extents in the area of the Tschierva rock avalanche. During the Little Ice Age (around 1850), the flank was not covered by ice. A small tributary glacier was located below the investigated rock slope. During the Pleistocene, the area was affected by a series of several glacial advance and retreat cycles (Maisch et al., 2000, Ivy-Ochs et al., 2008). The last glaciation of the entire rock slope occurred during the LGM (Late Pleistocene), when the ice thickness at the location of the detachment zone is estimated to have been between 50 and 150 m (Jäckli, 1962; Maisch, 1992).

3.5 Permafrost distribution

Rock wall surface temperature is a function of the energy balance at the rock surface, and has a strong influence on subsurface temperatures and permafrost occurrence. The primary factors determining the surface temperature of a rock wall are aspect (shortwave radiation), altitude (sensible heat and longwave incoming radiation), and lithology (albedo; Noetzli et al., 2003). Temperature estimations by Noetzli et al. (2003) were complemented with distributed temperature modeling by Noetzli using the topography and energy balance model TEBAL (Gruber, 2005). A 25 m digital elevation model (DHM25 Level 2; Swisstopo) and climate time series data from 1990-1999 from the Corvatsch meteorological station were used in this analysis (data provided by MeteoSchweiz). Based on the key assumption that a mean annual ground surface temperature (MAGST) of 0° C indicates the limit of permafrost existence, the spatial permafrost distribution was assessed.

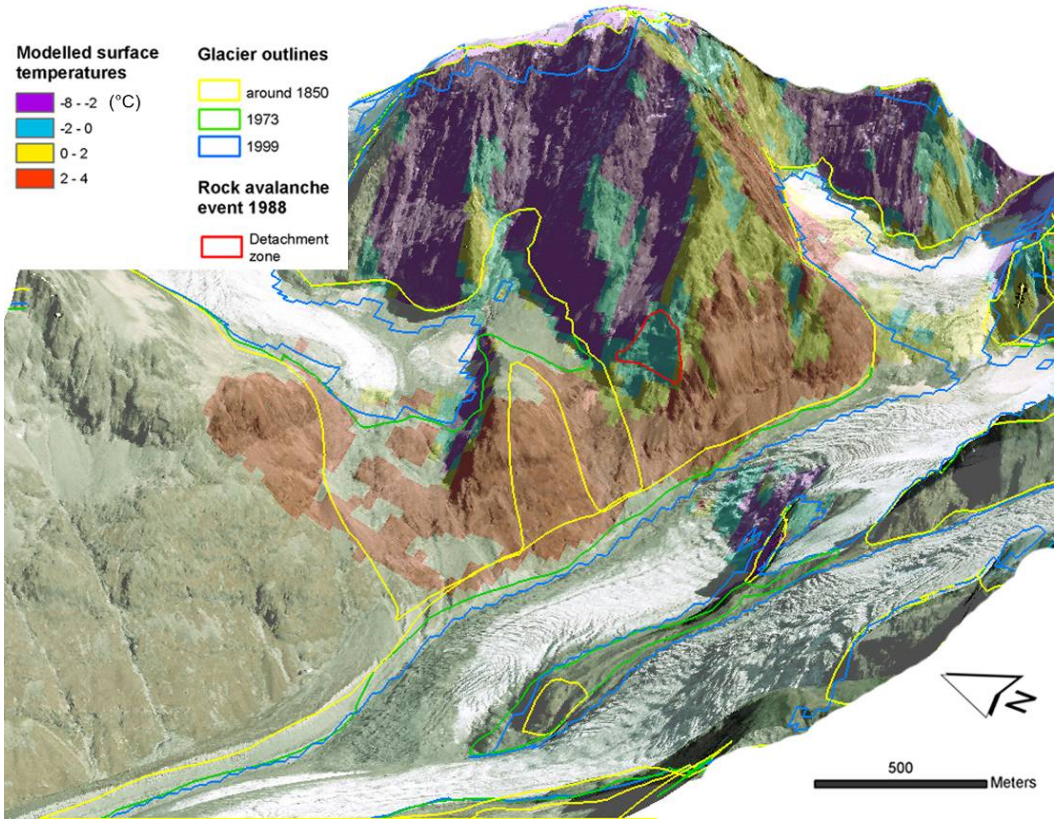

Fig. 5. Modeled ground surface temperatures (in °C) and glacier outlines at three different times for the Piz Morteratsch area. The synthetic view is computed from a 2003 orthophoto and 25 m DHM (reproduced with permission from Swisstopo; BA091428).

Fig. 5 shows the results of temperature modeling for the Piz Morteratsch area. Due to the delayed reaction of permafrost to 20th century warming, permafrost in rock walls may still occur below the surface down to about 150m lower than simulated here (Noetzli et al., 2007).

Mean annual ground surface temperatures in steep rock in the Piz Morteratsch area range, depending on aspect and altitude, from about -8° C (dark blue) to +4° C (red, Fig. 5). In the area of the detachment zone, the modeled surface temperatures are between -2° C and 0° C. This result indicates probable permafrost in close proximity to the limit of permafrost existence. Interstitial ice would thus be close to the melting point, and the combined occurrence of ice and water could be present in discontinuities. Observation of ice within the detachment zone after the 1988 failure (personal communication A. Amstutz) confirms the modeled negative surface temperatures. In the area of the detachment zone, complex surface temperature fields are observed. The modeled surface temperatures are positive on the southern side of the ridge and negative on the northern side. This introduces a complex subsurface temperature field, which can strongly influence the permafrost distribution and also groundwater flow paths from the assumed infiltration zone in cirque.

3.6 Meteorological data

Precipitation and temperature data were analyzed to help understand any possible role of meteorological factors in triggering the slope failure. Temperature and precipitation data are available since 1980 for the Corvatsch meteorological station located 6 km to the west of the detachment zone at an elevation of 3315 m a.s.l. (data provided by MeteoSchweiz). Due to the proximity and similar altitude of the climate station, the data are considered to be directly transferable.

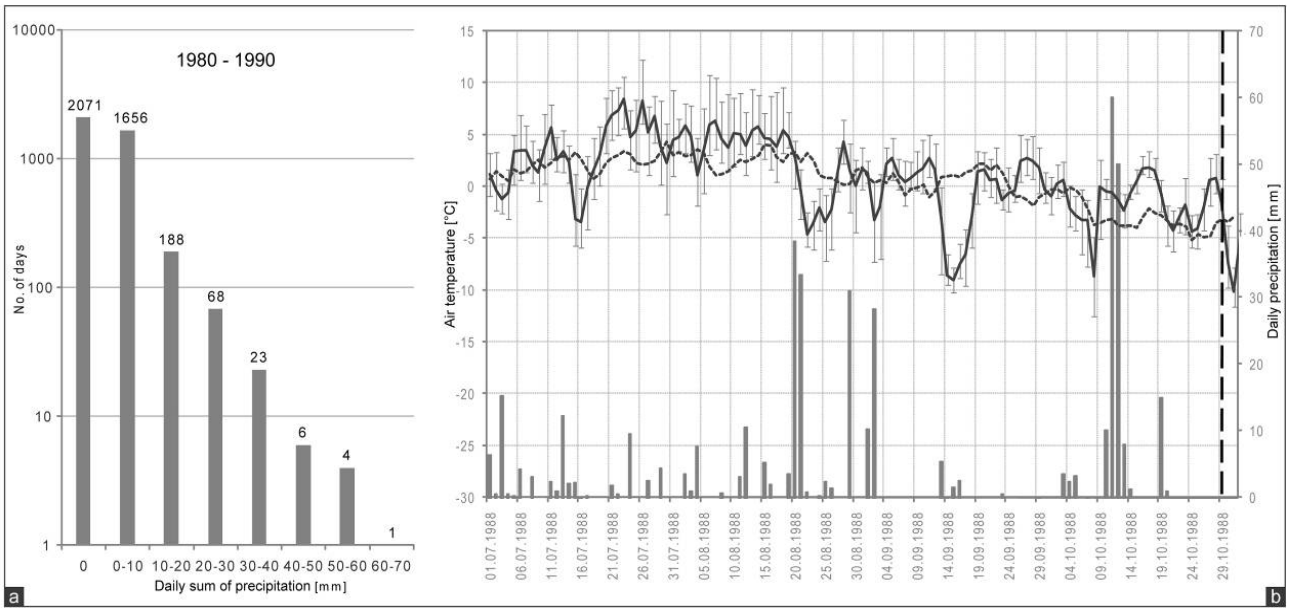

Fig. 6. Temperature and precipitation data from the Corvatsch climate station near to the Tschierva rock avalanche (data provided by MeteoSchweiz). [a]: Number of days with particular daily sum of precipitation from 1980 to1990; note the logarithmic scale on the number of days. [b]: Daily precipitation and mean daily air temperature (with indicated minimum and maximum values) during the four months prior to the Tschierva rock avalanche (marked by a vertical dashed line). The dotted line indicates the mean daily air temperature from 1980 to 1990.

Meteorological data were analyzed for a timeframe from 1980 to 1995 in order to obtain reliable mean values and identify outliers. Fig. 6a shows the total number of days between 1980 and 1990 with different daily sums of precipitation. The maximum daily precipitation during this period is between 60 and 70 mm, and the data show only five days with more than 50 mm precipitation. Precipitation data from July 1988 to October 1988 (Fig. 6b), show that two of these five days of heavy precipitation occurred just two weeks before the slope failure (vertical dashed line). This precipitation in October 1988 likely occurred as snowfall, as indicated by sub-zero air temperatures, which can delay potential water infiltration.

Fig. 6b also shows daily air temperatures between July and October 1988. The solid line is the daily mean temperature during this period with indicated daily minimum and maximum, while the dashed line shows the long-term (1980 to 1990) mean daily air temperature. The 1988 summer temperatures are, in general, slightly higher than the long-term mean, but the differences are relatively minor. The meteorological data show an exceptional precipitation event on 11 and 12 October, 1988, and reveal two periods with above-zero temperatures between this snowfall event and the rock avalanche, which could allow for melting of the newly fallen snow. However, it is difficult to estimate the amount of snowmelt and subsequent infiltration based on these data.

3.7 Hypotheses based on site investigation

Results of the site investigation lead to the following hypotheses to be addressed with kinematic and numerical slope stability analyses:

1. Discontinuity and rock slope geometry determine the location of potential slope failures.
2. The regional morphology shows a strong glacial overprint, and the failed flank had been modified by repeat Pleistocene glaciations. The oversteepened topography, in combination with debuttressing accompanying glacial retreat, creates an unfavourable condition for slope stability.
3. Permafrost and permafrost degradation may have contributed to the slope destabilization.
4. Different permeabilities within the fault zone and the underlying diorite can induce an unfavorable groundwater setting. Increased water pressure after heavy precipitation in mid-October, 1988 may have adversely influenced slope stability.

4. Geomechanical analyses

4.1 Kinematic analysis

4.1.1 Method

Kinematic analysis of discontinuity-controlled slope instabilities takes into account comparison of joint orientation and friction angle with the geometry of the slope free face. Due to field evidence, planar sliding is anticipated to be the dominant failure mechanism at our site, and therefore exclusively investigated in this study. The kinematic analysis is based on the stereographic projection method according to Norrish and Wyllie (1996). To approximate failure conditions, the following fundamental mechanical criteria for discontinuity-controlled planar failure in rock slopes were considered:

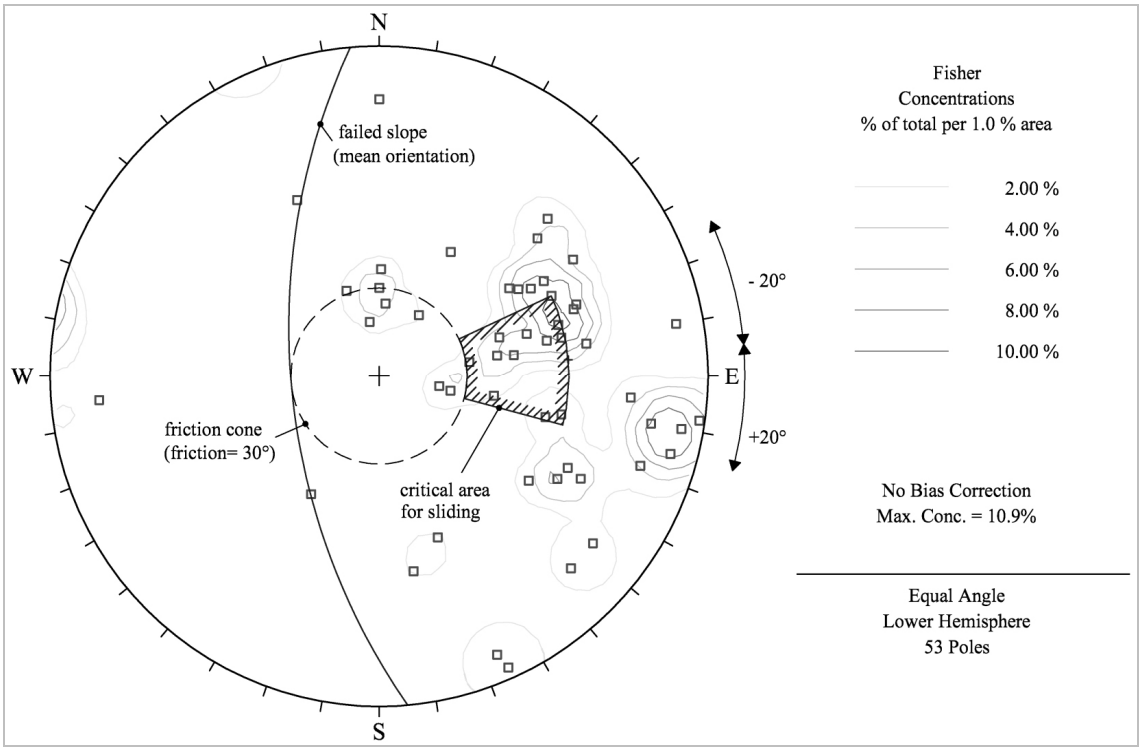

Fig. 7. Kinematic conditions for discontinuity-controlled planar failure in rock slopes. Based on the assumed failure criteria, a critical area for sliding can be distinguished (hatched outline). Fisher concentrations show the density of poles from field discontinuity data.

The slope fails if: $\Psi_f > \Psi_p > \Phi$ and

$$\alpha_f - \alpha_p \leq 20°$$

where Ψ_f: rock face dip angle, Ψ_p: joint dip angle; Φ: joint friction angle (assumed to be 30°). The critical departure between dip direction of the slope (α_f) and discontinuity (α_p) was assumed to be 20° (Fig. 7).

To account for the variability of slope and discontinuity geometry (Fig. 7), a probabilistic approach was applied in our kinematic analysis (Rosenbleuth, 1981; Christian and Baecher, 2002). The approach is based on the assumption that the slope and fracture geometry are representative, and the variability of the slope orientation is known. In order to highlight the influence of discontinuity geometry in relation to slope orientation, the adjacent stable slopes in vicinity of the failure zone were also analyzed. The two investigated slopes were: [A] the failed portion of the rock slope, and [B] the adjacent stable flank. For the probabilistic analysis of different rock slope orientations (according to Rosenbleuth, 1981), the corresponding geometrical variables were chosen: [A] dip angle of 55-70° and dip direction of 260-270°, and [B] dip angle of 55-70° and dip direction of 205-225°. These values were extracted from a 25 m gridded digital elevation model (DHM25 Level 2, Swisstopo). Based on field measurements and observations, the orientation of discontinuities is assumed to be the same for flanks [A] and [B].

4.1.2 Results

Results of the kinematic analysis indicate the potential for planar sliding along pre-existing discontinuities K1 and K2 in the failed portion of the slope. The likelihood of planar sliding is significantly higher in the detachment area [A] in comparison to the adjacent stable slopes [B]. For

a representative variability of slope and discontinuity geometry in the failed area, 10 to 33% of the poles indicate the potential for planar sliding (90% confidence interval, normal distribution assumed). For the adjacent stable slope [B], only 1 to 6% of the poles plot within the critical area for planar sliding. These results confirm that the slope and discontinuity geometry have a significant influence on the degree of kinematic freedom and slope stability.

The analysis of kinematic conditions shows that the probability of planar sliding along existing discontinuities is significantly higher in the area of the slope failure than in the adjacent stable flank. Minor changes in slope orientation and angle reduce the occurrence of daylighting discontinuities and consequently limit the degree of kinematic freedom. Planar sliding is impossible when no discontinuity sets daylight on the slope.

4.2 Numerical slope stability assessment

4.2.1 Method

Numerical slope stability modeling was performed using the Universal Distinct Element Code UDEC (Itasca, 2004) to investigate the influence of different factors and underlying mechanisms contributing to the rock avalanche.

UDEC is a two-dimensional distinct element code appropriate for analysis of discontinuous materials. Rock joints are viewed as interfaces between blocks along which contact forces and displacements can be calculated. Movement of the block system results from applied loads or forces, which in the current study is gravitational force. Additionally, fully-coupled mechanical-hydraulic analysis can be performed. In this study, numerical modeling was used in a conceptual manner to test the hypotheses developed from the site characterization.

4.2.2 Modeling setup

The profile for the numerical modeling is positioned in the central portion of the detachment zone and extends from the Tschierva glacier to the ridge approximately 50 m above the detachment zone (Fig. 3). The two dominant discontinuity sets K1 and K2, as well as the fault zone, were included in the model. The slope surface geometry after the rock avalanche was not implemented.

For model initialization introducing the in situ stress conditions, all joints were assumed to follow Mohr-Coulomb behavior, i.e. perfectly elasto-plastic joints, so as to avoid brittle failure during this stage. For all subsequent simulations, the joint model was set to Mohr-Coulomb slip with residual strength, i.e. perfect brittle joints. The intact rock material was assumed to be linear-elastic for all modeling series. Modeling of glacier retreat was performed neglecting the influence of water pressure in the rock mass in order to analyze the mechanical and hydrological aspects independently.

The input parameters for the intact rock and discontinuity properties are summarized in Table 2. Discontinuity persistence is a key factor influencing rock mass strength and slope stability (Einstein et al., 1983). Failure along non-persistent discontinuities may require fracturing through intact rock bridges. The combined strength of non-persistent joints and intact rock pieces can be approximated by applying Jennings' equivalent cohesion and friction criterion. Jennings (1970) offered a fundamental method to estimate the shear resistance (R) on a sliding surface that is partitioned into intact rock bridges of area A_r and a joint area of $A_j = A - A_r$. The shear resistance to

sliding can be evaluated as a weighted combination of the shear resistance of intact rock bridges (R_r) and the shear resistance of joint surface (R_j) (Einstein et al., 1983):

$$R = A_r/A \cdot R_r + A_j/A \cdot R_j$$

The equivalent friction and cohesion are then given by:

$$c_a = (1\text{-}K); \cdot c_r + K \cdot c_j$$

$$\tan\Phi_a = (1\text{-}K); \cdot \tan\Phi_r + K \cdot \tan\Phi_j$$

Where K = Persistence = A_j/A, c_a = apparent cohesion, c_r = cohesion of the intact rock bridges, c_j = joint surface cohesion, Φ_a = apparent friction angle, Φ_r = friction angle of intact rock bridges and Φ_j = friction angle of the joint surface. Einstein et al. (1983) discussed the shortcomings and limitations of the method (e.g. the failure surface is restricted to joint planes and en-echelon failures are neglected).

The first series of discontinuum models were calculated in order to establish an equilibrium stability state. Stresses were initialized and run to equilibrium with a standard horizontal to vertical stress ratio of 0.5 (i.e. $k = \sigma_H / \sigma_V = 0.5$).

Considering the large uncertainties associated with specific conditions, in particular the state of stress, deformability, and strength properties, a sensitivity analysis was performed for key geotechnical parameters. The primary emphasis in this sensitivity analysis was to constrain the joint friction angle and cohesion. The sensitivity analysis showed, that for the given geometry with persistent discontinuities, the stability threshold requires cohesion between 0.1 - 0.3 MPa and a friction angle between 30 - 50°. The slope becomes unstable with cohesion values lower than 0.1 MPa.

Table 2

Material properties for the discontinuum slope stability modeling.

Parameter	Diorite	Fault zone	Glacial ice
Young's modulus (GPa)	20	15	10
Poisson's ratio	0.25	0.25	0.3
Density (kg/m^3)	2700	2700	900
Persistence K (%)	0.95-0.97	0.95-0.97	
Joint normal stiffness (GPa/m)	10	10	
Joint shear stiffness (GPa/m)	1	1	
Joint cohesion (MPa)	0.5-1	0.5-1	
Joint friction (°)	30-35	30-35	
Joint dilatation angle (kPa)	0	0	
Joint tensile strength (kPa)	0-0.5	0-0.5	
Joint residual cohesion (MPa)	0.1	0.1	
Joint residual friction (°)	30	30	
Joint residual tensile strength	0	0	

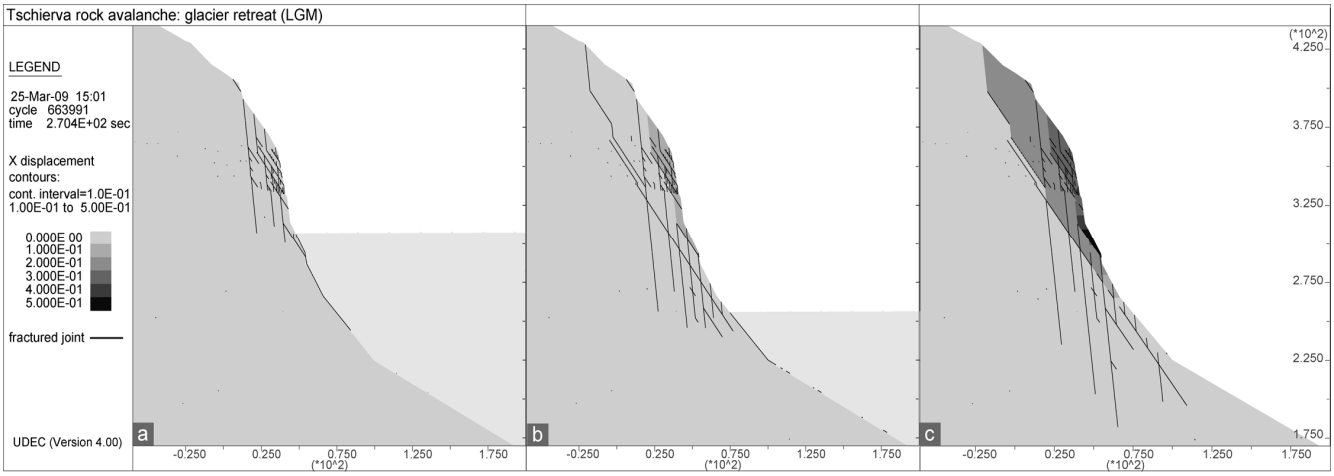

Fig. 8. [a-c]: Retreat of Pleistocene glaciers and associated confinement loss alters the stress field in the rock slope and induces progressive failure through non-persistent discontinuities (black lines). Horizontal displacements between 10 and 40 cm can be observed in stage [c] along a stepped sliding surface that matches well with the observed 1988 failure surface.

4.2.3 Results I: Glacier retreat

Glacial unloading was simulated by assuming glacier down-wasting of approximately 450 m to the current level. This value is in accordance with reconstructed glacial ice surface maximums during the LGM (Jäckli, 1962). The process of glacier retreat was modeled with nineteen stages of ice surface lowering in the 2D profile.

Fig. 8 shows three stages of the glacier retreat. The results reveal fracturing of intact rock bridges in the near-surface areas with lowering of the glacier ice level. In Fig. 8b, horizontal displacements in the range of 10 cm can be observed in the steep frontal portion of the flank; a result of this debuttressing. The model suggests that progressive development of fractured joint surfaces primarily occurs in steep zones of the slope. Changes in the stress field in this area were pronounced, while the main discontinuity set daylights on the slope, generating an unfavorable situation for slope stability.

Minor movements can be detected along a stepped surface (Fig. 8c), which corresponds well with the observed failure surface from the 1988 rock avalanche. This indicates that fracturing of intact rock bridges along non-persistent discontinuities, and planar sliding on the two main joint sets was already induced by glacial unloading. However, for bulk failure to occur the discontinuities must be fully persistent, and our numerical models show that the slope remains stable under the assumption of 3% intact rock bridges.

As shown in the kinematic analysis, the assumption of joint frictional strength alone results in failure immediately after the glacier has retreated to a critical level where sliding is permitted by the new kinematic freedom. Since the slope was stable for many thousands of years following retreat of LGM glaciers, we can assume that there were still intact rock bridges between discontinuities after deglaciation, and the influence of glacier retreat can be considered as preparatory degradation of rock mass strength but not the primary reason for slope failure.

4.2.4 Results II: Hydrologic loading conditions

Model simulations including groundwater loading were performed to assess the influence of water pressure on slope stability. Due to the lack of detailed measurements of water pressures and flow paths, this modeling describes only the basic concept based on visual observations.

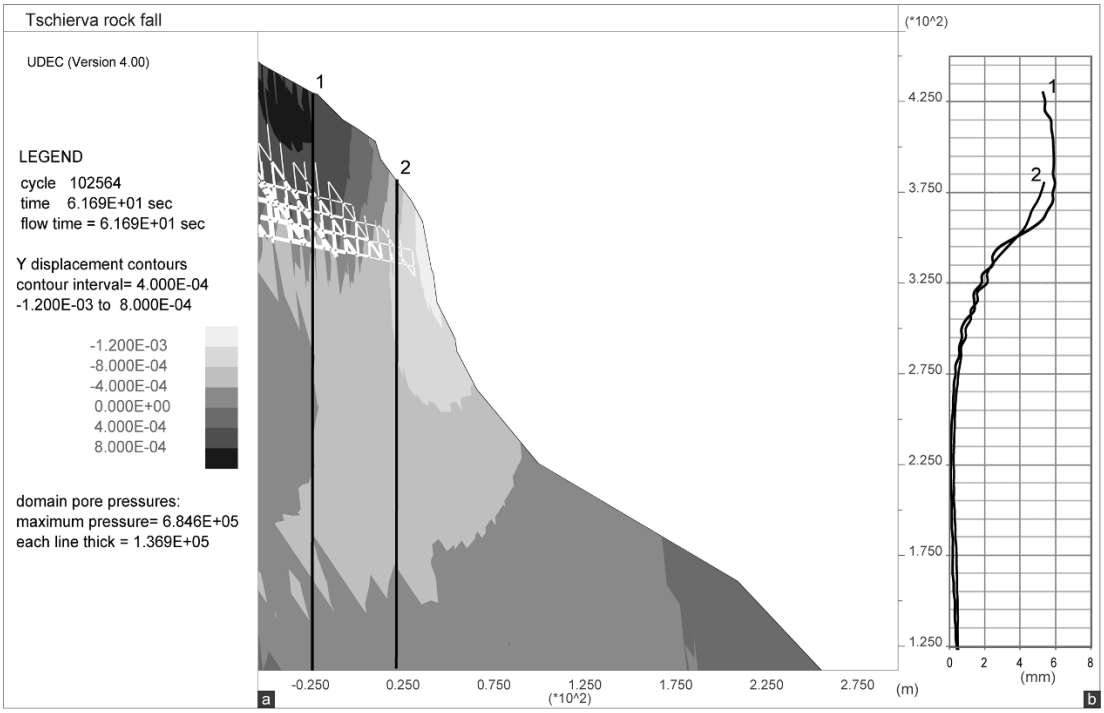

Fig. 9. The influence of hydrologic loading within the fault zone: [a] vertical displacement in the 2D profile after application of groundwater, [b] horizontal displacement along the two marked vertical profiles. Horizontal displacements concentrate in the area of high fluid pressures (white lines), while the vertical displacements proceed further down into the rock mass.

In first model runs, the groundwater conditions were simulated with a permanent water table at different elevations. The results showed that as soon as the steep portion of the rock slope is water saturated it becomes unstable. More realistic analyses incorporating the observed hydrological setting were then conducted. As observed during field investigations, the fault zone shows increased permeability compared to the underlying dioritic rock mass (Fig. 3 and 4). Therefore, permeability of the joints within the fault zone was increased by implementing a joint aperture 10 times higher than that for the dioritic rock mass. Additionally, permeability was decreased within a narrow layer at the lower boundary of the fault zone. Fluid flow was then introduced by applying a pressure gradient from the uphill boundary of the model. The zone of water infiltration into the model was limited to the upper part of the surface stopping at the lower boundary of the fault zone (Fig. 9, left boundary, between ~350 - 450 m on Y-axis). With this modeling setup, the groundwater reservoir in the upper part of the slope, originating from water infiltration in the cirque above the failed rock slope (Fig. 4), and aquiclude situation below the fault zone could be reproduced and their effect tested. One main assumption is that the discontinuities are fully water saturated.

Fig. 9 shows the water pressure along discontinuities (marked with white lines). Maximum fluid pressures generated are 0.6 MPa, which corresponds to a head of 60 m. Mean fluid pressures within the fault zone range from 0.3 and 0.4 MPa, and between 0.02 and 0.03 MPa in the less-permeable diorite below. Water outflow at the surface is allowed. Fig. 9a displays vertical displacements in the 2D profile after hydrologic loading, while Fig. 9b displays horizontal displacements along two vertical profiles. Horizontal displacements were found to concentrate in the area of higher fluid pressures, and amount to 6 mm. Vertical displacements, however, extend further downwards and indicate maximum subsidence of 2 mm in the steep part of the flank. On the shoulder of the ridge, uplift displacements up to 8 mm can be recognized. Expansion of the flank due to water pressure in

the upper portion of the slope can induce displacements throughout the steep face, only ceasing where the slope becomes flatter. The 1988 slope failure occurred in the area with modeled vertical displacement. These results indicate that water pressure not only induces reversible displacements, but also provokes irreversible vertical settlement.

5. Discussion

This research addresses different environmental factors and processes possibly influencing slope stability and contributing to the 1988 Tschierva rock avalanche. Various approaches and data sets have been combined in an integrated analysis of the slope failure. The discussion is structured based on the hypotheses in section 3.8.

5.1 Discontinuity and rock slope geometry

Detailed site investigations yielded important insight into the current state of the slope and changes in the past. Although in situ access was limited, a comprehensive data set could be compiled from field work and remote sensing. Topographic and morphologic investigations revealed oversteepened topography resulting from glacial erosion in the area of the slope failure. Inspection of neighboring flanks, however, showed that most rock slopes in this area are also steep with similar oversteepened morphology. This suggests that, although slope angle, orientation, and morphology are key factors for rock slope stability, in this case the slope angle and morphology are not the primary factors provoking the slope failure.

Kinematic analyses highlighted the strong influence of the two main discontinuity sets on the slope stability. Joint geometry controls the dominant failure mode in hard rock slopes, which in this case is planar sliding. The moderately-dipping and daylighting discontinuity set, K1, induces a kinematically unfavorable situation. Analyzing the neighboring flanks with similar discontinuity patterns, however, no unstable areas were observed and kinematic analyses reveal minor criticality for planar sliding failure in these adjacent areas. Therefore, the two predominant discontinuity sets have a significant effect on slope stability only in combination with the particular slope orientation. Even minor changes in either slope or discontinuity geometry may alter the kinematic conditions and the overall stability of the slope.

5.2 Glacial retreat and debuttressing

The rock avalanche detachment area was subject to high glacial confining pressure and significant redistribution of internal stress following glacier retreat. Numerical modeling of glacier retreat has shown that removal of the glacial buttress and subsequent decompression allowed propagation of fractures through previously intact rock bridges. The investigated rock slope was apparently stable after glacier retreat until 1988, despite significant stress redistribution and induced displacements. Our modeling has shown that the slope would have failed sooner if we assumed fully-persistent discontinuities. Therefore, our results suggest important contributions to rock mass strength from intact rock bridges along non-persistent discontinuities. Any occurrence of interstitial ice along joint surfaces is assumed to have a similar and complementary effect on rock mass strength as rock bridges. The effect of glacier retreat and debuttressing on rock slope strength deterioration likely occurred slowly and progressively over a long period of time through brittle fracturing of intact rock bridges (Eberhardt et al., 2004). This indicates that for our study site, the failure mechanism was not a simple process but rather a complex combination of increasing stress and the progressive

development of persistent discontinuities. Numerical model results revealed irreversible displacements along a stepped surface connecting discontinuity sets, which matched well with the eventual geometry of the 1988 failure surface. Only one deglaciation cycle has been simulated in our modeling. In reality, the flank experienced several cycles of glaciation and deglaciation during the Late Pleistocene (Maisch et al., 2000, Ivy-Ochs et al., 2008), possibly intensifying the process of progressive failure. However, rock slope failure can also occur shortly after deglaciation, as observed in several cases (e.g. Porter and Orombelli, 1981; McSaveney, 1993; Abele, 1997; Fischer et al., 2006; Oppikofer et al., 2008).

5.3 Permafrost

Ground surface temperature modeling has shown that permafrost occurrence is likely in the area of the failed slope, primarily on the northern side of the ridge and possibly also in the detachment zone. The probable occurrence of ice on the failure surface after the rock avalanche (personal communication A. Amstutz) confirms this estimation. The presence of ice in joints influences the strength of a jointed rock mass, however, geotechnical parameters and the behavior of ice-filled joints are not well known. Davies et al. (2001) showed on the basis of direct shear box tests that a rise in temperature might lead to a reduction in the shear strength of ice-bonded discontinuities between -2 and 0°C, and Mellor (1973) showed that the compressive and tensile strength of water saturated rocks increases strongly when temperatures decrease further below zero. This indicates an increased strength of ice-bonded fractures at lower negative temperatures. The observed water outflow in the upper part of the flank after the failure indicates subsurface temperatures above 0° C, at least along the flow paths. The presence of ice within joints in permafrost areas influences the hydrologic conditions. Groundwater flow can be cut off or diverted by frozen zones with much lower permeabilities (Tart, 1996). Permafrost thaw and consecutive water flow can strongly increase hydrostatic pressures, e.g. in fractures where ice may be thawing, in areas impermeable due to ice, or in areas where ice is thawing above. We assume that changes in permafrost could influenced slope stability due to a rise in ice temperature, a reduction in shear strength, and formation of new groundwater flow paths. However, more detailed conclusions are currently not possible, as they require further information on the permafrost and temperature distribution, and improved process knowledge linking permafrost and rock slope mechanics.

Meteorological data from the nearby Corvatsch station cannot conclusively demonstrate that the slope failure reported in this paper is related to recent climate warming, due to of a lack of detailed long-term data. The mean daily temperatures in the summer and autumn of 1988 show no significant anomalies compared to the data from 1980 to 1995. For conclusions about changes in permafrost occurrence and temperature, however, longer data series would be necessary, and 3D and transient effects with depth must be modeled (Noetzli and Gruber, 2009). Theoretical considerations and modeling suggest that effects of 20th century warming have reached bedrock depths on the order of decameters (Gruber and Haeberli, 2007; Noetzli et al., 2007; Harris et al., 2009). Accordingly, recent subsurface temperature changes at the Tschierva site are likely.

5.4 Groundwater

Increased fracture density within the fault zone crossing the detachment area may have adversely affected slope stability. Model results suggest that irreversible displacements can occur due to high water pressures generated within the fault zone. Since the input data necessary to design predictions are limited in this study, the numerical results should be used primarily to understand

the mechanisms affecting the system behavior, and no predictions can be made whether such water pressure acted as an ultimate triggering factor.

Meteorological data show significant precipitation events in the weeks preceding the rock avalanche. Within the considered time frame of 15 years, the daily precipitation reached 50 mm on only five occasions, and two of these were consecutive days in October 1988. However, this precipitation was in the form of snow and occurred 16 days prior to the slope failure. Storage of precipitation as snow, and delayed melting in the days before the event likely influenced the slope failure. It is not clear to what extent the snow had melted within the two weeks preceding the rock avalanche, given the relatively short periods of above-freezing temperatures. The pronounced freezing periods in the days before slope failure could also have lead to a superficial freezing and consequently to a trapping of groundwater beneath a surface cap. Under such artesian conditions, quite high water pressure can build up. Although water outflow observed directly after the 1988 rock avalanche is evidence of a considerable amount of groundwater within the flank, the preceding heavy precipitation cannot be clearly assigned as a triggering factor. Local observations indicated that there was rockfall activity from the flank during preceding months, which indicates a generally unstable state. Krähenbühl (2004) showed, based on long-term measurement of meteorological and displacement data in other parts of the eastern Swiss Alps, that heavy precipitation in autumn may have a stronger influence on displacements than comparable events during summer and spring because fracture opening is largest in autumn and therefore maximal joint water pressure can be built up. Such irreversible displacements have also been shown in our coupled hydro-mechanical modeling for the investigated rock slope. Based on the results of one loading cycle with high fluid pressures, we suggest that repeated small infiltration events and cyclic fluid pressure may have contributed to slow, progressive failure of intact rock bridges and ultimately to the failure of the slope.

6. Conclusions

Analysis of the 1988 Tschierva rock avalanche indicates that the slope failure was the result of a number of contributing factors and cannot be ascribed to one single cause. Among these factors, rock mass characteristics, namely the geometry of the two prominent joint sets with respect to the slope free face, played an important role in the failure. Slow, progressive formation or extension of discontinuities following glacial debutressing likely played a key role in long-term degradation of rock mass strength. Similarly, cyclic loading of fluid pressure in joints following precipitation or snow melt events likely contributed to progressive failure of intact rock bridges. The occurrence of permafrost within the failed flank may have influenced slope stability, as changes in the temperature and ice distribution related to ongoing climate warming combine to reduce discontinuity shear strength while contributing to the formation of new groundwater flow paths. The heavy precipitation several days before the slope failure may have acted as a final trigger of the rock avalanche, as high water pressures could have resulted in irreversible displacements along persistent fractures. The delay of 16 days could be explained by the snowfall and subsequent snow melting. However, air temperatures were in this period only slightly above 0°C, provoking probably slow snow melting. Therefore, no distinct trigger event can be conclusively assigned.

Rock slope stability assessments are particularly challenging in high-mountain regions due to difficult or impossible site access. Poor data availability and specific characteristics of cold mountain environments, such as glacier and permafrost occurrence, that are particularly sensitive to climatic change, introduce further complexity. In such environments it is important to proceed with an integrated approach slope stability, which considers a broad range influencing factors.

Our approach of multi-factor analysis in combination with geomechanical modeling proved appropriate for failure analyses in such complex terrain, despite existing data limitations. Initial topography and glaciation history can be reconstructed by the means of remote sensing and surface temperature distribution can be modeled if climatic and topographic data are available. It has been shown that permafrost occurrence, related water pressure conditions, and stability modeling can be interrelated. However, even though the surface ground temperature can be approximated with some reliability, temperatures at depth strongly depend on thermal fluxes associated with three-dimensional effects, joint systems and other factors. The prevailing uncertainties that propagate into the groundwater conditions are a challenge for geomechanical modeling, and therefore more research is needed. This study has also pointed out that sufficient information on rock mass characteristics for reliable analyses can only obtained by in situ investigations, a particular challenge that can only partly be overcome by advanced technology such as high resolution remote sensing. In summary, the strength of our approach in this work is consideration of an integrated set of controlling factors that influence slope stability in high mountain regions, and the development of a framework for geomechanical modeling based on limited data availability, as is typical for these environments.

Acknowledgements

The authors thank Frank Lemy for the valuable collaboration in initial phase of this project, Jeannette Noetzli and Frank Paul for providing the temperature modeling and glaciation data, and Wilfried Haeberli for general support. We thank A. Amstutz for providing imagery and valuable information about the Tschierva rock avalanche. This work was supported by the Swiss National Science Foundation (project no. 200021-111967).

References

Abele, G., 1997. Influence of glacier and climatic variation on rockslide activity in the Alps. Paläoklimaforschung-Paleoclimate Research, 19, 1-6.

Augustinus, P., 1995. Rock mass strength and the stability of some glacial valley slopes. Z. Geomorph. N.F., 1, 55-68.

Ballantyne, C.K., 2002. Paraglacial Geomorphology. Quarternary Science Reviews 21, 1935-2017.

Barla, G., Barla, M., 2001. Investigation and modelling of the Brenva Glacier rock avalanche on the Mount Blanc Range. Proceedings of the ISRM Regional Symposium Eurock 2001, Espoo, Finlandia, 3-7 giugno, 2001, 35-40.

Barla, G., Dutto, F., Mortara, G., 2000. Brenva glacier rock avalanche of 18 January 1997 on the Mont Blanc range, Northwest Italy. Landslide News 13, 2–5.

Bieniawski, Z.T., 1989. Engineering rock mass classifications. Johns Wiley & Sons, New York.

Bottino, G., Chiarle, M., Joly, A., Mortara, G., 2002. Modelling rock avalanches and their relation to permafrost degradation in glacial environments. Permafrost Periglacial Processes, 13, 283-288.

Christian, J.T., Baecher, G.B., 2002. The point-estimate method with large numbers of variables. Int. J. Numer. Anal. Meth. Geomech. 26, 15151-1529.

Cola, G., 2005. The large landslide of the south-east face of Thurwieser peak (Thurwieser-Spitze) 3658 m (Upper Valtellina, Italy). Terra Glacialis. 8, 38-45.

Cruden, D.M., Hu, X-Q., 1993. Exhaustion and steady state models for predicting landslide hazards in the Canadian Rocky Mountains. Geomorphology, 8: 279-285.

Davies, M.C.R., Hamza, O., Harris, C., 2001. The effect of rise in mean annual temperature on the stability of rock slopes containing ice-filled discontinuities, Permafrost Periglacial Processes, 12(1), 137-144.

Dramis, F., Govi, M., Guglielmin, M., Mortara, G., 1995. Mountain permafrost and slope instability in the Italian Alps: The Val Pola landslide, Permafrost Periglacial Processes, 6(1), 73– 82.

Eberhardt, E., Stead, D., Coggan, J.S., 2004. Numerical analysis of initiation and progressive failure in natural rock slopes – the 1991 Randa rockslide. Int. J. Rock Mech. Min. Sci. 41, 69-87.

Einstein, H.H., Veneziano, D., Baecher, G.B., O'Reilly, K.J., 1983. The effect of discontinuity persistence on rock slope stability. Int. J. Rock. Mech. Min. Sci. Geomech. Abst., 20(5), 227-236.

Evans, S.G., Clague, J.J., 1988. Catastrophic rock avalanches in glacial environments. Proc. Fifth Int. Symp. on Landslides, Vol. 2, pp. 1153-1158.

Evans, S.G., Clague, J.J., 1993. Glacier-related hazards and climatic change, In Bras, R. (ed.), The World at Risk: Natural Hazards and Climatic Change, American Institute of Physics Conference Proceedings, 277, 48-60.

Evans, S.G., Clague, J.J., 1994. Recent climatic change and catastrophic geomorphic processes in mountain environments. Geomorphology 10, 107–128.

Fischer, L., Huggel, C., 2008. Methodical design for stability assessments of permafrost affected high-mountain rock walls. Proceedings of the 9th International Conference on Permafrost 2008, Fairbanks, Alaska, USA, 29.6.-3.7.2008, 1, 439-444.

Fischer, L., Kääb, A., Huggel, C., Noetzli, J., 2006. Geology, glacier retreat and permafrost degradation as controlling factors of slope instabilities in a high-mountain rock wall: the Monte Rosa east face. Nat. Hazards Earth Syst. Sci., 6, 761-772.

Geertsema, M., Clague, J.J, Schwab, J.W., Evans, S.G., 2006. An overview of recent large catastrophic landslides in northern British Columbia, Canada. Eng. Geol., 83, 120-143.

Giani, G.P., 1992. Rock slope stability analysis. A.A. Balkema, Rotterdam, pp. 361.

Goodman, R. E., 1989. Introduction to rock mechanics. Wiley, New York, pp. 562.

Gruber, S. (2005): Mountain permafrost: transient spatial modelling, model verification and the use of remote sensing, PhD dissertation, Department of Geography, University of Zurich, Switzerland, 123pp.

Gruber, S., Haeberli, W., 2007. Permafrost in steep bedrock and its temperature-related destabilization following climate change. J. Geophys. Research 112, F02S18.

Haeberli, W., Wegmann, M., Vonder Muehll, D., 1997. Slope stability problems related to glacier shrinkage and permafrost degradation in the Alps, Eclogae Geol. Helv., 90, 407-414.

Haeberli,W., Huggel, C., Kääb, A., Oswald, S., Polkvoj, A., Zotikov, I., Osokin, N., 2004. The Kolka-Karmadon rock/ice slide of 20 September 2002 – an extraordinary event of historical dimensions in North Ossetia (Russian Caucasus). Journal ofGlaciology 50, 533–546.

Harris, C., Davies, M., Etzelmüller, B., 2001. The assessment of potential geotechnical hazards associated with mountain permafrost in a warming global climate, Permafrost Periglacial Processes, 12, 145–156.

Harris, C., Vonder Mühll, C., Isaksen, K., Haeberli, W., Sollid, J.L., King, L., Holmlund, P., Dramis, F., Gugliemin, M., Palacios, D., 2003. Warming permafrost in European mountains, Global Planet. Change, 39, 215-225.

Harris, C., Arenson, L.U., Christiansen, H.H., Etzelmüller, B., Frauenfelder, R., Gruber, S., Haeberli, W., Hauck, C., Hölzle, M., Humlum, O., Isaksen, K., Kääb, A., Kern-Lütschg, M.A., Lehning, M., Matsuoka, N., Murton,J.B., Nötzli, J., Phillips, M., Ross, N., Seppälä, M., Springman, S.M., Vonder Mühll, D., 2009. Permafrost and climate in Europe: Monitoring and modelling thermal, geomorphological and geotechnical responses. Earth Science Reviews, 92, 117-171.

Hoek, E., Brown, E.T., 1980. Empirical strength criterion for rock masses. J. Geotech. Engng Div., ASCE 106 (GT9), 1013-1035.

Hoek, E., J. Bray, 1981. Rock Slope Engineering, Inst. of Min. and Metal., London.

Hoek, E., Brown, E.T., 1997. Practical estimates of rock mass strength. Int. J. Rock Mech. & Mining Sci. & Geomechanics Abstracts. 34 (8), 1165-1186.

Huggel, C., 2009. Recent extreme slope failures in glacial environments: effects of thermal perturbation. Quaternary Science Reviews, 28, 1119-1130.

Itasca, 2004. Itasca Software Products – UDEC (Universal Distinct Element Code), Version 4.0. Itasca Consulting group Inc., Minneapolis.

Ivy-Ochs, S., Kerschner, H., Reuther, A., Preusser, F., Heine, K. Maisch, M., Kubik, P.W., Schlüchter, C., 2008. Chronology of the last glacial cycle in the European Alps. J. Quat. Sci., 23, 559-573.

Jäckli, H., 1962. Die Vergletscherung der Schweiz im Würmmaximum. Eclogae geol. Helv. 55/2, 285-293.

Jennings, J.E., 1970. A mathematical theory for the calculation of the stability of open cast mines. In: Proceedings of the symposium on theoretical background to the planning of open pit mines. Johannesburg, 1970, p. 87-102.

Krähenbühl, R., 2004. Temperatur und Kluftwasser als Ursachen von Felssturz. Bull. angew. Geol., 9(1), 19-35.

Mellor, M., 1973. Mechanical properties of rocks at low temperatures. In: Permafrost: North American contribution [to the] Second International Conference. Proceedings of the United States Planning Committee for the 2d International Conference on Permafrost, National Academy of Sciences (U.S.), 334-344.

Maisch, M., 1992. Die Gletscher Graubündens. Rekonstruktion und Auswertung der Gletscher und deren Veränderungen seit dem Hochstand von 1850 im Gebiet der östlichen Schweizer Alpen (Bündnerland und angrenzende Regionen). Geographisches Institut der Universität Zürich, Physische Geographie, 33, Part A: 324 p., Part B: 128 p.

Maisch, M., Wipf, A., Denneler, B., Battaglia, J., Benz, C., 2000. Die Gletscher der Schweizer Alpen. Gletscherhochstand 1850, Aktuelle Vergletscherung, Gletscherschwund-Szenarien (2nd Ed.). VdF Hochschulverlag, ETH Zürich, Schlussbericht NFP31, 373 p.

McSaveney, M.J., 1993. Rock avalanches of 2 May and 6 September 1992, Mount Fletcher, New Zealand. Landslide News 7, 2-4.

Moore, J.R., Sanders, J.W., Dietrich, W.E., Glaser, S.D., 2009. Influence of rock mass strength on the erosion rate of alpine cliffs. Earth Surface Processes and Landforms, doi: 10.1002/esp.1821.

Müller, F., Caflish, T., Müller, G., 1976. Firn und Eis der Schweizer Alpen, Gletscherinventar. Geographisches Institut, vdf-Verlag, ETH Zürich, 57, 174 p.

Noetzli, J., Gruber, S., 2009. Transient thermal effects in Alpine permafrost. The Cryosphere 3, 85-99.

Noetzli, J., Hoelzle, M., Haeberli, W., 2003. Mountain permafrost and recent Alpine rock-fall events: a GIS-based approach to determine critical factors. Proceedings of the 8th International Conference on Permafrost, Zurich, Switzerland, 2, 827-832.

Noetzli, J., Gruber, S., Kohl, T., Salzmann, N., Haeberli, W., 2007. Three-dimensional distribution and evolution of permafrost temperatures in idealized high-mountain topography. Journal of Geophysical Research, 112, F02S13, doi:10.1029/ 2006JF000545.

Norrish, H.L., Wyllie, D.C., 1996. Rock slope stability analysis. In Turner, A.K., Schuster, R.L. (Eds.), Landslides: Investigation and Mitigation, Transportation Research Board National Research Council. Special Report 247 Washington D.C., USA. National Academy Press.

Oppikofer T., Jaboyedoff, M., Keusen, H.-R., 2008. Collapse of the eastern Eiger flank in the Swiss Alps. Nature Geosciences 1(8), 531-535.

Paul, F., 2004. The new Swiss glacier inventory 2000 - Application of remote sensing and GIS. PhD Thesis, Department of Geography, University of Zurich, pp. 198.

Porter, S.C., Orombelli, G., 1981. Alpine rockfall hazards. American Scientist, 69, 67-75.

Prudencio, M., Van Sint Jan, M., 2007. Strength and failure modes of rock mass models with non-persistent joints. Int. J. Rock Mech. Min. Sci. 44, 890-902.

Rosenbleuth, E., 1981. Two-point estimates in probabilities. J. Appl. Math. Modelling 5, 329-335.

Sartori, M., Baillifard, F., Jaboyedoff, M., Rouiller, J.D., 2003. Kinematics of the 1991 Randa rockslide (Valais, Switzerland). Nat. Hazards Earth Syst. Sci., 3, 423-433.

Spillmann, P., Trommsdorff, V., 2005. Geologischer Atlas der Schweiz 1:25 000 , Piz Bernina. Ed. Bundesamt für Wasser und Geologie, Wabern, pp. 140.

Stead, D., Eberhardt, E., Coggan, J., Benko, B., 2001. Advanced numerical techniques in rock slope stability analyses-applications and limitations. Proceedings of the International Conference on Landslides-Causes, Impacts and Countermeasures, Davos 2001: 615-624.

Stead, D., Eberhardt, E., Coggan, J.S., 2006. Developments in the characterization of complex rock slope deformation and failure using numerical modelling techniques. Eng. Geol., 83, 217-235.

Schweizer, J., 1990. Short note on Rockslide to Tschiervaglacier. VAW, ETH Zurich, unpublished manuscript.

Swisstopo, DHM25: Das digitale Hoehenmodell der Schweiz, Level 2, Bundesamt fuer Landestopographie, Wabern, Switzerland, 2002.

Tart, R.G., 1996. Permafrost. In Turner, A.K., Schuster, R.L. (Eds.), Landslides: Investigation and Mitigation, Transportation Research Board National Research Council. Special Report 247 Washington D.C., USA. National Academy Press.

Wegmann, M., G.H. Gudmundsson, W. Haeberli, 1998. Permafrost changes in rock walls and the retreat of Alpine glaciers: a thermal modelling approach, Permafrost Periglacial Processes, 9, 23-33.

Zemp, M., Haeberli, W., Hoelzle, M., Paul, F., 2006. Alpine glaciers to disappear within decades? Geophysical Research Letters, 33, L13504, doi:10.1029/2006GL026319.